A NOVEL RHEOLOGICAL AND FRICTIONAL PRESSURE LOSS EQUATIONS FOR NON-AQUEOUS DRILLING FLUID SYSTEMS BY CONSIDERING THE PRESSURE EFFECT

A THESIS SUBMITTED TO
THE GRADUATE SCHOOL OF NATURAL AND APPLIED SCIENCES
OF
MIDDLE EAST TECHNICAL UNIVERSITY

BY

MUZAFFER GÖRKEM GÖKDEMİR

IN PARTIAL FULFILLMENT OF THE REQUIREMENTS
FOR
THE DEGREE OF DOCTOR OF PHILOSOPHY
IN
PETROLEUM AND NATURAL GAS ENGINEERING

MARCH 2023

Approval of the thesis:

A NOVEL RHEOLOGICAL AND FRICTIONAL PRESSURE LOSS EQUATIONS FOR NON-AQUEOUS DRILLING FLUID SYSTEMS BY CONSIDERING THE PRESSURE EFFECT

submitted by **Muzaffer Görkem Gökdemir** in partial fulfillment of the requirements for the degree of **Doctor of Philosophy in Petroleum and Natural Gas Engineering, Middle East Technical University** by,

Prof. Dr. Halil Kalıpçılar
Dean, Graduate School of **Natural and Applied Sciences** _____

Asst. Prof. Dr. İsmail Durgut
Head of the Department, **Petroleum and Natural Gas Eng.** _____

Prof. Dr. Mahmut Parlaktuna
Supervisor, **Petroleum and Natural Gas Eng., METU** _____

Examining Committee Members:

Prof. Dr. Gürşat Altun
Petroleum and Natural Gas Eng., ITU _____

Prof. Dr. Mahmut Parlaktuna
Petroleum and Natural Gas Eng., METU _____

Assoc. Prof. Dr. Çağlar Sınayuç
Petroleum and Natural Gas Eng., METU _____

Asst. Prof. Dr. İsmail Durgut
Petroleum and Natural Gas Eng., METU _____

Asst. Prof. Dr. Ali Ettehadi
Petroleum and Natural Gas Eng., Katip Çelebi Uni. _____

Date: 31.03.2023

I hereby declare that all information in this document has been obtained and presented in accordance with academic rules and ethical conduct. I also declare that, as required by these rules and conduct, I have fully cited and referenced all material and results that are not original to this work.

Name Last name : Muzaffer Görkem Gökdemir

Signature :

ABSTRACT

A NOVEL RHEOLOGICAL AND FRICTIONAL PRESSURE LOSS EQUATIONS FOR NON-AQUEOUS BASED DRILLING FLUID SYSTEMS BY CONSIDERING THE PRESSURE EFFECT

Gökdemir, Muzaffer Görkem
Doctor of Philosophy, Petroleum and Natural Gas Engineering
Supervisor: Prof. Dr. Mahmut Parlaktuna

March 2023, 183 pages

Non-aqueous conventional drilling fluid systems (NAF) are preferred due to lubricity effect, high inhibitive characteristic and temperature-rheological stability in deep formations. However their flow characteristics prone to change with pressure due to slightly compressibility nature of them.

This study is designed to investigate the effect of pressure on the flow characteristics of sightly compressible drilling fluids, both experimental and theoretical work, at constant temperature conditions. Diesel and synthetic based samples are used as slightly compressible systems while water base muds are tested as incompressible drilling fluids. Rheological tests are conducted on Anton Paar MCR-302 high pressure high temperature (HPHT) rheometer. Pressure dependent constitutive stress equations are proposed and based on those rheological equations, frictional pressure loss calculation methodology is developed during the theoretical work.

While a difference in pressure doesn't affect Fluid Flow Behaviour Index (m parameter), both the Yield Stress or Point – τ_y and Consistency Index, (also known

as K parameter), are strongly dependent on pressure change as rheological parameter analysis indicates.

The hydraulic calculations obtained using the proposed constitutive stress equations were verified through real field application, where the drilling fluid system demonstrated a yield behavior with shear-thinning deformation characteristics. Field measurements were taken at two different flow rates along with pressure readings and when compared to model calculations in the annular geometry, the on-bottom pressure values were slightly overestimated with a negligible difference in absolute terms.

When the oil (continuous) fraction of a non-aqueous drilling fluid system is increased in volume relative to the water (brine) phase, pressures shows more effect on the rheological parameters or stress requirements of flow for the non-aqueous based drilling fluid systems.

The oil water ratio affects the level of yield stress significantly. When the o/w ratio is reduced, higher yield stress values are observed.

Under the same experimental conditions, an increase in Barite content in the system results in the rise of both yield stress and consistency index.

On higher mud weights, even though the relatively compressible fluid amount is decreased; the percentage increase of rheological parameters τy and K in terms of pressure is higher due to solid particle effect.

Keywords: Rheology, Slightly Compressible, Drilling Fluids, Hydraulic Calculation Methodology

ÖZ

SU BAZLI OLMAYAN SONDAJ AKIŞKANI SİSTEMLERİNDE BASINÇ ETKİSİNİ GÖZ ÖNÜNE ALAN YENİLİKÇİ BİR REOLOJİ VE SÜRTÜNME BASINÇ KAYBI DENKLEMLERİ

Gökdemir, Muzaffer Görkem
Doktora, Petrol ve Doğal Gaz Mühendisliği
Tez Yöneticisi: Prof. Dr. Mahmut Parlaktuna

Mart 2023, 183 sayfa

Su bazlı olmayan sondaj çamurları (NAF) bünyesinde sentetik bazlı (SBM) ve petrol bazlı (OBM) sistemleri barındırmaktadır. NAF sistemleri; yüksek yağlama, yüksek korunma mekanizması, yüksek sıcaklıkta kararlılık ve kuvvetli kuyu stabilitesi sağlama özelliklerinden dolayı operasyonel olarak daha çok tercih edilir. NAF sistemleri sıkıştırılabilen akışkanlar olduklarından akış karakterleri basınca bağlı olarak değişim gösterir.

Bu çalışmada, sabit sıcaklık koşullarında basıncın etkisi az sıkıştırılabilir sondaj sıvılarının akış davranışlarında deneysel ve teorik olarak gerçekleştirilmiştir. Dizel ve sentetik bazlı örnekler az sıkıştırılabilir sistemler, su bazlı çamurlar sıkıştırılamayan sondaj sıvıları olarak kullanılmıştır. Reolojik testler Anton Paar-302 yüksek basınç yüksek sıcaklık (YBYS) reometresinde gerçekleştirilmiştir. Basınca bağlı temel stres denklemleri önerilmiş ve teorik çalışmada sürtünme basınç kaybı hesaplama metodolojisi reolojik denklemlere bağlı olarak geliştirilmiştir. Reoloji parametre analizinin gösterdiği üzere Akışkan Akışı Davranış Endeksi (m parametresi), basınç değişimi ile değiştirilemez. Fakat hem Akma Gerilimi ya da

noktası – τy, hem de Kıvam Endeksi (K parametresi) basınç değişimine fazlasıyla bağımlıdır.

Önerilen yapısal stres denklemlerine dayalı şekilde elde edilen hidrolik hesaplamalar, gerçek saha uygulamalarıyla doğrulanmıştır. Sondaj akışkanı sistemi kayma incelmesi deformasyon davranışına sahip bir akma karakteri göstermiştir. Saha ölçümleri iki farklı akış hızında, basınç okumalarıyla beraber alınmıştır. Annüler geometrideki model hesaplamaları, on-bottom basınç değerlerini çok düşük bir mutlak fark ile olduğundan sadece biraz fazla tahmin etmiştir.

Petrol (sürekli faz) yüzdesi, su (brine) yüzdesine göre hacimsel olarak arttırıldığı zaman, reolojik parametreleri basınç domine etmektedir. Yani akış için stres gereksinimleri, su-bazlı-olmayan sondaj akışkanı sistemleri için daha yüksek seviyededir.

Petrol/su (O/W) oranı, akma gerilimi değerini yüksek oranda etkiler. O/W oranı düşürüldüğünde daha yüksek akma gerilimi değerleri gözlenmiştir.

Aynı deneysel koşullarda, sistemdeki Barit miktarı arttırıldıkça hem akma gerilimi hem de kıvam endeksi yükselmektedir.

Daha yüksek çamur ağırlıklarında, her ne kadar sıkıştırılabilir akışkan miktarı göreceli olarak düşmüş olsa da basıncın yüzdesel artışı τy ve K reolojik parametreleri için katı madde etkisi sebebiyle daha fazladır.

Anahtar Kelimeler: Reoloji, Az Sıkıştırılabilir, Sondaj Akışkanları, Hidrolik Hesaplama Metodolojisi

To My Family

ACKNOWLEDGMENTS

First of all, I would like to express sincere thanks to my advisor, Prof.Dr. Mahmut Parlaktuna, for his valuable support and guidance in every step of this research. The shared experience and academic freedom he gave me, inspired me and made me more confident. I would like to give special thanks to Prof.Dr. Gürşat Altun and Assoc.Prof.Dr. Çağlar Sınayuç who devoted a large amount of time to help me endlessly and to make this thesis possible.

I extend thanks to the Turkish Petroleum Corporation Research and Development Centre and Drilling Technology Management Department who provided me endless support to get my degree. My colleague Çağdaş Yalçın for his contributive assistance, also deserves special thanks.

Finally, my family who believed in me and supported me without any expectations deserves the most appreciation. I dedicate this work to my daughter, Gülten Duru and my wife, Gökçe.

TABLE OF CONTENTS

ABSTRACT v

ÖZ vii

ACKNOWLEDGMENTS x

TABLE OF CONTENTS xi

LIST OF TABLES xiii

LIST OF FIGURES xv

LIST OF ABBREVIATIONS xviii

LIST OF SYMBOLS xxi

CHAPTERS

1 INTRODUCTION 1

2 LITERATURE REVIEW 3

2.1 Rheology 3

2.1.1 Yield Stress Phonemena and Viscoelasticity 6

2.1.2 Previously Pressure Dependent Rheological Models 7

3 STATEMENT OF THE PROBLEM 9

4 EXPERIMENTAL SET-UP, TEST METHODOLOGY and TEST FLUIDS 11

4.1 Experimental Set-Up 11

4.2 Test Methodology and Test Fluids 12

5 EXPERIMENTAL RESULTS and DISCUSSIONS 19

6 PROPOSED MATHEMATICAL PRESSURE – DEPENDENT EQUATIONS and EVALUATION 29

6.1 Constitutive - Stress Equation 29

6.2 Frictional Pressure Loss Equation 35
6.2.1 Power Law Pipe Flow 35
6.2.2 Power Law Annular Flow 36
6.2.3 Yield Power Law Pipe Flow 48
6.2.4 Yield Power Law Annular Flow 40
6.3 Model Validation and Discussion from Real Field Application and Pressure Measurements 43
7 RHEOLOGICAL MODEL SENSIVITY IN REFERENCE TO THE BASE FLUID RATIO, TEMPERATURE AND VOLUME of SOLID 63
7.1 Base Fluid Effect 63
7.2 Temperature Effect 76
7.3 Mud Weight - Solid Effect 82
8 CONCLUSIONS 103
9 RECOMMENDATIONS 107
REFERRENCES 109
APPENDICES
A. 0.03 M3/SEC FLOW RATE CALCULATION RESULTS 113
CURRICULUM VITAE 183

LIST OF TABLES

TABLES

Table 1 Chemical Composition of Test Fluids 15

Table 2 Test Conditions of Sample Fluids.....18

Table 3 Rheological Parameters of Field OBM at Different Pressure and 25°C.....23

Table 4 Rheological Parameters of SBM-1 at Different Pressure and 25°C 25

Table 5 Rheological Parameters of SBM-2 at Different Pressure, 50°C and 75°C.27

Table 6 F-OBM Model Parameters at Test Temperatures.....47

Table 7 String Geometry of Well XX.....51

Table 8 Operated Mud Pump Properties in Well XX 51

Table 9 Mud Properties of Validation Sample.....52

Table 10 Rheological Parameters of F-OBM at Different Pressure at 55°C 53

Table 11 Model Parameters of F-OBM at 55°C 53

Table 12 F-OBM Newtonian Viscosity at 55°C.....60

Table 13 Rheological Parameters of 30/70 w/o F-OBM at Different Pressure at 45°C 66

Table 14 30/70 w/o F-OBM Model Parameters at 45°C 67

Table 15 Rheological Parameters of 40/60 w/o F-OBM at Different Pressure at 45°C 71

Table 16 40/60 w/o F-OBM Model Parameters at 45°C 72

Table 17 Rheological Parameters of 40/60 w/o F-OBM at Different Pressure at 100°C 78

Table 18 40/60 w/o F-OBM Model Parameters at 100°C 79

Table 19 Formulation of Different Mud Weight DBMs 83

Table 20 Rheological Parameters of 1044 kg/m^3 80/20 o/w at 25°C..... 85

Table 21 1044 kg/m3 DBF Model Parameters at 25°C..... 86

Table 22 Rheological Parameters of 1404.4 kg/m^3 80/20 o/w at 25°C..... 91

Table 23 1404.4 kg/m^3 DBF Model Parameters at 25°C 92

Table 24 Rheological Parameters of 1764.7 kg/m^3 80/20 o/w at 25°C..... 97

Table 25 1764.7 kg/m^3 DBF Model Parameters at 25°C 98

LIST OF FIGURES

FIGURES

Figure 1 Diagram of Fluid Flow between Stationary and Moving Plates 4
Figure 2 Picture and Schematic Drawing of Experimental Setup 12
Figure 3 Magnetic Coupling and High Pressure Measuring Geometry..... 13
Figure 4 Silverson High Shear Mixer 16
Figure 5 Beach Mixer 17
Figure 6 Data Analysis Example 19
Figure 7 Rheogram for Drill-In Fluids..... 20
Figure 8 Rheogram for PMIC Fluids 21
Figure 9 Rheogram for Field OBM 22
Figure 10 Rheogram for Field SBM-1..... 24
Figure 11 Rheogram for SBM-2 at 50°C..... 28
Figure 12 Rheogram for SBM-2 at 75°C..... 28
Figure 13 Consistency Index for Field OBM at 25°C 31
Figure 14 Model Rheogram Example for Field OBM at 25°C..... 31
Figure 15 Predicted and Measured τ_y for SBM Systems 32
Figure 16 Predicted and Measured *K* for SBM Systems 33
Figure 17 Model Rheogram Example for SBM at 25°C..... 33
Figure 18 Model Rheogram Example for SBM at 50°C..... 34
Figure 19 Model Rheogram Example for SBM at 75°C..... 34
Figure 20 Rheogram-1 for F-OBM at 45°C..... 44
Figure 21 Rheogram-2 for F-OBM at 45°C..... 44
Figure 22 Rheogram-1 for F-OBM at 55°C..... 45
Figure 23 Rheogram-2 for F-OBM at 55°C..... 45
Figure 24 Rheogram-1 for F-OBM at 68°C..... 46
Figure 25 Rheogram-2 for F-OBM at 68°C..... 46
Figure 26 F-OBM Predicted and Measured Yield Stress 47
Figure 27 F-OBM Predicted and Measured Consistency Index 48

Figure 28 Pressure Calculation Methodology in the Hole Trajectory 54
Figure 29 Calculated Pressure in the Well Bore at 0.3 m^3/s Circulation Rate 55
Figure 30 Calculated Pressure in the Well Bore at 0.3 m3/s Circulation Rate..... 56
Figure 31 Calculated Pressure in the Well Bore at 0.022 m3/s Circulation Rate ... 57
Figure 32 Calculated Pressure in the Well Bore at 0.022 m3/s Circulation Rate ... 57
Figure 33 F-OBM Newtonian Viscosity with Different Pressure at 55°C 58
Figure 34 Calculated Pressure in the Well Bore at 0.3 m^3/s Circulation Rate with Newtonian Model 59
Figure 35 Frictional Pressure Loss Gradient Change at 0.3 m^3/s Circulation Rate with Newtonian Model 61
Figure 36 Rheogram-1 for 30/70 F-OBM at 45°C 64
Figure 37 Rheogram-2 for 30/70 F-OBM at 45°C 65
Figure 38 30/70 w/o F-OBM Predicted and Measured Yield Stress 45°C 67
Figure 39 30/70 w/o F-OBM Predicted and Measured Consistency Index 45°C ... 68
Figure 40 Rheogram-1 for 40/60 F-OBM at 45°C 70
Figure 41 Rheogram-2 for 40/60 F-OBM at 45°C 70
Figure 42 40/60 w/o F-OBM Predicted and Measured Yield Stress 45°C 72
Figure 43 40/60 w/o F-OBM Predicted and Measured Consistency Index 45°C ... 73
Figure 44 Compressible Fluid Fraction and Pressure Effect on Yield Stress 75
Figure 45 Compressible Fluid Fraction and Pressure Effect on Consistency Index 75
Figure 46 Rheogram-1 for 40/60 F-OBM at 100°C 77
Figure 47 Rheogram-2 for 40/60 F-OBM at 100°C 77
Figure 48 40/60 w/o F-OBM Predicted and Measured Yield Stress 100°C 79
Figure 49 40/60 w/o F-OBM Predicted and Measured Consistency Index 100ºC .. 80
Figure 50 Temperature and Pressure Effect on Yield Stress 81
Figure 51 Temperature and Pressure Effect on Consistency Index 82
Figure 52 Rheogram-1 for 1044 kg/m^3 DBM at 25°C 84
Figure 53 Rheogram-2 for 1044 kg/m^3 DBM at 25°C 84
Figure 54 1044 kg/m3 ppg DBM Predicted and Measured Yield Stress 25°C 87

Figure 55 1044 kg/m3 DBM Predicted and Measured Consistency Index 25°C ... 87
Figure 56 1044 kg/m3 DBM Predicted and Measured Stress Values 88
Figure 57 Rheogram-1 for 1404.4 kg/m^3 DBM at 25°C 89
Figure 58 Rheogram-2 for 1404.4 kg/m^3 DBM at 25°C 90
Figure 59 1404.4 kg/m^3 DBM Predicted and Measured Yield Stress 25°C 92
Figure 60 1404.4 kg/m^3 DBM Predicted and Measured Consistency Index 25°C . 93
Figure 61 1404.4 kg/m^3 DBM Predicted and Measured Stress Values 94
Figure 62 Rheogram-1 for 1767.7 kg/m^3 DBM at 25°C 95
Figure 63 Rheogram-2 for 1767.7 kg/m^3 DBM at 25°C 96
Figure 64 1767.7 kg/m^3 DBM Predicted and Measured Yield Stress 25°C 98
Figure 65 1767.7 kg/m^3 DBM Predicted and Measured Consistency Index 25°C . 99
Figure 66 1767.7 kg/m^3 DBM Predicted and Measured Stress Values 100
Figure 67 Mud Weight and Pressure Effect on Yield Stress 101
Figure 68 Mud Weight and Pressure Effect on Consistency Index 102

LIST OF ABBREVIATIONS

a: Model Constant in Equation 7 and 8 (Pa s)

A: Model Constant in Equation 6 (Pa s)

A`: Model Constant in Equation 9 (Pa s)

A'': Model Constant in Equation 10 (Pa s)

A_n: Model Constant in Equation 12 (Pa s)

b: Model Constant in Equation 7 (Bar^{-1})

B: Model Constant in Equation 6 (Bar^{-1})

B`: Model Constant in Equation 9 (Kelvin)

B": Model Constant in Equation 10 (Kelvin)

C_{ca}: Correction Factor in Equation 60

D: Diameter (m)

D_{eff}: Effective Diameter (m)

D_{hyd}: Hydraulic Diameter (m)

f: Fanning Friction Factor

F: Model Parameter in Equation 37

E_a: Model Constant in Equation 12 (Kelvin)

F_{Bin}: Model Constant in Equation 9 (Kelvin Pa^{-1} Bar^{-1})

F_{Cas}: Model Constant in Equation 10 (Kelvin Pa^{-1} Bar^{-1})

g: Model Constant in Equation 13 and 14

h: Height of the Annular Flow Area in *Narrow Slot Approximation* (m)

K: Consistency Index (Pa s^m)

l: Length (m)

L: Model Constant in Equation 14 (Pa)

m: Fluid Flow Behavior Index

N: Model Constant in Equation 14 (Pa Bar^{-v})

P: Pressure (Bar)

PV: Plastic Viscosity (Pa s)

Q: Flow Rate (m^3)

r: Radius (m)

R: Model Constant in Equation 13 and 14 (Pa s^m)

Re: Reynolds Number (d'less)

Re_{YPL}: Yield Power Law Reynolds Number (d'less)

ref: Reference Measurement

S: Model Constant in Equation 13 and 14 (Pa s^m Bar^{-g})

t: Model Constant in Equation 8 (Kelvin)

T: Temperature (Kelvin or °C)

U: Model Constant in Equation 48 and 49 (Pa)

v: Model Constant in Equation 14

W: Model Constant in Equation 48 and 50 (Pa^2)

w: Width of the Annular Flow Area in *Narrow Slot Approximation* (m)

Y_{Bin}: Bingham Yield Point (Pa)

Y_{Cas}: Casson Yield Point (Pa)

YP: Yield Point (Pa)

LIST OF SYMBOLS

μ: Viscosity (Pa s)

ρ : Density (kg/m^3)

τ: Shear Stress (Pa)

τ_y: Yield Stress (Pa)

τ_w: Yield Stress at Wall (Pa)

γ: Shear Rate (s^{-1})

β: Model Constant in Equation 11 and 12 (Bar^{-1})

α: Model Constant in Equation 12

CHAPTER 1

INTRODUCTION

The aim of a drilling operation is to drill and complete a well and to produce the hydrocarbon sources in a more economical and efficient way. There are various components in the drilling system to manage the operation. Drilling fluid (called drilling mud in the field term) is one component, which is circulated from surface through the drill string, passes to the bit and continues up the annulus to the final destination-surface again. The drilling fluid or drilling mud ia a colloidal system a mixture of a base fluid and special chemicals designed to meet the operational requirements. This colloidal system should have certain properties throughout the drilling process, namely, its primary well control role over the pressure in the formation pores, counterbalancing against the in-situ formation stresses by its pressure force or carrying formation cuttings, preventing precipitation of these cuttings and chemical additives using viscous forces.

Drilling fluids are the life blood of the well and operations cannot survive without them. Rheological properties of drilling fluids are adjusted to provide some properties based on operational conditions and to affect the functionality of drilling fluid. Viscosity and yield stress play a vital role to control specific functions such as carrying the formation cuttings from down hole to the surface while circulating in the well bore, preventing the precipitation of cutting particles and chemical additives during the pump-off period and to pump easily; i.e., to decrease the apparent viscosity with increasing the shear rate (Ahmadi T. and Andy P., 2009). That means, drilling fluid should show solid-like gelled and fluid-like behavior. More viscous fluids or fluids with high yield stress are preferred to achieve this goal, but they cause high frictional pressure loss which is detrimental when the mud operating window between pore pressure and fracture gradient is shrinking especially in deep water wells and horizontal drilling (Gokdemir M.G., 2010).

Increasing energy demand and the depletion of the shallow hydrocarbon reserves have led the industry to explore deeper reservoirs. It is stated that 87 percent of industry players have some form of involvement in High Pressure High Temperature - HPHT assets and that 60 percent of this capacity will be involved in an HPHT program in the next few years (Lee J., et al, 2012). Drilling ultra-deep HPHT wells, deviated wells or offshore wells can be managed by formulating stable and accurate drilling fluid systems (Ibeh C., et al., 2008). Drilling with non-aqueous conventional drilling fluids (NAF), containing SBM and OBM, is more favorable than Water Based Mud (WMB) in challenging environments due to lubricity, high inhibitive character in shale and salt formations, corrosion control, contamination resistance and thermal rheological stability.

Despite the advantages of NAF over WBM, their flow properties vary with pressure due to compressibility. The effects of, pressure and temperature on the density and rheological behavior of slightly compressible fluids are indeed complex (Gokdemir M.G., et al., 2017).

Generally, rheological measurements are defined at the surface conditions and extrapolated to downhole conditions, that resulting in a perversity of the actual high-pressure deformation behavior. Davison et al. mentioned this drawback in their research. They focused on the rheological phenomena in hydraulic calculations or equivalent circulation density (ECD) and found that ECD calculation with pressure-temperature independent rheology and density, underestimates the measured values by about 10 percent (Davison J.M., et al, 1999).

The goal of this research is to get better understanding on the effects of pressure on NAF rheology, to obtain an accurate model in terms of the previously developed equations, and to compare it to WBM via the rheological tests. Rheological parameters are determined, and a pressure dependent mathematical model is proposed to characterize the deformation behavior under in-situ high-pressure conditions.

CHAPTER 2

LITERATURE REVIEW

2.1 Rheology

Rheology is the study of flow and deformation of any kind of matter. In rheology, the relationship between the applied forces (i.e., stress), the deformation caused by that force, called strain, and the deformation behavior are studied. Typically, for fluid rheology, the flow behavior is explained by the flow of fluid between two solid plates. As presented in Figure 1, a force F is applied parallel to the upper plate of area A, which made the plate move at velocity v to the distance Δh while the bottom plate is held stationary; the distance between the plates is h. The fluid layer attached to the plates will move at the same velocity of the plates, for example, the layer underneath the upper plate move with the same velocity of the upper plate and the bottom fluid layer has zero velocity because of the stationary. Thus, the fluid layers in between these two layers travel at different velocities; there is the velocity variation or velocity gradient (dv/dh). By considering the deformation mechanism in fluids, velocity fluctuations or velocity gradients are usually observed due to the cohesive and viscous forces between fluid layers. This velocity gradient or so-called shear rate is defined as the rate of fluid movement between the plates. The force exerted on the region of the fluid area to provide fluid movement is defined as the shear stress. In addition, the shear rate represents the rate of change of strain (ΔL/h). It can be stated that the shear stress (force divided by the area parallel to the force, F/A) has the relationship with the shear rate (dv/dh).

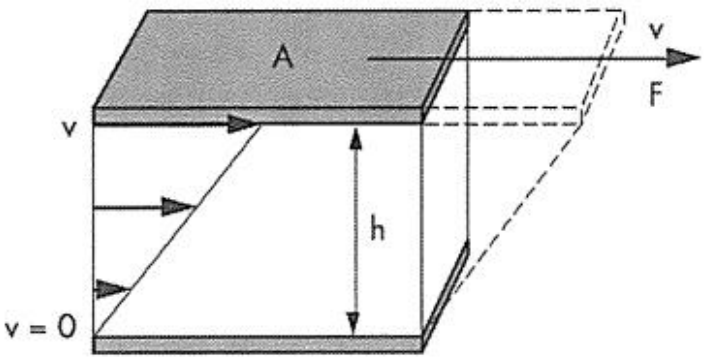


Figure-1: Diagram of Fluid Flow between Stationary and Moving Plates (Thomas M.G., 2011)

The viscous fluids can be classified by considering the relationship between shear stress (τ) and shear rate ($\dot{\gamma}$). Generally, they are divided into two groups as the followings:

- Newtonian fluids
- Non-Newtonian fluids, time independent. Time dependent fluids develop some structure with time, therefore stress – rate explanation needs time function to represent the real deformation character (Gokdemir M.G., et al., 2011)

To classify the fluids, the apparent viscosity which is defined as the ratio of shear stress to shear rate ($\eta(\dot{\gamma}) = \tau(\dot{\gamma}) / \dot{\gamma}$) is applied. Newton's law states that the applied shear stress is proportional to resulting shear rate; and, the proportionality constant known as the dynamic viscosity (μ) is independent of shear rate; the relationship is expressed as $\tau = \mu\dot{\gamma}$. The fluid behaves like this kind of deformation is called Newtonian fluid.

The Non-Newtonian fluids are generally complex mixtures such as drilling fluids, gels, slurries, etc.; their viscosity changes as a function of shear rate. The viscous flow behavior, as a function of shear stress and shear rate, is modeled by mathematical models.

Main mathematical models that can be used for the drilling industry are;
Newtonian Model, graphically explained by straight line with a slope of Newtonian Viscosity and starts from the origin (Dipankar C. et al, 2009).

$$\tau = \mu \gamma \quad (1)$$

Bingham Plastic Model *(BP)* requires as a threshold value for fluid flow, is called Yield Point (YP). After the yield point, shear stress and shear point mathematically show constant slope value of Plastic Viscosity (PV).

$$\tau = YP + PV\,\gamma \quad (2)$$

Power Law Model *(PL)*, which is pseudoplastic behavior of fluids (Dipankar C. et al, 2009). In this model, Consistency Index (K) shows the resistance of deformation or thickness of the fluid under specific deformation conditions.

$$\tau = K\,\gamma^{m} \quad (3)$$

Yield-Power Law (Herschel Bulkley) Model *(YPL)*, is mathematically combination of Bingham Plastic and Power Law rheological models. After a certain value of stress application, fluid can flow with a thickness or viscosity at a specific degree of slope.

$$\tau = \tau_y + K\,\gamma^{m} \quad (4)$$

Casson Model is mathematically similar to Yield-Power Law model with the difference of root in mechanism.

$$\sqrt{\tau} = \sqrt{\tau_y} + \sqrt{K\gamma} \quad (5)$$

2.1.1 Yield Stress Phenomena and Viscoelasticity

The general definition of yield stress in aqueous systems is a critical value, below which elastic or plastic deformation is observed. Contrarily viscous deformation occurs above this critical value.

Viscoelastic fluids exhibit both fluid-like (viscous) and solid-like (elastic) deformation behavior at the same time due to the high elastic component. Elasticity stems from the resistance of the bonds in a material to extension or bending; i.e., deformation increases bond energy. When stress, which is in the elastic region, is removed in real solid materials, the materials go back to their original shape and no bonds are broken between molecules. However, some bonds are broken upon deformation in viscoelastic materials and no permanent bonds are observed in purely viscous materials (Walstra P., 2003).

Viscoelastic phenomena occur due to the normal stress difference in fluid. This stress difference characterizes the elastic component of the fluid; i.e., viscoelastic behavior. Compared to viscoelastic fluid, normal stress difference in inelastic or Newtonian fluids is zero; Newtonian fluids do not exhibit any solid-like behavior (Coussot P., et al, 2002).

Another characteristic of viscoelastic fluids is the existence of stress relaxation with given deformation. Stress value decays exponentially to zero with constant applied strain in a finite period of time (Wilkinson W.L., 1960). Furthermore, recoil phenomena is encountered in viscoelastic fluids due to tensile forces in the system which cause the back and forth movements of particles.

Maxey defines the yield stress as a condition in which a fluid can support its own weight to a certain extent; i.e., it resists flowing to a certain value at a given shear (Maxey J, 2007). A continuous solid network can be formed in time-dependent fluids when they are not mobilized hence, it is necessary to apply a minimum shear stress to start the flow. This stress value is called yield stress, which varies with time and temperature. Above this critical value, materials exhibit a fluid-like deformation

(Rubinho H. and Galindo R., 2009). Peder et al. give the theoretical definition of yield stress as the stress value at which fluid starts or stops moving or flowing, or the viscosity alternates between finite and infinite value, the highest stress at which no flow is observed (Peder C.F.M et al., 2006). Steffe states that yield stress is the first stress in a test where the increase in strain occurs without increase in stress; i.e., a finite stress required to achieve flow (Steefe J.F., 1996). Below the yield stress, materials can store the energy in a small strain level like the one solids do. Some authors (Power P. and Zamora M., 2003) believe that yield stress is the 6 rpm stabilized reading; others use the 3 rpm reading or even lower rates. There are various values of this critical stress from this point of view. Yield stress is the minimum stress to initiate flow. This intrinsic property is affected by temperature, pressure, chemical content and flow history.

Yield stress is a shear stress threshold that defines the boundary between solid and fluid-like behavior. The fluid does not begin to flow until the yield stress threshold is exceeded.

2.1.2 Previous Pressure Dependent Rheological Models

The sensitivity of the viscosity of the continuous phase in colloidal fluid systems controls the viscosity or rheological properties of the system (Lee J., et al, 2012).

Rommetveit and Bjorkevoll found that for the specific rate of deformation conditions, shear stress increases with pressure increment and proves their statement in an experimental work (Rommetveit R. and Bjorkevoll K.S., 1997).

Conventional constitutive equations explain the rheological deformation of the system at certain temperatures and pressures. Various studies have been carried out in the literature to integrate the temperature or pressure effect to predict the viscosity and rheological parameters of the fluid system. Most of them use Arrhenius equations in the developed models (Joseph R.R., et al, 2000), where rate of a reaction has exponential dependency on activation and kinetic energy (Thomas M.G., 2011).

$$k = A\,exp\ (-Ea/RT) \quad (6)$$

Lee et al., develop an equation to predict the compressible fluid viscosity at specific pressure (Lee J. et al., 2012).

$$\mu = A\,exp\ (B.P) \quad (7)$$

Amani uses a similar approach like Lee, also establishes the temperature term in the viscosity equation (Amani M., 2012).

$$\mu = a\,exp\ (b.P) \quad (8)$$

and

$$\mu = a\,\exp\ (t/T) \quad (9)$$

Houwen and Geehan improve the yielding term of Bingham and Casson constitutive equations as (Houwen O.H. and Geehan T., 1986);

$$YP_{Bingham} = A^{\iota}\ \left(\frac{B^{\iota}}{T} + \frac{Y_{Bin}F_{Bin}P}{T}\right) \quad (10)$$

$$YP_{Casson} = A^{\iota\iota}\ \left(\frac{B^{\iota\iota}}{T} + \frac{Y_{Cas}F_{Cas}P}{T}\right) \quad (11)$$

Martin-Alfonso et al., use the reference viscosity value at the defined pressure in the proposed viscosity equation (Martin-Alfons M.J. et.al., 2007).

$$\mu = \mu_{ref}\,\exp\left(\beta\left(P - P_{ref}\right)\right) \quad (12)$$

Alderman et al., extend the Arrhenius equation in both considering the temperature and pressure effect in their viscosity calculation (Alderman N.J. et al, 1988).

$$\mu(P,T) = A_n(1 + \alpha(\varphi)\beta(P)P)\,\exp\left(\frac{E_a + P(BT - C)}{T}\right) \quad (13)$$

CHAPTER 3

STATEMENT OF THE PROBLEM

Increasing energy demand and the depletion of the shallow hydrocarbon reserves have led the oil industry to explore deeper reservoirs. Majority of these deep exploration activities have some form of involvement in High Pressure High Temperature (HPHT) assets. One of the challenges of drilling ultra-deep HPHT wells, deviated wells or offshore wells is to formulate stable and accurate drilling fluid systems. One of the primary concerns in deep offshore wells or horizontal drilling is to maintain a proper mud pressure due to the narrow window between the pore pressure and the fracture gradient curves. If the mud weight is not maintained within this window, it might result in either lost circulation or blowouts.

Non-aqueous conventional drilling fluid systems (NAF) are more than water base muds (WBM) favorable due to their lubricity effect, high inhibitive characteristics in shale and salt formations, corrosion control and temperature-rheological stability in deep formations.

Despite the advantages of NAF over WBM, their flow properties vary with pressure due to compressibility. The effects of, pressure and temperature on the density and rheological behavior of slightly compressible fluids are indeed complex. On the other hand, the equivalent pressure exerted by the drilling fluid under downhole conditions should outweigh the pressure exerted by the pore fluid, which may be extremely high. In extreme wellbore conditions, horizontal wells or ultra-deep sections, only small changes in overpressure can be tolerated because of the small margin between pore pressure and fracture gradient of the formation. Incompetent fluid formulation and hydraulic design will result in adverse and vital problems. A static and dynamic pressure profile and all parameters that affect the pressure profile, such as drilling fluid density, depth, flow rate, and downhole rheological properties, are critical.

Unfortunately, generated rheological data under extreme HPHT conditions are rare due to inadequate measurement systems and drilling fluid formulation. Generally, rheological measurements are defined at the surface conditions and extrapolated to downhole conditions, that resulting in deviation of the actual high-pressure deformation behavior.

The main purpose of this study is to experimentally investigate the pressure effect on slightly compressible drilling fluid rheology under high pressure but moderate temperature conditions and propose new rheological models to cover all constitutive stress behavior. As a consequence, a new calculation methodology will be proposed for frictional pressure loss determination of NAF systems based on determined rheological aspects under high pressure.

CHAPTER 4

EXPERIMENTAL SET-UP, TEST METHODOLOGY and TEST FLUIDS

The testing methodology was developed based on previous studies. Lee used 5 different HPHT viscometers in the experimental part; however 5 different results were obtained for the same fluid under the same experimental conditions (Lee J. et al., 2012). Although the manufacturers recommend the frictionless pivot and the measuring stone for the viscometer design, the rotation damages the pivot and leads to inaccurate readings. In addition, viscometers or some HPHT rheometers that limit the mixing of fluids are the main problem that harms the fluid system. Considering the disadvantages of viscometers, rheological experiments are conducted by using an Anton Paar MCR 302 Rheometer with an HPHT measuring cell in this research. The Rheometer has an air-bearing system in the measuring coupling part to minimize the metal-to-metal friction effect in the measurements compared to HPHT viscometers in which metal friction leads to misreading, and no confining fluid is needed to pressurize the test fluid.

4.1 Experimental Set-Up

The measurement system consists of four main parts; the rheometer test cell, the pressure gauge, the pressurized sample chamber, and the high-pressure hydraulic oil pump, as shown in Figure 2.

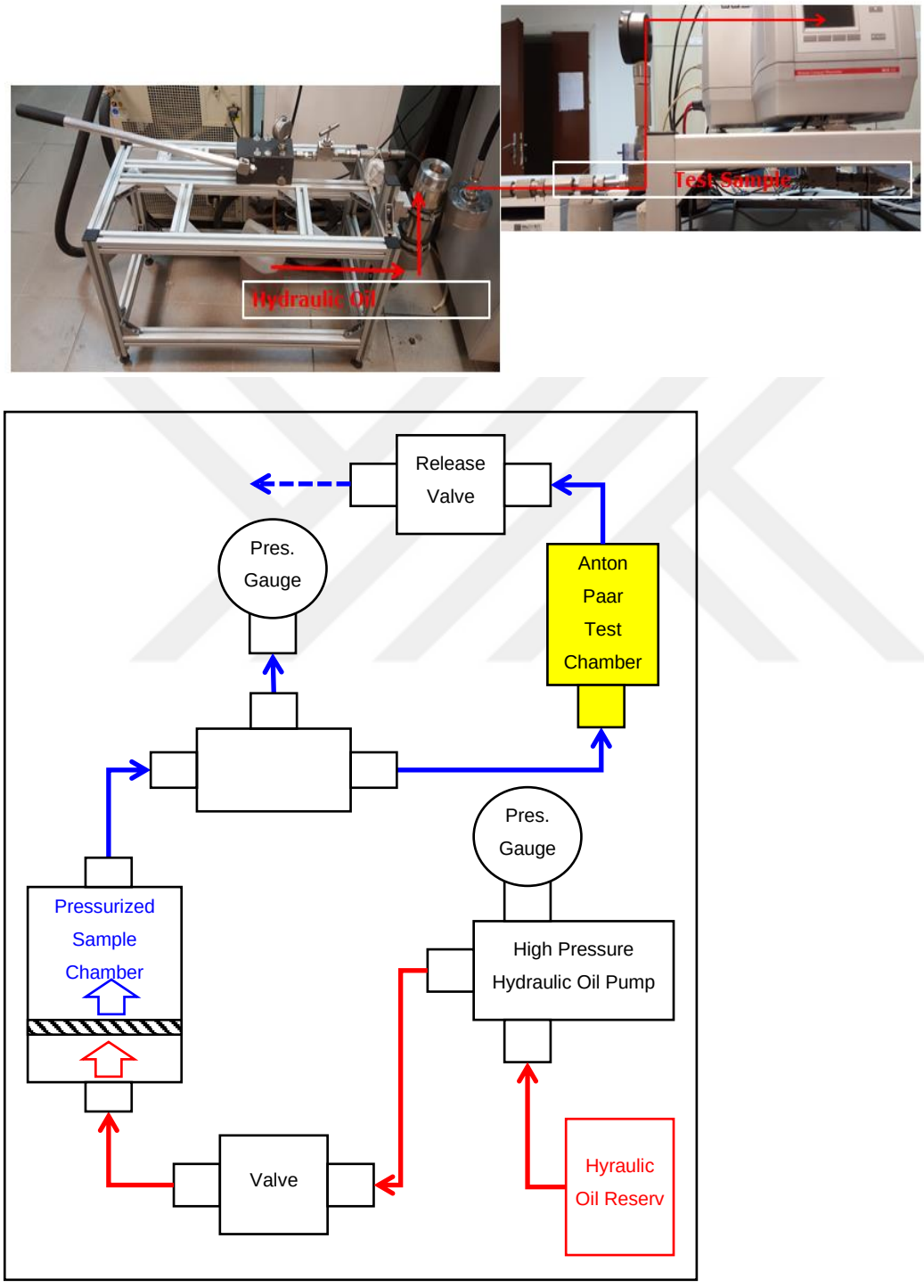


Figure-2: Picture and Schematic Drawing of Experimental Setup

The system uses the concentric cylinder systems as the test cell with electrical resistance heating, which limits the temperature up to 300°C and the pressure to 1000 bar (14500 psi). The geometry is equipped with a magnetic coupling that transmits the torque of the measuring drive to the measuring cylinder in the pressure cup, illustrated in Figure 3. The inner diameter of the pressure cup is 30 mm and the outer diameters of the gauges used in this research are 29 mm and 29.5 mm. The 29.5 mm bob is preferred for fluids that exhibits wall slippage. Since the colloidal system may not be used in the pump, a new-modified pressure unit was developed to be used in the rheological tests with different pressure values. The new pressurized sample chamber is separated by a piston. It holds the test fluids and keeps the test fluid and hydraulic oil in a separate position. The high-pressure hydraulic oil pump, which serves as the pressure source, is directly connected to the pressure cup.



Figure-3: Magnetic Coupling and High Pressure Measuring Geometry

The sample is placed in the 200 ml capacity pressure chamber. The pump, using the special hydraulic oil under the chamber, pressurizes the chamber. The sample and the hydraulic oil are removed from the packing disk. When the oil is pumped, the packing disk directs the sample through the hose, at the desired pressure value, directly into the pressure chamber of the rheometer. The applied pressure is measured on the manometer that is placed, in the hoses in front of the inlet of the measuring cell.

4.2 Test Methodology and Test Fluids

Water-Based Drilling Fluids are used as incompressible fluids to see if pressure can affect the rheological behavior of incompressible fluids. A Drill-In fluid system and a low-weight bubble coated system, Polymeric Multiphase Invasion Control Mud (PMICM), commercially called Aphron, are selected as incompressible fluid samples. Aphron system is created by an air-core and outer shell is provided by surfactants. Bubbles are protected by a both monolayer and trilayer surfactants. Aphrons are surrounded by high viscous fluid that should show thixotropic behavior. Aphron mud is used in depleted zones and drilling operations where high mud loss is encountered (Growcock F.B. et.al., 2004). On the other hand, a field oil-based mud, a diesel-based drilling fluid system (denoted F-OBM) and two different synthetic drilling fluid systems with different chemical compositions (denoted SBM-1 and SBM-2) were used as slightly compressible fluid systems for rheological tests. The main chemical compositions of the fluid systems are shown in Table 1. Diesel Based, Drill-In and Aphron chemicals are field used commercial grades, synthetic system chemicals are obtained from Baker Hughes and DFT drilling fluid providers. In this study, all the drilling fluid systems, which has hydrocarbon derivatives base fluid is generalized as Non-Aqueous Fluids (NAF).

Table-1 Chemical Composition of Test Fluids

Chemicals	Diesel Based Fluids	Synthetic Based Fluid*	Drill-In Fluid	PMICM (Aphron System)
Base Fluid	Diesel	Synthetic Oil	Water	Water
Primary Emulsifier, v%	1.5-5	1	-	-
Secondary Emulsifier, v%	0.3-1	0.3	-	-
Lime, gr/l	28.6-43	11.4	-	-
Brine	25% $CaCl_2$	25% $CaCl_2$	-	-
Viscosifier, g/l	23-34.3	34.3-48.6		14.3
Filtration Control Agent, g/l	28.6	14.3		15.7
pH Buffer Agent, g/l	-	-		6.6
Surfactant, g/l	-	-	-	3.4
Bacterial Controller, g/l	-	-		0.6
Low Shear Rate Viscosity (LSRV) Agent, v%	0-1	1-1.5	-	-
Barite, g/l	Depends on Test Formulation	100	-	-
Low Gravity Solid, g/l	0-86	43	-	-
Soda Ash, g/l	-	-	0.70	0.57
System Weight, gr/l	Depends on Test Formulation	28.6		18.6
Oil-Water Ratio, v/v	Depends on Test Formulation	80/20	-	-

*In the sample of SMB-2, only LSRV agent concentration is increased to 3.25% by volume.

Mixing protocol for OBM/SBM in the laboratory are as followed;

1) Taking the base fluid into the Silverson high shear mixer (shown in Figure 4). The mixer has 7000 to 10000 rpm value depends on the fluid rheology and density,
2) Mixing the primary emulsifier and lime then shear 1 hour,
3) $CaCl_2$ Brine is prepared in the beach mixer (shown in Figure 5), and added to the slurry. It should be noted that both laboratory and field preparation

system should be sheared at least 4 hours. Shearing with emulsion creates heating up effect on the fluid. To minimize this effect, shearing cup is covered by small hoses and water is circulated inside hoses that connected to water bath for cooling,

4) Then secondary emulsifier is mixed,
5) Fluid Loss Polymers and Rheology Modifiers are blended to the system, and sheared at least 2 hours,
6) Rheology and Electrical stability of the mud are measured,
7) Weighting Agents are mixed with the mud, and sheared 2 hours,
8) In the final stage, density, emulsion stability and rheological properties are checked. If any unintended mud properties are observed, modification with chemicals are performed.



Figure-4: Silverson high shear mixer



Figure-5: Beach mixer

Equipment in the experimental set-up and chemical sensitivity of the system, fluid preparation, test methodology and aging history can affect the rheological data generation. A consistent preparation phase and test methodology is followed in this study to obtain accurate data. The samples are prepared using a high shear mixer. After the preparation time, the sample is poured into the chamber and pumped into the test cup. Air is completely displaced from the system and the test cell is sealed. The system is sheared at a medium level, between 600 to 800 s^{-1}, when the required temperature is reached by the sample, and then the fluid is held still for about ten seconds to relax and to orient the structure. After the relaxation period, the test interval is started. The controlled shear rate method is used to obtain rheological results. The shear rate is ramped down from 1200 s^{-1} to 30, 20 or 10 s^{-1}. If ramp increase methodology in shear rate is performed, low shear period may create the time-dependent effect and hence affect the dynamic readings in lower plateau in rate of deformation situation. Moreover, 60 to 100 data points are collected from all test intervals using the rheometer software program. The duration of the data points starts at 2 seconds and increases logarithmically to ten seconds to obtain the steady stress

or torque readings. The sample is changed after 3 hours that corresponds to any applied pressure test interval to avoid any possible problem of chemical additive precipitation. At each pressure point, the test is repeated three times to obtain a data set within ± five percent, if not interval is repeated to stay in the defined limit. As mentioned, the objective of this work is to study the effect of pressure on fluid rheology. For this reason, only the applied pressures are changed from 1.01 to 830 bar (0.1 MPa to 82.7 MPa) or 14.7 to 12000 psi at constant temperature during the test periods. The physical conditions of the tested fluid systems are listed in Table 2.

Table-2 Test Conditions of Sample Fluids

Test Fluid	Temperature, °C	Pressure, MPa (Psi)
Diesel Based, Synthetic Based, Aphron System, Drill-In System	25	0.1 (14.7); 0.7 (100); 1.7 (250); 3.5 (500); 6.9 (1000); 13.8 (2000); 20.7 (3000); 27.6 (4000); 34.5 (5000); 41.4 (6000); 48.3 (7000); 55.2 (8000); 62.1 (9000); 69 (10000); 75.8 (11000); 82.7 (12000)

CHAPTER 5

EXPERIMENTAL RESULTS and DISCUSSIONS

In low shear rate applications, viscoelastic deformation, the sol-gel or solid-liquid transition is observed. It depends on the deformation rate and history for both solid like and fluid like deformation, shown most of the colloidal non-Newtonian fluids. Therefore, measurement points below the critical shear rate values are excluded from the analysis in order to obtain the equilibrium values of viscous deformation for the graphical representation of the rheograms of the different systems. This approach has been illustrated in Figure 6 for Drill-In Fluid system. The plot is limited to 400 s^{-1} shear rate application to highlight the effect at low shear rate values. The critical shear rate for the limit of viscous flow condition is around 30 s^{-1} shear rate where reading anomaly ends or stress trend changed, for this test interval. In this study all the rheological parameters are found by "non-linear estimation method". Statistica (https://www.statistica.com/en/) is used to analyze and find the rheological parameters of the samples. In the analyses, regression is specified, Quasi-Newton estimation methodology is applied with the convergence criteria of 0.00001.

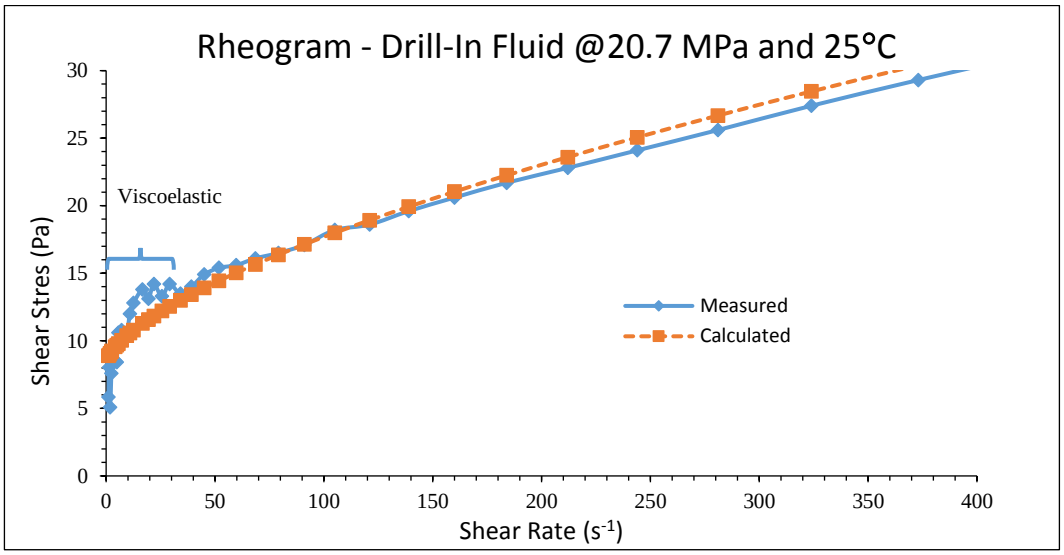


Figure-6: Data Analysis Example

Incompressible fluid samples used in this research, namely Drill-In and PMICM systems, show stress threshold before flow initiation, i.e., yield stress. This flow character is required for drilling fluids to reduce the precipitation rate of cutting materials and chemical additives. In addition, a shear-thinning deformation response is observed for both samples, which is also required for drilling fluids with lower energy requirements at high deformation rates. The Yield Power Law rheological model describes the mathematical stress equations for both the Drill-In and PMIC systems. The rheograms of the incompressible systems are shown in Figures 7 and 8, respectively.

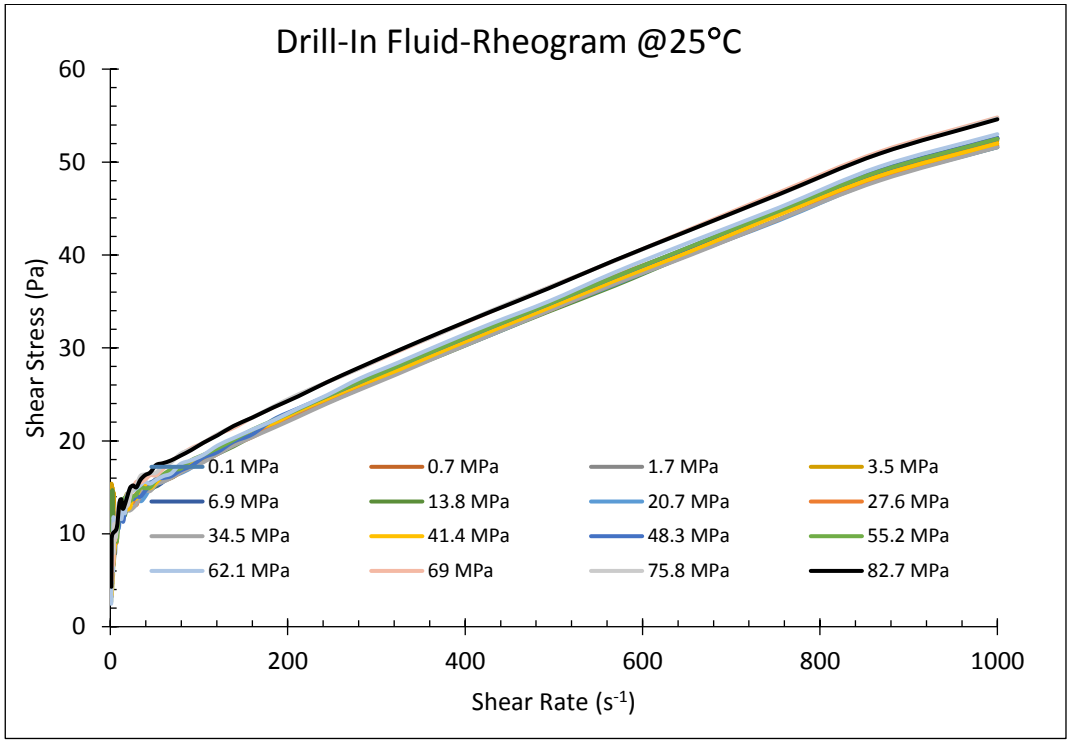


Figure-7: Rheogram for Drill-In Fluids

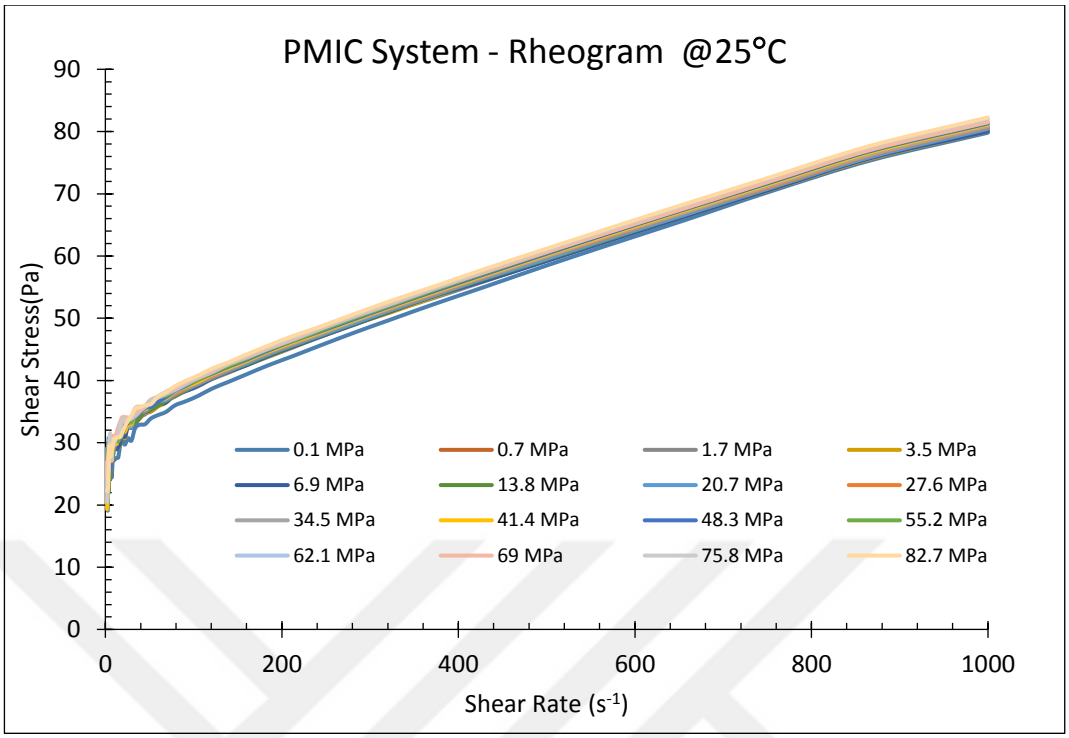


Figure-8: Rheogram for PMIC Fluids

Pressure has a negligible effect on the deformation behavior and rheological parameters of the Drill-In and PMICM systems at constant temperature conditions. This statement is expected for Drill-In Fluid system. However, the PMICM system contains entrapped air bubbles that are dispersed in the water medium and enables to the system having a lower mud weight (Growcock F.B. et al., 2004). Therefore, system is expected to have pressure effect on rheological behaviour. Though air is compressible and hence affected by pressure, the surfactant coating creates durable multiphase structures that resist the effects of pressure also stated in the product bulletin.

Field used OBM (F-OBM), base fluid of diesel, is tested at 25°C temperature under atmospheric conditions up to a high pressure of 82.7 MPa as a slightly compressible fluid mud sample. The system density is 1260 kg/m^3. According to the statistical analysis of the measured rheological data the non-linear regression - R^2 is more than 99.9% for F-OBM. The mathematical equation Power Law describes the rheological behavior of F-OBM best among the other mathematical equations. The system does

not exhibit elastic deformation character, but shear-thinning behavior is observed. The pressure affects the deformation behavior of the fluid. For a test application of 13.8 MPa; the read shear rate of 1200 s^{-1} increases by almost 25% compared with the measurement at 27.6 MPa. A similar trend can be observed in the lower shear rate data under the same pressure conditions, i.e., 21% increase at 105 s^{-1} or 20% increase at 50 s^{-1} when the pressure changes from 13.8 MPa to 27.6 MPa. The effect of pressure on the shear stress or apparent viscosity measurement is remarkable when comparing results between atmospheric and 82.7 MPa high pressure conditions. The values increase around 1.75 times compared to the lower ones. The Rheogram of the F-OBM is given in Figure 9.

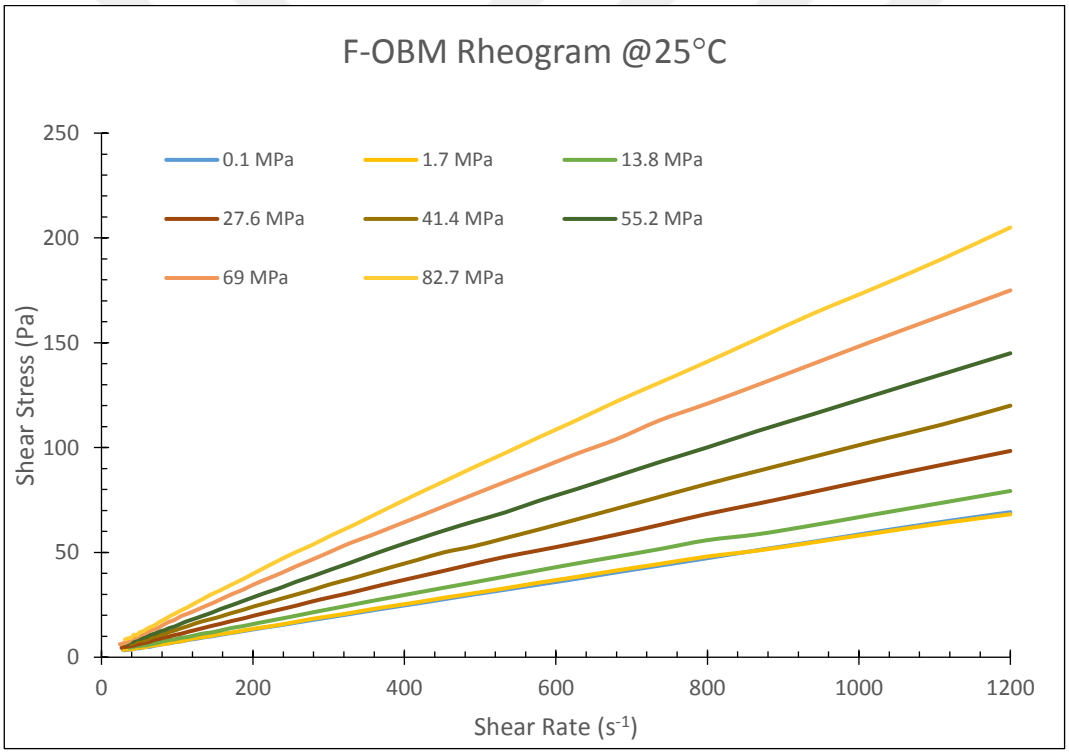


Figure-9: Rheogram for Field OBM

Fluid Flow Behavior index, known as m-value, is not affected by the change of pressure and ranges from 0.89 to 0.92 in all test intervals. This was also observed by Houwen, stated that the flow index is a fluid-shear dependent property and cannot be changed by pressure (Houwen O.H. and Geehan T., 1986). On the other hand, the

consistency index, denoted by K, can increase steadily with increasing pressure. It already doubles when the applied pressure is changed from 0.1 MPa to 41.4 MPa and at 75.8 MPa the - K value is three times higher than the atmospheric one. The rheological parameters of F-OBM are shown in Table 3 with respect to the applied pressure conditions.

Table-3 Rheological Parameters of Field OBM at Different Pressure and 25°C

Pressure (MPa)	K (Pa sec^m)	m
0.1	0.1022	0.9184
1.7	0.1092	0.9073
3.5	0.1200	0.8948
6.9	0.1346	0.8849
13.8	0.1473	0.8865
20.7	0.1654	0.8845
27.6	0.1809	0.8877
34.5	0.1842	0.8994
41.4	0.2145	0.8909
48.3	0.2341	0.8926
55.2	0.2423	0.9016
62.1	0.2627	0.9016
69	0.2869	0.9043
75.8	0.3112	0.9075
82.7	0.3257	0.9207

The Synthetic Base Fluid System-1 (SBM-1) is tested at constant temperature of 25°C under various pressure conditions, likewise the F-OBM. The fluid density is 1200.5 kg/m^3 and the chemical formulation is given in Table-1. Stress responses

when shear stresses applied increase with increasing pressure. As an example for atmospheric conditions, shear stress readings increase 63% at 1200 s^{-1} and 55% at 30.1 s^{-1} shear rates compared to test results at 34.5 MPa. A similar trend is observed for at higher pressure applications. The Rheogram of the SBM-1 is presented in Figure 10.

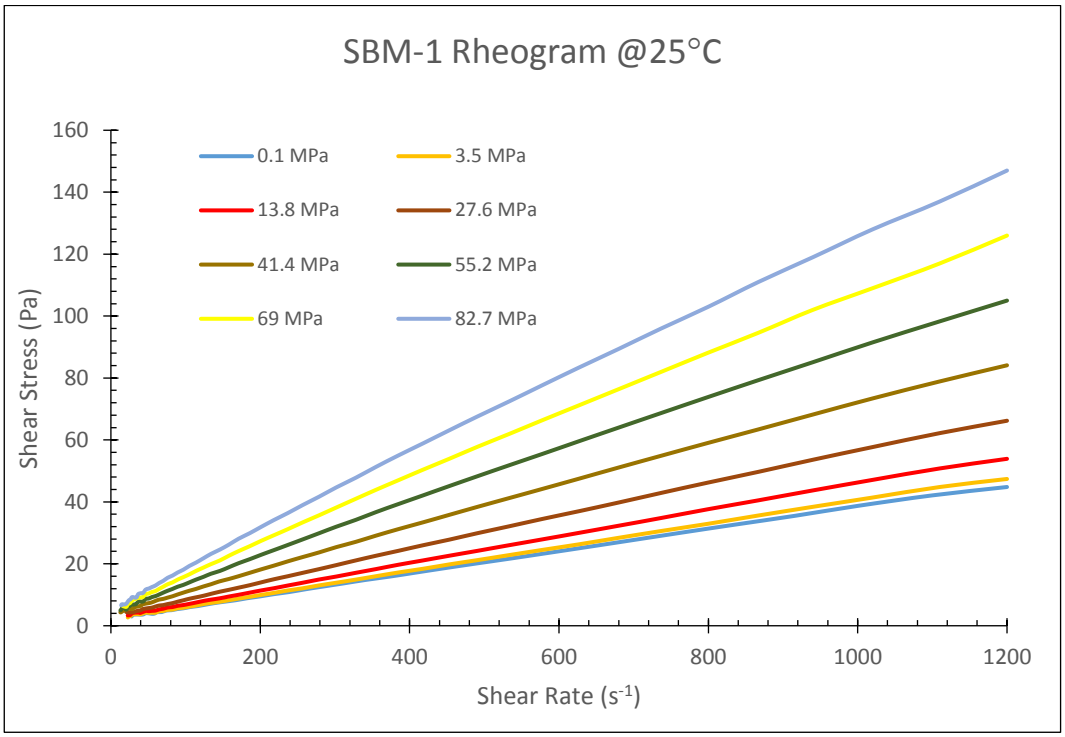


Figure-10: Rheogram for Field SBM-1

According to non-linear regression analysis, SBM-1 follows the Yield Power Law equation with a threshold value that initiates permanent deformation and shear behavior. Table 4 shows the rheological parameters of SBM-1. Fluid flow behavior, or shear thinning index, hardly changes with pressure and ranges from 0.91 to 0.96 for all the pressure conditions, which is also consistent with F-OBM and previous data in the literature. The yield stress and the consistency index change and increase with pressure application, which explains the clear pressure shift in the rheogram. Both the τ_y and K increase by 10% and 9%, respectively, when the pressure is doubled from 6.9 MPa, and τ_y doubles when the pressure is changed from atmospheric one to 82.7 MPA. The K value at an 82.7 MPa is more than four times

higher than the atmospheric reading. This example of extreme pressure explains that, at least two times more energy is required to initiate the fluid flow at an 82.7 MPa pressure across the SBM-1 system, which can lead to formation rupture and more severe operational problems like; lost circulation, stability issues or well control incidents.

Table-4 Rheological Parameters of SBM-1 at Different Pressure and 25°C

Pressure (MPa)	τ_y (Pa)	K (Pa sec^m)	m
0.1	1.9389	0.0442	0.9500
3.5	2.0154	0.04448	0.9500
6.9	2.0739	0.0488	0.9500
13.8	2.2723	0.0530	0.9500
20.7	2.3756	0.0629	0.9500
27.6	2.5798	0.0705	0.9500
34.5	2.8804	0.0871	0.9500
41.4	3.1596	0.1023	0.9500
48.3	3.2664	0.1205	0.9500
55.2	3.3779	0.1465	0.9500
62.1	3.6544	0.1843	0.9500
69	3.7479	0.2154	0.9500
75.8	3.9291	0.2216	0.9500

The chemical composition of SBM-2 system is different from that of SBM-1 system due to the low-shear rate viscosity agent to analyze the proposed model responses under elevated yielding conditions. In addition, SMB-2 are tested at a temperature of 50°C and 75 °C with the same pressure conditions to verify the functionality of the model at different temperature conditions. The Yield Power Law model explains

the deformation of SBM-2 in both temperatures. Pressure effect, on the SBM-2 fluid rheology is similar to the previously analyzed slightly compressible fluids' rheology. Rheograms of SBM-2 at 50°C and 75°C are illustrated in Figures 11 and 12, respectively. At 50°C stress recordings with the application of 302 s^{-1} shear rate is 11.8 Pascal at atmospheric condition, 39% increase is observed when the pressure reaches 34.5 MPa, even more than doubled in the 82.7 MPa test interval. The m index does not change with pressure and found between 0.95-0.98. However, both τ_y and K parameters increased with increased pressure. Similar pressure effect is found at 75°C test intervals. All the stress responses and pressure dependent rheological parameters are increased with the pressure. τ_y values are normally decreased with temperature, yet increased at 75°C compared to the 50°C test conditions; this could be due to the temperature stability of the chemicals or due to the sagging. Model parameters are presented in Table 5.

Table-5 Rheological Parameters of SBM-2 at Different Pressure, 50°C and 75°C

Temperature (°C)	Pressure (psi)	τ_y (Pa)	K (Pa sec^m)	m
50	0.1	4.0358	0.0257	0.9700
	1.7	4.0476	0.0246	0.9700
	6.9	4.0256	0.0279	0.9700
	13.8	4.0703	0.0346	0.9700
	20.7	4.1698	0.0427	0.9700
	27.6	4.2083	0.0477	0.9700
	34.5	4.2578	0.0513	0.9700
	41.4	4.3290	0.0460	0.9700
	48.3	4.3661	0.0524	0.9700
	55.2	4.3945	0.0574	0.9700
	69	4.4322	0.0696	0.9700
	75.8	4.4482	0.0794	0.9700
	82.7	4.4603	0.0847	0.9700
75	0.1	6.0673	0.0144	0.9300
	1.7	6.1858	0.0156	0.9300
	3.5	6.1951	0.0161	0.9300
	6.9	6.3528	0.0174	0.9300
	13.8	6.4138	0.0242	0.9300
	20.7	6.4672	0.0276	0.9300
	27.6	6.6197	0.0270	0.9300
	34.5	6.7418	0.0295	0.9300
	41.4	6.8141	0.0404	0.9300
	48.3	6.8169	0.0414	0.9300
	55.2	6.8797	0.0463	0.9300
	62.1	6.9060	0.0518	0.9300
	69	7.0430	0.0597	0.9300

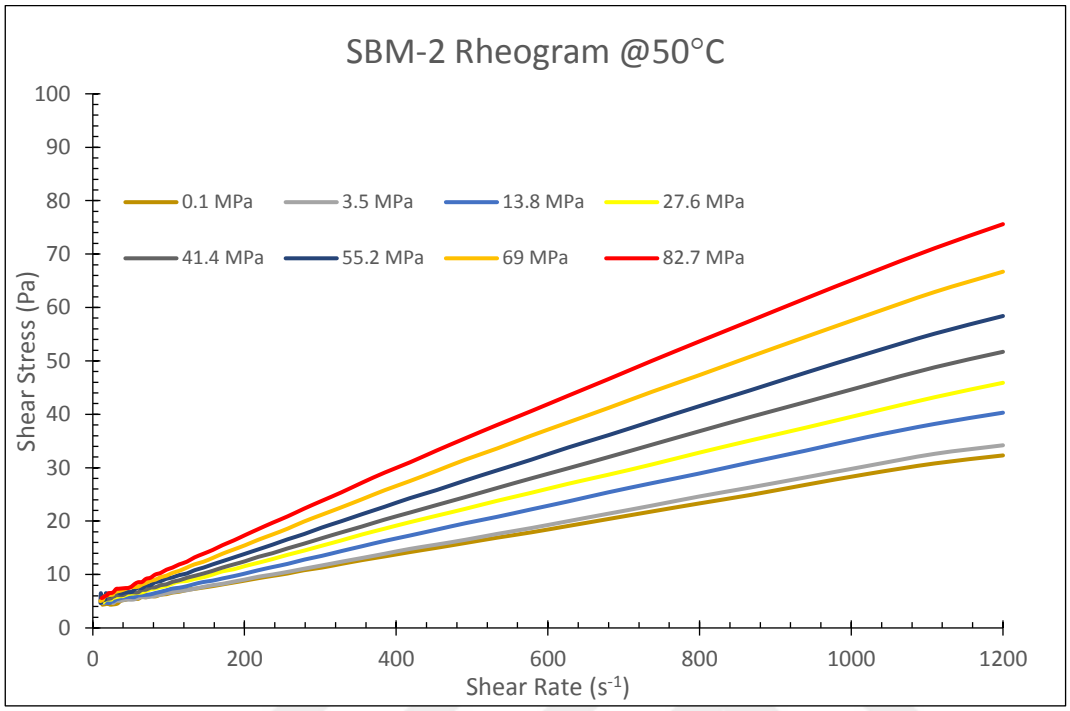


Figure-11: Rheogram for SBM-2 at 50°C

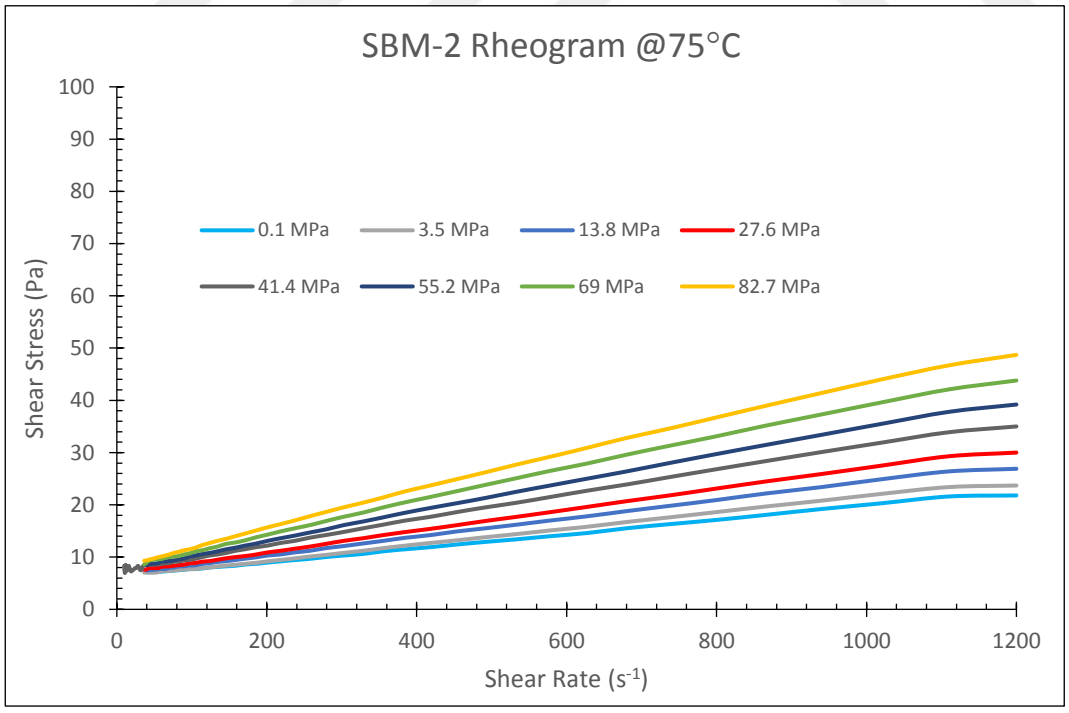


Figure-12: Rheogram for SBM-2 at 75°C

CHAPTER 6

PROPOSED MATHEMATICAL PRESSURE-DEPENDENT EQUATIONS and EVALUATION

6.1 Constitutive – Stress Equations

The conventional steady-state stress equations define the mathematical deformation behavior of fluids at a specific constant pressure and temperature. In literature, very few constitutive equations exist to model the stress-strain rate deformation by considering pressure or temperature. In literature, previous temperature and pressure dependent equations can only consider the viscosity term, and hence does not represent the constitutive stress equation except the Houwen's equation, equations 10 and 11 (Houwen O.H. and Geehan T., 1986).

A pressure dependent constitutive stress equation is proposed in this thesis. The mathematical model is developed from the Power-Law and Yield Power-Law equations. Temperature effect is not considered in the proposed equations and estimated constant, because the response of chemical additives are strongly affected at some critical high temperature value, typically after 275°F for polymers and 350° F for surfactants. Thermal stability of the chemicals alter the deformation behavior of the system and led to incompatibility of the trend and equations, also it is stated that pressure effect on fluid rheology or viscosity is prevail rather than temperature when the temperature is below 177°C (Ibeh C. et al., 2008). Similar activity is observed in Valentin's, case study; and they concluded that pressure change is more dominant compared to temperature alteration in specific temperature limits. (Valentin V. and Mario B., 2013). Also Rommetveit and Bjorkevoll gives the

domination effect of pressure rather than temperature below 150 - 160°C on OBM's rheology according to laboratory results (Rommetveit R. and Bjorkevoll K.S., 1997).

In the Power-Law model, pressure effect is placed in to the Consistency Index (K) term and the proposed equation is;

$$\tau = (R + S \times P^{g})\,\gamma^{m} \quad (14)$$

The first term in the right side (in the bracket) of the equation represents the pressure effect on *K*. All *R*, *S* and *g* are fluid and temperature-dependent model constants and found to be in non-linear regression methodology. The unit of the pressure is Pa or Bar.

In the Yield-Power Law model, pressure effect is arranged in both the yield stress and the consistency index; the developed equations is;

$$\tau = (L + N \times P^{v}) + (R + S \times P^{g})\,\gamma^{m} \quad (15)$$

The first bracket and second bracket terms in the right side of the equation represents the pressure effect on the τ_y and *K*, respectively. Like the Power-Law equation; *L*, *N* and *v* are model constants and changed with fluid type and temperature. The unit of the pressure is again Pa or Bar.

Proposed pressure dependent stress Equation-14 is applied on the F-OBM system, which does not show any creeping or elastic deformation, i.e. does not have any yield stress. Consistency index increased with pressure increment and the model points the *K* value almost at a measured readings with an R^2 of 0.9936, only the model over-predicts the *K* value at an atmospheric condition with a difference of 7.5%. The *K* value determination and stress prediction examples are illustrated in Figures 13 and 14.

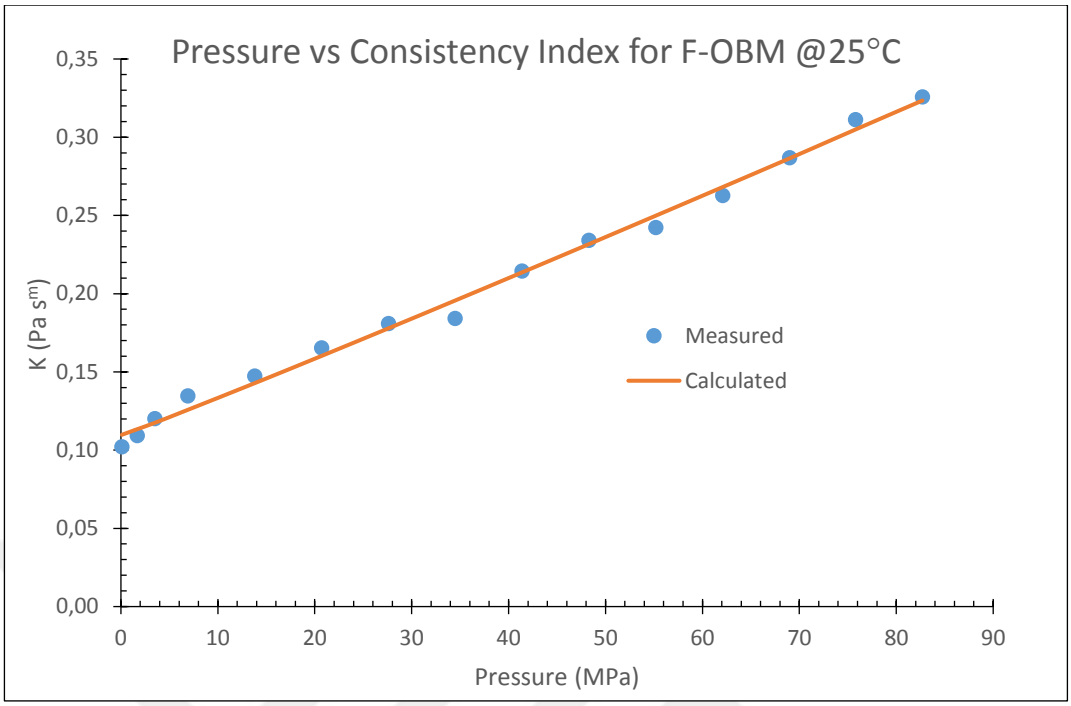


Figure-13: Consistency Index for Field OBM at 25°C

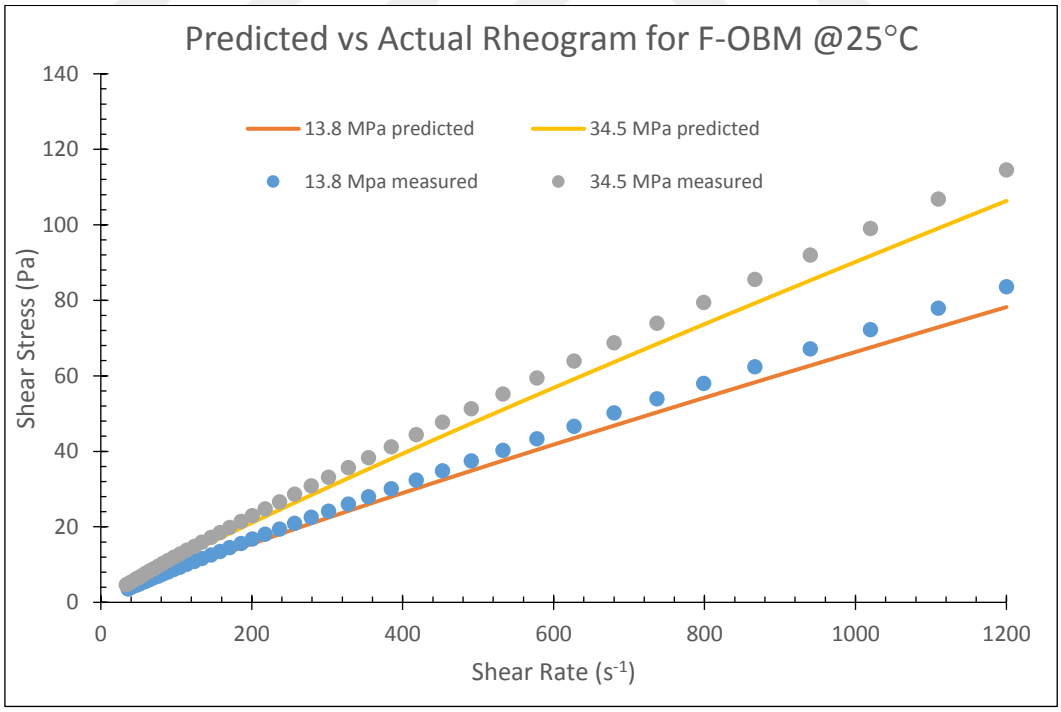


Figure-14: Model Rheogram Example for Field OBM at 25°C

Equation-15 validation is checked by using the synthetic base fluid samples, showing stress threshold to initiate the flow and shear thinning behavior simultaneously. Each test fluids are examined separately at the constant temperature conditions and model parameters are found by non-linear estimation methodology. Temperature change for SBM-2 is applied just to see the model functionality for the same fluid at different temperature environments. Model predicts both τ_y and K values in some levels. Measured variables and predicted ones' linear fit level in the regression model, so called R^2, for SBM samples are; for τ_y at 25°C 0.9888, at 50°C 0.9648, at 75°C 0.9545. Similarly, R^2 values for K parameter are 0.9952, 0.9566 and 0.9871 respectively. Figure 15 and 16 illustrate the measured and predicted τ_y and K values. Stress prediction examples about the SBM samples are shown in Figures 17 through 19.

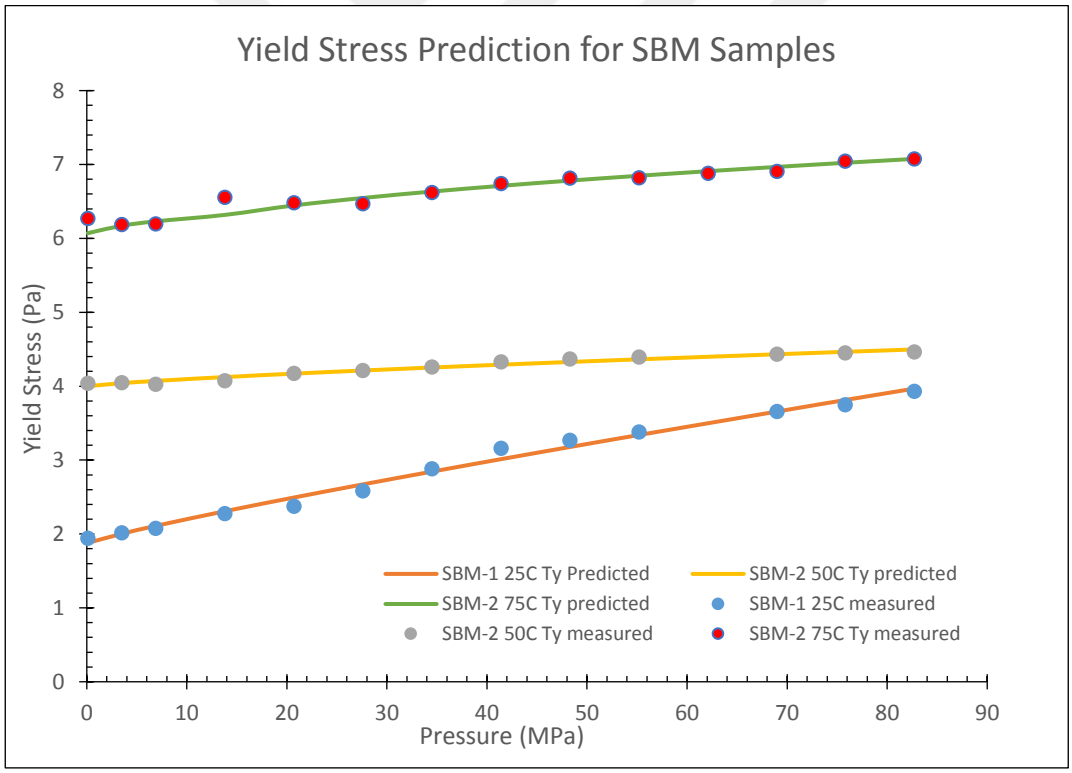


Figure-15: Predicted and Measured τ_y for SBM Systems

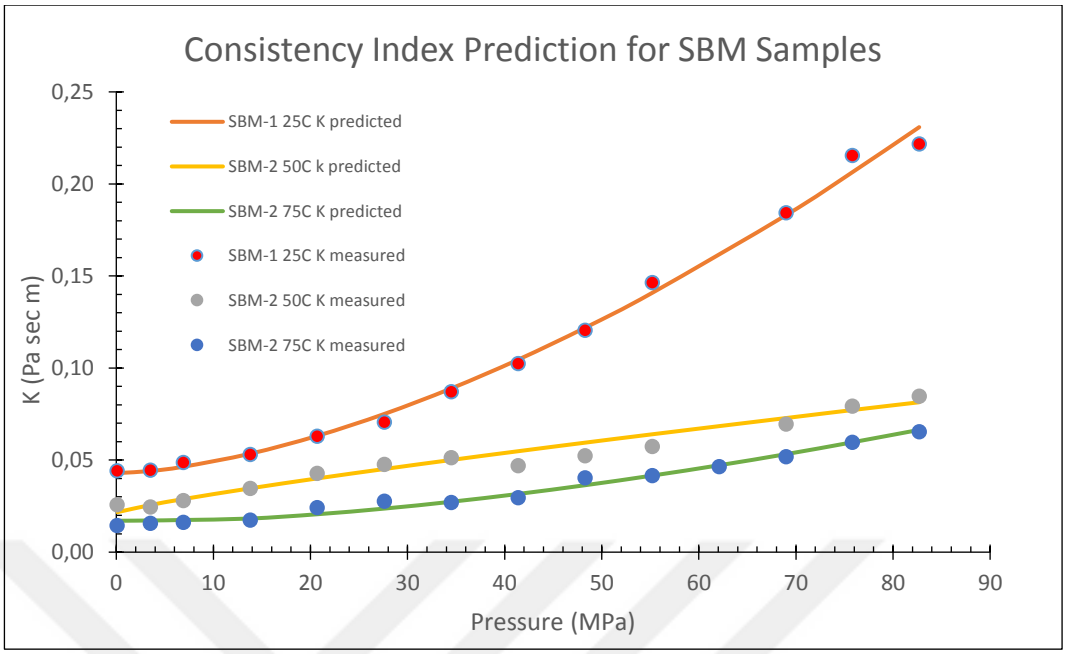


Figure-16: Predicted and Measured *K* for SBM Systems

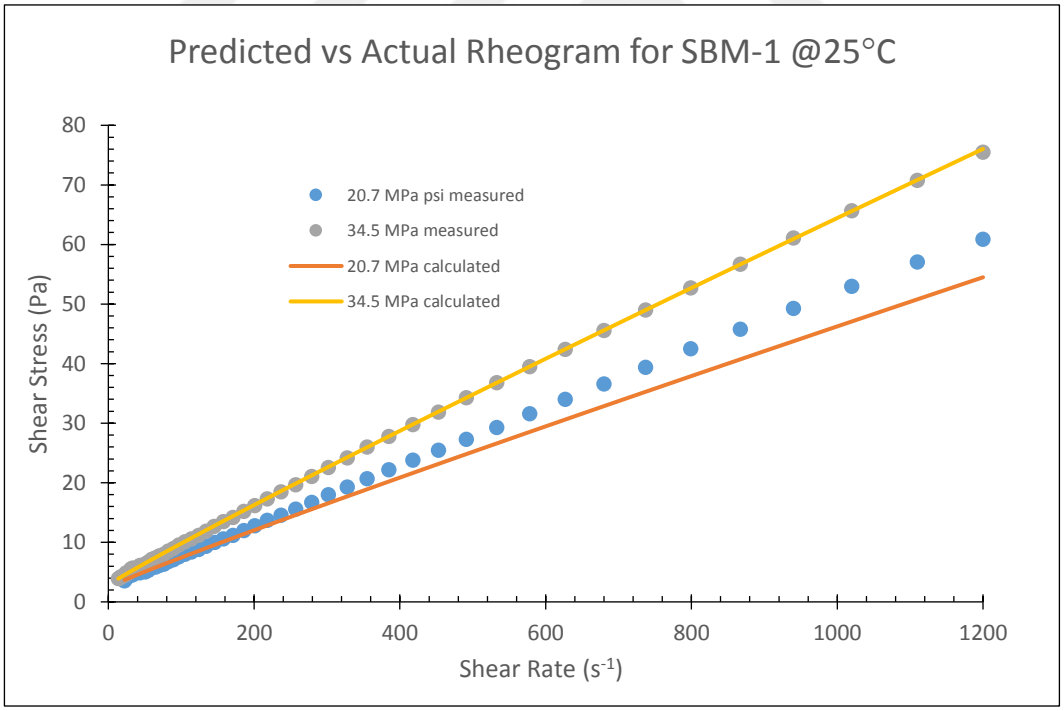


Figure-17: Model Rheogram Example for SBM-1 at 25°C

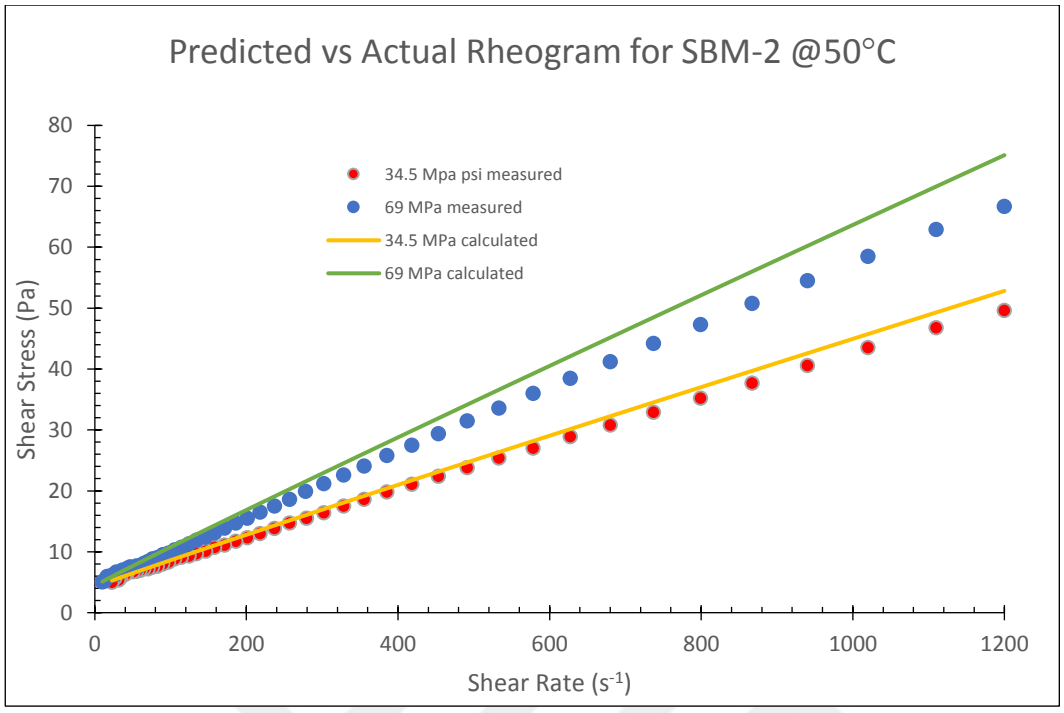


Figure-18: Model Rheogram Example for SBM-2 at 50°C

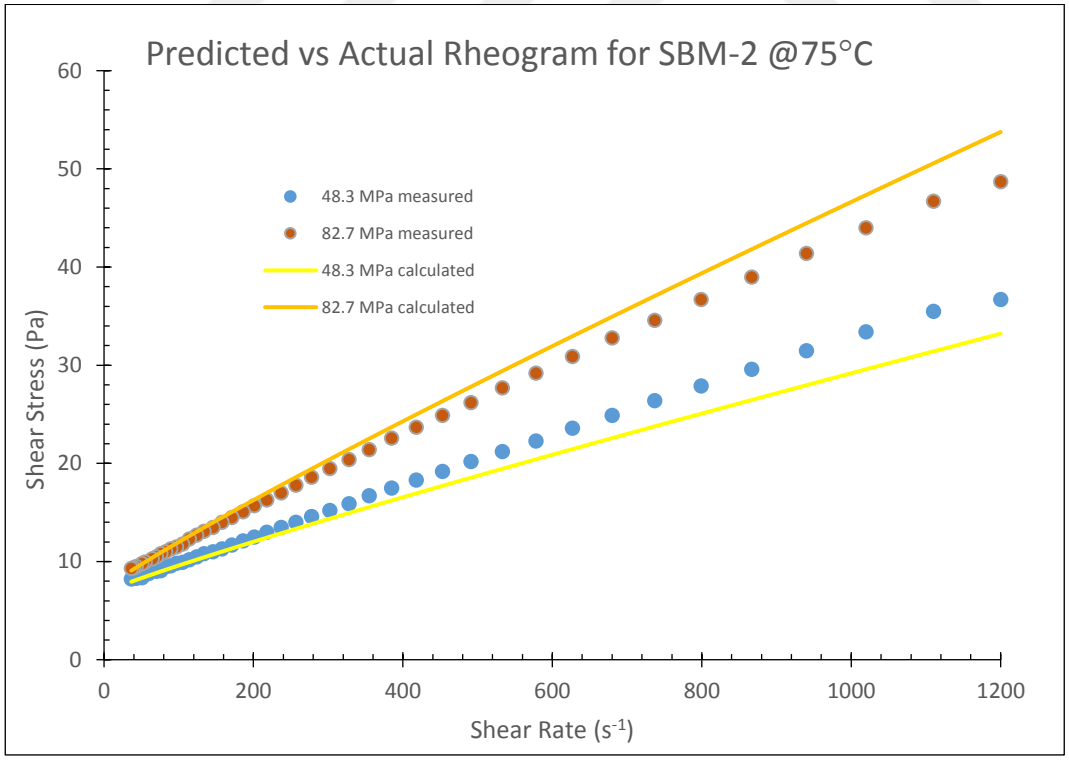


Figure-19: Model Rheogram Example for SBM-2 at 75°C

6.2 Frictional Pressure Loss Equations

Friction may be observed as the resistance required for moving a body through the external surface. Nevertheless, the friction loss is related to the flow of liquid through some conduit. Thus, it is a kind of energy loss due to the drag, viscous and cohesive forces inside the flow area. It is therefore related to the velocity, mass and rheology of the fluid, (Bourgoyne Jr. A.T. et al., 1991).

According to conservation of mass and conservation of energy equations, Newtonian annular laminar flow equation for constant density is defined as;

$$\frac{dP}{dl} = \frac{1}{r}\,\frac{d(\tau r)}{dr} \quad (16)$$

In this research, pipe and annular flow hydraulic equations are redefined for Power-Law and Yield Power Law deformation behaviors. In this manner, fluid density is assumed constant in the small-defined grids or the represented conduit hence conservation of energy and mass equations are applied, (Aadnoy B.S. et al., 2009).

6.2.1 Power-Law Pipe Flow

EXLOG staff developed laminar flow equation of Power Law fluid's in pipes, so called Ex-log solution. They use effective diameter concept (D_{eff}) to simulate non-Newtonian effect (Whittaker A. and Exlog Staff, 1985). Power-Law Laminar Pipe flow is restated according to Equation-14 as;

$$\frac{dP}{dl} = \left(\frac{4K}{D_{eff}}\right)\left(\frac{8\,v\,G}{D_{eff}}\right)^{n} \quad (17)$$

Where G and D_{eff} is given in the following equations;

$$G = \frac{3m+1}{4m} \quad (18)$$

$$D_{eff} = \frac{D}{G} \quad (19)$$

$$\tau w_{avr} = (R + S\ x\ P^{g})\ (\frac{8v}{D})^{m}\ (\frac{3m+1}{4m})^{m} \quad (20)$$

Hence, the Reynolds Number for Power-Law Pipe flow is derived as;

$$Re_{PL} = \frac{{D_{eff}}^{m}\ v^{(2-m)}\ \rho(P)}{8^{(m-1)}\ (R+S\ x\ P^{g})} \quad (21)$$

If the calculated Reynolds number is below 2100, the flow regime is assumed laminar and the frictional pressure loss is calculated;

$$\frac{dP}{dl} = \frac{2\ f\ \rho(P)\ v^{2}}{D} \quad (22)$$

Where the friction factor "f" is;

$$f = \frac{16}{Re_{PL}} \quad (23)$$

If the calculated Reynolds number is above 2100, the flow regime is assumed turbulent, and the fanning frictional factor is calculated according to Dodge-Metzner approximation as (Bourgoyne Jr, A.T. et al, 1991);

$$\frac{1}{\sqrt{f}} = \frac{4}{m^{0.75}} \log(Re_{PL}\ f^{1-\frac{m}{2}}) - \frac{0.4}{m^{1.2}} \quad (24)$$

After obtaining the *friction factor*, frictional pressure loss equation is;

$$\frac{dP}{dl} = \frac{2\ f\ \rho(P)\ v^{2}}{D} \quad (25)$$

6.2.2 Power-Law Annular Flow

In the annular conduit, Ex-Log solution is used Power-Law geometry similar to Power-Law Laminar Pipe flow. In this concept, both hydraulic diameter (D_{hyd}) and effective diameter (D_{eff}) are used (Whittaker A. and Exlog Staff, 1985). Annular flow calculations are performed according to Equation-14 followed by;

$$\frac{dP}{dl} = \left(\frac{4K}{D_{hyd}}\right)\left(\frac{8\,v\,G}{D_{hyd}}\right)^{n} \quad (26)$$

Where;

$$D_{hyd} = D_o - D_i \quad (27)$$

$$G = \frac{\left(1+\frac{z}{2}\right)\{(3-z)m+1\}}{m\,(4-z)} \quad (28)$$

$$D_{eff} = \frac{D_{hyd}}{G} \quad (29)$$

In addition, z parameter in Equation 28 is found by "Y" parameter;

$$Y = 0.37\,m^{-0.14} \quad (30)$$

$$z = 1 - \left(1 - \left(\frac{D_i}{D_o}\right)^{Y}\right)^{1/Y} \quad (31)$$

$$\tau w_{avr} = (R + S\,x\,P^{g})\left(\frac{8v}{Deff}\right)^{m} \quad (32)$$

$$Re_{PL} = \frac{D_{eff}{}^{m}\,v^{(2-m)}\,\rho(P)}{8^{(m-1)}\,(R+S\,x\,P^{g})} \quad (33)$$

If the calculated Reynolds number is below 2100, the flow regime is presumed laminar and the frictional pressure loss is calculated;

$$\frac{dP}{dl} = \frac{2\,f\,\rho(P)v^{2}}{Dhyd} \quad (34)$$

Where the friction factor "f" is;

$$f = \frac{16}{Re_{PL}} \quad (35)$$

If the calculated Reynolds number is above 2100, the flow regime is accepted as turbulent, and the fanning frictional factor is calculated according to Dodge-Metzner approximation as (Bourgoyne Jr. A.T. et al, 1991).

$$\frac{1}{\sqrt{f}} = \frac{4}{m^{0.75}} \log(Re_{PL}\, f^{(1-\frac{m}{2})}) - \frac{0{,}4}{m^{1.2}} \quad (36)$$

After obtaining the *friction factor*, frictional pressure loss equation is;

$$\frac{dP}{dl} = \frac{2\, f\, \rho(P)\, v^2}{Dhyd} \quad (37)$$

6.2.3 Yield Power Law Pipe Flow

Hydraulic or frictional pressure drop equation for YPL Laminar Pipe flow is reestablished according to proposed Equation 15 from the algorithm presented by Reed and Pilehvari (Reed T.D. and Pilehvari A.A., 1993). In this algorithm flow rate, trajectory and pipe diameters, and rheological properties should be known.

$$v = \frac{4\, Q}{\pi D^2} \quad (38)$$

In the first trial, assuming the flow behavior index is "m" is equal to F parameter.

$$D_{eff1} = \frac{4F}{3F+1} \quad (39)$$

$$\gamma_{w1} = \frac{8v}{D_{eff1}} \quad (40)$$

Then the shear stress at the wall is re-defined as;

$$\tau_{w1} = (L + N\ x\ P^v) + (R + S\ x\ P^g)(\gamma_{w1})^m \quad (41)$$

Hence the effective viscosity is;

$$\mu_{eff} = \frac{\tau_{w1}}{\gamma_{w1}} \quad (42)$$

$$Re_1 = \frac{D_{eff1}\, v\, \rho(P)}{\mu_{eff}} \quad (43)$$

If the calculated Reynolds number is below 2100, the flow regime is laminar and the frictional factor is;

$$f_1 = \frac{16}{Re_1} \quad (44)$$

If the calculated Reynolds number is above 2100, the flow regime is accepted as turbulent and the frictional factor is;

$$\frac{1}{\sqrt{f1}} = \frac{4}{F^{0.75}} \log(Re_1 \, f^{1-F/2}) \frac{0,4}{F^{1,2}} \quad (45)$$

$$\tau_{w2} = \frac{f_1 v^2 \, \rho(P)}{2} \quad (46)$$

After calculating the τ_{w2} , the convergence of τ_{w1} is checked.

$$\left|\frac{\tau_{w2} - \tau_{w1}}{\tau_{w2}}\right| x \, 100 < convergence \; criteria \; (1) \quad (47)$$

If the convergence factor is within the accepted criteria;

Frictional pressure loss for laminar flow is;

$$\frac{dP}{dl} = 4 \frac{\tau_{w2}}{D} \quad (48)$$

Frictional pressure loss for turbulent flow is;

$$\frac{dP}{dl} = \frac{2 \, f \, \rho(P) \, v^2}{D} \quad (49)$$

If the convergence is not approached, new "F" factor should be re-calculated and start from Equations 39 until 47 when the convergence is attained.

$$\frac{1}{F} = -3 + \tau_{w2} \left(\left(\frac{1+m}{m \, U} \right) + 2(U) \big(W(3m+1) \big) + 2 \frac{(L + N \, x \, P^v}{W \, (2m+1)} \right) \quad (50)$$

Where;

$$U = \left(\tau_{w2} - (L + N \, x \, P^v) \right) \quad (51)$$

and

$$W = \frac{U^2}{3m+1} + 2\,\frac{(L+N\,x\,P^{v})U}{2m+1} + \frac{(L+N\,x\,P^{v})^2}{m+1} \quad (52)$$

6.2.4 Yield Power Law Annular Flow

There is no exact solution for Yield Power Laws Fluids to calculate the frictional pressure loss in the annulus. Rectangular slot approximation is frequently used in practical engineering operations. This approximation assumes the annular geometry as a rectangular slot with a height (*h*) and a width (*w*). Total flowing area in the annular geometry is represented by the multiplication of *h* and *w*. The formulation of h and w is:

$$h = \frac{D_o - D_i}{2} \quad \text{And} \quad w = \frac{\pi}{2}(D_o - D_i) \quad (53)$$

Where D_o and D_i are outer and inner diameters of annular conduit respectively.

A calculation methodology for frictional pressure losses of YPL fluids is presented in reference (Aadnoy B.S. et al., 2009), assuming; inner pipe or geometry is concentrically located in the annular section. As our model systems' are slightly compressible fluid and assumed incompressible in density manner and flow is isothermal. According to Newton's Law of Motion, the relation between pressure drop gradient and the shear stress is;

$$\tau = y\left(-\frac{dP}{dl}\right) \quad (54)$$

Where *y* is the vertical distance between the center and any point from center of the slot. *y* value is equal to the half of the *h* value at the wall of the slot. Therefore, the pressure gradient is redefined with respect to shear stress at the wall (τ_w).

$$\tau_w = \frac{h}{2}\left(-\frac{dP}{dl}\right) \quad (55)$$

The equations for wall shear rate (γ_w) and flow rate (Q) are defined in terms of pressure gradient and YPL rheological parameters in the equations 56 and 57, respectively.

$$\dot{\gamma}_w = \frac{1}{\left(R + SxP^g\right)^{\frac{1}{m}}}\left[\frac{h}{2}\left(-\frac{dP}{dl}\right) - \left(L + NxP^v\right)\right]^{\frac{1}{m}} = \frac{1}{\left(R + SxP^g\right)^{\frac{1}{m}}}\left(\tau_w - \left(L + NxP^v\right)\right)^{\frac{1}{m}} \quad (56)$$

$$Q = \frac{wh^2}{2\left(R + SxP^g\right)^{\frac{1}{m}}\tau_w^{\,2}}\left(\frac{1}{1+2m}\right)\left(\tau_w - \left(L + NxP^v\right)\right)^{\frac{1+m}{m}}\left(\tau_w + \frac{m}{m+1}\left(L + NxP^v\right)\right) \quad (57)$$

Moreover, the velocity equation is;

$$\frac{12\,v}{D_o - D_i} = \frac{\left(\tau_w - (L + NxP^v)\right)^{\frac{1+m}{m}}}{(R + SxP^g)^{\frac{1}{m}}\,\tau_w^2}\left(\frac{3m}{1+2m}\right)\left(\tau_w + \frac{m}{1+m}(L + NxP^v)\right) \quad (58)$$

Equation 58 needs to be solved iteratively to find shear stress at the wall;

Also the velocity equation for the given flow rate in the annular media is written,

$$v = \frac{Q}{h\,w} \quad (59)$$

By assuming *N=n*, the Shear Stress at the wall is;

$$\dot{\gamma}_w = \frac{1+2m}{3m}\frac{12v}{D_o - D_i} \quad (60)$$

Hence the shear stress at the wall is;

$$\tau_w = \left(L + NxP^v\right) + \left(R + SxP^g\right)\left(\dot{\gamma}\right)^m \quad (61)$$

After obtaining the rheological equations, correction factor-C_{ca} should be defined:

$$C_{ca} = 1 - \frac{1}{1+m}\frac{\left(L + NxP^v\right)}{\tau_w} - \frac{m}{1+m}\left(\frac{\left(L + NxP^v\right)}{\tau_w}\right)^2 \quad (62)$$

Shear stress can be recalculated in terms of the correction factor to check the iteration convergence,

$$\tau_{wc} = \left(L + NxP^{v}\right) + \left(R + SxP^{g}\right)\left[\left(\frac{1}{C_{ca}}\frac{1+2m}{3m}\right)\frac{12v}{D_o - D_i}\right]^{m} \quad (63)$$

The convergence criterion is,

$$\frac{\tau_{wc} - \tau_w}{\tau_{wc}}\ 100 \leq 1 \quad (64)$$

If the convergence criterion is satisfied, Reynolds Number is calculated:

$$\mathrm{Re}_{YPL} = \frac{12\rho(P)v^2}{\tau_w} \quad (65)$$

Otherwise, continue iteration from Equation 62 until 65 by using τ_{wc} as a new shear stress at wall.

If $Re_{YPL} \leq 2100$, flow is laminar and

$$\frac{dP}{dl} = \frac{4\tau_w}{D_o - D_i} \quad (66)$$

If the calculated Reynolds number is above 2100, the flow regime is assumed turbulent and the frictional factor is;

$$\frac{1}{\sqrt{f}} = \frac{4}{N^{0,75}}\ \log\left(Re_{YPL} f^{1-\frac{N}{2}}\right) - \frac{0.4}{N^{1,2}} \quad (67)$$

Where,

$$N = \frac{(m\ C_{ca})}{1+2m(1-C_{ca})} \quad (68)$$

Finally the frictional pressure drop equation is;

$$\frac{dP}{dl} = \frac{2\, f\rho(P)v^2}{D_o - D_i} \qquad (69)$$

6.3 Model Validation and Discussion from Real Field Application and Pressure Measurements

Proposed pressure dependent Rheological and Frictional Pressure loss equations are validated by field used Oil Based Drilling Fluid System (F-OBM) in real field application. This system was in the Well XX in drilling operation in August 2019, in Turkey. As the main objective of this research is investigation of pressure effect on slightly compressible fluids rheology and friction loss at constant temperature, validation rheological tests will be performed at constant temperatures on the Anton Paar MCR 302 HPHT Rheometer with 29 mm pressure cell. According to logging while drilling data (LWD), bottom hole temperature was measured as 68°C and average temperature through the bore was given as 55°C, meanwhile flow line temperature was 45°C. Rheological tests were performed from that temperature information, proposed hydraulic model validation will be run at average temperature profile. Average temperature results, used in validation calculations, are tabulated in Table 6.

Data analysis are performed and model parameters are calculated. In every constant temperature; deformation regime or energy requirement increases as pressure increments. Each temperature results are divided into two parts (0.1 MPa to 27.6 MPa and 34.5 MPa to 82.7 MPa) to highlight the stress elevation with different pressure intervals. Rheological results with different temperature and pressure conditions are illustrated from Figure 20 to 25.

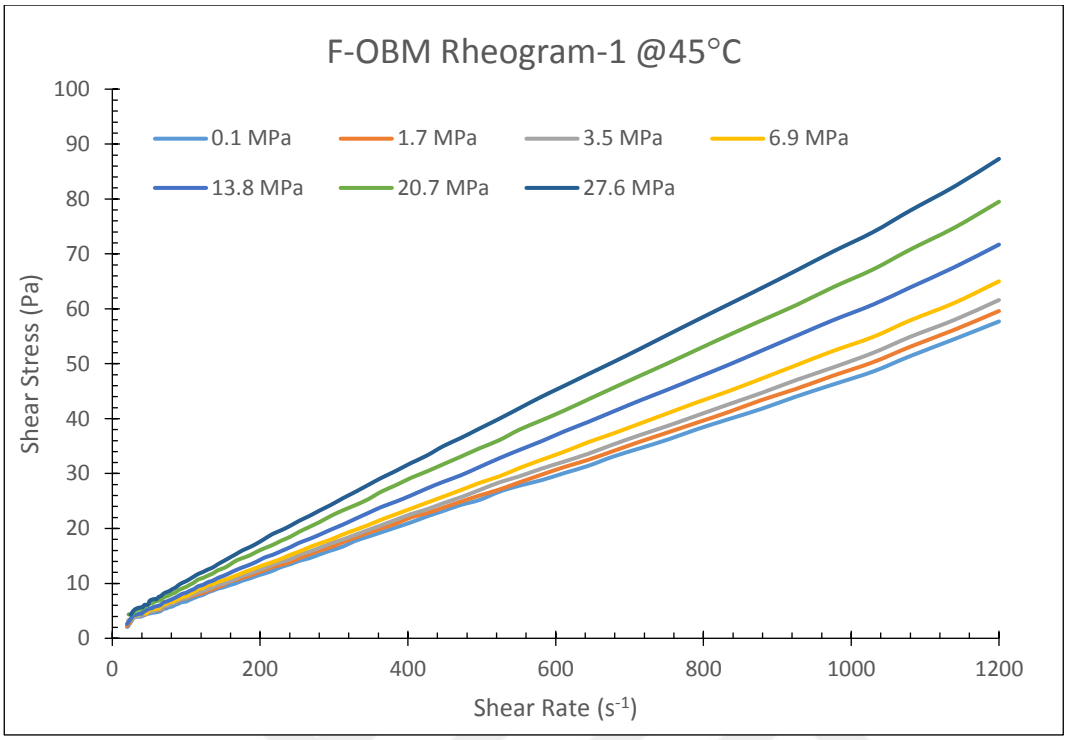


Figure-20: Rheogram-1 for F-OBM at 45°C (0.1 to 27.6 MPa)

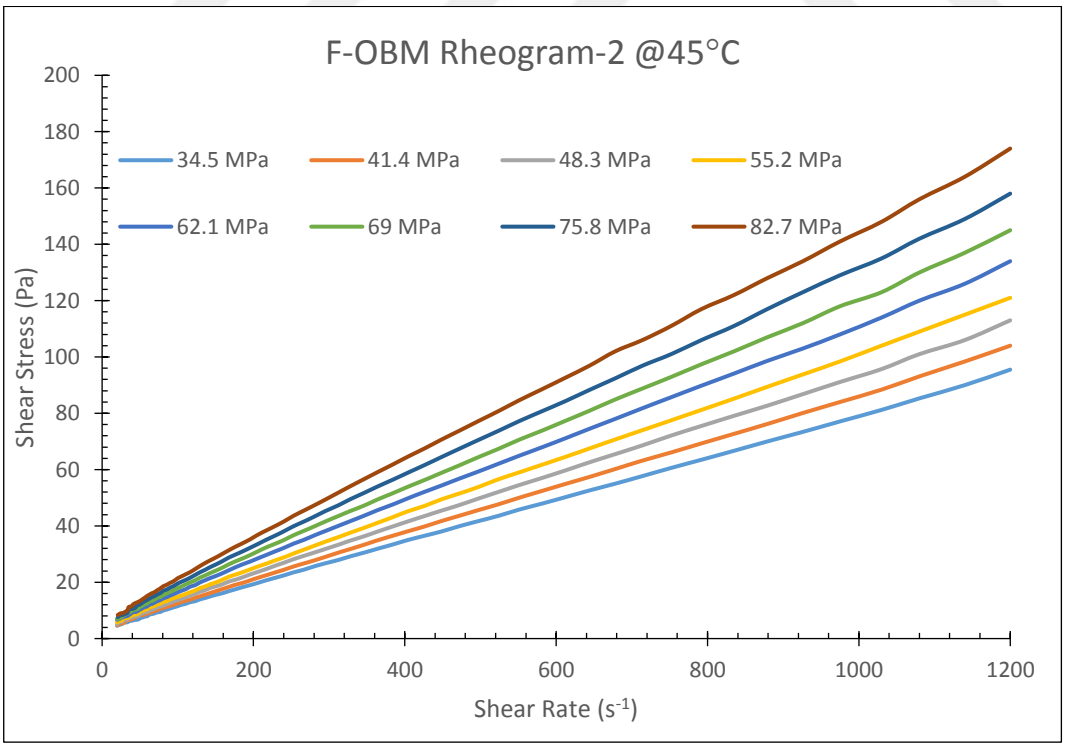


Figure-21: Rheogram-2 for F-OBM at 45°C (34.5 to 82.7 MPa)

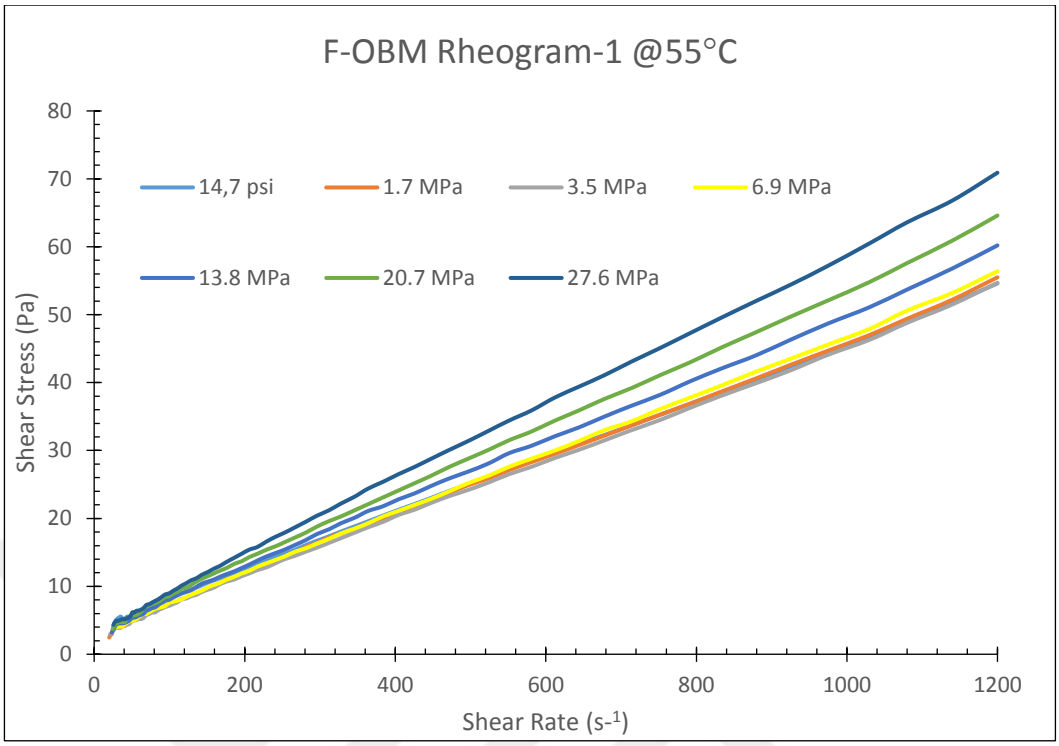


Figure-22: Rheogram-1 for F-OBM at 55°C (0.1 to 27.6 MPa)

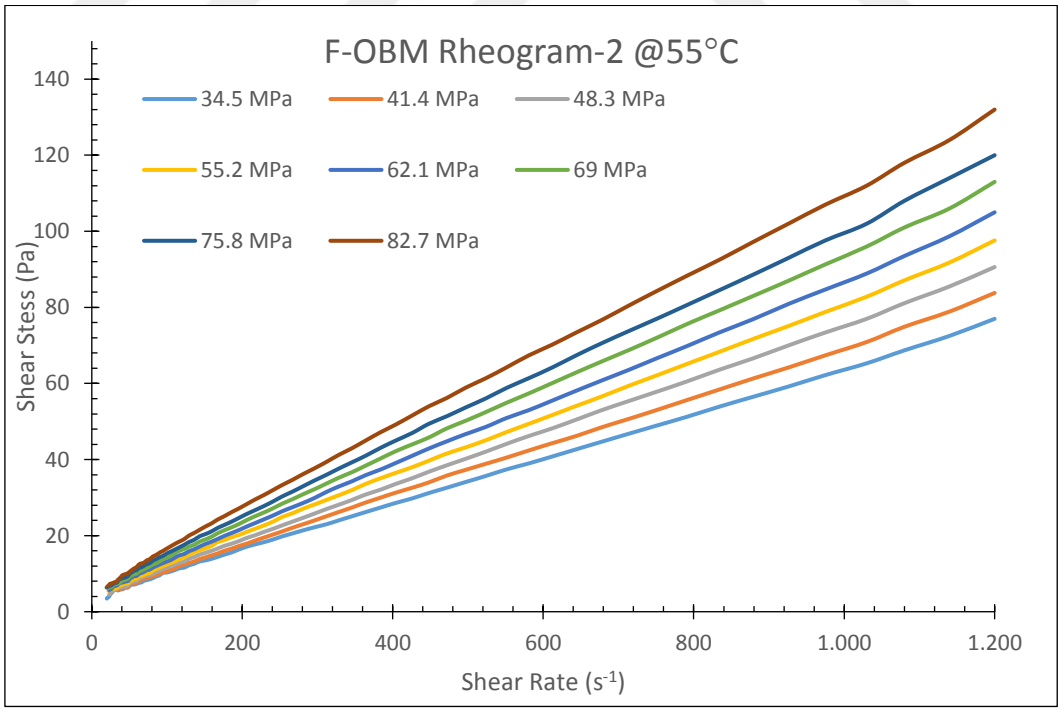


Figure-23: Rheogram-2 for F-OBM at 55°C (34.5 to 82.7 MPa)

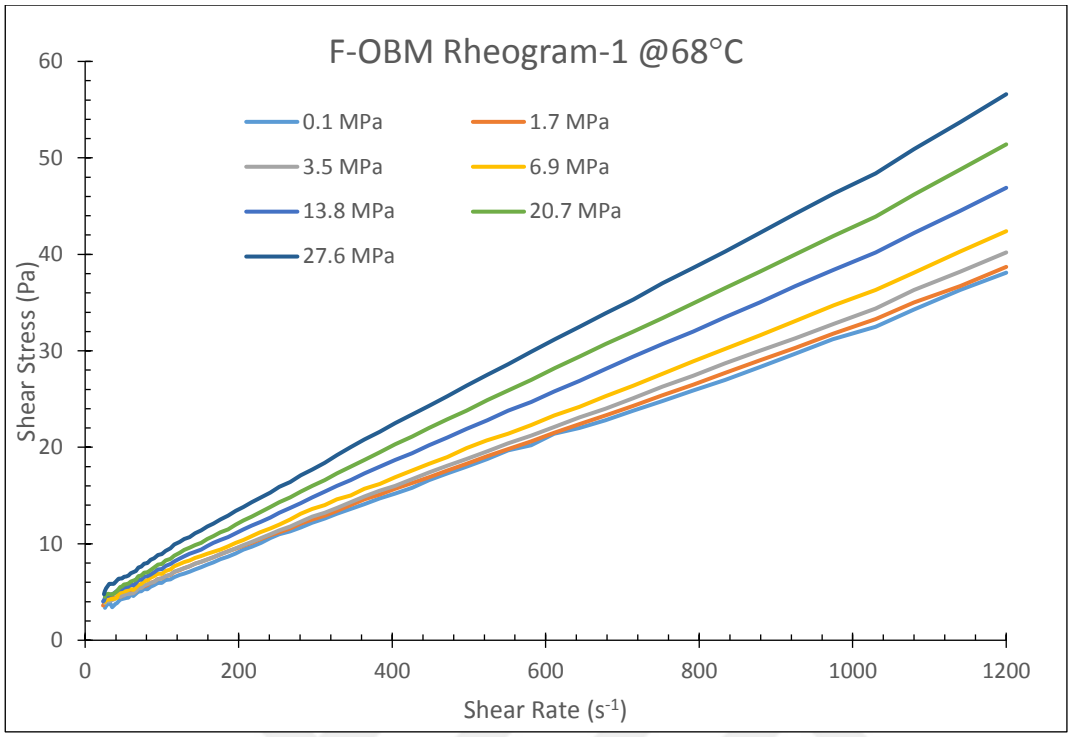


Figure-24: Rheogram-1 for F-OBM at 68°C (0.1 to 27.6 MPa)

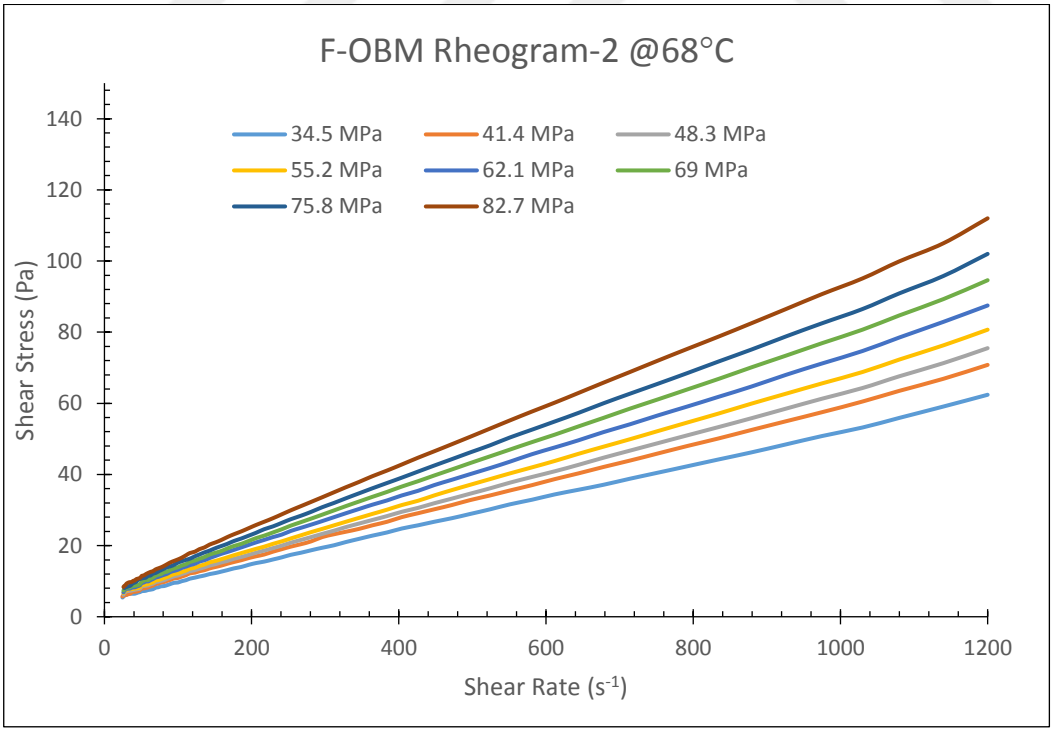


Figure-25: Rheogram-2 for F-OBM at 68°C (34.5 to 82.7 MPa)

Table 6 illustrates the model parameters belongs to F-OBM used in validation calculations. Parameters are obtained via regression analyses. Figures 26 and 27 shows the measured and predicted rheological parameters; yield stress and consistency index, obtained from proposed rheological models respectively. From this prediction R^2 values at 45°C are 0.9859 for yield stress and 0.9982 for consistency index, likewise at 55°C analyses calculated R^2 are 0.9411 for yield stress and 0.9773 for consistency index terms.

Table 6- F-OBM Model Parameters at Test Temperatures

Temperature (°C)	L (Pa)	N (Pa Bar^{-v})	v	R (Pa sec^{-m})	S (Pa sec^{m} Bar^{-g})	g
45	2.0280	0.0009	1.2122	0.0584	4.0639E-06	1.5635
55	2.3192	0.0025	1.0075	0.0552	2.8452E-06	1.5466
68	2,6257	0.0093	0.8965	0.0435	9.6330E-06	1.3221

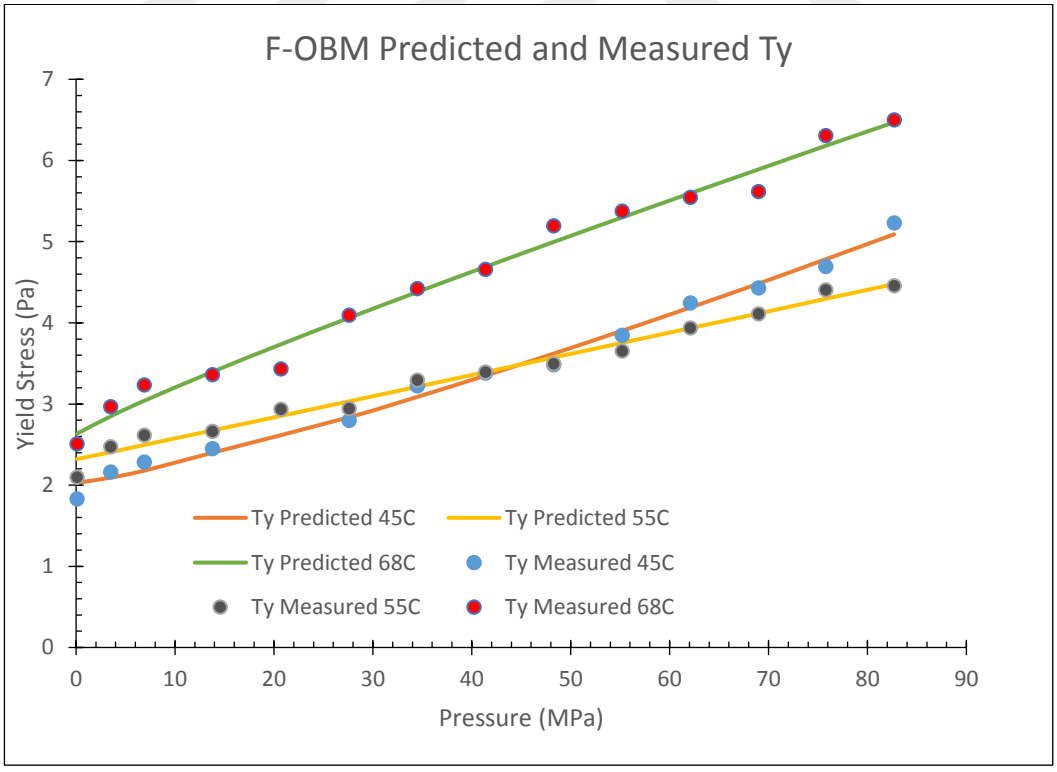


Figure-26: F-OBM Predicted and Measured Yield Stress

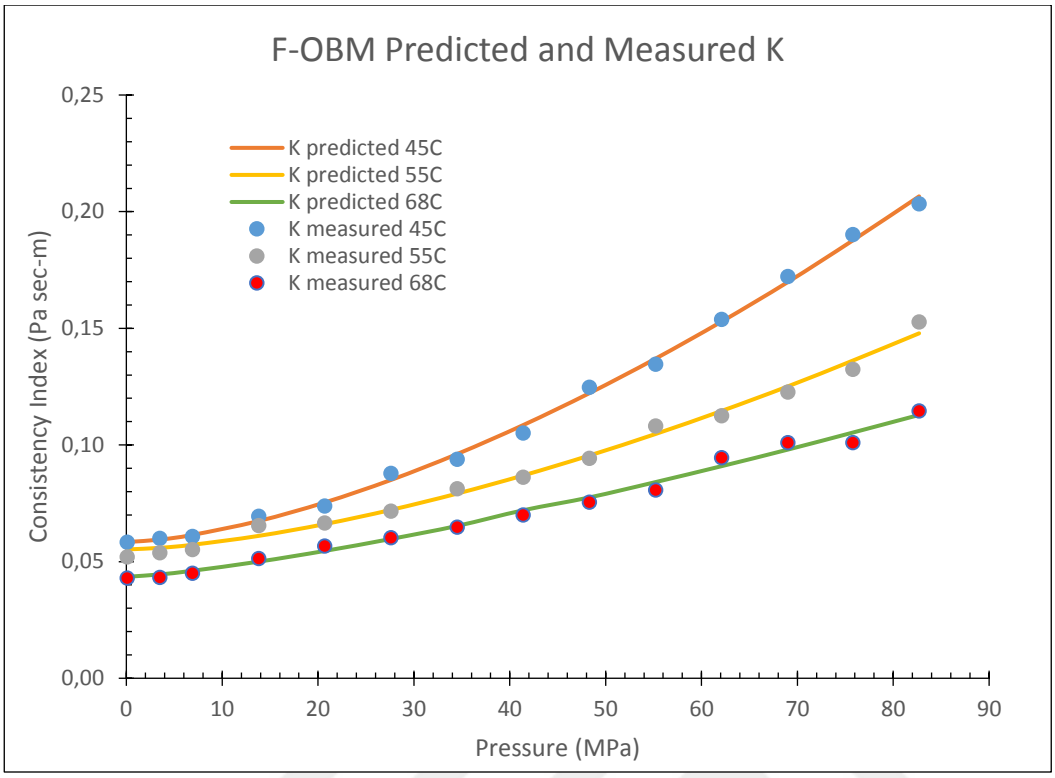


Figure-27 F-OBM Predicted and Measured Consistency Index

Calculation algorithm for the given mud properties, hole geometry and operational parameters is as follows;

First annular velocity profile is calculated;

$$Ann_vel = \frac{4Q}{(Do - Di)^2 Pi}$$

Then Shear Rate at the wall is found;

$$\Upsilon = \frac{1 + 2m}{3m} \frac{12x}{Do - Di}$$

Followed by Shear Stress at wall and Correction Factor equations;

$$\tau_w = \left(L + NxP^v\right) + \left(R + SxP^g\right)\left(\dot{\gamma}\right)^m$$

$$C_{ca} = 1 - \frac{1}{1+m}\frac{\left(L + NxP^v\right)}{\tau_w} - \frac{m}{1+m}\left(\frac{\left(L + NxP^v\right)}{\tau_w}\right)^2$$

From that information Critical Shear Stress at wall is;

$$\tau_{wc} = \left(L + NxP^v\right) + \left(R + SxP^g\right)\left[\left(\frac{1}{C_{ca}}\frac{1+2m}{3m}\right)\frac{12v}{D_o - D_i}\right]^m$$

Convergence criteria is checked;

$$\frac{\tau_{wc} - \tau_w}{\tau_{wc}}\ 100 \le 1$$

If satisfied new Shear Stress at wall is Critical Shear Stress at wall ($\tau_w = \tau_{wc}$),

If not, attain as $\tau_{wc} = \tau_w$ and turn back to equation till convergence satisfied.

After obtaining the corrected Shear Stress at wall, check the Reynolds Number

$$\text{Re}=\frac{12\rho v\text{^}2}{\tau w}$$

If Re<2100 flow is laminar

If Re>2100 flow is assumed turbulent.

In laminar flow frictional pressure loss is,

$$\frac{dP}{dl}=\frac{4\tau_w}{D_o-D_i}$$

In turbulent flow, friction factor needs to calculate frictional loss gradient;

$$\frac{1}{\sqrt{f}}=\frac{4}{N^{0,75}}\log\left(Re_{YPL}f^{1-\frac{N}{2}}\right)-\frac{0.4}{N^{1,2}}$$

$$N=\frac{(m\,C_{ca})}{1+2m(1-C_{ca})}$$

Finally;

$$\frac{dp}{dl}=\frac{2f\rho v\text{^}2}{Do-Di}$$

As stated, real field data is used to validate both the proposed constitutive and hydraulic equations. Data is obtained from Well XX, drilled 8.5-inch (0.2159 m) bit to 2694 m. with the 9 5/8 inch (0.2445 m) casing set at 2667 m. Tables 7 and 8 illustrate the bottom hole assembly - string geometries and length. In addition, mud

pump properties are illustrated for the upcoming table. According to third party smart pressure tool (LWD) measurement, at the 2662 m depth of interest, 120 lb/cuft (1925.9 kg/m^3) circulation density is recorded at the 110 strokes – 0.03 m^3/s of mud pump circulation. Moreover, 113 lb/cuft (1813.6 kg/m^3) density is recorded at the 80 strokes – 0.022 m^3/s of mud pump condition.

Table 7 - String Geometry of Well XX

String	Outer Diameter cm (in)	Inner Diameter cm (in)	Length (m)
Smart Tools	17.15 (6.75)	9.53 (3.75)	31.50
Drill Collar	16.51 (6.50)	6.99 (2.75)	144.60
Heavy Weight	12.7 (5.00)	7.62 (3.00)	113.50
Drill Pipe	12.7 (5.00)	10.86 (4.28)	2372.40

Table 8 – Operated Mud Pump Properties in Well XX

Mud Pump Properties	
Stroke Length cm (in)	30.48 (12)
Stroke Diameter cm (in)	15.24 (6)
Efficiency, %	98

Table 9 gives the daily mud properties reported by third party services at the depth of interest.

Table-9 Mud Properties of Validation Sample

Sample From	Flow Line	Flow Line
Check Time	04:59	14:59
Depth (m)	2694	2696
Bit Depth (m)	2694	2696
Density (kg/m^3)	1685	1685
Funnel Viscosity (s/quart)	75	68
Test Temperature (°F)	150	150
R600/R300/R200	92/57/43	84/54/42
R100/R6/R3	29/12/11	29/13/12
Plastic Viscosity (cP)	35	30
Yield Point (lbf/100sqft)	22	24
Gel 10 s (lbf/100 sqft)	13	12
Gel 10 min (lbf/100 sqft)	23	23
HTHP API-Filter (ml)	2,1	2,2
HTHP API-Cake (in/32)	1	1
Retort Water (%)	15	15
Retort Base Fluid (%)	56	56
Oil/Water Ratio	21/79	21/79
Alkalinity (ml)	2	2
Chloride (mg/l)	30000	30000
Electrical Satbility (nV)	620	860

Rheological and model parameters in the validation calculation are given in the Tables 10 and 11, respectively. Rheological model parameters are redefined in terms of Pascal unit to provide the compatibility throughout the calculation.

Table-10 Rheological Parameters of F-OBM at Different Pressure at 55°C

Pressure (MPa)	τ_y (Pa)	K (Pa sec^m)	m
0.1	2.5108	0.0552	0.9580
3.5	2.4780	0.0538	0.9580
6.9	2.6169	0.0552	0.9580
13.8	2.6636	0.0655	0.9580
20.7	2.9360	0.0665	0.9580
27.6	2.9441	0.0716	0.9580
34.5	3.2922	0.0812	0.9580
41.4	3.3933	0.0862	0.9580
48.3	3.4962	0.0942	0.9580
55.2	3.6518	0.1081	0.9580
62.1	3.9377	0.1125	0.9580
69	4.1094	0.1227	0.9580
75.8	4.4072	0.1323	0.9580

Table-11 Model Parameters of F-OBM at 55°C

Temperature (°C)	**L (Pa)**	**N (Pa $^{1-v}$)**	**v**	**R (Pa sec^{-m})**	**S (Pa sec^m Pa^{-g})**	**g**
55	2.3192	2.48E-08	1.0073	0.0552	5.28E-14	1.5464

Annular frictional pressure loss calculations are solved iteratively by using the Visual Basic Computer program. As explained, string is in the casing at 2662 m, medium flow rate are used in check-shots to prevent any wear on the casing. Calculation starts from surface and annular geometry is divided into 1-meter grids.

In the 1-meter conduit, frictional pressure loss is calculated and add to 1-meter hydrostatic head and pressure at the starting point of grid, which is attained as end pressure of the grid. Calculations continue until the bottom of the hole. Figure 28 shows the schematic calculation methodology in the well bore trajectory. Calculation results are tabulated in the Appendix-A.

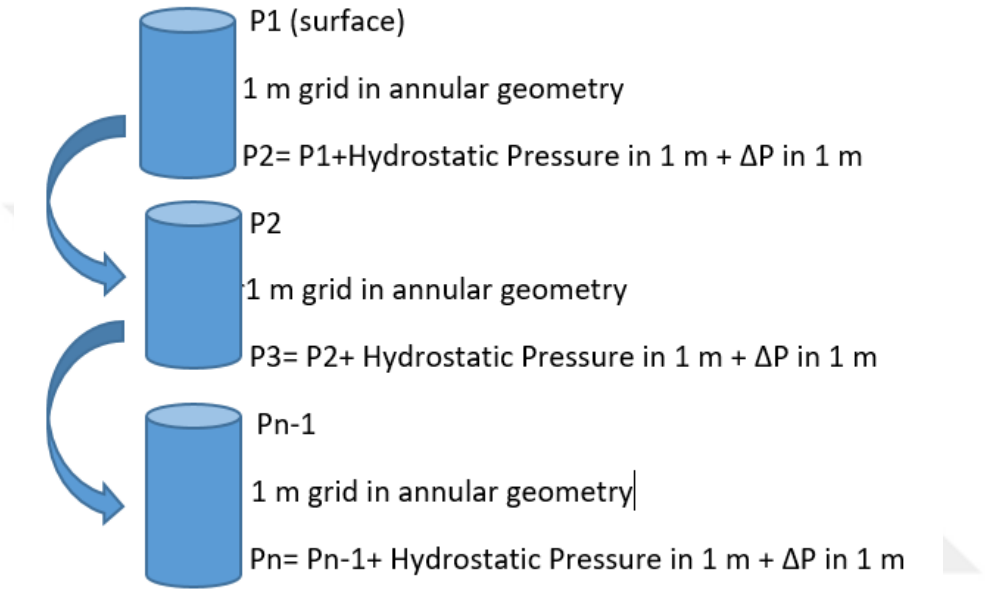


Figure-28: Pressure Calculation Methodology in the Hole Trajectory

At 0.03 m^3/s flow rate, measured 1925.9 kg/m^3 equivalent density creates 50.24 MPa pressure at this depth, calculation shows 50.93 MPa pressure value. Model slightly overestimates 1.36% of the in-situ measurements. The entire flow regime is in the laminar region according to program illustration. This is expected in check shots for smart units records wants to be taken in steady conditions, lack of chaotic flow. Furthermore, without considering the pressure effect on slightly compressible fluids, i.e., if calculations are performed according to atmospheric conditions, pressure at 2662 m is calculated as 47.14 MPa. This value strengths the hypothesis of the thesis. In the surface, 1357.56 Pa/m gradient is calculated, at 1000 meter depth of interest gradient is 1546.24 Pa/m and reaches to 1913.57 Pa/m at 2000 m in the same annular geometry. Figure 29 displays the annular pressure with depth. Figure 30 illustrates

the fictional pressure loss gradient in the trajectory. At 2486-meter gradient, there is a sharp increase in the gradient values. This is due to annular velocity increase or flow in the Bottom Hole Assembly.

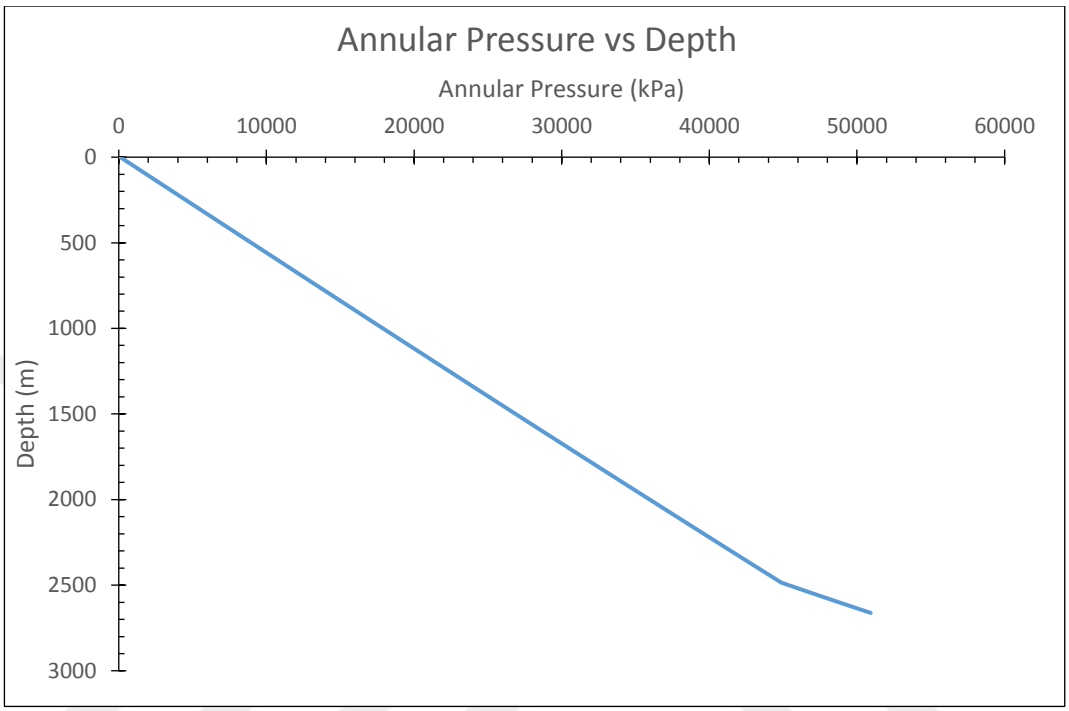


Figure-29: Calculated Pressure in the Well Bore at 0.3 m^3/s circulation rate

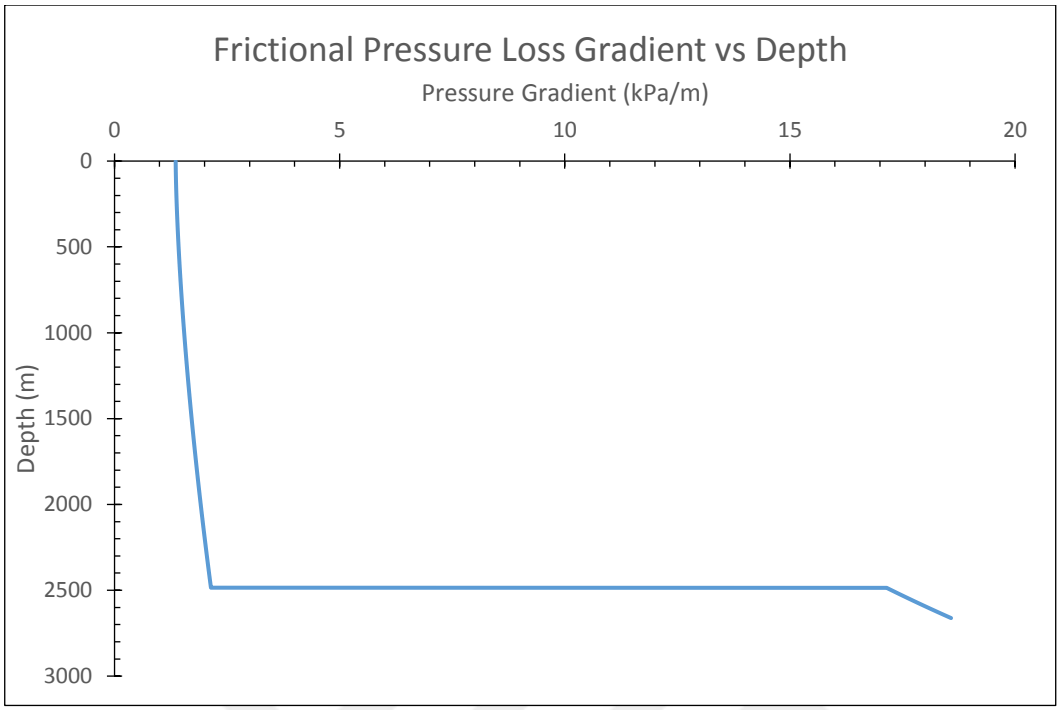


Figure-30: Frictional Pressure Loss Gradient Change at 0.3 m^3/s circulation rate

Second validation calculation is performed 0.022 m^3/s flow rate; measured 1813.6 kg/m^3 equivalent density creates 47.40 MPa pressure, shown in Figure 31. Same calculation algorithm and methodology is followed. Program gives 49.05 MPa pressure value at 2662 m. The absolute discrepancy is 3.48% of the in-situ measurements. The entire flow regime is in the laminar region according to program illustration. In addition, without considering the pressure effect on slightly compressible fluids, i.e., if calculations are performed according to atmospheric conditions, pressure at 2662 m is calculated as 46 MPa. In atmospheric condition, friction gradient is 1040.58 Pa/m, due to overhead pressure it is not constant and changed to 1175.68 Pa/m at 1000 m and reaches to 1437.28 Pa/m at 2000 m. If pressure effect is not considered in the rheological aspect and surface conditions are used in hydraulic calculations, 38% of underestimation happens in our calculations. Figure 32 illustrates the fictional pressure loss gradient in the trajectory. At 2486 meter, again there is an increase in gradient values. This is due to annular velocity increase or flow in the Bottom Hole Assembly.

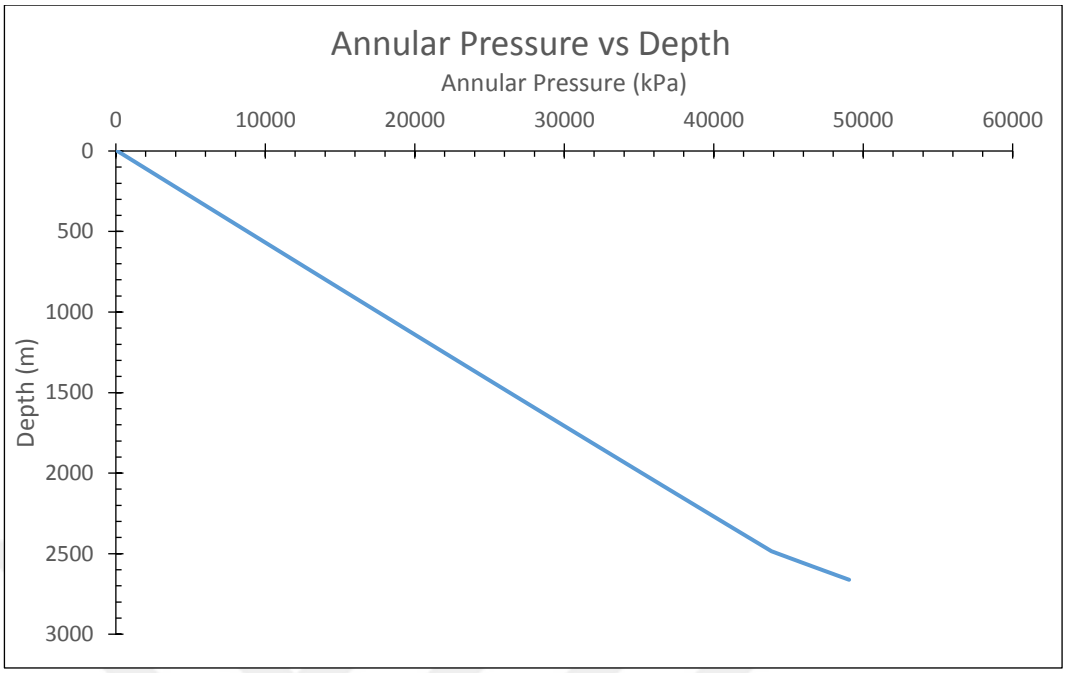


Figure-31: Calculated Pressure in the Well Bore at 0.022 m^3/s circulation rate

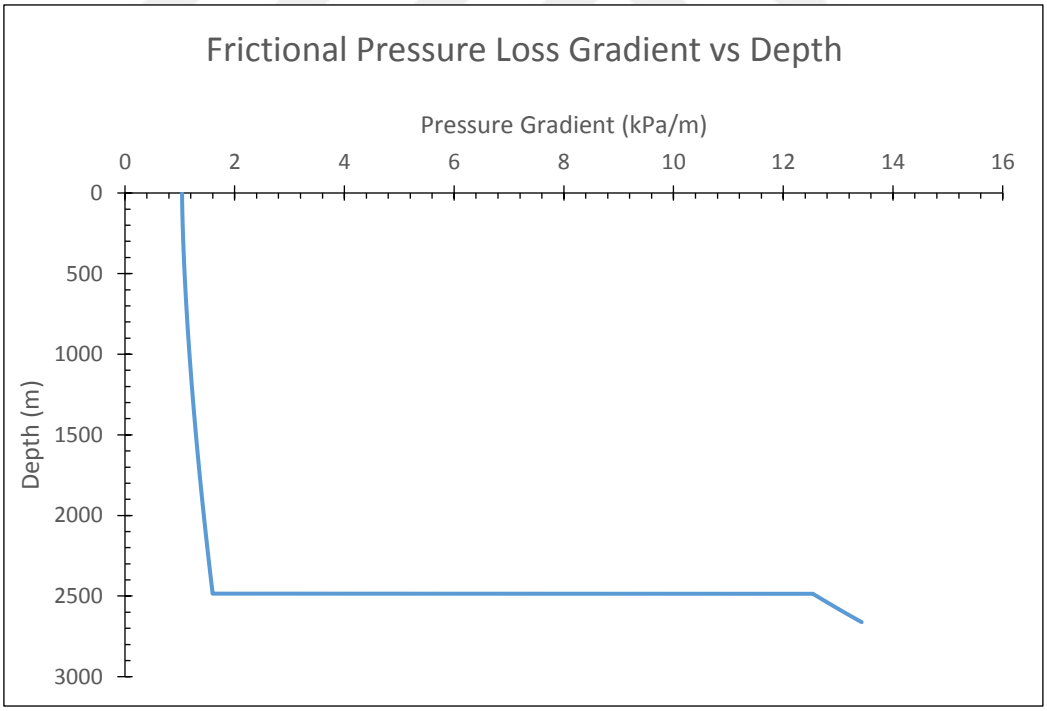


Figure-32: Frictional Pressure Loss Gradient Change at 0.022 m^3/s circulation rate

Proposed rheological equations and hydraulic calculation methodology is compared with Lee et.al.'s equation (Equation-7). In their equation, Newtonian viscosity is related to pressure change in an exponential way. F-OBM viscosity results at constant 55°C temperature test conditions are reviewed (shown in Table 12). Figure 33 illustrates the viscosity change with pressure and Lee et.al.'s model constants are calculated as; *A:* 0.0455 Pa-s and *B:* 0.011 Pa^{-1}.

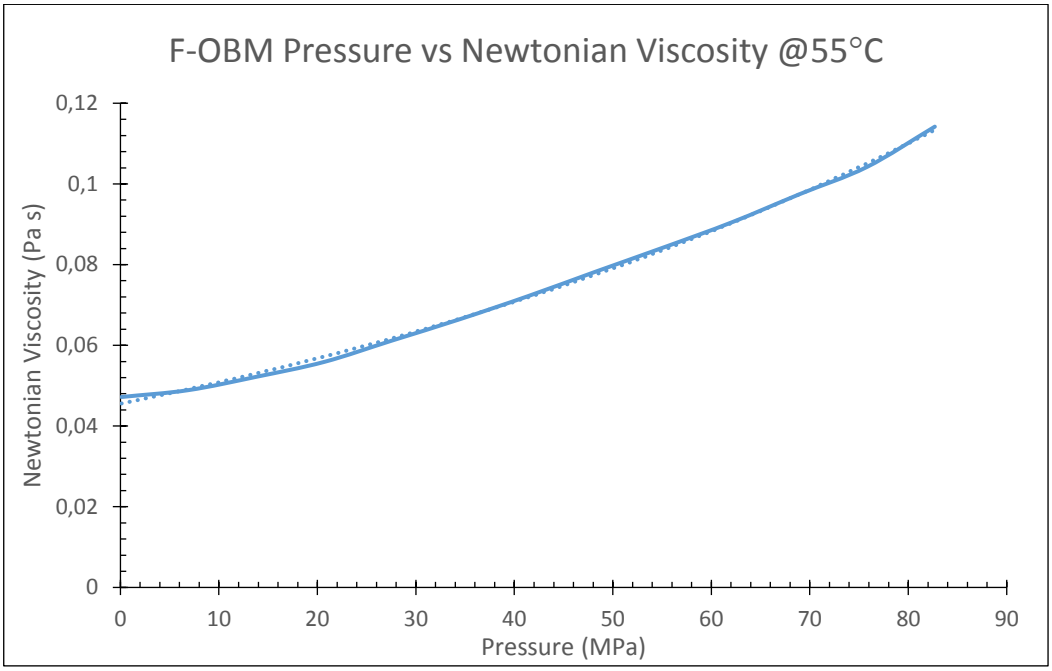


Figure-33: F-OBM Newtonian Viscosity with Different Pressure at 55°C

For Newtonian frictional loss calculations, Lamb's equation is used in annular conduit (Bourgoyne Jr. A.T., et.al., 1991), where r_2 is the inner radius of casing or open hole and r_1 is the outer radius of string.

$$\frac{dP}{dl} = \frac{8\,\mu\,v}{\left(r_2^2 + r_1^2 - \frac{r_2^2 - r_1^2}{Ln^{r_2}/_{r_1}}\right)} \quad (70)$$

Where viscosity is;

$$\mu = 0.0455\, exp^{(0.011\,P)} \quad (71)$$

Similar methodology is followed and viscosity is changed with pressure. Calculations are performed at 0.3 m^3/s flow rate and 55°C with the same hole and string geometry. For example, in frictional loss gradient calculations, there has been 62.8% increase is observed at 2486 m (where drill pipe - heavy weight strings end) compared to surface gradient due to viscosity change with pressure.

Calculations give 45.47 MPa pressure at 2662 m where measured pressure is 50.24 MPa at this point of interest (50.93 MPa is calculated via proposed equations in this study). That means, Newtonian calculation with previously developed pressure dependent viscosity equations underestimate the measured one with a difference 9.5% or calculated equivalent density is 182.66 kg/m^3 (1.52 ppg) less than the real case. That findings show that, design or calculation with Newtonian – Lee approach cause some design and operational troubles. Calculated annular pressure at each depth with Lee-Newtonian equations is drawn in Figure 34.

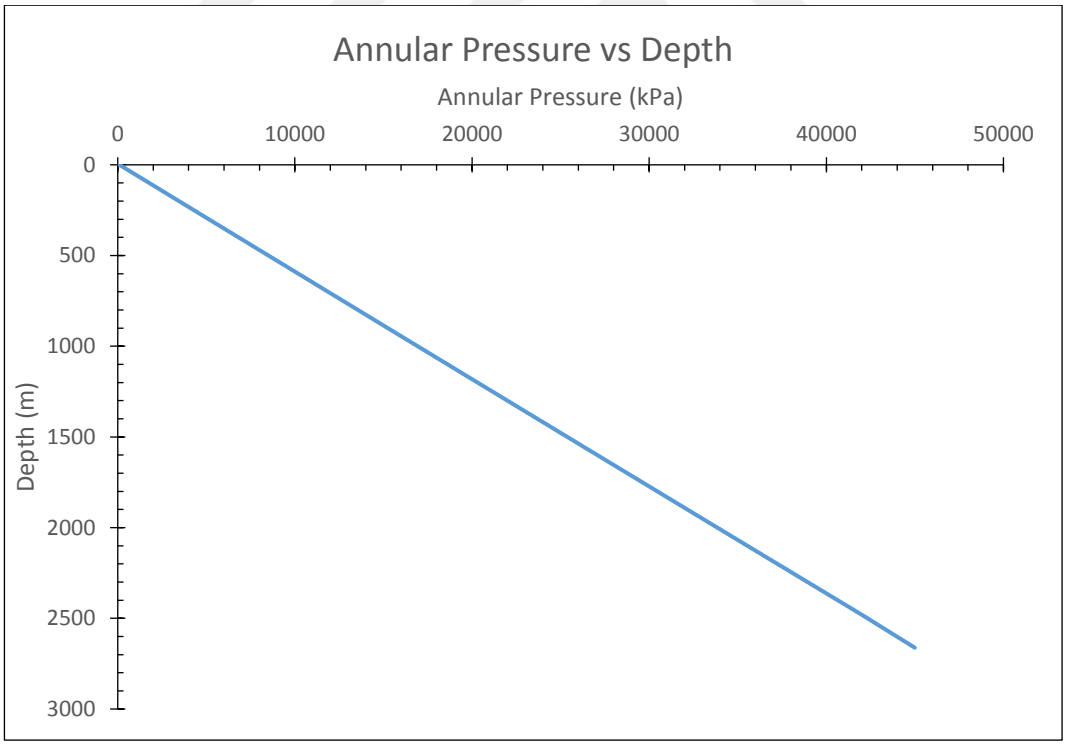


Figure-34: Calculated Pressure in the Well Bore at 0.3 m^3/s circulation rate with Newtonian Model

Table-12 F-OBM Newtonian Viscosity at 55°C

Pressure (MPa)	Newtonian Viscosity (Pa-s)
0.1	0.0482
6.9	0.0489
13.8	0.0522
20.7	0.0559
27.6	0.0612
34.5	0.0665
41.4	0.0722
48.3	0.0783
55.2	0.0843
62.1	0.0905
69	0.0975
75.8	0.1042
82.7	0.1142

Measured total annular frictional pressure loss is around 6.26 MPa. Newtonian calculation methodology with Lee et.al.'s viscosity equation gives 1.49 MPa at 2662 m. Calculated value is around 4.2 times less than the real case. Nevertheless, calculated annular frictional loss with the proposed rheological and hydraulic equations is 6.94 MPa at this depth of interest. Figure 35 illustrates Newtonian frictional pressure gradient at 0.3 m^3/s flow rate.

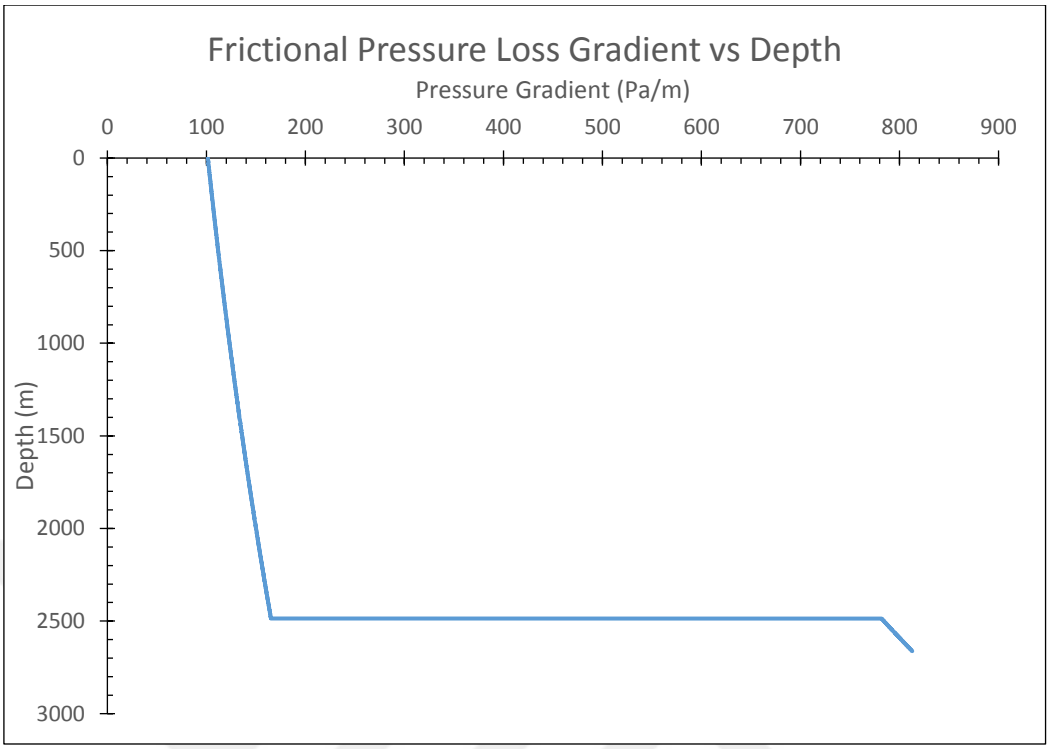


Figure-35: Frictional Pressure Loss Gradient Change at 0.3 m^3/s circulation rate with Newtonian Model

CHAPTER 7

RHEOLOGICAL MODEL SENSIVITY IN REFERENCE TO THE BASE FLUID RATIO, TEMPERATURE and VOLUME OF SOLID

Proposed rheological models are checked by analyzing different slightly compressible and incompressible fluids at moderate temperature conditions. In both the diesel and synthetic base samples are mixed with 20/80 water/oil ratio (w/o), chemical contents are given in Table 1. Model predictions show accurate match with the measured ones at this formulated systems, in between 25°C to 68°C temperature conditions. Model performance is reviewed by decreasing the oil ratio in the drilling fluid system. F-OBM sample is selected in this analysis. Besides the 20/80 w/o, already mentioned and shown in the previous parts, 30/70 and 40/60 w/o systems are prepared by increasing the brine phase and primary emulsifier ratio (1% in each 10% water phase change) in the main formulation. All of the prepared samples, emulsion stability values are more than 600 nV at room temperature.

7.1 Base Fluid Effect

Like the previous ones, the rheological tests are conducted on Anton Paar Physica MCR 302 HPHT Rheometer. Controlled shear rate methodology is followed in this sample, also. After the relaxation period, test interval is started. Shear rate is ramped decreasing from 1200 s^{-1} to 10 s^{-1}. To minimize the barite or any colloidal system precipitation, samples are changed in every 3 hours of test intervals. At each pressure points test is repeated three times to get the data set in the ± five-percent range. Base fluid effect on the rheological behavior are analyzed at 45°C.

Deformation behavior of 30/70 w/o diesel-based fluid obeys the Yield Power Law model at 45°C, shown in Figures 36 and 37. Pressure increments result in the energy requirement to flow hence, there has been an uplift in the Rheogram in the Pressure side.

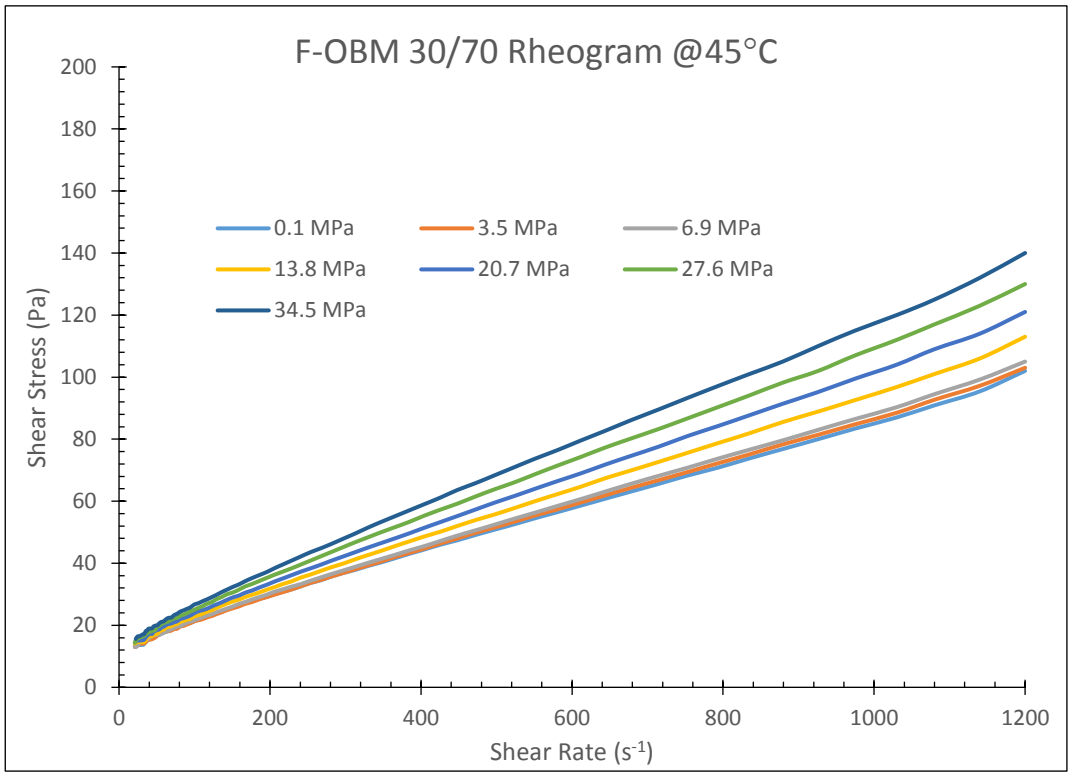


Figure-36: Rheogram-1 for 30/70 F-OBM at 45°C (0.1 to 34.5 MPa)

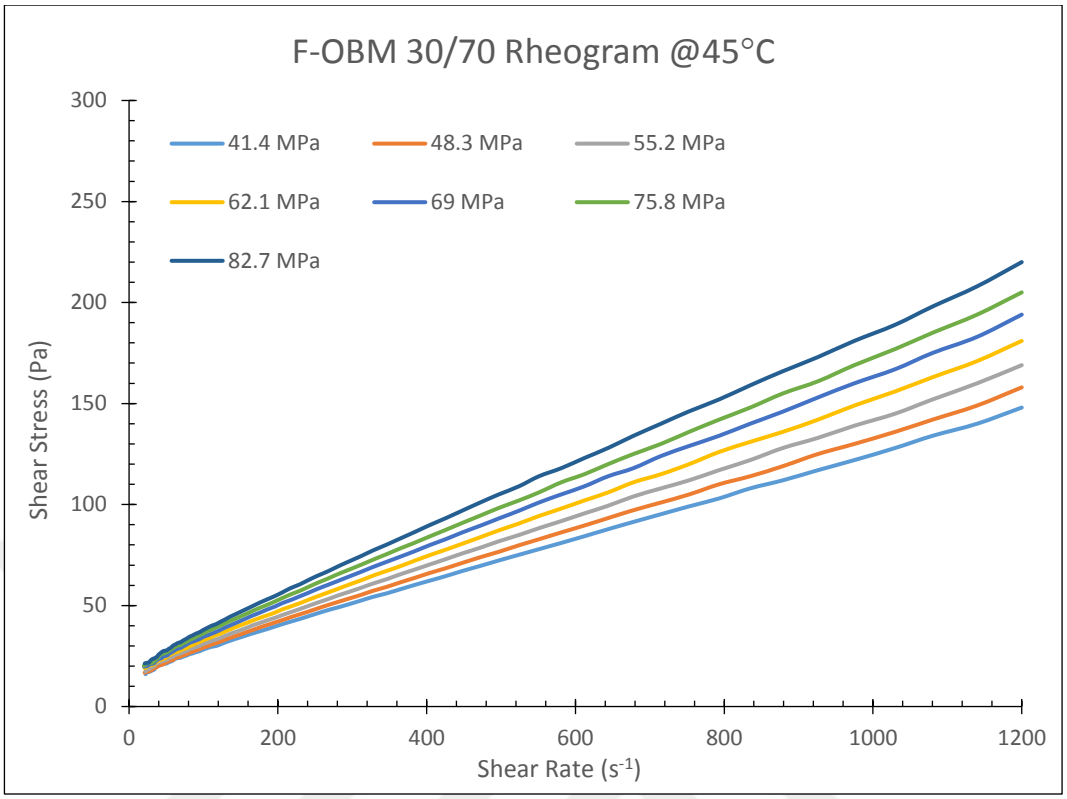


Figure-37: Rheogram-2 for 30/70 F-OBM at 45°C (41.4 to 82.7 MPa)

The system needs some degree of stress threshold to initiate the flow, yield stress, and shows shear-thinning behavior. Rheological parameters are found by nonlinear regression technique. Fluid flow behavior index, *m*, is almost constant (between 0.905 and 0.920) in every pressure level. Pressure influences the deformation responses of the fluid. At 41.4 MPa test application; 1200 s^{-1} shear rate reading almost increases by 35% at 82.7 MPa measurement. Similar trend is also identified in lower shear rate data at the same pressure conditions i.e.; 23% increase in 105 s^{-1} readings when the pressure changes from 6.9 MPa to 34.5 MPa. Rheological parameters are illustrated in Table 13.

Table-13 Rheological Parameters of 30/70 w/o F-OBM at Different Pressure at 45°C

Pressure (MPa)	τ_y (Pa)	K (Pa sec^m)	m
0.1	11.7171	0.1491	0.9150
3.5	11.3977	0.1500	0.9150
6.9	11.7027	0.1527	0.9150
13.8	12.3224	0.1547	0.9150
20.7	12.7889	0.1553	0.9150
27.6	12.9550	0.1784	0.9150
34.5	13.4364	0.1896	0.9150
41.4	14.4244	0.1930	0.9150
48.3	14.2070	0.2171	0.9150
55.2	15.1542	0.2206	0.9150
69	16.2020	0.2229	0.9150
75.8	16.4206	0.2479	0.9150
82.7	17.1903	0.2579	0.9150

Table 14 illustrates the model parameters belongs to 30/70 w/o F-OBM in validation to Equation-15. Figures 38 and 39 show the measured and predicted rheological parameters; yield stress and consistency index, obtained from the proposed rheological models respectively. There has been a good match with an R^2 value of 0.9863 in every pressure level for Yield Stress and 0.9852 in every pressure level for consistency index.

Table-14 30/70 w/o F-OBM Model Parameters at 45°C

Temperature (°C)	L (Pa)	N (Pa Bar^{-v})	v	R (Pa sec^{-m})	S (Pa sec^{m} Bar^{-g})	g
45	11.3065	0.0037	1.1280	0.1470	1.3240E-05	1.3635

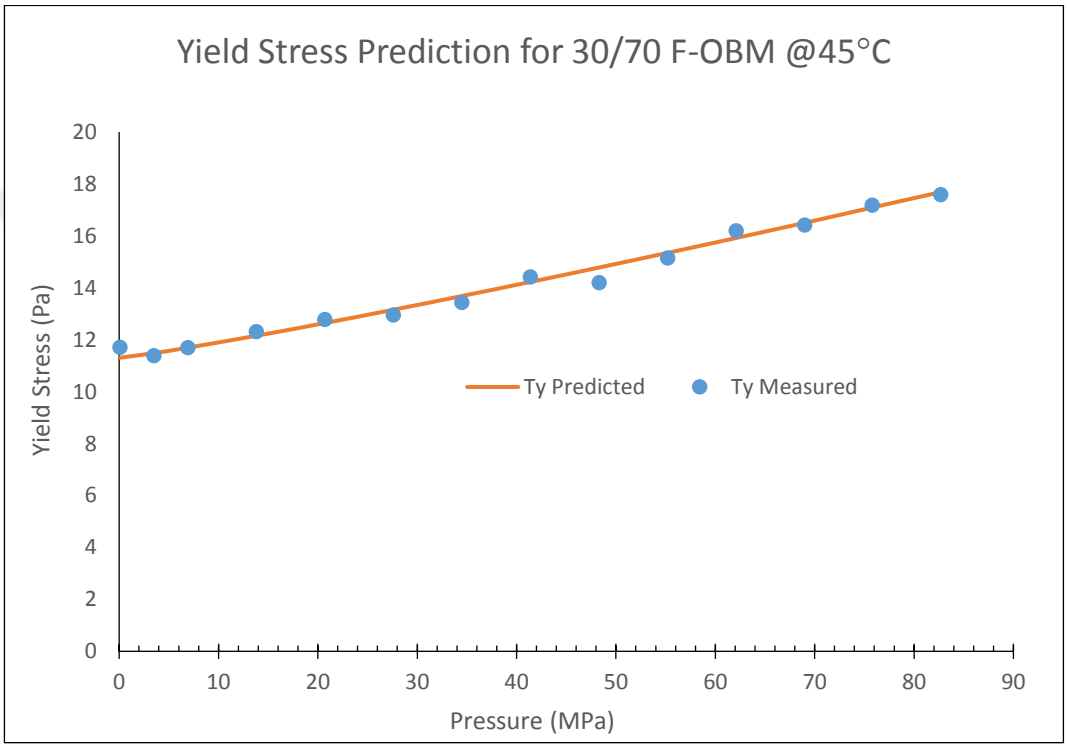


Figure-38: 30/70 w/o F-OBM Predicted and Measured Yield Stress 45°C

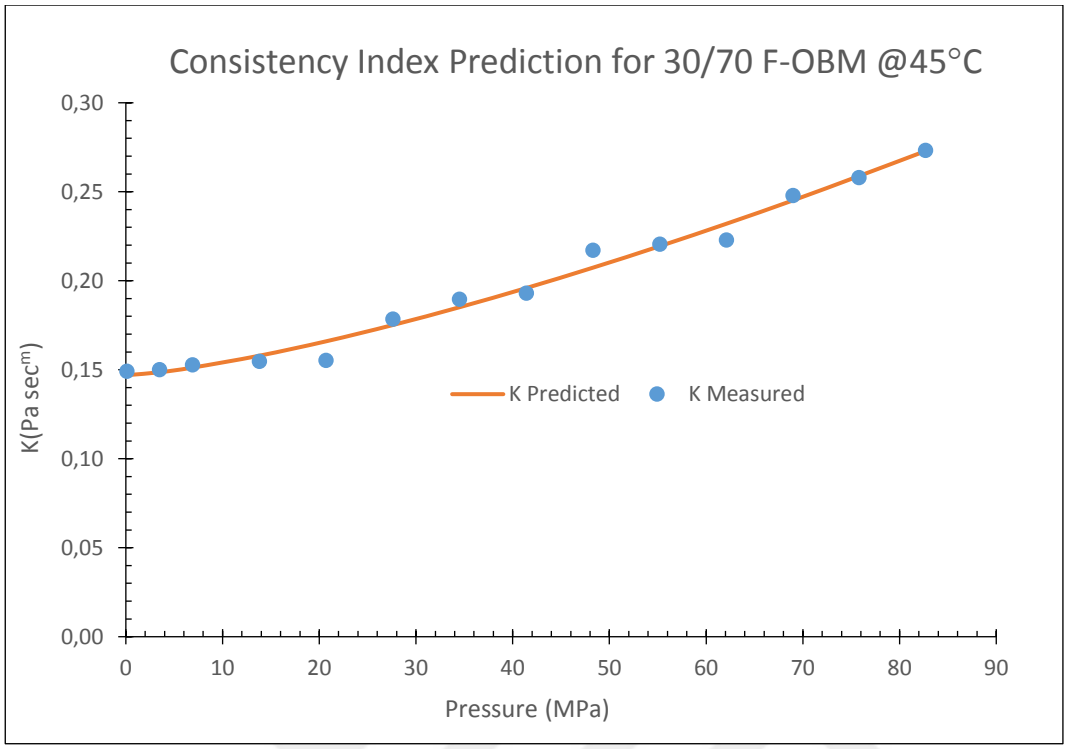


Figure-39: 30/70 w/o F-OBM Predicted and Measured Consistency Index 45°C

Similar mixing protocol is followed to prepare 40/60 w/o F-OBM, to investigate the kind of compressible base fluid – pressure sensitivity on the deformation phase. The main chemical composition F-OBM, for 20/80 w/o, is given in Table 1, however to obtain the 40/60 more brine phase is needed and so more primary emulsifier is used to obtain the emulsion stability. Like the 30/70 w/o sample, 2% more primary emulsifier is added to the mixing procedure to achieve the 600 nV emulsion stability value at room temperature.

As well the previous rheological tests, controlled shear rate methodology is used. First, the sample is sheared and allowed to rest for relaxation and then test interval is initiated. Shear rate is ramped decreasing from 1200 s^{-1} to 10 s^{-1}. To minimize the barite or any colloidal chemical sag, samples are changed in every 3 hours of test interval. At each pressure points, test is repeated three times to get the data set in the ± five-percent range.

Higher yield stress values are measured at 40/60 sample at 45°C, compared to the 20/80 and 30/70 w/o samples. This effect is also observed by another research, which concluded that oil water ratio play a big role in yield stress level. Higher yield stress values are observed when the w/o ratio is increased (Eldar D. et.al., 2004). This is because of the continuous phase reduction and more brine phase addition, acting like solid droplets and causing in resistance to flow. Moreover water molecule spacing changes the colloidal forces between droplets (attractive and repulsive forces), even observed at stagnant period. Both the hydrodynamic and electrostatic communication led to increase in internal friction when the volume amount of brine increased in the system (Eldar D. et.al., 2004).

Rheograms of the 40/60 w/o sample at 45°C are illustrated in Figures 40 and 41. Samples show the yield stress or creeping in the early stage of viscous deformation, and then followed shear thinning behavior is recognized. Even the slightly compressible fluid volumetric ratio is decreased; pressure can play a significant role on the deformation behavior.

Energy requirement for flow is increased when the pressure application is in higher level. For example, at 1200 s^{-1} shear rate, stress measurement is doubled at 82.7 MPa compared to 6.9 MPa readings. In addition, at moderate drilling shear rate simulation as the flow in annular medium - 206 s^{-1} deformation rate, there has been a 33% increased stress is recorded when the pressure is altered from 27.6 MPa to 69 MPa. Similar trend is also identified in lower shear rate data i.e.; 27% increase in 20 s^{-1} readings when the pressure increased from 13.8 MPa to 75.8 MPa.

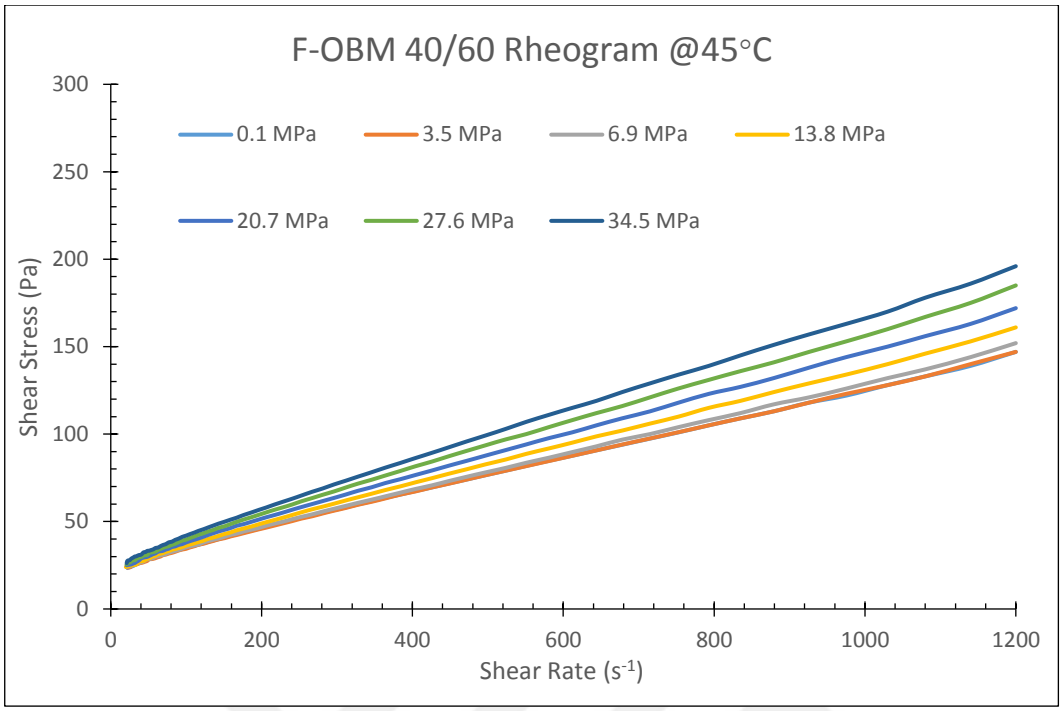


Figure-40: Rheogram-1 for 40/60 F-OBM at 45°C (0.1 to 34.5 MPa)

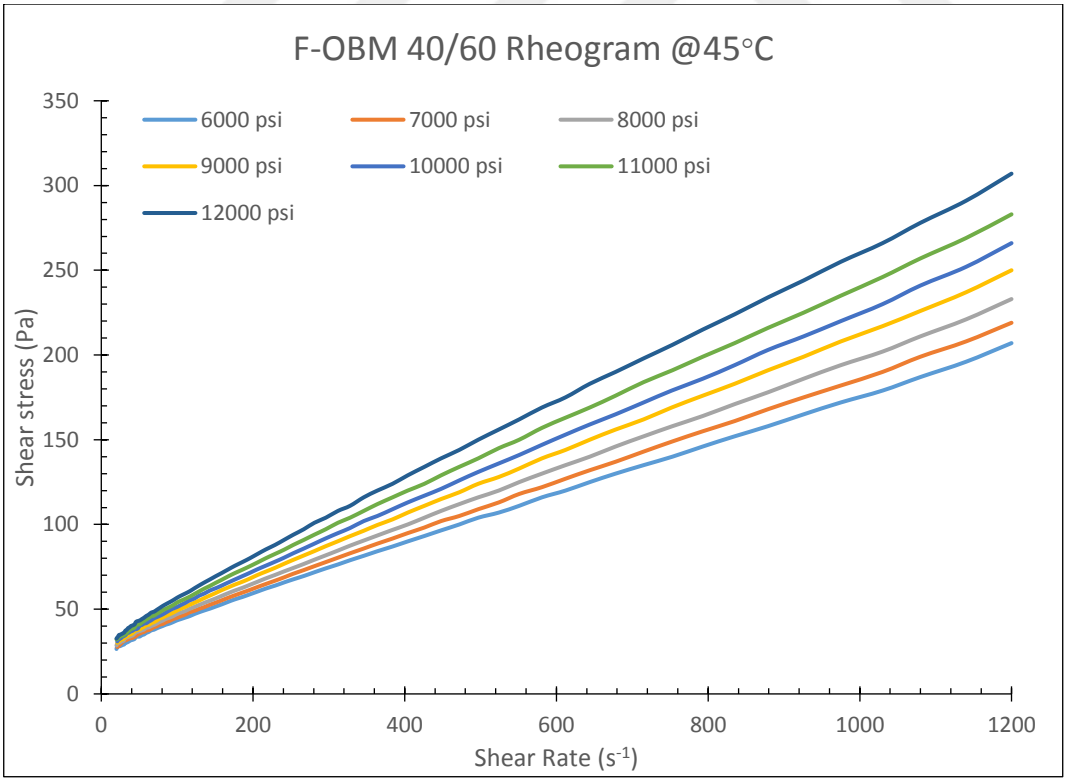


Figure-41: Rheogram-1 for 40/60 F-OBM at 45°C (41.4 to 82.7 MPa)

All the rheological parameters are identified through a nonlinear regression technique and listed in Table 15. Fluid flow behavior index, *m*, is constant (between 0.90 and 0.91) in every pressure level and consistent with previous samples and literature statements. Both the yield stress - τ_y , and Consistency Index - *K*, increase with pressure, being not as dramatic as 30/70 or 20/80 samples. That observation is expected, because the relatively compressible continuous fluid phase is decreased in the volumetric ratio.

Table-15 Rheological Parameters of 40/60 w/o F-OBM at Different Pressure at 45°C

Pressure (MPa)	τ_y (Pa)	K (Pa sec^m)	m
0.1	21.2480	0.2159	0.9100
1.7	21.0850	0.2064	0.9100
6.9	21.4169	0.2015	0.9100
13.8	21.3117	0.2274	0.9100
20.7	22.0377	0.2397	0.9100
27.6	22.7828	0.2512	0.9100
34.5	23.9093	0.2617	0.9100
41.4	24.2726	0.2706	0.9100
48.3	25.1511	0.2757	0.9100
55.2	25.7455	0.2957	0.9100
69	26.2382	0.3235	0.9100
75.8	27.1618	0.3353	0.9100
82.7	27.5799	0.3704	0.9100

Proposed pressure dependent rheological model, Equation-15, is applied for the data to find the model parameters. These parameters are presented in the Table 16 for the

40/60 w/o F-OBM at 45°C temperature. Predicted and measured Yield stress analyses is exhibited in the Figure 42. The highest identified difference is 2.4% at 13.8 MPa values with R^2 of 0.9906. Figure 43 illustrates the Consistency Index analysis. Except the 6.9 MPa comparison that has 9% difference by overestimation, other pressure conditions have a R^2 value of 0.9825.

Table-16 40/60 w/o F-OBM Model Parameters at 45°C

Temperature (°C)	**L (Pa)**	**N (Pa Bar^{-v})**	**v**	**R (Pa sec^{-m})**	**S (Pa sec^{m} Bar^{-g})**	**g**
45	20,8201	0,0038	1,1332	0,2180	1,1700E-06	1,7723

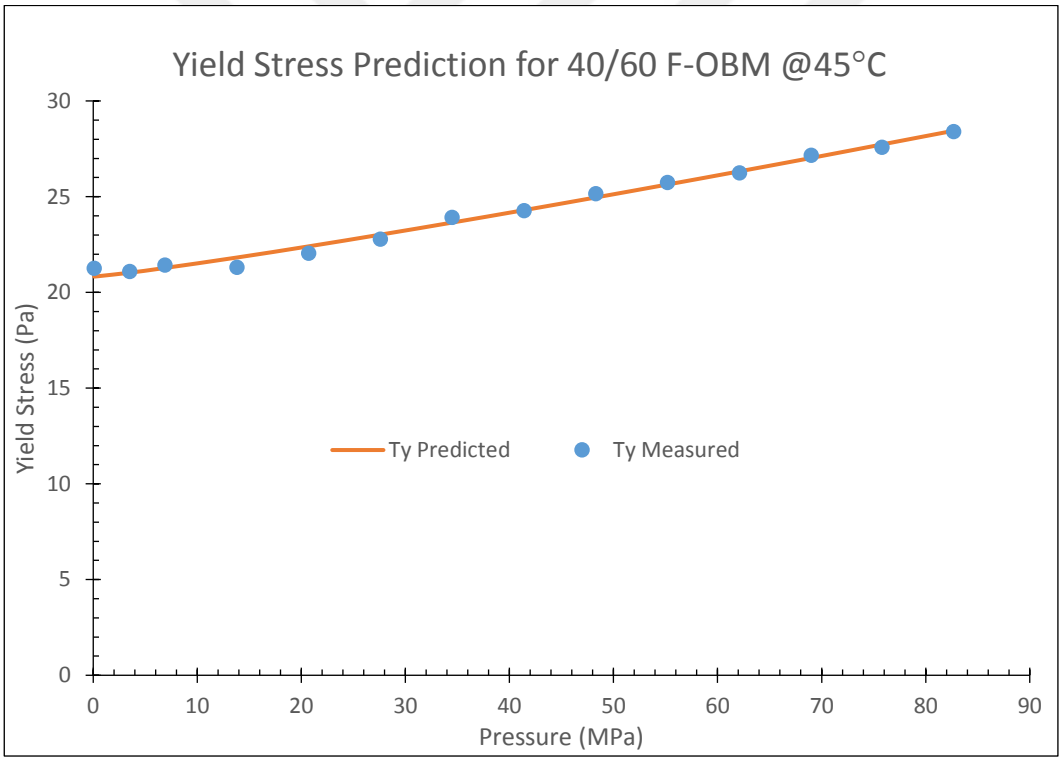


Figure-42: 40/60 w/o F-OBM Predicted and Measured Yield Stress 45°C

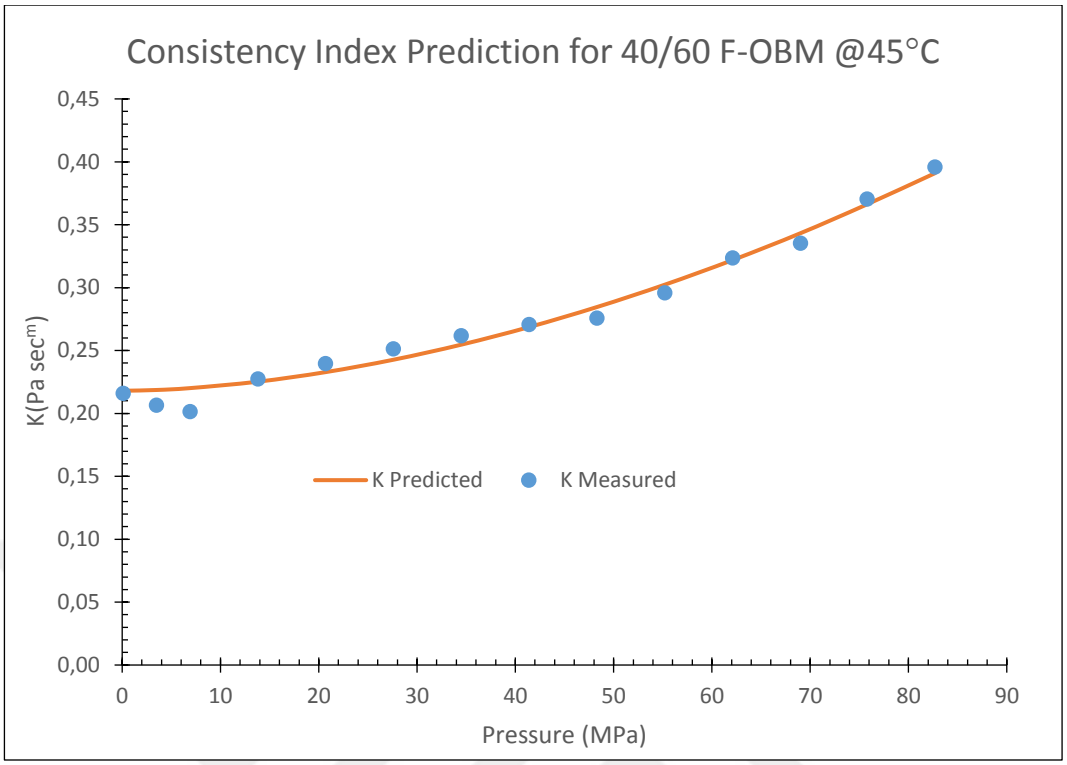


Figure-43: 40/60 w/o F-OBM Predicted and Measured Consistency Index 45°C

Compressible fluid fraction in the drilling fluid system and pressure effect on the yield stress is illustrated in Figure 44. As the temperature is another alteration factor for rheological parameters, same temperature results are interpreted. In this graph, 45°C test results for F-OBM with 20/80 w/o, 30/70 w/o and 40/60 w/o ratio fluid systems are analyzed. This evaluation is carried out by taking the atmospheric yield stress values at each temperature conditions as a reference point. Then calculate the percentage increment at 20.7 MPa, 41.4 MPa, 62.1 MPa and 82.7 MPa, respectively. The higher percentage increase is observed at 20/80 w/o samples compared to other fraction ratios. As stated more volume of compressible fluid in the system, change in the yield stress is more dramatic with respect to pressure change. When the pressure is changed from atmospheric condition to 20.7 MPa; yield stress reached more than 55% of atmospheric one, or it is 132% at 62.1 MPa. Energy requirement to initiate the fluid flow or pump start-up is 186% higher than the atmospheric condition that may leads to formation breakdown in the operational conditions. The

increment is in modest level in 30/70 w/o F-OBM system, but higher than the 40/60 fraction system in the percentage values. For example, 20.7 MPa yield stress is 13% more than the atmospheric yield stress, at 41.4 MPa it reaches to 28% or at 82.7 MPa, there is a 56% increment compared to the atmospheric one. At 45°C test conditions 40/60 w/o samples show the least percent increase on the reference-atmospheric yield stress readings. The system is barely affected by the pressure change because of the diminished compressible fluid volumetric ratio. The percentage of reference – atmospheric yield stress increment for 20.7 MPa, 41.4 MPa, 62.1 MPa and 82.7 MPa values are; 5%, 16%, 25% and 37%, respectively.

In addition, Figure 45 illustrates Consistency Index and Pressure susceptibility in terms of compressible fluid fraction in the drilling fluid system, thus atmospheric Consistency Index is kept as a reference point at the constant temperature, 45°C. Likewise the Yield Stress, there is a sharp change observed for 20/80 w/o samples compared to the other fractions. Increase in the Consistency Index is 80% at 41.4 MPa or 164% at 62.1 MPa. On the other hand, the pace in the increment is decreased as the water phase is increased in the fluid. For 30/70 w/o samples, the increase is 34% when the pressure is changed to 41.4 MPa, 55% at 62.1 MPa.

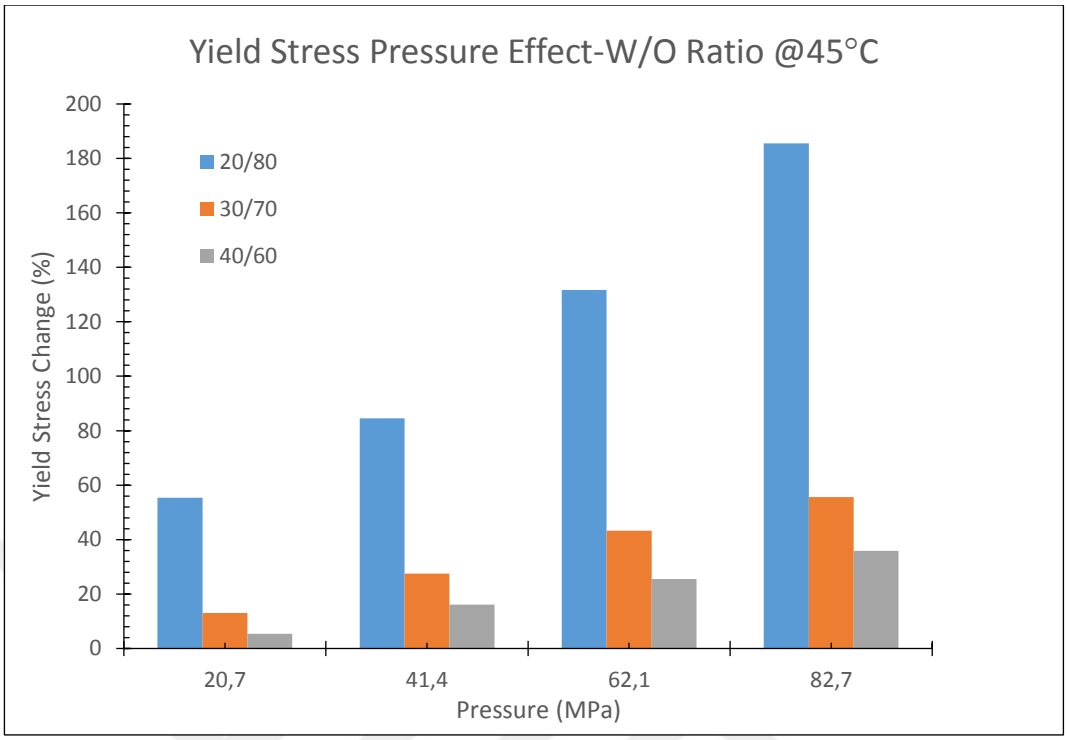


Figure-44: Compressible Fluid Fraction and Pressure Effect on Yield Stress

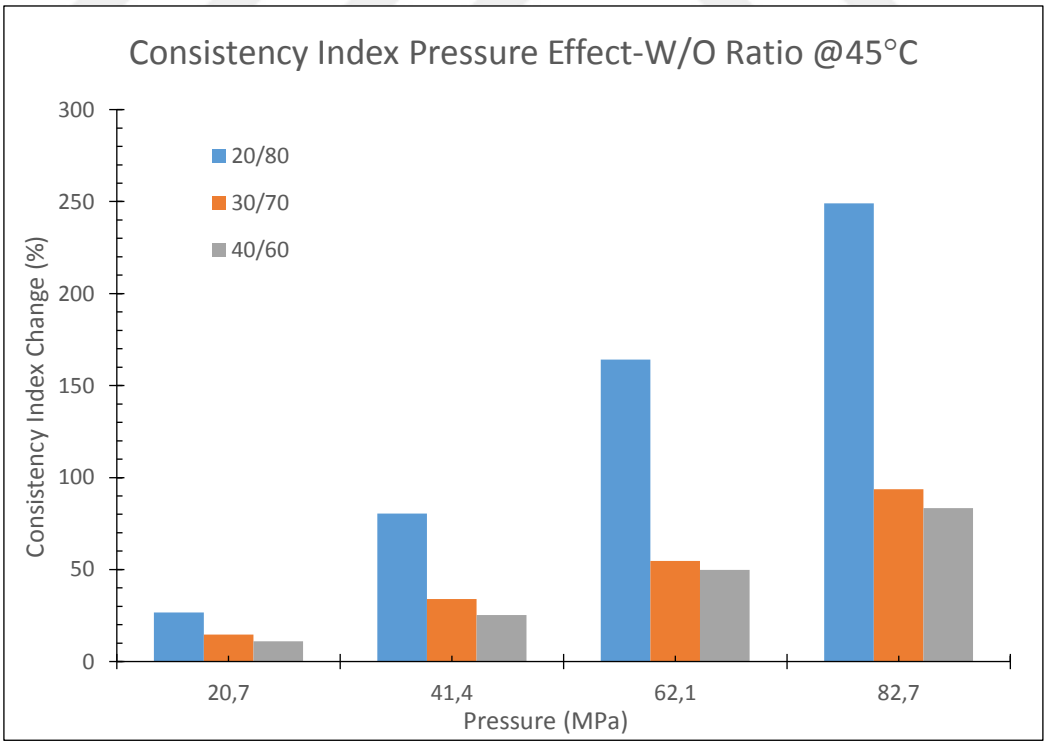


Figure-45: Compressible Fluid Fraction and Pressure Effect on Consistency Index

7.2 Temperature Effect

Proposed pressure dependent rheological equations work properly at constant temperature conditions. So far, mid-temperature operational conditions are tested and simulated. In addition, model functionality at higher temperatures, needed to be validated. When the w/o ratio is increased, Yield Stress and Consistency Index terms reached higher values compared to lower w/o ratio formulated systems. Also stated, at higher temperature conditions rheological parameters are decreased and very low numerical values are observed in temperature effect sensivity data. Therefore, 40/60 w/o formulated F-OBM are analyzed at 100°C temperature. Sample preparation is the same but test methodology is altered to obtain the steady constant temperature in the test chamber. After preparation and set-up the test protocol, fluid is pre-sheared at 1000 s^{-1} rate of deformation in the pre-heated chamber (100°C) at half an hour. The Rheometer-Physica program measures steady sample temperature with in the accuracy of ± 0.3 °C. When reached the target temperature, test intervals has been started. Shear rate is ramped decreasing from 1200 s^{-1} to 10 s^{-1}. To minimize the barite or any colloidal system sag, samples are changed in every 3 hours of test interval. At each pressure points test is repeated three times to get data set in the plus/minus five-percentage range. Figures 46 and 47 illustrate the deformation behavior of 40/60 w/o sample at 100°C with different pressure conditions. A characteristic behavior of Yield Power Law rheological equation is shown in the deformation phase of samples. First fluid needs a stress value to start the viscous flow, followed by shear thinning behavior in some degree. Yield stress values of 100°C readings at 40/60 w/o are lower than the 45°C measurements. That is expected, because streamlines or fluid molecules has higher energy level inside the system and shows less resistance to flow. However, pressure increments led to increase in deformation-stress responses. Shear stress value is almost doubled when the pressure is changed from 6.9 MPa to 82.7 MPa at the 1200 s^{-1} shear rate condition. In addition, there has been a 24% increase in stress response at 404 s^{-1} shear rate at the 55.2 MPa test interval compared to 20.7 MPa.

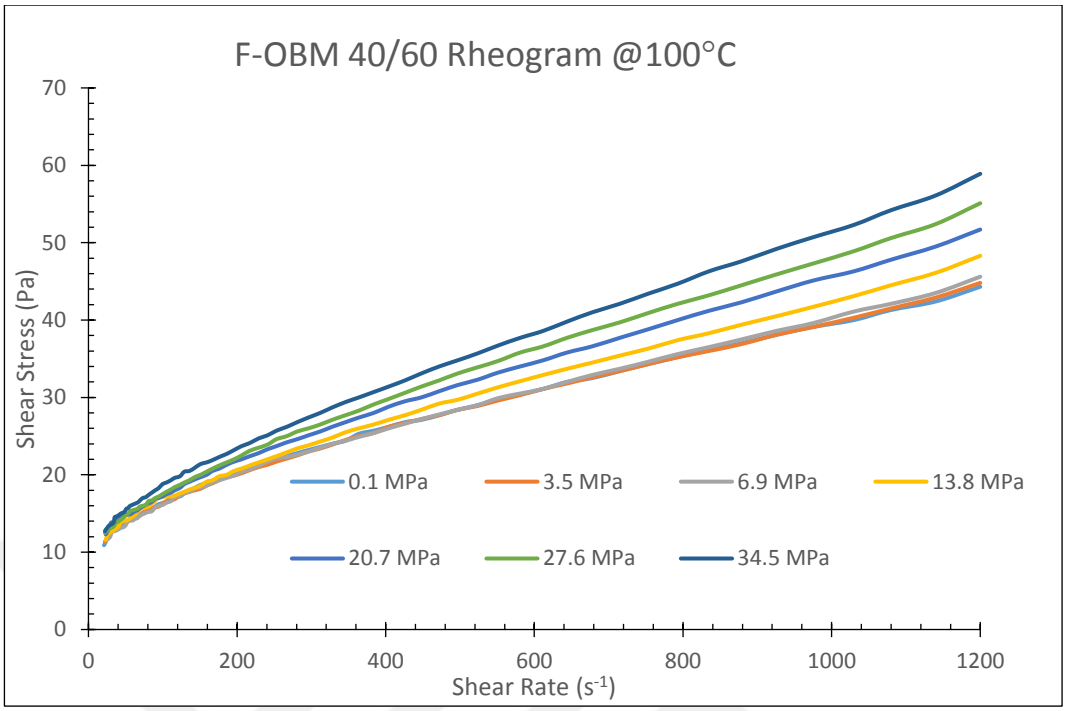


Figure-46: Rheogram-1 for 40/60 F-OBM at 100°C (0.1 to 34.5 MPa)

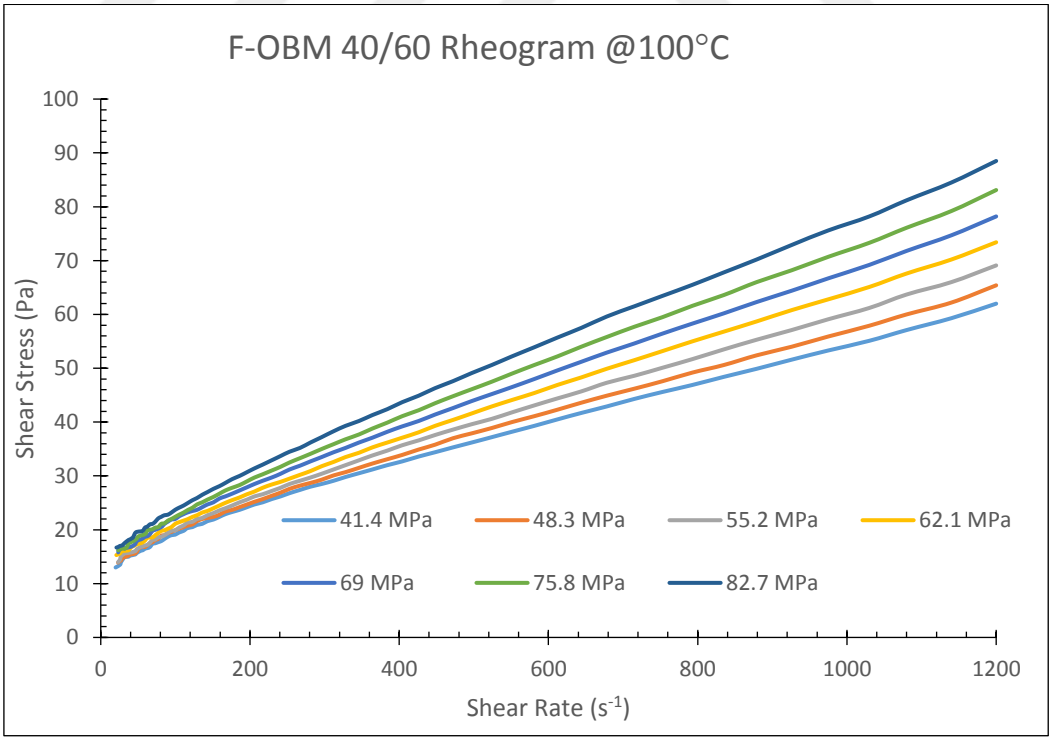


Figure-47: Rheogram-2 for 40/60 F-OBM at 100°C (41.4 to 82.7 MPa)

Nonlinear regression analyses is followed Yield Stress - τ_y, Consistency Index - K and Fluid Flow Behavior Index – m, of Yield Power Law model. Fluid flow behavior index is almost constant and obtained between 0.74 and 0.77, the average value of 0.76, which is also consistent with previous samples and literature statements. Both the yield stress, τ_y, and Consistency Index, K, increase with pressure. Parameters are tabulated in Table 17.

Table-17 Rheological Parameters of 40/60 w/o F-OBM at Different Pressure at 100°C

Pressure (MPa)	τ_y (Pa)	K (Pa sec^m)	m
0.1	11.2200	0.1466	0.7600
3.5	11.2294	0.1466	0.7600
6.9	11.0682	0.1498	0.7600
13.8	11.1287	0.1604	0.7600
20.7	11.3718	0.1747	0.7600
27.6	11.0516	0.1896	0.7600
34.5	11.4566	0.2036	0.7600
41.4	11.6831	0.2155	0.7600
48.3	11.7449	0.2284	0.7600
55.2	11.5934	0.2455	0.7600
69	11.8857	0.2619	0.7600
75.8	12.1612	0.2805	0.7600
82.7	12.2060	0.3009	0.7600

Proposed pressure dependent rheological equation's parameters are presented in Table 18. Yield stress comparison with respect to measured and model prediction is illustrated in Figure 48. Model curve perfectly fits the rheometer data with a 0.9189

value of R^2 and maximum differ of 2.4% at the 55.2 MPa condition. Figure 49 demonstrates the predicted and measured Consistency Index values. Model calculation coincides the rheometer Consistency Index values with a maximum 1.8% differ at the 27.6 MPa pressure application of 0.9986 fitting regression.

Table-18 40/60 w/o F-OBM Model Parameters at 100°C

Temperature (°C)	L (Pa)	N (Pa Bar^{-v})	v	R (Pa sec^{-m})	S (Pa sec^{m} Bar^{-g})	g
100	11.0696	9.6200E-05	1.4288	0.1445	2.7100E-05	1.3058

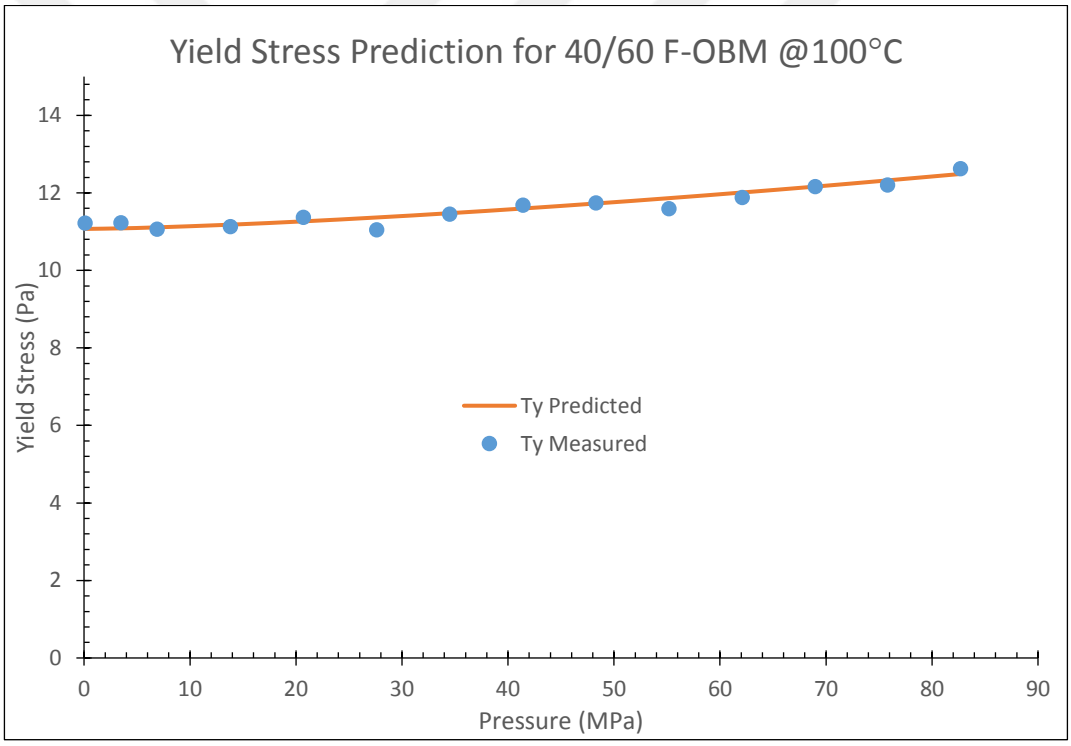


Figure-48: 40/60 w/o F-OBM Predicted and Measured Yield Stress 100°C

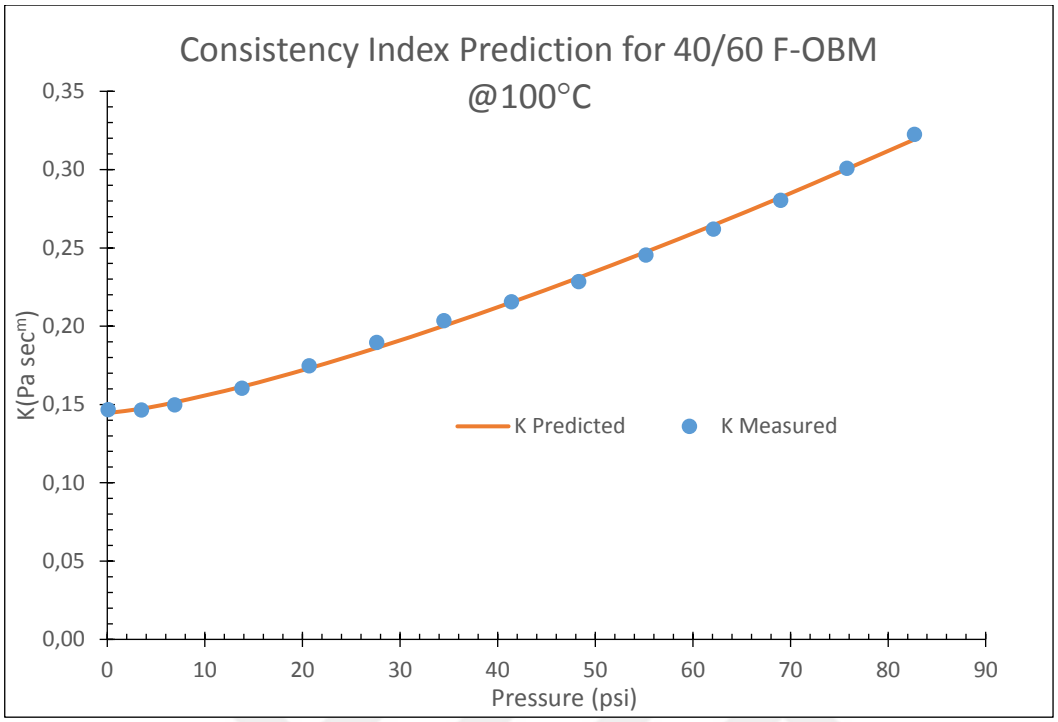


Figure-49: 40/60 w/o F-OBM Predicted and Measured Consistency Index at 100°C

Temperature affects the rheological behavior of colloidal systems. Percentage change in both yield stress and consistency index are shown in the Figures 50 and 51, respectively. At these analyses, 40/60 w/o ratio F-OBM is used at 45°C and 100°C readings are used. Two temperature conditions have same fluid and measurement methodology. Atmospheric values of both yield stress and consistency index are kept constant and percentage change at 20.7 MPa, 41.4 MPa, 62.1 MPa and 82.7 MPa are calculated.

According to Figure 50, the change in yield stress at 45°C is 5% when the pressure is 20.7 MPa, 16% at 41.4 MPa, 25% at 62.1 MPa and 35% at 82.7 Mpa, compared to atmospheric pressure reference value. On the other hand, the rate of change is less at 100°C interest, namely 4% at 20.7 MPa, 7% at 41.4 MPa, 9% at 62.1 MPa and finally 16% at 82.7 MPa.

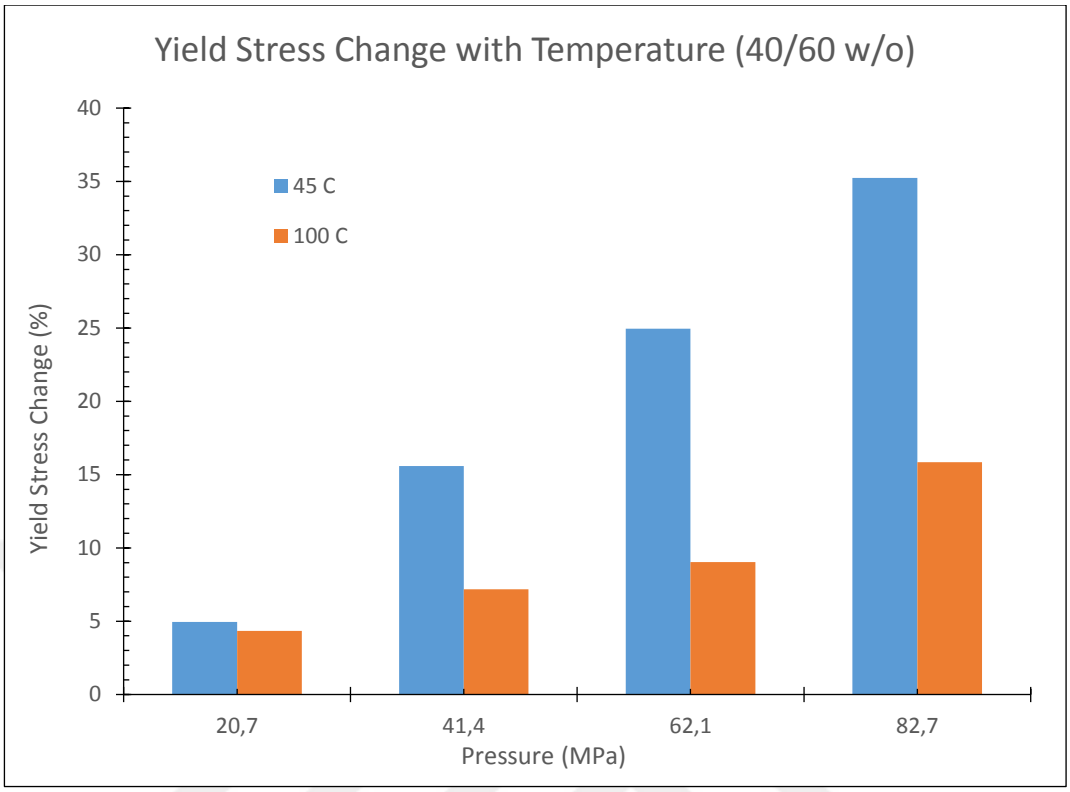


Figure-50: Temperature and Pressure Effect on Yield Stress

For considering the K value change at 45°C results, illustarted in Figure 51, 20% increase is observed at 20.7 MPa compared to atmospheric condition. When pressure is changed to 41.4 MPa, 35% increase is calculated. At 62.1 MPA change is 61%, at 82.7 MPa there has been a 98% increase. In 100°C analyses, calculated values are; 19% at 20.7 MPa, 47% at 41.4 MPa, 79% at 62.1 MPa and 120% at 82.7 MPa.

Unlike the yield stress trend, the percentage change in consistency index is higher at 100°C than 45°C. Also fluid flow index , m value is changed to 0.91 to 0.76 when temperature is changed from 45°C to 100°C. As shown, it is not easy to state any temperature trend on the rheological paremeters like the pressure phonemena for the slightly compressible fluids.

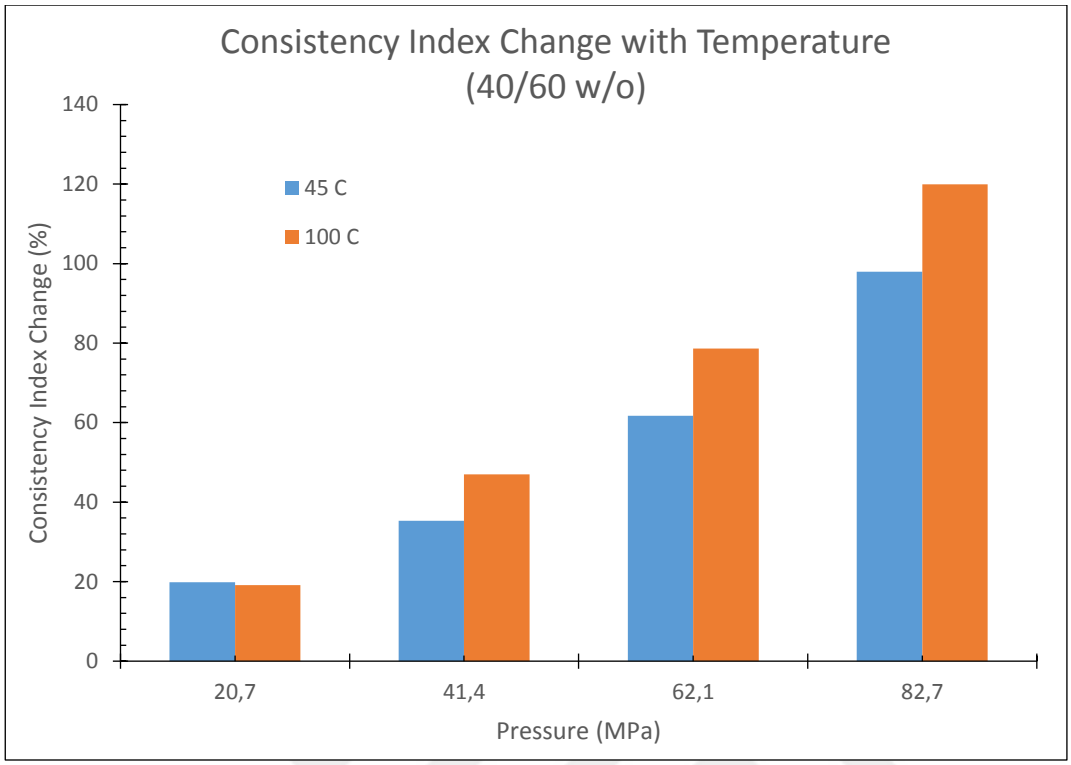


Figure-51: Temperature and Pressure Effect on Consistency Index

7.3 Mud Weight – Solid Effect

In this analysis, Diesel Based NAFs (DBF) with different mud weight are used to analyze any solid effect on slightly compressible fluid rheology. Controlled shear rate methodology is followed in all sample tests. 80/20 oil/water ratio systems are mixed with 3 different barite amount to obtain mud with 1044 kg/m^3 (8.7 ppg), 1404.4 kg/m^3 (11.7 ppg) and 1764.7 kg/m^3 (14.7 ppg) densities. To prevent any emulsifier or viscosifier effect on the rheology, three samples are formulated with same chemical ingredients except the Barite content. All the samples have 25%-wt $CaCl_2$ Brine phase. Chemical additives and formulation of fluids are illustrated in Table 19.

Table-19 Formulation of Different Mud Weight DBMs

CHEMICAL ITEM	SAMPLE COMPOSITION		
	1044 kg/m^3	1404.4 kg/m^3	1764.7 kg/m^3
Diesel (vol %)	80	80	80
Brine Phase (vol %)	20	20	20
Primary Emulsifier (vol %)	4	4	4
Secondary Emulsifier (vol %)	2	2	2
Fluid Loss Agent (g/l)	22.9	22.9	22.9
Viscosifier (g/l)	17.1	17.1	17.1
LSRV Agent (vol %)	3.5	3.5	3.5
Lime (g/l)	18.6	18.6	18.6
Barite (g/l)	157	715	1443

Tests are performed at 25°C for all samples. Fluids are pre-sheared in the pressure cell and let to be rest to obtain the relaxation period, then test interval is started with the shear rate ramped decreased methodology from 1200 s^{-1} to 20 s^{-1}. To minimize the barite or any colloidal chemical precipitation, samples are changed in every 3 hours of test intervals. At each pressure points, test is repeated three times to get the data set in the ± five-percent range.

Deformation behavior of 1044 kg/m^3, lowest weighted DBF follows the Yield Power Law model at 25°C. Graphs are divided into two parts to prevent any complexity, shown in Figures 51 and 52.

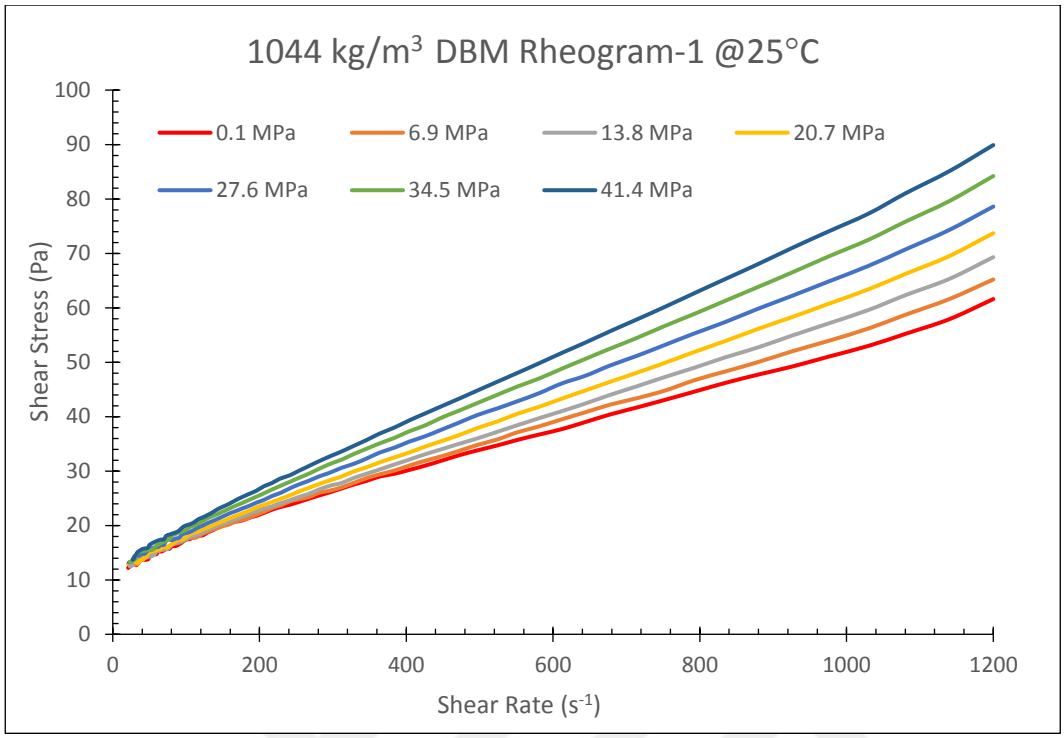


Figure-52: Rheogram-1 for 1044 kg/m^3 DBM at 25°C (0.1 to 41.4 MPa)

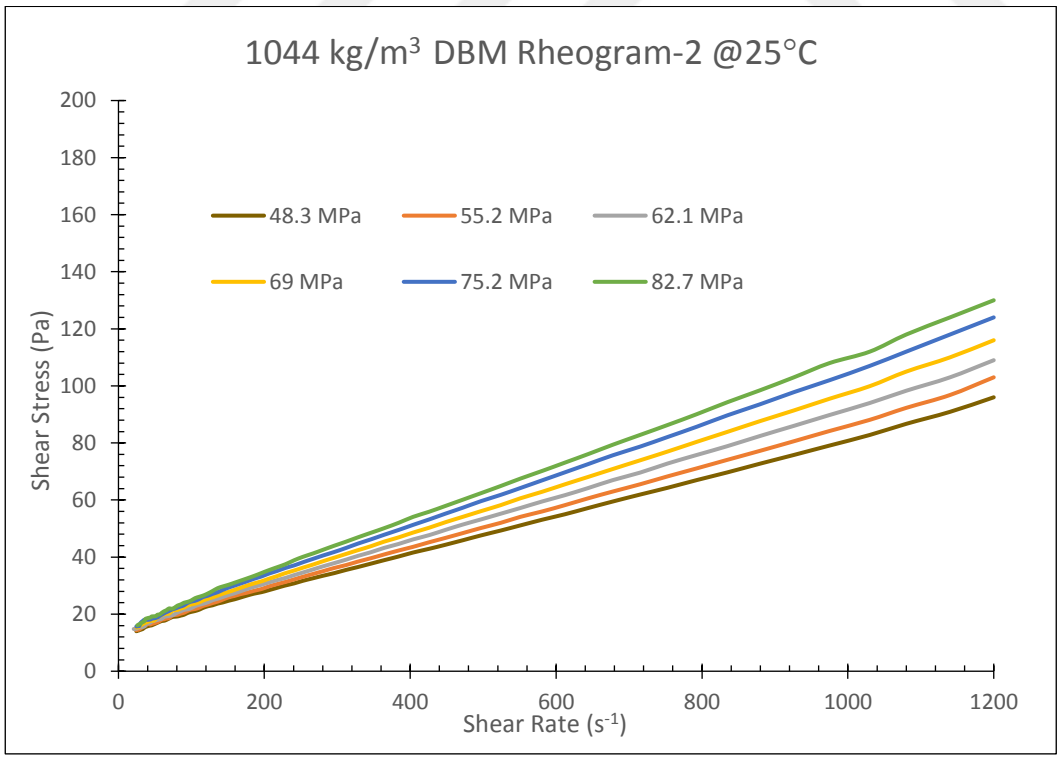


Figure-53: Rheogram-2 for 1044 kg/m^3 DBM at 25°C (48.3 to 82.7 MPa)

Results show, some stress level is required to initiate the deformation, called the yield stress, and show some degree of shear thinning behavior. Rheological parameters are found by nonlinear regression technique. Fluid flow behavior index, *m,* is not affected by pressure and almost constant an average value of 0.95. Stress response is increased in levels when the ambient pressure is increased. Pressure influences the deformation responses of the fluid. One third of increase in deformation practice is observed at the 600 s^{-1} rate of shear application when pressure is changed from atmospheric condition to 34.5 MPa, even doubled at 82.7 MPa. At the highest shear rate of application, stress reading reaches 50% higher values from atmospheric ones to 41.4 MPa or 110% higher at 82.7 MPa. Rheological parameters of 1044 kg/m^3 DBF are tabulated in Table 20.

Table-20 Rheological Parameters of 1044 kg/m^3 80/20 o/w at 25°C

Pressure (MPa)	τ_y (Pa)	K (Pa sec^m)	m
0.1	11.0740	0.1040	0.9500
3.5	11.5191	0.1198	0.9500
6.9	11.7768	0.0845	0.9500
13.8	11.7690	0.0843	0.9500
20.7	11.8947	0.0867	0.9500
27.6	12.4320	0.0869	0.9500
34.5	12.4080	0.0864	0.9500
41.4	12.9300	0.0914	0.9500
48.3	12.9540	0.0936	0.9500
55.2	13.3288	0.0928	0.9500
62.1	13.4190	0.1003	0.9500
69	13.9920	0.1013	0.9500
75.8	14.4750	0.1019	0.9500
82.7	14.5520	0.1148	0.9500

Consistency index of fluid is counted in the low value due to small amount of solid, which is less than 4% by volume in the system and cannot affected by pressure alteration. On the other hand, Yield stress is increased when pressure increases. In order to depict the pressure effect importance, "pump start-up pressure" is reached to 1.3 of surface design when 82.7 MPa of bottom hole head is subjected in-situ hole conditions. As stated before, system shows in a small degree of thinning behavior due to small amount of solid-surfactant interaction, common behavior of post-chemical rheological responses of OBMs.

All the stress inputs are examined through the proposed Equation-15 to find the model parameters, shown in Table 21.

Table-21 1044 kg/m^3 DBF Model Parameters at 25^{o}C

Temperature (°C)	**L (Pa)**	**N (Pa Bar^{-v})**	**v**	**R (Pa sec^{-m})**	**S (Pa sec^m Bar^{-g})**	**g**
25	11.3176	0.0022	1.0867	0.0681	1.50E-14	1.5750

Comparison of measured and model predicted Yield Stress is illustrated in Figure 54. There has been a good match is identified with a R^2 value of 0.9781 in every pressure level for Yield Stress parameter in 1044 kg/m^3 sample. Better convergence is identified in Consistency Index calculation, illustrated in Figure 55, except the atmospheric measured K value, which is out of trend.

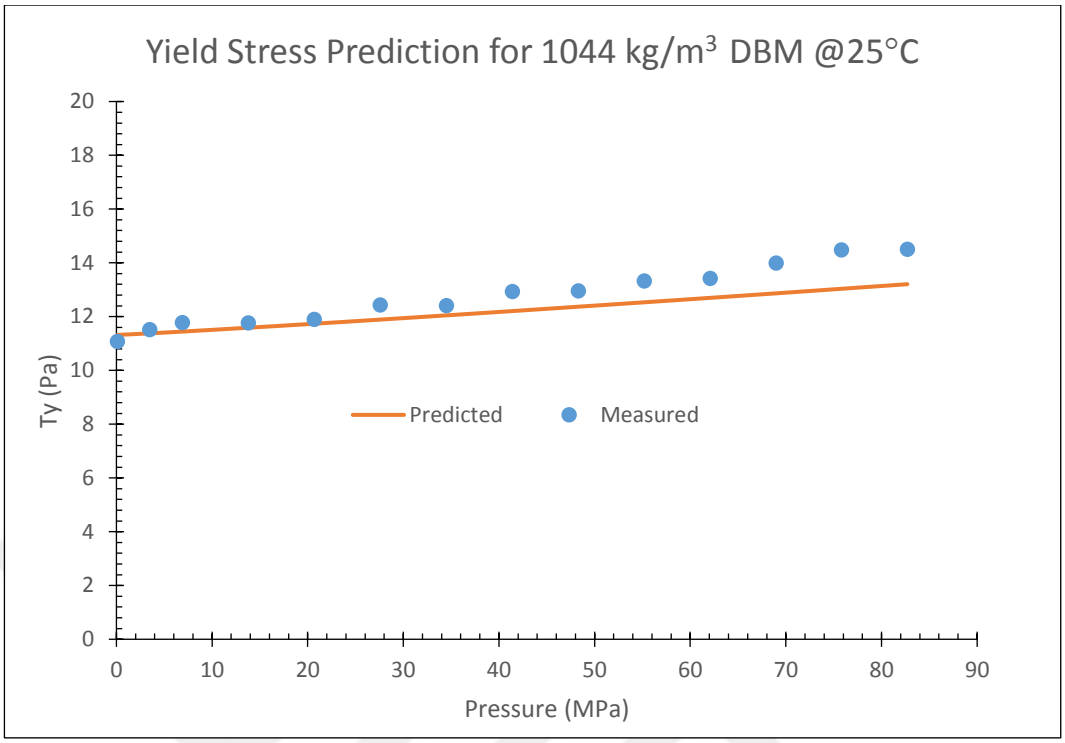


Figure-54: 1044 kg/m^3 DBM Predicted and Measured Yield Stress 25°C

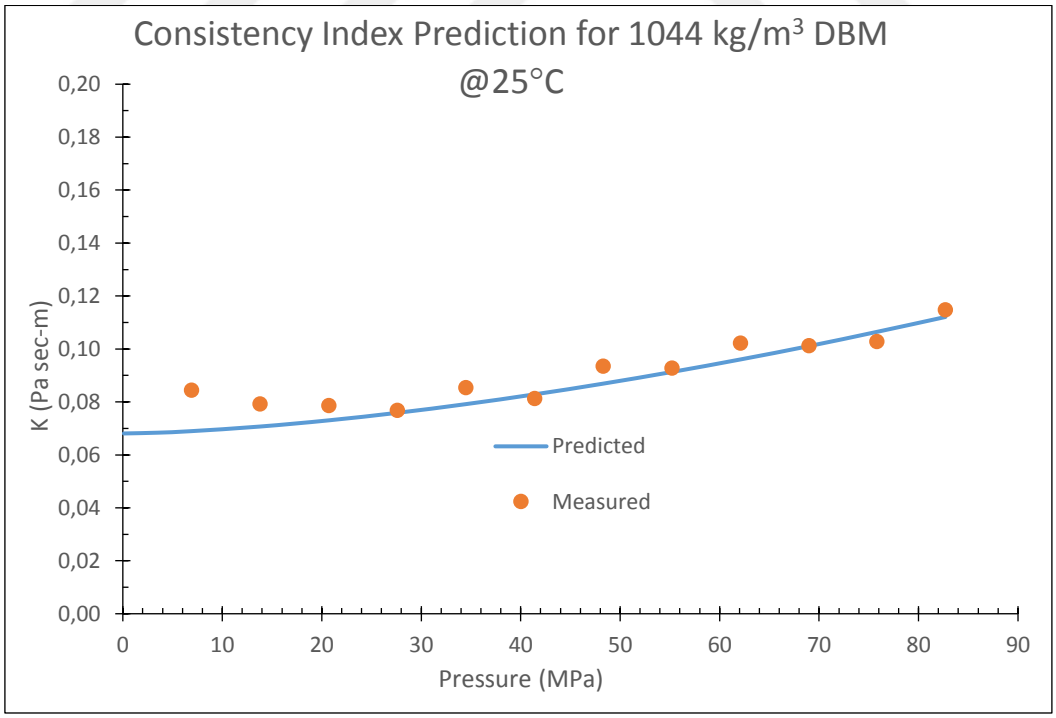


Figure-55: 1044 kg/m^3 DBM Predicted and Measured Consistency Index 25°C

Rheometer measurements and Model Prediction of constitutive stress levels are exemplified in Figure 56 which consists measurements at atmospheric, 41.4 MPa and 82.7 MPa pressures. Model overestimates the stress level at the higher level of deformation at the atmospheric conditions. Maximum 29% of difference is identified. Model converges the measured ones after the 300 s^{-1} shear rate and crosses in lower values with a maximum differ of 6.5%. However, at 41.4 MPa, good match and similar values in both higher – moderate and lower deformation levels are observed in the rheogram with a maximum discrepancy of 9.2% in all readings. Highest-pressure measurements and model prediction can almost be coincidence with each other. Divergence level is an average value of 3.3%.

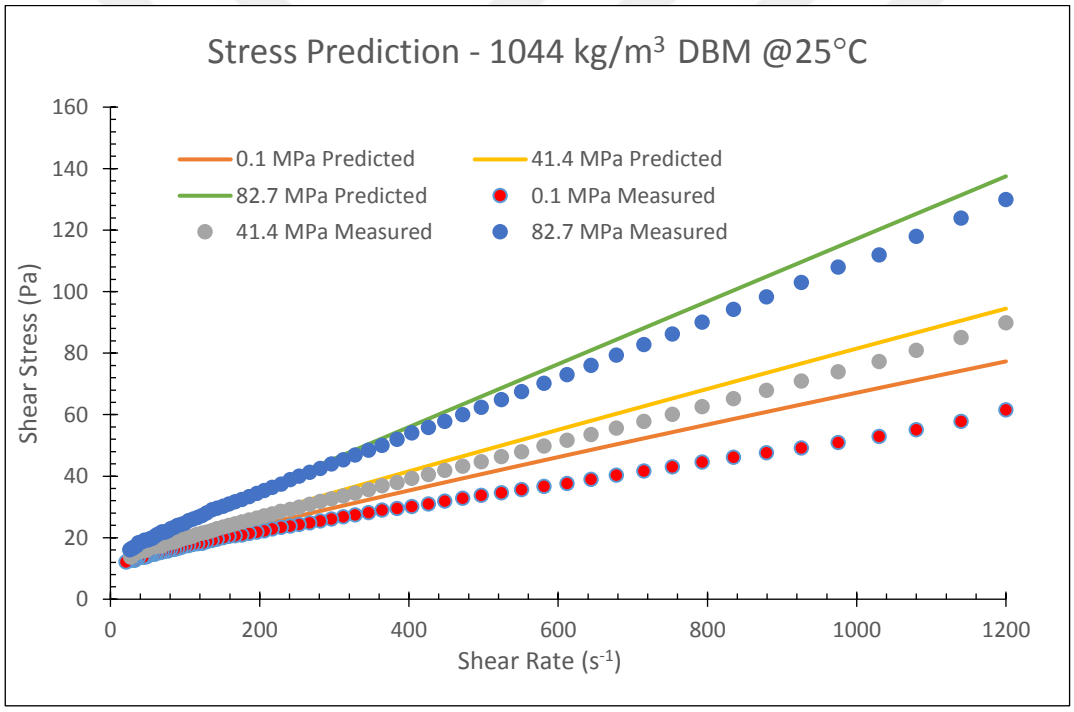


Figure-56: 1044 kg/m^3 DBM Predicted and Measured Stress Values

Mixing protocol of moderate weight sample, 1404.4 kg/m^3 DBF, is the same with the previous test fluid. In addition, chemical concentration is the same, already stated in Table 19, except the Barite content. 714.3 g/l of Barite is added to base system to obtain the desired mud weight. That leads to 14.5% volume increase in the system, hence diesel volume fraction reduces to 68.5%, but still the system has 80/20 o/w

ratio. During the rheological tests, temperature kept constant at 25°C, only pressure is changed within the intervals. For the test procedure, first samples are pre-sheared in the pressure cell; second fluid stays stagnant for a short time period to have the relaxation period. Finally measurements are started with the decreasing Shear rate ramped methodology from 1200 s^{-1} to 10 s^{-1}. To minimize the barite or any colloidal chemical precipitation, samples are changed in every 3 hours of test intervals. At each pressure points test is repeated three times to get the data set in the ± five-percent range.

Rheogram and stress behavior of 1404.4 kg/m^3 DBM are exhibited in Figures 57 and 58. Deformation behavior follows the yielding in the early rate of deformation levels, then curvature is followed with the slope less than 1 at higher shear rate application, thus data set typically follows the Yield Power Law model at 25°C.

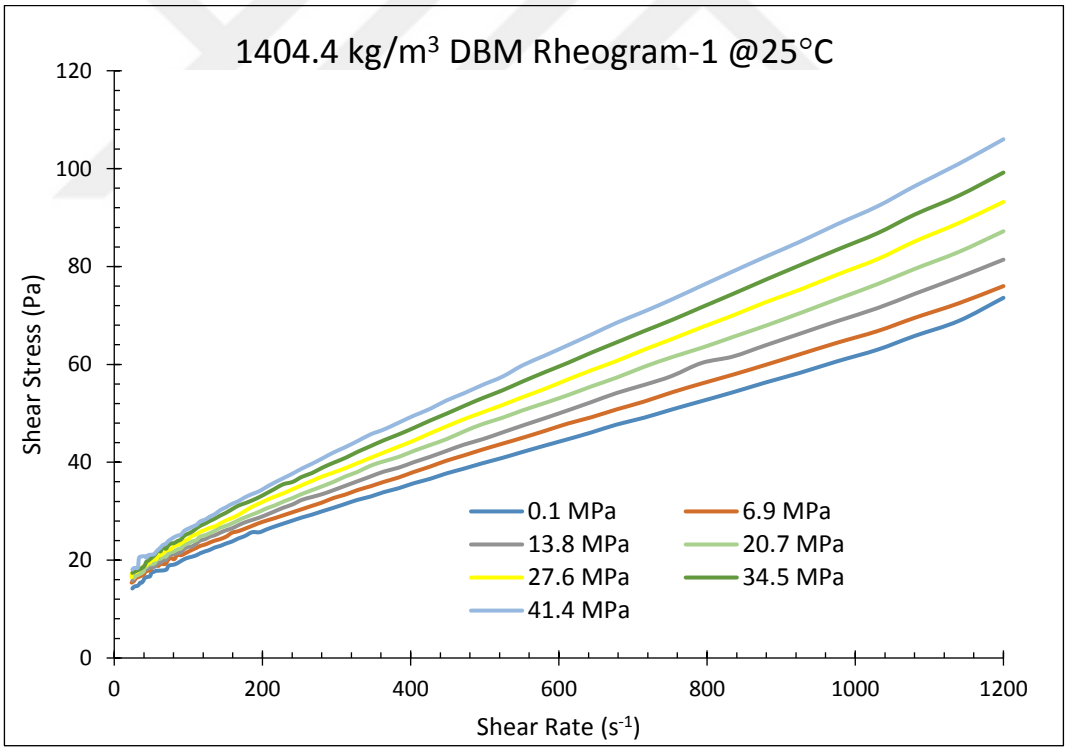


Figure-57: Rheogram-1 for 1404.4 kg/m3 DBM at 25°C (0.1 to 41.4 MPa)

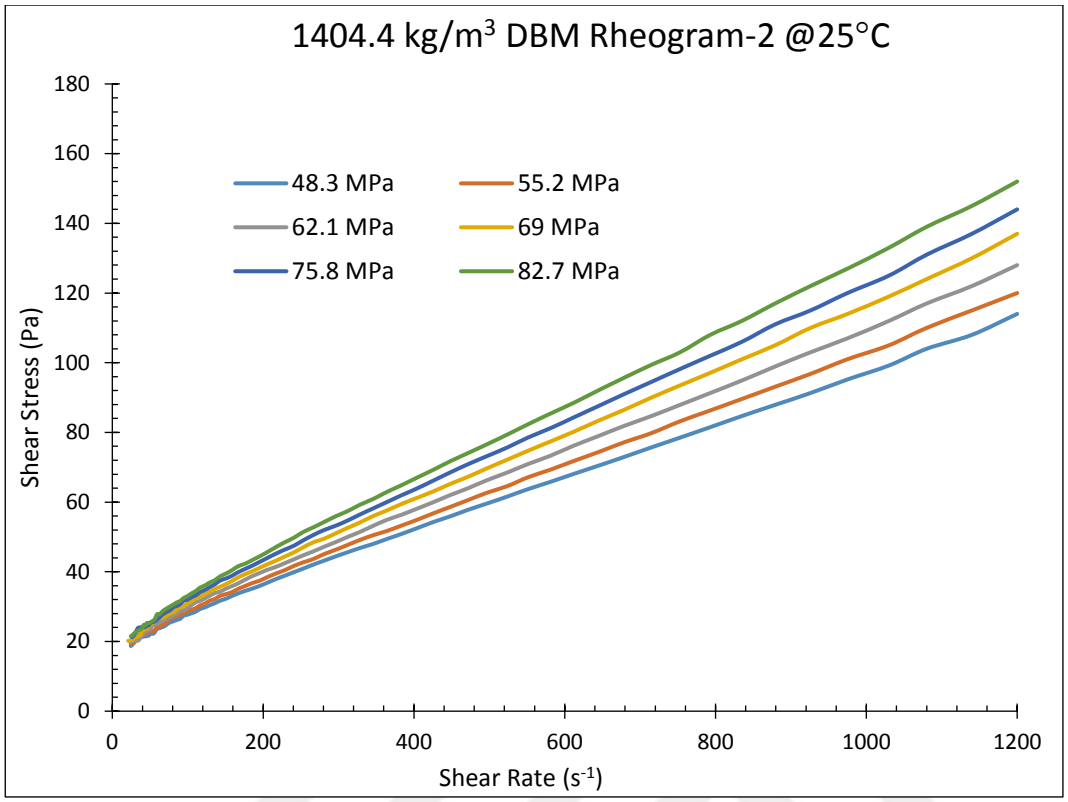


Figure-58: Rheogram-2 for 1404.4 kg/m3 DBM at 25°C (48.3 to 82.7 MPa)

Readings states that, a threshold value is required to trigger the creep flow, where the fluid velocity is too slow, or any irreversible deformation behavior. Furthermore, this "flow start-up stress" value is increased with pressure due to the compressible fluid effect. Three YPL Model parameters, namely Yield Stress, Consistency Index and Fluid Flow Behavior Index, are obtained from nonlinear regression calculations. Like the Yield Stress, Consistency Index is sensitive to subjected pressure and increased with pressure. Similar to previous hydrocarbon based drilling fluid muds, Fluid flow behavior index, *m*, is not affected by pressure and almost constant with an average value of 0.89.

Besides the rheological parameters, stress reaction of the sample is highly dependent on pressure alteration. At highest shear rate condition, 82.7 MPa reading is more than two times of atmospheric one. Furthermore; at 600 s^{-1} deformation rate, 34% increment is recorded with respect to 6.9 MPa value and within the same rate; 84.3%

increment is measured when the pressure is increased from 6.9 MPa to 75.8 MPa. Rheological parameters of 1404.4 kg/m^3 DBF are shown in Table 22.

Table-22 Rheological Parameters of 1404.4 kg/m^3 80/20 o/w at 25°C

Pressure (MPa)	τ_y (Pa)	K (Pa sec^m)	m
0.1	13.5560	0.1266	0.8900
6.9	14.0500	0.1459	0.8900
13.8	14.5430	0.1461	0.8900
20.7	15.0320	0.1551	0.8900
27.6	15.5202	0.1529	0.8900
34.5	16.0068	0.1560	0.8900
41.4	16.4932	0.1635	0.8900
48.3	16.9781	0.1597	0.8900
55.2	17.4618	0.1673	0.8900
62.1	17.9463	0.1900	0.8900
69	18.4290	0.1860	0.8900
75.8	18.9113	0.1875	0.8900
82.7	19.3932	0.1924	0.8900

Compared to atmospheric Yield Stress, additional 22% and 43% energy is required in the solid-liquid transition phase when test pressure showed up 41.4 MPa and 82.7 MPa respectively. Increment in the Consistency Index terms are; 23% at 20.7 MPa, 30% at 41.4 MPa, 42% at 62.1 MPa and 52% at 82.7 MPa compared to surface readings.

Proposed pressure dependent rheological model parameters in the Equation-15, are analyzed and illustrated in Table 23.

Table-23 1404.4 kg/m^3 DBF Model Parameters at 25°C

Temperature (°C)	L (Pa)	N (Pa Bar^{-v})	v	R (Pa sec^{-m})	S (Pa sec^m Bar^{-g})	g
25	13.5511	0.0076	0.9900	0.1287	3.0752E-07	0.6690

Model Yield Stress calculation overlaps the measured ones, illustrated in the Figure 59. Maximum discrepancy for 1404.4 kg/m^3 DBM is observed only 1.5% at 6.9 MPa condition. Comparison of measured and model predicted Consistency is illustrated in the Figure 60. There has been also a good match is identified with a R^2 value of 0.9179.

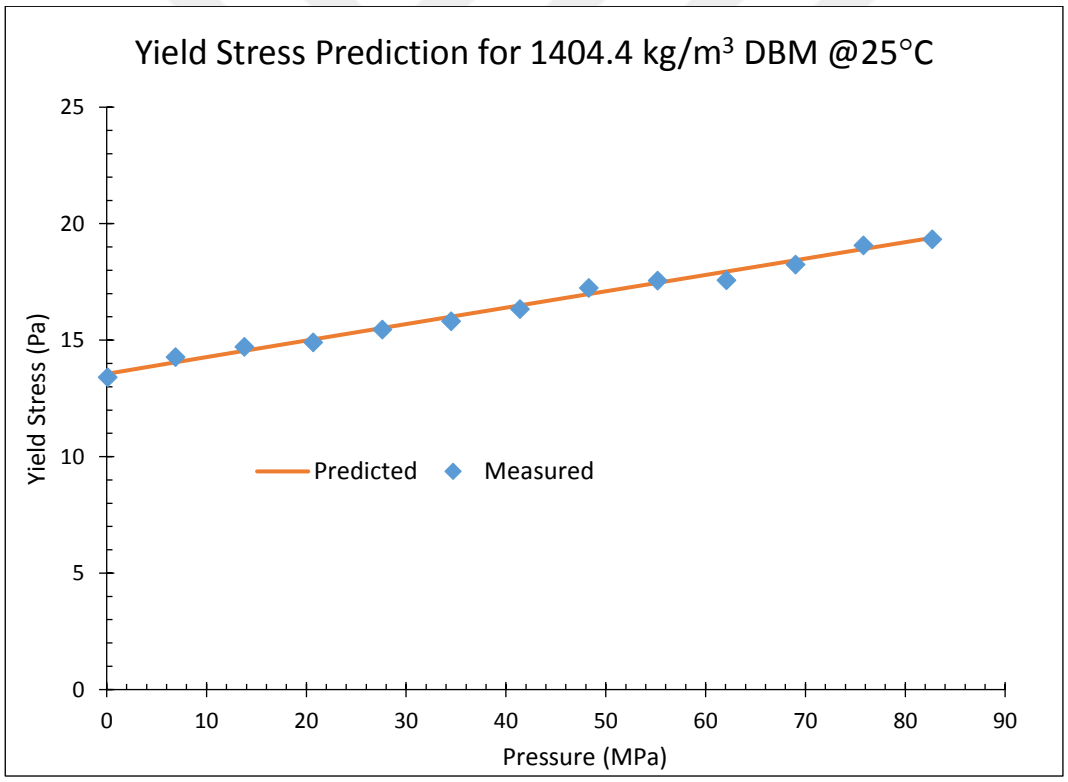


Figure-59: 1404.4 kg/m^3 DBM Predicted and Measured Yield Stress 25°C

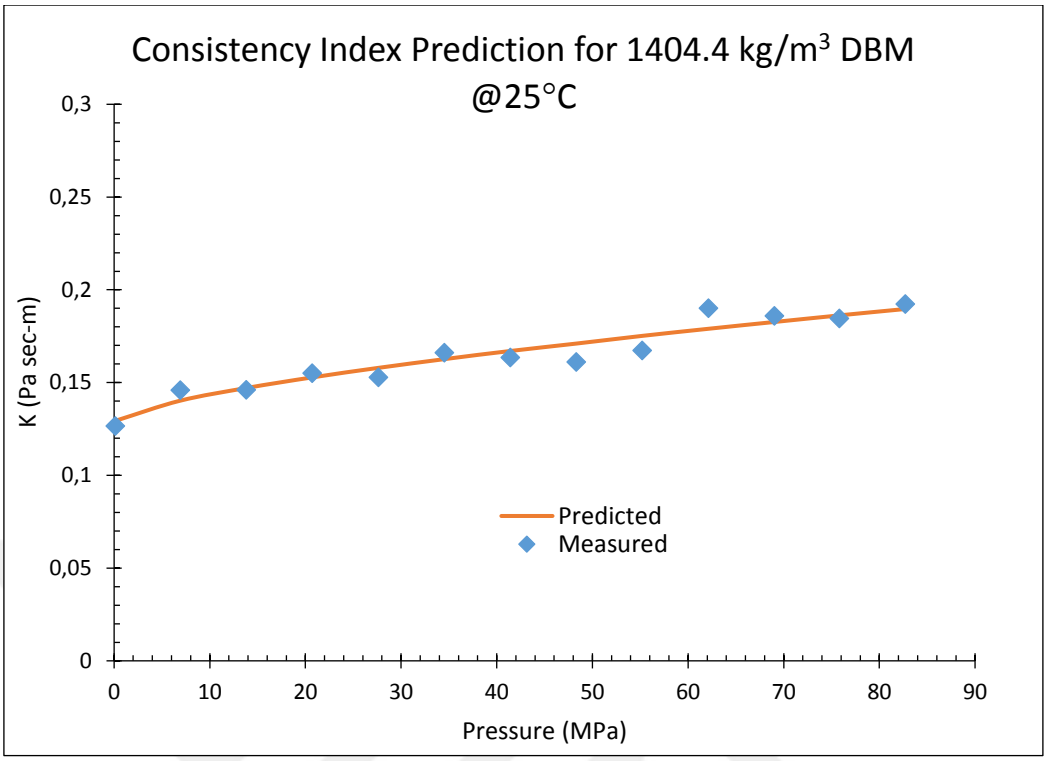


Figure-60: 1404.4 kg/m^3 DBM Predicted and Measured Consistency Index 25°C

Figure 61 delineates the measured stress values and Model calculations within the test shear rate levels. At 6.9 MPa curve, model overestimates the measured ones until the 300 s^{-1} shear rate point with a maximum of 13% divergence. In contrast, after this shear rate model gets closer and almost gives the measured values. At 41.4 MPa curve, in all the upper plateau rates, moderate levels and low shear conditions, model predicts the measured values. The difference is less than 6% in all constitutive stresses. At 82.7 MPa curve, model slightly underestimates the measured ones until the 1000 s^{-1} shear rate levels with a maximum of 7% divergence. After 1000 s^{-1} shear rate, model converges and fits the measured values.

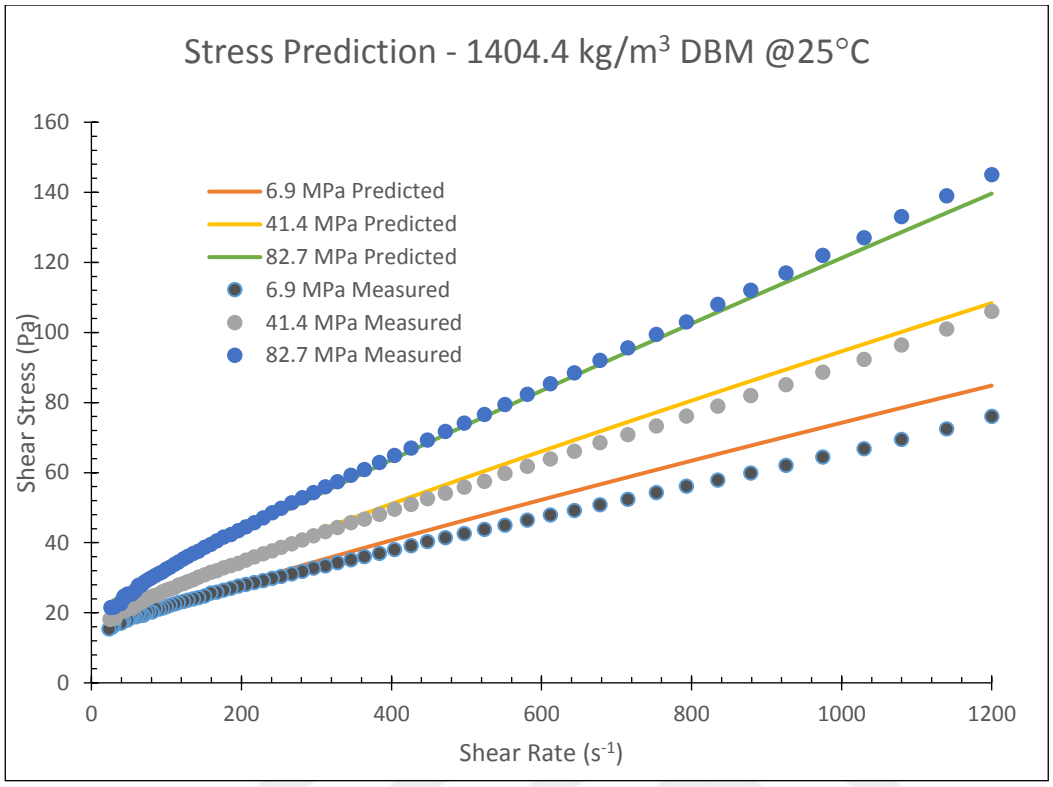


Figure-61: 1404.4 kg/m^3 DBM Predicted and Measured Stress Values

Third and maximum weighted sample, 1764.7 kg/m^3 DBM, chemical formulation has already been stated in the Table 19. Barite is used to obtain this weight, and 1443 g/l of Barite is added. This amount of solid causes 34% increase in volume. Compressible fluid volume ratio reduces to 59.5%, brine ratio reduces to 14.5%, yet the oil-water ratio remains 80/20. Rheological tests are performed at constant 25°C temperature; pressure is only the varying parameter to be investigated. Before the data recording, similar procedures are followed, "pre-shearing and resting". Like the previous rheological experiments, shear rate is ramped from 1200 s^{-1} to 10 s^{-1}. To minimize the barite or any colloidal chemical precipitation, samples are changed in every 3 hours of test intervals. At each pressure points test is repeated three times to get the data set in the ± five-percent range.

All the stress behavior of 1764.7 kg/m^3 DBM, from atmospheric conditions to 82.7 MPa, are illustrated in Figures 62 and 63. Fluid deforms after a certain point of stress level and continues as a viscous flow with a shear-thinning behavior at 25°C. This

elastic-viscous transition is typical character of Hersley-Buckley fluids and expressed by Yield Power Law mathematical model.

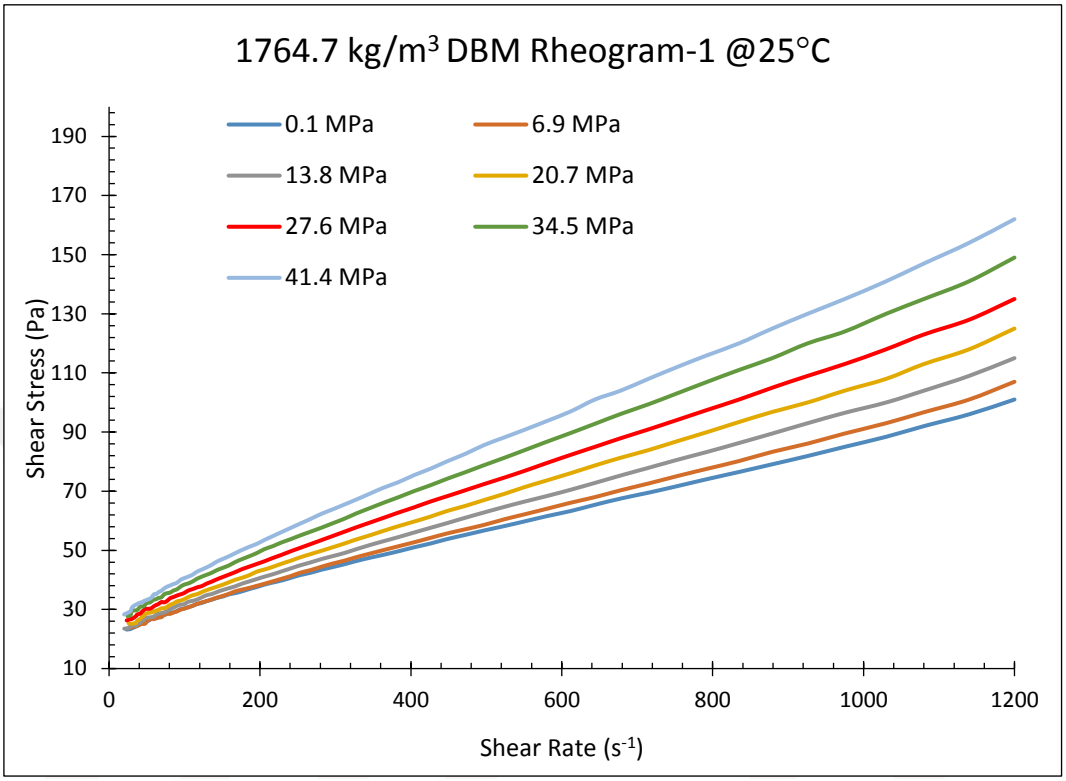


Figure-62: Rheogram-1 for 1764.7 kg/m^3 DBM at 25°C (0.1 to 41.4 MPa)

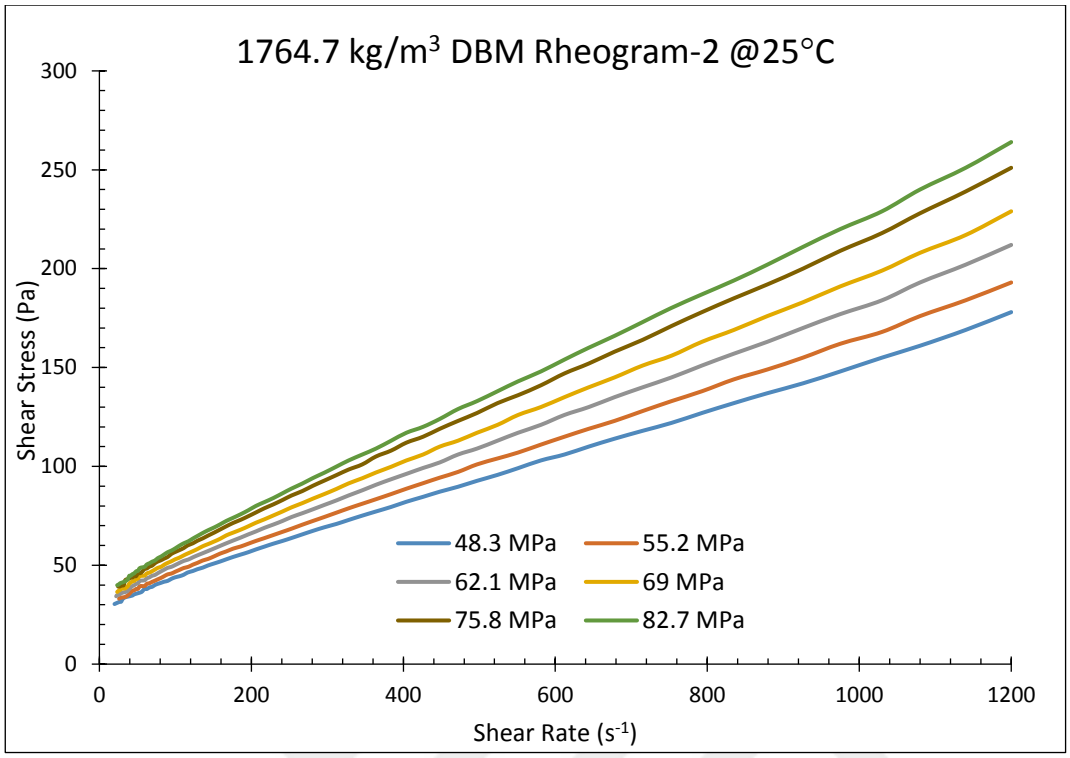


Figure-63: Rheogram-2 for 1764.7 kg/m^3 DBM at 25°C (48.3 to 82.7 MPa)

Yield Stress, Consistency Index and Fluid Flow Behavior Index, are also calculated from nonlinear regression method. Besides the physical-chemical interaction due to chemicals and temperature, pressure is another key factor that influences the rheological behavior in hydrocarbon-derived fluids. Permanent deformation value or transition to viscous flow is increased with pressure due to the compressible fluid effect. Degree of flow resistance, represented by Consistency Index, is increased with pressure. Similar to previous hydrocarbon based drilling fluid muds, Fluid flow behavior index, *m*, is not affected by pressure and almost constant an average value of 0.90.

At the 6.9 MPa condition having 30 s^{-1} shear rate, stress response is 24% higher when the applied pressure is doubled and reaches 53.5% value when the pressure is extended to 69 MPa. At the mid-level of rheogram, 600 s^{-1} rate of deformation, atmospheric measurement is boosted to 50% of original value in 41.4 MPa, and

almost 2.3 times in the highest-pressure condition. Rheological parameters of 1764.7 kg/m^3 DBF are shown in the Table 24.

Table-24 Rheological Parameters of 1764.7 kg/m^3 80/20 o/w at 25°C

Pressure (MPa)	τ_y (Pa)	K (Pa sec^m)	m
0.1	21.4333	0.1548	0.9000
6.9	21.2702	0.1481	0.9000
13.8	21.5477	0.1720	0.9000
20.7	22.8221	0.1644	0.9000
27.6	23.9750	0.1782	0.9000
34.5	25.5950	0.1831	0.9000
41.4	26.4602	0.2071	0.9000
48.3	28.4643	0.2168	0.9000
55.2	29.6479	0.2440	0.9000
62.1	31.3781	0.2622	0.9000
69	33.0902	0.2727	0.9000
75.8	34.9941	0.2825	0.9000
82.7	35.8367	0.2970	0.9000

There has been a 53% increase identified at the 69 MPa condition compared to the surface Yield Stress. Likewise, increase in 13.8 MPa Yield Stress value reaches to 38% when pressure is increased to 55.2 MPa. Increment in the Consistency Index terms are; 14% at 27.6 MPa, 30% at 41.4 MPa, 57% at 55.2 MPa and 90% at 82.7 MPa compared to surface reading.

Proposed pressure dependent rheological model parameters in the Equation-15, are analyzed and illustrated in Table 25.

Table-25 1764.7 kg/m^3 DBF Model Parameters at 25°C

Temperature (°C)	L (Pa)	N (Pa Bar^{-v})	v	R (Pa sec^{-m})	S (Pa sec^m Bar^{-g})	g
25	20.3012	0.0025	1.3060	0.1542	6.93E-06	1.4850

Predicted Yield Stress term in the Equqtion-15 and real data exemplification is presented in Figure 64. The absolute difference is less than 1.5% in all pressure intervals, except the atmospheric one. Surface prediction underestimates 5.3% of the measured yield stress. Comparison of measured and model predicted Consistency is illustrated in the Figure 65. Both the curvature trend of the graph and data fits each other. Calculated maximum difference value is 6.2% at 6.9 MPa.

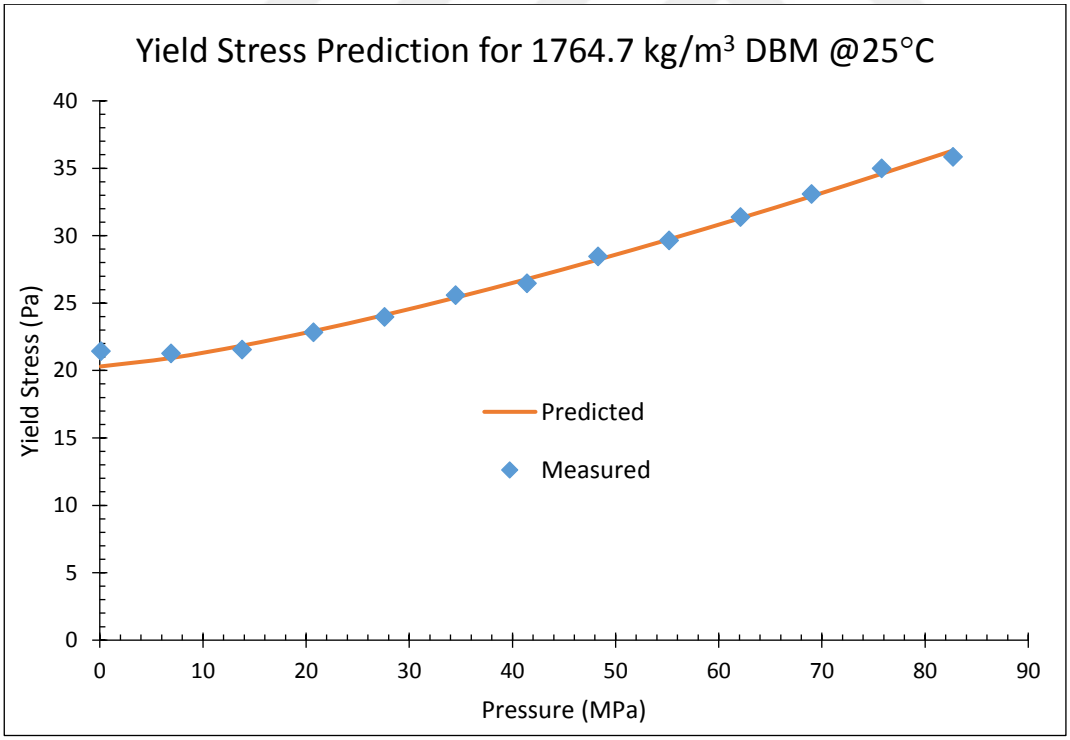


Figure-64: 1764.7 kg/m^3 DBM Predicted and Measured Yield Stress 25°C

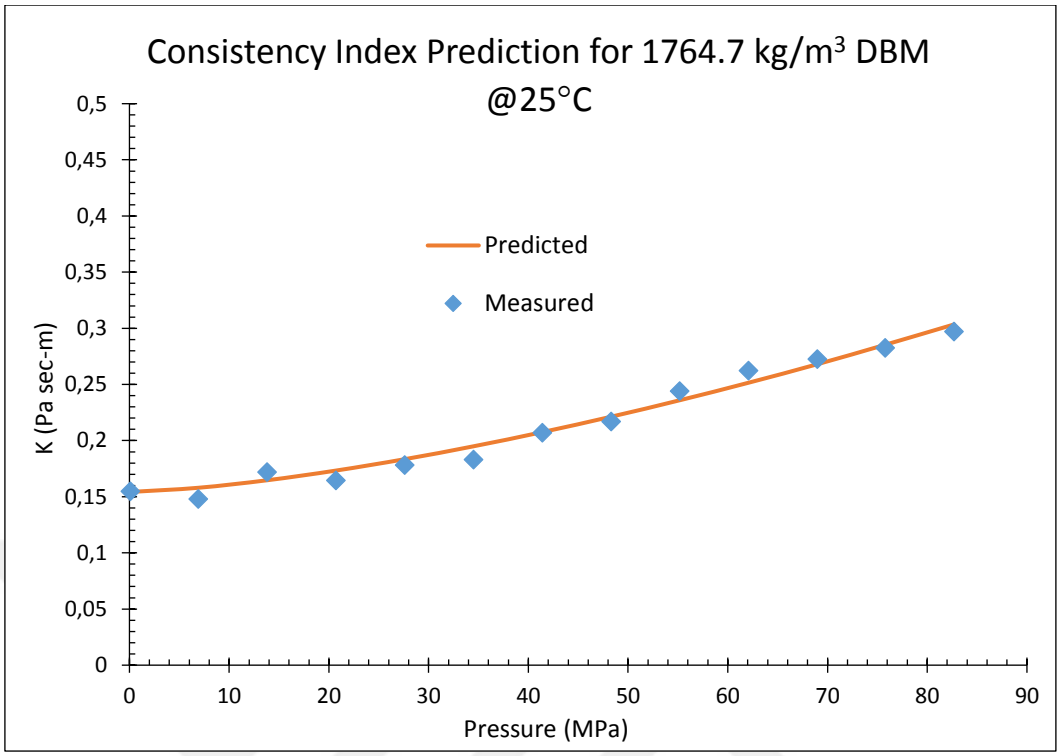


Figure-65: 1764.7 kg/m^3 DBM Predicted and Measured Consistency Index 25°C

All the deformation responses of rheometer and model data are illustrated in Figure 66. Graph belongs to 13.8, 48.3 and 75.8 MPa pressure conditions. Prediction slightly overestimates the 13.8 MPa data only the difference of maximum 6.5% between 600 to 1050 s^{-1}shear rate interval, and getting closer after 400 s^{-1}. At 48.3 MPa, model calculation almost gives the rheometer data with an average difference of 2.1%. In the 75.8 MPa curve, model slightly underestimates the measured ones and model converges and fits the low shear rate values.

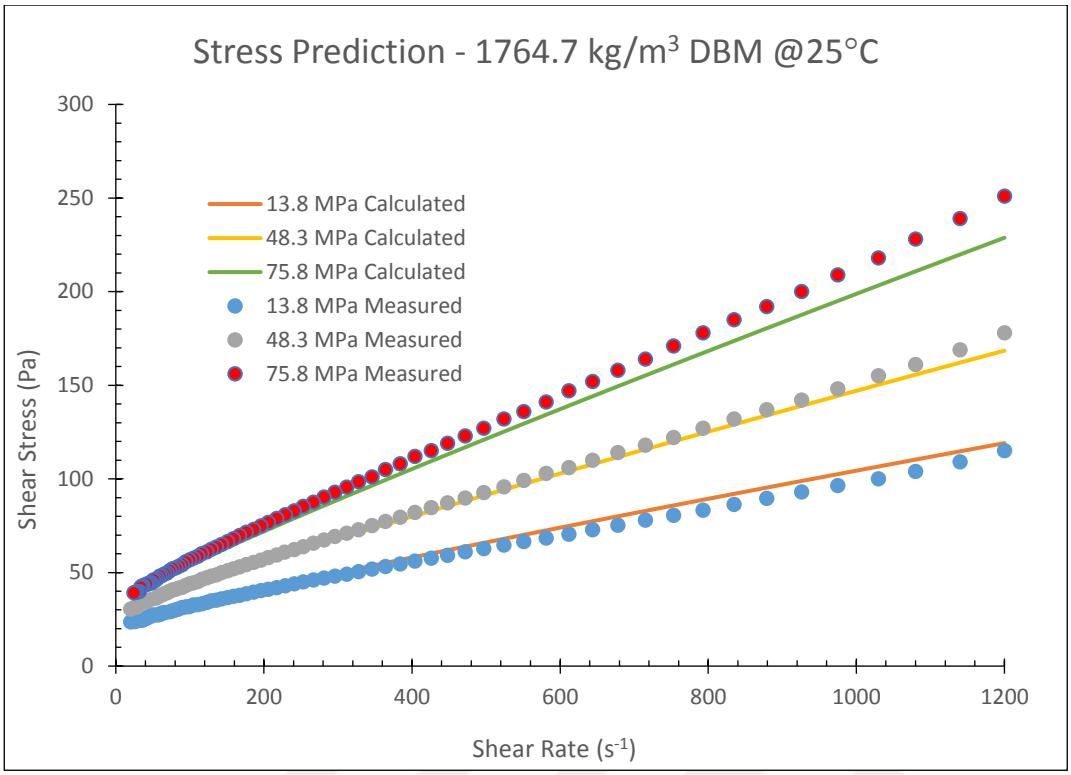


Figure-66: 1764.7 kg/m^3 DBM Predicted and Measured Stress Values

The oil-water ratio or the relatively compressible fluid volume analysis has already mentioned in terms of rheological parameters; yield stress and consistency index terms. Results states that the intensity in Yield Stress increase is higher when the oil ratio rises in the system.

Mud weight analyses based on similar approach. Except the weighting agent, other chemical formulation is the same for all three samples. Chemical additives and formulation of fluids are shown in Table 19. Even the 1044 kg/m^3 sample has the limited amount of Barite, concentration of Organophilic Clay, Secondary Emulsifier and LSRV agent amounts are designed in terms of 1404.4 kg/m^3 fluid requirements. Formulation based on wettability of Barite requirement and prevention of Barite precipitation. Highest level of yielding and consistency can observed in 1764.7 kg/m^3 fluid as expected because of highest solid amount. The volume of slightly compressible fluid portion is decreased when the mud weight increased. Therefore, it is supposed that, percentage of increase in rheological parameter get the maximum

value in the lowest weighed sample. However, physical-chemical phenomena and new generation surfactants and viscosifiers determines the trend responses.

Organophilic clays are specially blended clays, mostly treated with amines and became hydrocarbon-wetted used as main viscosifiers in NAF systems. It adjust the moderate level and high plateau of rheological behavior, LSRV agents directly increase the force requirement in elastic limit of system. Figure 67 shows that these two component are susceptible to solid amount in the system hence solid amount alters the magnitude of increase in Yield Stress. This graph is established by keeping the atmospheric Yield Stress as a reference point in each sample, and percentage change of Yield Stress at 20.7, 41.4, 62.1 and 82.7 MPa are investigated. For the 1044 kg/m^3 system; increase of percentages are; 7.5%, 16.8%, 21.2% and 31% when the pressure is varied from atmospheric condition to 20.7, 41.4, 62.1 and 82.7 MPa, respectively. Those values are; 11.1%, 21.7%, 31% and 44.1% for 1404.4 kg/m^3 system and 8.5%, 26%, 49.2% and 70.4% for 1764.7 kg/m^3 DBM.

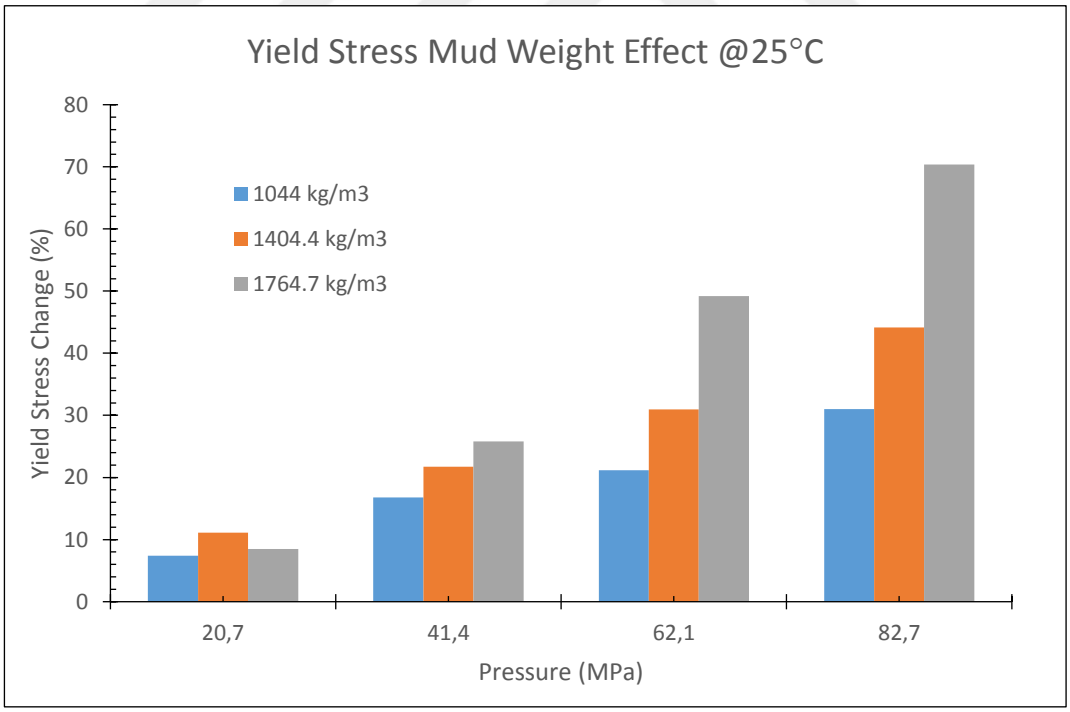


Figure-67: Mud Weight and Pressure Effect on Yield Stress

In YPL model, consistency index defines the degree of resistance to flow. Main solid in the test fluid is Barite. Secondary emulsifier coats the water-wet Barite particles and to be oil-wet in the final process. “In the oil medium environment” streamlines are not free to flow because of solid molecules and leads to increase in apparent viscosity. That statement is observed in the rheological analyses; Consistency Index rises as the Barite amount is increased in the system. Similar to Yield Stress – Mud weight relation, atmospheric Consistency Index is kept as a reference point at the constant temperature, 25°C and percentage change of Consistency Index at 20.7, 41.4, 62.1 and 82.7 MPa are calculated. Even the relatively compressible fluid amount is decreased; percentage increase in terms of pressure is more, in higher mud weight due to solid particle effect. For example; Consistency index increase is; 91.7% in 1404.4 kg/m^3 sample, 40.8% in 1404.4 kg/m^3 sample but 20% in 1044 kg/m^3 fluid, when the pressure is varied from 1764.7 kg/m^3 to 82.7 MPa. Percentage change is illustrated in Figure 68.

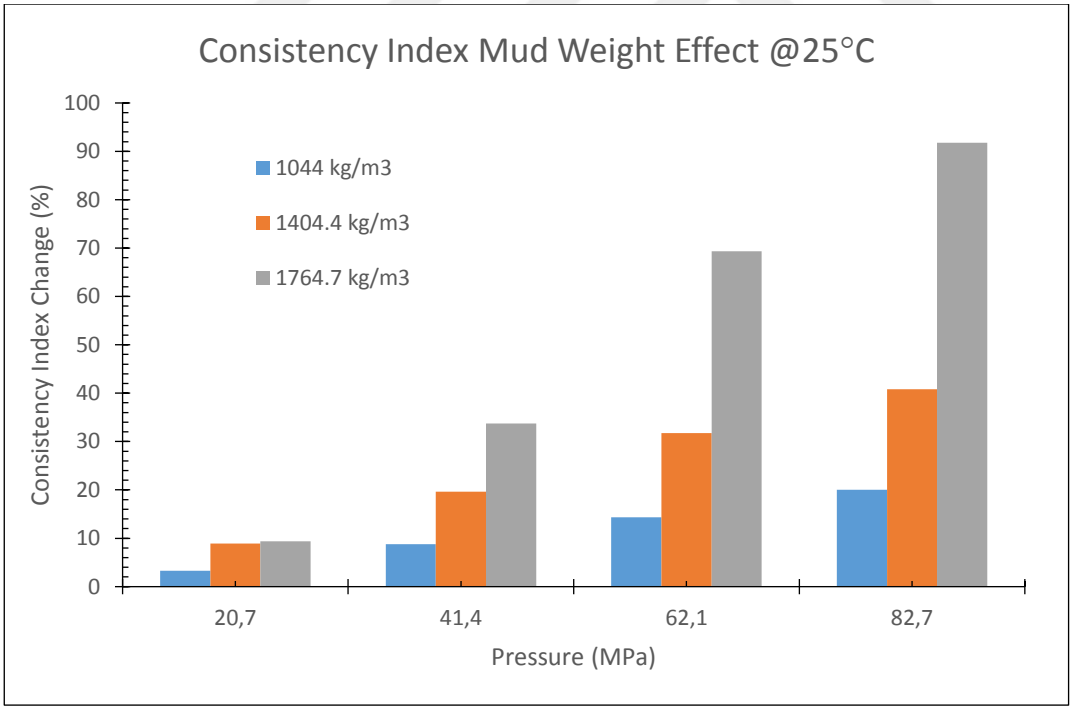


Figure-68: Mud Weight and Pressure Effect on Consistency Index

CHAPTER 8

CONCLUSIONS

In this study, pressure effect on slightly compressible drilling fluids are investigated, in both experimental study and theoretical work, at constant temperature conditions. In experimental work, diesel and synthetic based samples are used as a slightly compressible system; also water based muds are tested to see any pressure effect in theoretically incompressible drilling fluid. Rheological tests are conducted on Anton Paar MCR-302 HPHT rheometer. In theoretical work, pressure dependent constitutive stress equations are proposed and based on those rheological equations, frictional pressure loss calculation methodology is developed.

According to rheological analyses;

- The rheology of incompressible fluid based Drilling Mud systems can be affected in negligible level by pressure change at a constant temperature. Surface measurements can be used in operational calculations.
- Drilling Fluids that contains bubble coated low-weight systems' rheological deformation parameters also affected in negligible level by applied pressure change and proven by the experiments.
- Pressure phenomenon changes the slightly compressible fluid based Drilling Mud systems' rheology and stress requirement is increased with pressure increment.
- Rheological parameter analysis show that Fluid Flow Behavior Index, m parameter, cannot be changed with pressure change. On the other hand, both the Yield Stress or Point – τy and Consistency Index, so-called K parameter, are strongly dependent on pressure change.

For the proposed equations;

- It is identified that good match is observed for the proposed pressure dependent rheological equation in this study, with different test samples, chemical compositions and different deformation characteristics, compared to measured data. All the calculated rheological parameters have R^2 values between 0.92 and 0.99. Moreover, the model predicts the constitutive stress equations with different constant temperature intervals and chemical compositions.
- Derived hydraulic calculations based on proposed constitutive stress equations are validated with real field application. In this situation, drilling fluid system shows yield character with shear-thinning deformation behavior. Two different flow rate checks with pressure readings were obtained from the field measurements. Model calculations in the annular geometry slightly overestimates the on bottom pressure values with a very low absolute difference.
- Hydraulic calculations based on a rheological characterization underestimates the in-situ annular pressure frictional pressure loss for slightly compressible drilling fluid systems. This can also cause operational problems.
- Hydraulic calculation based on Lee et.al.'s equation underestimates around 9.5% measured pressure at 2662 m. at 0.3 m^3/s flow rate and 55°C. At this point of interest, proposed rheological and hydraulic equations have the discrepancy of 1.36%.

In addition to pressure effect on slightly compressible systems' rheology examination, oil/water volumetric ratio, solid amount and temperature effects are examined in both on rheological parameters and proposed equations.

For the oil/water ratio effect;

- As the oil fraction - as a continuous phase, is increased volumetrically compared to the water – brine phase, pressure dominates the rheological

parameters or stress requirements of flow is in the higher levels for the non-aqueous based drilling fluid systems.

- Oil water ratio play a big role in yield stress level. Higher yield stress values are observed when the o/w ratio is diminished.

For the solid amount effect;

- Both yield stress and consistency index rises as the Barite amount is increased in the system by considering the same experiment conditions.
- Even the relatively compressible fluid amount is decreased; percentage increase in terms of pressure is more for rheological parameters τ_y and K, in higher mud weight due to solid particle effect.

For temperature effect;

- Percentage change of Yield Stress is more at lower temperature test intervals compared to higher temperatures. Unlike the yield stress trend, the percentage change in consistency index is higher at 100°C temperature then 45°C.
- Moreover, at higher temperature situations with the same chemical compositions, fluid shows more shear thinning behaviour. Fluid flow index, m, is changed to 0.91 to 0.76 when temperature is changed from 45°C to 100°C.

CHAPTER 9

RECOMMENDATIONS

1. Validity of hydraulic calculations will be tested at higher flow rate and turbulent flow regime conditions.
2. Pipe rotation effect or a correlation factor may be added to hydraulic equataions.
3. Temperature effect shall be added into the rheological equations and frictional pressure loss calculation methodology.
4. Drilling fluid systems, which show higher properties of compressibility, can be tested for the proposed equations and calculation methodologies.

REFERENCES

Aadnoy B.S., Cooper I., Miska S.Z., Mitchell R.F., Payne M.L., Advanced Drilling and Well Technology, SPE Press, 2009, pp 191-301.

Ahmadi T., Andy P., 2009, "Modelling The Gelling Properties of Water-Based Drilling Fluids", AADE-2009-NTCE-12-02 presented at 2009 National Technical Conference and Exhibition held in New Orleans, Louisiana.

Alderman, N.J., Gavignet, A., Forex, S., Guillot, D., Maitland, G.J., 1988, "High-Temperature, High-Pressure Rheology of Water-Based Muds" SPE 18035, presented at the 63rd Annual Technical Conference and Exhibition held in Houston, Texas, 2-5 October.

Amani, M., "The Rheological Properties of Oil-Based Mud Under High Pressure and High Temperature Conditions", Advances in Petroleum Exploration and Development, Vol.3, No.2, 2012, pp 21-30.

Bland, R., Mullen, G., Gonzalez, Y., Harvey, F., Pless, M., 2006, "HP/HT Drilling Fluid Challenges", SPE 103731, presented at Asia Pacific Drilling Technology and Conference held in Bangkok, Thailand, 13-15 November.

Bourgoyne Jr, A.T., Milheim, K.K, Chenevert, M.E., Yonug Jr, F.S., Applied Drilling Engineering, Society of Petroleum Engineers Press, 1991, 2rd Edition, pp 113-183.

Coussot, P., Nguyen, O.D., Huynh, H.T., Bonn, D.,: "Viscosity Bifurcation in Thixotropic, Yielding Fluids", The Society of Rheology, May/June 2002, 46(3), 573-589. 18.

Davison, J.M., Clary, S., Saasen, A., Allouche, M., Bodin, D., Nguyen, V-A., 1999, "Rheology of Various Drilling Fluid Systems Under Deepwater Drilling Conditions and the Importance of Accurate Predictions of Downhole Fluid Hydraulics" SPE 56630, presented at the Annual Technical Conference and Exhibition held in Houston, Texas, 3-6 October.

Dipankar, C., Pal, S., Mohammed, M.R., 2009, "Prediction of Stand Pipe Pressure Using Conventional Approach" Chemical Engineering Research Bulletin, 13, 2009, pp 7-11.

Drilling Fluid Technologies, Aphron ICS Formulation and Maintenance Product Bulletin.

Eldar, D., Erlend, P., Knut, T., 2004, "Oil Based Drilling Fluids With Tailor-Made Rheological Properties: Results from A Multivariate Analysis" Annual Transactions of The Nordic Rheology Society, Vol.12, 2004.

Gandelman, R.A., Leal, R.F., Goncalves, J.T., Aragao, A.L., Lomba, R.F. and Martins, A.L., 2007, "Study on Gelation and Freezing Phenomena of Synthetic Drilling Fluids in Ultra Deepwater Environments", SPE/IADC 105881 presented at the SPE/IADC Drilling Conference held in Amsterdam, The Netherland, 20-22 February.

Gokdemir, M.G., 2010, "Modelling of Time Effect in Synteq – 11 ppg Drilling Fluid", The University of Tulsa Master Thesis, Tulsa, Oklohoma, 2010.

Gokdemir, M.G., Ozbayoglu, E.M., Majidi, R., Miska, S.Z., Takach, N., Yu, M., Merlo, A., 2011, "Gelation and Time-Dependent Rheological Behavior of Oil/Synthetic Based Drilling Fluids", AADE-11-NTCE-81 presented at the 2011 AADE National Technical Conference held in Houston, Texas, 12-14 April.

Gokdemir, M.G., Erkekol S. and Doğan H.A., 2017. "Investigation of High Pressure Effect on Drilling Fluid Rheology", OMAE2017-61449, Norway.

Growcock, F.B., Simon, G.A., Guzman, J. And Paiuk, B., 2004, "Application of Novel Aphron Drilling Fluids", AADE-04-DF-18 presented at the 2004 AADE Drilling Fluid Conference held in Houston, Texas, 6-7 April.

Houwen, O.H., Geehan, T., 1986, "Rheology of Oil-Base Muds" SPE 15416, presented at the 61st Annual Technical Conference and Exhibition held in New Orleans, LA, 5-8 October.

Ibeh, C., Schubert, J., Teodoriu, C., 2008, "Investigation on the Effects of Ultra-High Pressure and Temperature on the Rheological Properties of Oil-Based Drilling Fluids", AADE-08-DF-HO-13 presented at AADE Fluids Conference and Exhibition held in Houston, Texas, 8-9 April.

Joseph, R.R., Joseph, M.D., Saad, A.K., 2000, "High Pressure Rheology and Viscoelastic Scaling Predictions of Polymer Melts Containing Liquid and Supercritical Carbon Dioxide" Journal of Polimer Science, Vol.39, 2001 pp 3055-3066.

Lee, J., Shadravan, A., Young, S., 2012, "Rheological Properties of Invert Emulsion Drilling Fluid under Extreme HPHT Condition", SPE 151413 presented at the Drilling Conference and Exhibition held in San Diego, California, 6-8 March.

Martin-Alfonso, M.J., Martinez-Boza, F.J., Navarro, F.J., Fernandez, M., Gallegos, C., 2005, "Pressure-Temperature-Viscosity Relationship for Heavy Petroleum Fractions" Scient Direct, Fuel 86, 2007, pp 227-233.

M-I Fluid Company, M-I Drilling Fluid Engineering Handbook, Revised Edition, March 1998.

Maxey, J., 2007, “Thixotropy and Yield Stress Behavior in Drilling Fluids”, AADE-07-NTCE-20 presented at the 2007 AADE National Technical Conference held in Houston, Texas, 10-12 April.

Mezger, T.G., The Rheology Handbook, Vincentz Network Press, 2011, 3rd Revised Edition, 86.

Peder, C.F.M, Jan, M., Daniel, B., “Yield Stress and Thixotropy: On the Difficulty of Measuring Yield Stresses in Practice”, 2006, Soft Matter. 4.

Power, D., Catalian, D., Ivan and Steve W., 2003, “ The Top 10 lost Circulation Concern in Deepwater Drilling ”, SPE 81133 presented at the SPE Latin American Petroleum Engineering Conference held in Port of Spain, Trinidan, 27-30 April.

Power, P. and Zamora, M., 2003, “ Drilling Fluid Yield Stress: Measurement Techniques for Improved Understanding of Critical Drilling Fluid Parametres”, AADE-03-NTCE-35 presented at the 2003 AADE National Technical Conference held in Houston, Texas, 1-3 April.

Reed, T.D., Pilehvari, A.A., 1993, “A New Model for Laminar, Transitional, and Turbulent Flow of Drilling Muds” SPE 25456, presented at the Production Operations Symposium held in Oklahoma City, Oklahoma, 21-23 March.

Rommetveit R. and Bjorkevoll K.S., 1997 “Temperature and Pressure Effect on Drilling Fluid Rheologyand ECD in Very Deep Wells”, SPE 38282 presented at the Middle East Drilling Technology, Bahrain, 23-25 November.

Rubinho, H., Galindo, R., “Rheological Characterization of a Time-Dependent Fresh Cement Paste”, Mech. Time-Dependent Materials, 2009, 199-206.

Stefan S.Z., The University of Tulsa Advanced Drilling Engineering Class Notes, 2009.

Steefe, J.F., Rheological Methods in Food Process Engineering, Freeman Press, 1996, 2nd Edition, pp 294-348.

Valentin V. and Mario, B., 2013, “ Drilling Fluid for ERD: Rheology Requires More Than a Quick Look” AADE-13-FTCE-27 presented at the 2013 AADE National Technical Conference held in Oklohoma City, Oklohoma, 26-27 February.

Walstra, P.: Physical Chemistry of Foods, Marcel Dekker, 2003, pp 103-115.

Whittaker A. and Exlog Staff (ed), 1985 “Theory and Application of Drilling Fluid Hydraulics” International Human Development Corperations, Boston, 102.

Wilkinson, W.L.: Non-Newtonian Fluids, Peramon Press, 1960, pp 1-17, 22.

APPENDIX

A) 0.03 M^3/SEC FLOW RATE CALCULATION RESULTS

Depth (m)	Annular Velocity(m/s)	τ wall-corrected (Pa)	Reynolds Number	Flow Regime	Frictional Pressure Loss (Pa/m)
1	4.7354	30.4734	1315.2508	Laminar	1357.5416
2	4.7354	30.4738	1315.2334	Laminar	1357.5595
3	4.7354	30.4743	1315.2145	Laminar	1357.5790
4	4.7354	30.4747	1315.1943	Laminar	1357.5999
5	4.7354	30.4752	1315.1728	Laminar	1357.6221
6	4.7354	30.4758	1315.1500	Laminar	1357.6456
7	4.7354	30.4763	1315.1260	Laminar	1357.6704
8	4.7354	30.4769	1315.1008	Laminar	1357.6964
9	4.7354	30.4775	1315.0746	Laminar	1357.7234
10	4.7354	30.4781	1315.0473	Laminar	1357.7516
11	4.7354	30.4788	1315.0190	Laminar	1357.7809
12	4.7354	30.4795	1314.9896	Laminar	1357.8112
13	4.7354	30.4802	1314.9593	Laminar	1357.8425
14	4.7354	30.4809	1314.9281	Laminar	1357.8748
15	4.7354	30.4816	1314.8959	Laminar	1357.9080
16	4.7354	30.4824	1314.8628	Laminar	1357.9422
17	4.7354	30.4832	1314.8288	Laminar	1357.9772
18	4.7354	30.4840	1314.7940	Laminar	1358.0132
19	4.7354	30.4848	1314.7583	Laminar	1358.0501
20	4.7354	30.4857	1314.7218	Laminar	1358.0878
21	4.7354	30.4865	1314.6845	Laminar	1358.1263
22	4.7354	30.4874	1314.6464	Laminar	1358.1657
23	4.7354	30.4883	1314.6074	Laminar	1358.2059
24	4.7354	30.4892	1314.5678	Laminar	1358.2469
25	4.7354	30.4902	1314.5273	Laminar	1358.2887
26	4.7354	30.4911	1314.4861	Laminar	1358.3313
27	4.7354	30.4921	1314.4442	Laminar	1358.3746
28	4.7354	30.4931	1314.4016	Laminar	1358.4187
29	4.7354	30.4941	1314.3582	Laminar	1358.4635
30	4.7354	30.4951	1314.3141	Laminar	1358.5090
31	4.7354	30.4962	1314.2694	Laminar	1358.5553
32	4.7354	30.4972	1314.2239	Laminar	1358.6023
33	4.7354	30.4983	1314.1778	Laminar	1358.6500

Depth (m)	Annular Velocity(m/s)	τ wall-corrected (Pa)	Reynolds Number	Flow Regime	Frictional Pressure Loss (Pa/m)
34	4.7354	30.4994	1314.1310	Laminar	1358.6984
35	4.7354	30.5005	1314.0835	Laminar	1358.7474
36	4.7354	30.5016	1314.0354	Laminar	1358.7972
37	4.7354	30.5027	1313.9866	Laminar	1358.8476
38	4.7354	30.5039	1313.9372	Laminar	1358.8987
39	4.7354	30.5050	1313.8872	Laminar	1358.9505
40	4.7354	30.5062	1313.8365	Laminar	1359.0029
41	4.7354	30.5074	1313.7852	Laminar	1359.0559
42	4.7354	30.5086	1313.7334	Laminar	1359.1096
43	4.7354	30.5098	1313.6809	Laminar	1359.1639
44	4.7354	30.5111	1313.6277	Laminar	1359.2189
45	4.7354	30.5123	1313.5741	Laminar	1359.2744
46	4.7354	30.5136	1313.5198	Laminar	1359.3306
47	4.7354	30.5148	1313.4649	Laminar	1359.3874
48	4.7354	30.5161	1313.4095	Laminar	1359.4448
49	4.7354	30.5174	1313.3534	Laminar	1359.5028
50	4.7354	30.5188	1313.2968	Laminar	1359.5613
51	4.7354	30.5201	1313.2397	Laminar	1359.6205
52	4.7354	30.5214	1313.1820	Laminar	1359.6802
53	4.7354	30.5228	1313.1237	Laminar	1359.7406
54	4.7354	30.5241	1313.0649	Laminar	1359.8015
55	4.7354	30.5255	1313.0056	Laminar	1359.8629
56	4.7354	30.5269	1312.9457	Laminar	1359.9250
57	4.7354	30.5283	1312.8852	Laminar	1359.9876
58	4.7354	30.5297	1312.8243	Laminar	1360.0507
59	4.7354	30.5312	1312.7628	Laminar	1360.1144
60	4.7354	30.5326	1312.7008	Laminar	1360.1787
61	4.7354	30.5341	1312.6382	Laminar	1360.2435
62	4.7354	30.5355	1312.5752	Laminar	1360.3089
63	4.7354	30.5370	1312.5116	Laminar	1360.3747
64	4.7354	30.5385	1312.4475	Laminar	1360.4411
65	4.7354	30.5400	1312.3829	Laminar	1360.5081
66	4.7354	30.5415	1312.3179	Laminar	1360.5756
67	4.7354	30.5430	1312.2523	Laminar	1360.6436
68	4.7354	30.5446	1312.1862	Laminar	1360.7121
69	4.7354	30.5461	1312.1196	Laminar	1360.7811
70	4.7354	30.5477	1312.0526	Laminar	1360.8507
71	4.7354	30.5493	1311.9850	Laminar	1360.9207
72	4.7354	30.5509	1311.9170	Laminar	1360.9913

Depth (m)	Annular Velocity(m/s)	τ wall-corrected (Pa)	Reynolds Number	Flow Regime	Frictional Pressure Loss (Pa/m)
73	4.7354	30.5524	1311.8485	Laminar	1361.0624
74	4.7354	30.5541	1311.7795	Laminar	1361.1339
75	4.7354	30.5557	1311.7101	Laminar	1361.2060
76	4.7354	30.5573	1311.6401	Laminar	1361.2786
77	4.7354	30.5589	1311.5697	Laminar	1361.3516
78	4.7354	30.5606	1311.4989	Laminar	1361.4252
79	4.7354	30.5623	1311.4276	Laminar	1361.4992
80	4.7354	30.5639	1311.3558	Laminar	1361.5737
81	4.7354	30.5656	1311.2836	Laminar	1361.6487
82	4.7354	30.5673	1311.2109	Laminar	1361.7242
83	4.7354	30.5690	1311.1377	Laminar	1361.8002
84	4.7354	30.5707	1311.0641	Laminar	1361.8766
85	4.7354	30.5725	1310.9901	Laminar	1361.9535
86	4.7354	30.5742	1310.9156	Laminar	1362.0309
87	4.7354	30.5759	1310.8407	Laminar	1362.1088
88	4.7354	30.5777	1310.7653	Laminar	1362.1871
89	4.7354	30.5795	1310.6895	Laminar	1362.2659
90	4.7354	30.5812	1310.6133	Laminar	1362.3451
91	4.7354	30.5830	1310.5366	Laminar	1362.4248
92	4.7354	30.5848	1310.4595	Laminar	1362.5050
93	4.7354	30.5866	1310.3820	Laminar	1362.5856
94	4.7354	30.5885	1310.3041	Laminar	1362.6666
95	4.7354	30.5903	1310.2257	Laminar	1362.7481
96	4.7354	30.5921	1310.1469	Laminar	1362.8301
97	4.7354	30.5940	1310.0677	Laminar	1362.9125
98	4.7354	30.5958	1309.9880	Laminar	1362.9954
99	4.7354	30.5977	1309.9080	Laminar	1363.0787
100	4.7354	30.5996	1309.8275	Laminar	1363.1624
101	4.7354	30.6015	1309.7466	Laminar	1363.2466
102	4.7354	30.6034	1309.6654	Laminar	1363.3312
103	4.7354	30.6053	1309.5837	Laminar	1363.4162
104	4.7354	30.6072	1309.5016	Laminar	1363.5017
105	4.7354	30.6091	1309.4191	Laminar	1363.5876
106	4.7354	30.6111	1309.3362	Laminar	1363.6739
107	4.7354	30.6130	1309.2529	Laminar	1363.7607
108	4.7354	30.6150	1309.1692	Laminar	1363.8479
109	4.7354	30.6169	1309.0851	Laminar	1363.9355
110	4.7354	30.6189	1309.0006	Laminar	1364.0235
111	4.7354	30.6209	1308.9157	Laminar	1364.1120

Depth (m)	Annular Velocity(m/s)	τ wall-corrected (Pa)	Reynolds Number	Flow Regime	Frictional Pressure Loss (Pa/m)
112	4.7354	30.6229	1308.8304	Laminar	1364.2009
113	4.7354	30.6249	1308.7448	Laminar	1364.2902
114	4.7354	30.6269	1308.6587	Laminar	1364.3799
115	4.7354	30.6289	1308.5723	Laminar	1364.4700
116	4.7354	30.6310	1308.4854	Laminar	1364.5605
117	4.7354	30.6330	1308.3982	Laminar	1364.6515
118	4.7354	30.6351	1308.3106	Laminar	1364.7429
119	4.7354	30.6371	1308.2227	Laminar	1364.8346
120	4.7354	30.6392	1308.1343	Laminar	1364.9268
121	4.7354	30.6413	1308.0456	Laminar	1365.0194
122	4.7354	30.6434	1307.9565	Laminar	1365.1124
123	4.7354	30.6455	1307.8670	Laminar	1365.2057
124	4.7354	30.6476	1307.7772	Laminar	1365.2995
125	4.7354	30.6497	1307.6870	Laminar	1365.3937
126	4.7354	30.6518	1307.5964	Laminar	1365.4883
127	4.7354	30.6539	1307.5055	Laminar	1365.5833
128	4.7354	30.6561	1307.4142	Laminar	1365.6787
129	4.7354	30.6582	1307.3225	Laminar	1365.7744
130	4.7354	30.6604	1307.2304	Laminar	1365.8706
131	4.7354	30.6625	1307.1380	Laminar	1365.9671
132	4.7354	30.6647	1307.0453	Laminar	1366.0641
133	4.7354	30.6669	1306.9522	Laminar	1366.1614
134	4.7354	30.6691	1306.8587	Laminar	1366.2591
135	4.7354	30.6713	1306.7648	Laminar	1366.3572
136	4.7354	30.6735	1306.6706	Laminar	1366.4557
137	4.7354	30.6757	1306.5761	Laminar	1366.5546
138	4.7354	30.6780	1306.4812	Laminar	1366.6539
139	4.7354	30.6802	1306.3860	Laminar	1366.7535
140	4.7354	30.6824	1306.2904	Laminar	1366.8535
141	4.7354	30.6847	1306.1944	Laminar	1366.9539
142	4.7354	30.6870	1306.0981	Laminar	1367.0547
143	4.7354	30.6892	1306.0015	Laminar	1367.1559
144	4.7354	30.6915	1305.9045	Laminar	1367.2574
145	4.7354	30.6938	1305.8072	Laminar	1367.3593
146	4.7354	30.6961	1305.7095	Laminar	1367.4616
147	4.7354	30.6984	1305.6115	Laminar	1367.5642
148	4.7354	30.7007	1305.5132	Laminar	1367.6672
149	4.7354	30.7030	1305.4145	Laminar	1367.7706
150	4.7354	30.7054	1305.3155	Laminar	1367.8744

Depth (m)	Annular Velocity(m/s)	τ wall-corrected (Pa)	Reynolds Number	Flow Regime	Frictional Pressure Loss (Pa/m)
151	4.7354	30.7077	1305.2161	Laminar	1367.9785
152	4.7354	30.7100	1305.1164	Laminar	1368.0830
153	4.7354	30.7124	1305.0164	Laminar	1368.1879
154	4.7354	30.7148	1304.9160	Laminar	1368.2931
155	4.7354	30.7171	1304.8153	Laminar	1368.3987
156	4.7354	30.7195	1304.7143	Laminar	1368.5046
157	4.7354	30.7219	1304.6130	Laminar	1368.6109
158	4.7354	30.7243	1304.5113	Laminar	1368.7176
159	4.7354	30.7267	1304.4093	Laminar	1368.8247
160	4.7354	30.7291	1304.3070	Laminar	1368.9320
161	4.7354	30.7315	1304.2043	Laminar	1369.0398
162	4.7354	30.7339	1304.1013	Laminar	1369.1479
163	4.7354	30.7364	1303.9980	Laminar	1369.2564
164	4.7354	30.7388	1303.8944	Laminar	1369.3652
165	4.7354	30.7413	1303.7905	Laminar	1369.4743
166	4.7354	30.7437	1303.6862	Laminar	1369.5839
167	4.7354	30.7462	1303.5816	Laminar	1369.6937
168	4.7354	30.7487	1303.4768	Laminar	1369.8040
169	4.7354	30.7512	1303.3715	Laminar	1369.9145
170	4.7354	30.7536	1303.2660	Laminar	1370.0255
171	4.7354	30.7561	1303.1602	Laminar	1370.1367
172	4.7354	30.7586	1303.0540	Laminar	1370.2483
173	4.7354	30.7612	1302.9476	Laminar	1370.3603
174	4.7354	30.7637	1302.8408	Laminar	1370.4726
175	4.7354	30.7662	1302.7337	Laminar	1370.5853
176	4.7354	30.7687	1302.6263	Laminar	1370.6983
177	4.7354	30.7713	1302.5186	Laminar	1370.8116
178	4.7354	30.7738	1302.4106	Laminar	1370.9253
179	4.7354	30.7764	1302.3023	Laminar	1371.0393
180	4.7354	30.7790	1302.1936	Laminar	1371.1537
181	4.7354	30.7815	1302.0847	Laminar	1371.2684
182	4.7354	30.7841	1301.9755	Laminar	1371.3834
183	4.7354	30.7867	1301.8659	Laminar	1371.4988
184	4.7354	30.7893	1301.7561	Laminar	1371.6146
185	4.7354	30.7919	1301.6460	Laminar	1371.7306
186	4.7354	30.7945	1301.5355	Laminar	1371.8470
187	4.7354	30.7972	1301.4248	Laminar	1371.9637
188	4.7354	30.7998	1301.3138	Laminar	1372.0808
189	4.7354	30.8024	1301.2024	Laminar	1372.1982

Depth (m)	Annular Velocity(m/s)	τ wall-corrected (Pa)	Reynolds Number	Flow Regime	Frictional Pressure Loss (Pa/m)
190	4.7354	30.8051	1301.0908	Laminar	1372.3159
191	4.7354	30.8077	1300.9789	Laminar	1372.4340
192	4.7354	30.8104	1300.8667	Laminar	1372.5524
193	4.7354	30.8130	1300.7542	Laminar	1372.6711
194	4.7354	30.8157	1300.6414	Laminar	1372.7901
195	4.7354	30.8184	1300.5283	Laminar	1372.9095
196	4.7354	30.8211	1300.4149	Laminar	1373.0292
197	4.7354	30.8238	1300.3012	Laminar	1373.1492
198	4.7354	30.8265	1300.1872	Laminar	1373.2696
199	4.7354	30.8292	1300.0730	Laminar	1373.3903
200	4.7354	30.8319	1299.9584	Laminar	1373.5113
201	4.7354	30.8346	1299.8436	Laminar	1373.6326
202	4.7354	30.8373	1299.7285	Laminar	1373.7543
203	4.7354	30.8401	1299.6131	Laminar	1373.8763
204	4.7354	30.8428	1299.4974	Laminar	1373.9986
205	4.7354	30.8456	1299.3814	Laminar	1374.1212
206	4.7354	30.8483	1299.2652	Laminar	1374.2442
207	4.7354	30.8511	1299.1487	Laminar	1374.3674
208	4.7354	30.8539	1299.0319	Laminar	1374.4910
209	4.7354	30.8567	1298.9148	Laminar	1374.6149
210	4.7354	30.8595	1298.7974	Laminar	1374.7391
211	4.7354	30.8623	1298.6797	Laminar	1374.8637
212	4.7354	30.8651	1298.5618	Laminar	1374.9885
213	4.7354	30.8679	1298.4436	Laminar	1375.1137
214	4.7354	30.8707	1298.3251	Laminar	1375.2392
215	4.7354	30.8735	1298.2064	Laminar	1375.3650
216	4.7354	30.8763	1298.0873	Laminar	1375.4911
217	4.7354	30.8792	1297.9680	Laminar	1375.6176
218	4.7354	30.8820	1297.8484	Laminar	1375.7443
219	4.7354	30.8849	1297.7286	Laminar	1375.8714
220	4.7354	30.8877	1297.6085	Laminar	1375.9987
221	4.7354	30.8906	1297.4881	Laminar	1376.1264
222	4.7354	30.8935	1297.3674	Laminar	1376.2544
223	4.7354	30.8964	1297.2465	Laminar	1376.3827
224	4.7354	30.8992	1297.1253	Laminar	1376.5113
225	4.7354	30.9021	1297.0038	Laminar	1376.6402
226	4.7354	30.9050	1296.8820	Laminar	1376.7695
227	4.7354	30.9079	1296.7600	Laminar	1376.8990
228	4.7354	30.9109	1296.6378	Laminar	1377.0288

Depth (m)	Annular Velocity(m/s)	τ wall-corrected (Pa)	Reynolds Number	Flow Regime	Frictional Pressure Loss (Pa/m)
229	4.7354	30.9138	1296.5152	Laminar	1377.1590
230	4.7354	30.9167	1296.3924	Laminar	1377.2894
231	4.7354	30.9196	1296.2694	Laminar	1377.4202
232	4.7354	30.9226	1296.1460	Laminar	1377.5513
233	4.7354	30.9255	1296.0224	Laminar	1377.6826
234	4.7354	30.9285	1295.8986	Laminar	1377.8143
235	4.7354	30.9314	1295.7745	Laminar	1377.9463
236	4.7354	30.9344	1295.6501	Laminar	1378.0786
237	4.7354	30.9374	1295.5254	Laminar	1378.2111
238	4.7354	30.9404	1295.4006	Laminar	1378.3440
239	4.7354	30.9434	1295.2754	Laminar	1378.4772
240	4.7354	30.9464	1295.1500	Laminar	1378.6107
241	4.7354	30.9494	1295.0243	Laminar	1378.7445
242	4.7354	30.9524	1294.8984	Laminar	1378.8785
243	4.7354	30.9554	1294.7722	Laminar	1379.0129
244	4.7354	30.9584	1294.6458	Laminar	1379.1476
245	4.7354	30.9614	1294.5191	Laminar	1379.2826
246	4.7354	30.9645	1294.3921	Laminar	1379.4178
247	4.7354	30.9675	1294.2649	Laminar	1379.5534
248	4.7354	30.9706	1294.1375	Laminar	1379.6893
249	4.7354	30.9736	1294.0098	Laminar	1379.8254
250	4.7354	30.9767	1293.8818	Laminar	1379.9619
251	4.7354	30.9798	1293.7536	Laminar	1380.0986
252	4.7354	30.9828	1293.6252	Laminar	1380.2357
253	4.7354	30.9859	1293.4965	Laminar	1380.3730
254	4.7354	30.9890	1293.3675	Laminar	1380.5106
255	4.7354	30.9921	1293.2383	Laminar	1380.6485
256	4.7354	30.9952	1293.1089	Laminar	1380.7867
257	4.7354	30.9983	1292.9792	Laminar	1380.9252
258	4.7354	31.0014	1292.8492	Laminar	1381.0640
259	4.7354	31.0046	1292.7191	Laminar	1381.2031
260	4.7354	31.0077	1292.5886	Laminar	1381.3425
261	4.7354	31.0108	1292.4580	Laminar	1381.4822
262	4.7354	31.0140	1292.3270	Laminar	1381.6221
263	4.7354	31.0171	1292.1959	Laminar	1381.7623
264	4.7354	31.0203	1292.0645	Laminar	1381.9029
265	4.7354	31.0234	1291.9328	Laminar	1382.0437
266	4.7354	31.0266	1291.8009	Laminar	1382.1848
267	4.7354	31.0298	1291.6688	Laminar	1382.3262

Depth (m)	Annular Velocity(m/s)	τ wall-corrected (Pa)	Reynolds Number	Flow Regime	Frictional Pressure Loss (Pa/m)
268	4.7354	31.0329	1291.5364	Laminar	1382.4678
269	4.7354	31.0361	1291.4038	Laminar	1382.6098
270	4.7354	31.0393	1291.2710	Laminar	1382.7520
271	4.7354	31.0425	1291.1379	Laminar	1382.8946
272	4.7354	31.0457	1291.0046	Laminar	1383.0374
273	4.7354	31.0489	1290.8710	Laminar	1383.1805
274	4.7354	31.0522	1290.7372	Laminar	1383.3239
275	4.7354	31.0554	1290.6032	Laminar	1383.4675
276	4.7354	31.0586	1290.4689	Laminar	1383.6115
277	4.7354	31.0619	1290.3344	Laminar	1383.7557
278	4.7354	31.0651	1290.1997	Laminar	1383.9002
279	4.7354	31.0683	1290.0647	Laminar	1384.0450
280	4.7354	31.0716	1289.9295	Laminar	1384.1900
281	4.7354	31.0749	1289.7941	Laminar	1384.3354
282	4.7354	31.0781	1289.6584	Laminar	1384.4810
283	4.7354	31.0814	1289.5225	Laminar	1384.6269
284	4.7354	31.0847	1289.3864	Laminar	1384.7731
285	4.7354	31.0880	1289.2500	Laminar	1384.9196
286	4.7354	31.0913	1289.1134	Laminar	1385.0663
287	4.7354	31.0946	1288.9766	Laminar	1385.2133
288	4.7354	31.0979	1288.8396	Laminar	1385.3606
289	4.7354	31.1012	1288.7023	Laminar	1385.5082
290	4.7354	31.1045	1288.5648	Laminar	1385.6561
291	4.7354	31.1078	1288.4271	Laminar	1385.8042
292	4.7354	31.1112	1288.2891	Laminar	1385.9526
293	4.7354	31.1145	1288.1509	Laminar	1386.1013
294	4.7354	31.1179	1288.0125	Laminar	1386.2502
295	4.7354	31.1212	1287.8739	Laminar	1386.3994
296	4.7354	31.1246	1287.7350	Laminar	1386.5489
297	4.7354	31.1279	1287.5959	Laminar	1386.6987
298	4.7354	31.1313	1287.4566	Laminar	1386.8488
299	4.7354	31.1347	1287.3171	Laminar	1386.9991
300	4.7354	31.1380	1287.1773	Laminar	1387.1497
301	4.7354	31.1414	1287.0374	Laminar	1387.3005
302	4.7354	31.1448	1286.8972	Laminar	1387.4517
303	4.7354	31.1482	1286.7568	Laminar	1387.6031
304	4.7354	31.1516	1286.6161	Laminar	1387.7547
305	4.7354	31.1550	1286.4753	Laminar	1387.9067
306	4.7354	31.1585	1286.3342	Laminar	1388.0589

Depth (m)	Annular Velocity(m/s)	τ wall-corrected (Pa)	Reynolds Number	Flow Regime	Frictional Pressure Loss (Pa/m)
307	4.7354	31.1619	1286.1929	Laminar	1388.2114
308	4.7354	31.1653	1286.0514	Laminar	1388.3641
309	4.7354	31.1687	1285.9097	Laminar	1388.5172
310	4.7354	31.1722	1285.7677	Laminar	1388.6704
311	4.7354	31.1756	1285.6255	Laminar	1388.8240
312	4.7354	31.1791	1285.4832	Laminar	1388.9778
313	4.7354	31.1825	1285.3406	Laminar	1389.1319
314	4.7354	31.1860	1285.1978	Laminar	1389.2863
315	4.7354	31.1895	1285.0547	Laminar	1389.4409
316	4.7354	31.1930	1284.9115	Laminar	1389.5958
317	4.7354	31.1964	1284.7680	Laminar	1389.7510
318	4.7354	31.1999	1284.6244	Laminar	1389.9064
319	4.7354	31.2034	1284.4805	Laminar	1390.0621
320	4.7354	31.2069	1284.3364	Laminar	1390.2180
321	4.7354	31.2104	1284.1921	Laminar	1390.3742
322	4.7354	31.2139	1284.0476	Laminar	1390.5307
323	4.7354	31.2175	1283.9029	Laminar	1390.6875
324	4.7354	31.2210	1283.7579	Laminar	1390.8445
325	4.7354	31.2245	1283.6128	Laminar	1391.0017
326	4.7354	31.2280	1283.4674	Laminar	1391.1593
327	4.7354	31.2316	1283.3219	Laminar	1391.3171
328	4.7354	31.2351	1283.1761	Laminar	1391.4751
329	4.7354	31.2387	1283.0301	Laminar	1391.6334
330	4.7354	31.2423	1282.8839	Laminar	1391.7920
331	4.7354	31.2458	1282.7375	Laminar	1391.9509
332	4.7354	31.2494	1282.5909	Laminar	1392.1100
333	4.7354	31.2530	1282.4441	Laminar	1392.2693
334	4.7354	31.2565	1282.2971	Laminar	1392.4289
335	4.7354	31.2601	1282.1499	Laminar	1392.5888
336	4.7354	31.2637	1282.0025	Laminar	1392.7490
337	4.7354	31.2673	1281.8548	Laminar	1392.9094
338	4.7354	31.2709	1281.7070	Laminar	1393.0700
339	4.7354	31.2746	1281.5590	Laminar	1393.2309
340	4.7354	31.2782	1281.4107	Laminar	1393.3921
341	4.7354	31.2818	1281.2623	Laminar	1393.5535
342	4.7354	31.2854	1281.1137	Laminar	1393.7152
343	4.7354	31.2891	1280.9648	Laminar	1393.8772
344	4.7354	31.2927	1280.8158	Laminar	1394.0394
345	4.7354	31.2963	1280.6665	Laminar	1394.2018

Depth (m)	Annular Velocity(m/s)	τ wall-corrected (Pa)	Reynolds Number	Flow Regime	Frictional Pressure Loss (Pa/m)
346	4.7354	31.3000	1280.5171	Laminar	1394.3645
347	4.7354	31.3037	1280.3674	Laminar	1394.5275
348	4.7354	31.3073	1280.2176	Laminar	1394.6907
349	4.7354	31.3110	1280.0676	Laminar	1394.8542
350	4.7354	31.3147	1279.9173	Laminar	1395.0179
351	4.7354	31.3183	1279.7669	Laminar	1395.1819
352	4.7354	31.3220	1279.6163	Laminar	1395.3461
353	4.7354	31.3257	1279.4654	Laminar	1395.5106
354	4.7354	31.3294	1279.3144	Laminar	1395.6754
355	4.7354	31.3331	1279.1632	Laminar	1395.8404
356	4.7354	31.3368	1279.0117	Laminar	1396.0056
357	4.7354	31.3406	1278.8601	Laminar	1396.1711
358	4.7354	31.3443	1278.7083	Laminar	1396.3369
359	4.7354	31.3480	1278.5563	Laminar	1396.5029
360	4.7354	31.3517	1278.4041	Laminar	1396.6692
361	4.7354	31.3555	1278.2517	Laminar	1396.8357
362	4.7354	31.3592	1278.0991	Laminar	1397.0024
363	4.7354	31.3630	1277.9464	Laminar	1397.1695
364	4.7354	31.3667	1277.7934	Laminar	1397.3367
365	4.7354	31.3705	1277.6402	Laminar	1397.5042
366	4.7354	31.3742	1277.4869	Laminar	1397.6720
367	4.7354	31.3780	1277.3333	Laminar	1397.8400
368	4.7354	31.3818	1277.1796	Laminar	1398.0083
369	4.7354	31.3856	1277.0257	Laminar	1398.1768
370	4.7354	31.3894	1276.8715	Laminar	1398.3455
371	4.7354	31.3932	1276.7172	Laminar	1398.5145
372	4.7354	31.3970	1276.5627	Laminar	1398.6838
373	4.7354	31.4008	1276.4081	Laminar	1398.8533
374	4.7354	31.4046	1276.2532	Laminar	1399.0230
375	4.7354	31.4084	1276.0981	Laminar	1399.1930
376	4.7354	31.4122	1275.9429	Laminar	1399.3633
377	4.7354	31.4160	1275.7875	Laminar	1399.5338
378	4.7354	31.4199	1275.6318	Laminar	1399.7045
379	4.7354	31.4237	1275.4760	Laminar	1399.8755
380	4.7354	31.4275	1275.3200	Laminar	1400.0467
381	4.7354	31.4314	1275.1639	Laminar	1400.2182
382	4.7354	31.4353	1275.0075	Laminar	1400.3899
383	4.7354	31.4391	1274.8510	Laminar	1400.5618
384	4.7354	31.4430	1274.6942	Laminar	1400.7340

Depth (m)	Annular Velocity(m/s)	τ wall-corrected (Pa)	Reynolds Number	Flow Regime	Frictional Pressure Loss (Pa/m)
385	4.7354	31.4468	1274.5373	Laminar	1400.9065
386	4.7354	31.4507	1274.3802	Laminar	1401.0792
387	4.7354	31.4546	1274.2229	Laminar	1401.2521
388	4.7354	31.4585	1274.0655	Laminar	1401.4253
389	4.7354	31.4624	1273.9078	Laminar	1401.5987
390	4.7354	31.4663	1273.7500	Laminar	1401.7724
391	4.7354	31.4702	1273.5920	Laminar	1401.9463
392	4.7354	31.4741	1273.4338	Laminar	1402.1205
393	4.7354	31.4780	1273.2754	Laminar	1402.2949
394	4.7354	31.4819	1273.1169	Laminar	1402.4695
395	4.7354	31.4859	1272.9582	Laminar	1402.6444
396	4.7354	31.4898	1272.7993	Laminar	1402.8195
397	4.7354	31.4937	1272.6402	Laminar	1402.9948
398	4.7354	31.4977	1272.4809	Laminar	1403.1704
399	4.7354	31.5016	1272.3215	Laminar	1403.3463
400	4.7354	31.5056	1272.1618	Laminar	1403.5224
401	4.7354	31.5095	1272.0020	Laminar	1403.6987
402	4.7354	31.5135	1271.8421	Laminar	1403.8752
403	4.7354	31.5175	1271.6819	Laminar	1404.0520
404	4.7354	31.5214	1271.5216	Laminar	1404.2291
405	4.7354	31.5254	1271.3611	Laminar	1404.4064
406	4.7354	31.5294	1271.2004	Laminar	1404.5839
407	4.7354	31.5334	1271.0396	Laminar	1404.7616
408	4.7354	31.5374	1270.8785	Laminar	1404.9396
409	4.7354	31.5414	1270.7173	Laminar	1405.1179
410	4.7354	31.5454	1270.5559	Laminar	1405.2963
411	4.7354	31.5494	1270.3944	Laminar	1405.4750
412	4.7354	31.5534	1270.2327	Laminar	1405.6540
413	4.7354	31.5574	1270.0708	Laminar	1405.8332
414	4.7354	31.5615	1269.9087	Laminar	1406.0126
415	4.7354	31.5655	1269.7465	Laminar	1406.1922
416	4.7354	31.5695	1269.5840	Laminar	1406.3721
417	4.7354	31.5736	1269.4215	Laminar	1406.5522
418	4.7354	31.5776	1269.2587	Laminar	1406.7326
419	4.7354	31.5817	1269.0958	Laminar	1406.9132
420	4.7354	31.5857	1268.9327	Laminar	1407.0940
421	4.7354	31.5898	1268.7694	Laminar	1407.2751
422	4.7354	31.5939	1268.6060	Laminar	1407.4564
423	4.7354	31.5980	1268.4424	Laminar	1407.6379

Depth (m)	Annular Velocity(m/s)	τ wall-corrected (Pa)	Reynolds Number	Flow Regime	Frictional Pressure Loss (Pa/m)
424	4.7354	31.6020	1268.2786	Laminar	1407.8197
425	4.7354	31.6061	1268.1147	Laminar	1408.0017
426	4.7354	31.6102	1267.9505	Laminar	1408.1840
427	4.7354	31.6143	1267.7863	Laminar	1408.3664
428	4.7354	31.6184	1267.6218	Laminar	1408.5491
429	4.7354	31.6225	1267.4572	Laminar	1408.7321
430	4.7354	31.6266	1267.2924	Laminar	1408.9152
431	4.7354	31.6307	1267.1275	Laminar	1409.0986
432	4.7354	31.6349	1266.9624	Laminar	1409.2823
433	4.7354	31.6390	1266.7971	Laminar	1409.4661
434	4.7354	31.6431	1266.6316	Laminar	1409.6502
435	4.7354	31.6473	1266.4660	Laminar	1409.8346
436	4.7354	31.6514	1266.3003	Laminar	1410.0191
437	4.7354	31.6556	1266.1343	Laminar	1410.2039
438	4.7354	31.6597	1265.9682	Laminar	1410.3890
439	4.7354	31.6639	1265.8020	Laminar	1410.5742
440	4.7354	31.6680	1265.6355	Laminar	1410.7597
441	4.7354	31.6722	1265.4689	Laminar	1410.9454
442	4.7354	31.6764	1265.3022	Laminar	1411.1314
443	4.7354	31.6806	1265.1353	Laminar	1411.3176
444	4.7354	31.6847	1264.9682	Laminar	1411.5040
445	4.7354	31.6889	1264.8010	Laminar	1411.6906
446	4.7354	31.6931	1264.6336	Laminar	1411.8775
447	4.7354	31.6973	1264.4660	Laminar	1412.0646
448	4.7354	31.7015	1264.2983	Laminar	1412.2519
449	4.7354	31.7057	1264.1304	Laminar	1412.4394
450	4.7354	31.7099	1263.9623	Laminar	1412.6272
451	4.7354	31.7142	1263.7941	Laminar	1412.8152
452	4.7354	31.7184	1263.6258	Laminar	1413.0035
453	4.7354	31.7226	1263.4573	Laminar	1413.1919
454	4.7354	31.7269	1263.2886	Laminar	1413.3806
455	4.7354	31.7311	1263.1198	Laminar	1413.5695
456	4.7354	31.7353	1262.9508	Laminar	1413.7587
457	4.7354	31.7396	1262.7816	Laminar	1413.9481
458	4.7354	31.7439	1262.6123	Laminar	1414.1377
459	4.7354	31.7481	1262.4428	Laminar	1414.3275
460	4.7354	31.7524	1262.2732	Laminar	1414.5175
461	4.7354	31.7567	1262.1035	Laminar	1414.7078
462	4.7354	31.7609	1261.9335	Laminar	1414.8983

Depth (m)	Annular Velocity(m/s)	τ wall-corrected (Pa)	Reynolds Number	Flow Regime	Frictional Pressure Loss (Pa/m)
463	4.7354	31.7652	1261.7634	Laminar	1415.0890
464	4.7354	31.7695	1261.5932	Laminar	1415.2800
465	4.7354	31.7738	1261.4228	Laminar	1415.4712
466	4.7354	31.7781	1261.2522	Laminar	1415.6626
467	4.7354	31.7824	1261.0815	Laminar	1415.8542
468	4.7354	31.7867	1260.9107	Laminar	1416.0461
469	4.7354	31.7910	1260.7397	Laminar	1416.2381
470	4.7354	31.7953	1260.5685	Laminar	1416.4304
471	4.7354	31.7996	1260.3972	Laminar	1416.6230
472	4.7354	31.8040	1260.2257	Laminar	1416.8157
473	4.7354	31.8083	1260.0541	Laminar	1417.0087
474	4.7354	31.8126	1259.8823	Laminar	1417.2019
475	4.7354	31.8170	1259.7104	Laminar	1417.3953
476	4.7354	31.8213	1259.5383	Laminar	1417.5890
477	4.7354	31.8257	1259.3661	Laminar	1417.7828
478	4.7354	31.8300	1259.1937	Laminar	1417.9769
479	4.7354	31.8344	1259.0212	Laminar	1418.1712
480	4.7354	31.8388	1258.8485	Laminar	1418.3658
481	4.7354	31.8431	1258.6757	Laminar	1418.5605
482	4.7354	31.8475	1258.5027	Laminar	1418.7555
483	4.7354	31.8519	1258.3296	Laminar	1418.9507
484	4.7354	31.8563	1258.1563	Laminar	1419.1461
485	4.7354	31.8607	1257.9829	Laminar	1419.3418
486	4.7354	31.8651	1257.8093	Laminar	1419.5376
487	4.7354	31.8695	1257.6356	Laminar	1419.7337
488	4.7354	31.8739	1257.4617	Laminar	1419.9300
489	4.7354	31.8783	1257.2877	Laminar	1420.1265
490	4.7354	31.8827	1257.1135	Laminar	1420.3233
491	4.7354	31.8871	1256.9392	Laminar	1420.5202
492	4.7354	31.8916	1256.7648	Laminar	1420.7174
493	4.7354	31.8960	1256.5902	Laminar	1420.9148
494	4.7354	31.9004	1256.4154	Laminar	1421.1124
495	4.7354	31.9049	1256.2405	Laminar	1421.3103
496	4.7354	31.9093	1256.0655	Laminar	1421.5084
497	4.7354	31.9138	1255.8903	Laminar	1421.7066
498	4.7354	31.9182	1255.7150	Laminar	1421.9051
499	4.7354	31.9227	1255.5395	Laminar	1422.1038
500	4.7354	31.9271	1255.3639	Laminar	1422.3028
501	4.7354	31.9316	1255.1882	Laminar	1422.5019

Depth (m)	Annular Velocity(m/s)	τ wall-corrected (Pa)	Reynolds Number	Flow Regime	Frictional Pressure Loss (Pa/m)
502	4.7354	31.9361	1255.0123	Laminar	1422.7013
503	4.7354	31.9406	1254.8362	Laminar	1422.9009
504	4.7354	31.9451	1254.6601	Laminar	1423.1007
505	4.7354	31.9495	1254.4837	Laminar	1423.3007
506	4.7354	31.9540	1254.3073	Laminar	1423.5010
507	4.7354	31.9585	1254.1307	Laminar	1423.7014
508	4.7354	31.9630	1253.9539	Laminar	1423.9021
509	4.7354	31.9676	1253.7770	Laminar	1424.1030
510	4.7354	31.9721	1253.6000	Laminar	1424.3041
511	4.7354	31.9766	1253.4228	Laminar	1424.5054
512	4.7354	31.9811	1253.2455	Laminar	1424.7070
513	4.7354	31.9856	1253.0680	Laminar	1424.9087
514	4.7354	31.9902	1252.8905	Laminar	1425.1107
515	4.7354	31.9947	1252.7127	Laminar	1425.3129
516	4.7354	31.9993	1252.5349	Laminar	1425.5153
517	4.7354	32.0038	1252.3569	Laminar	1425.7179
518	4.7354	32.0084	1252.1787	Laminar	1425.9208
519	4.7354	32.0129	1252.0004	Laminar	1426.1238
520	4.7354	32.0175	1251.8220	Laminar	1426.3271
521	4.7354	32.0220	1251.6434	Laminar	1426.5305
522	4.7354	32.0266	1251.4648	Laminar	1426.7342
523	4.7354	32.0312	1251.2859	Laminar	1426.9381
524	4.7354	32.0358	1251.1069	Laminar	1427.1423
525	4.7354	32.0404	1250.9278	Laminar	1427.3466
526	4.7354	32.0450	1250.7486	Laminar	1427.5512
527	4.7354	32.0496	1250.5692	Laminar	1427.7559
528	4.7354	32.0542	1250.3897	Laminar	1427.9609
529	4.7354	32.0588	1250.2101	Laminar	1428.1661
530	4.7354	32.0634	1250.0303	Laminar	1428.3715
531	4.7354	32.0680	1249.8504	Laminar	1428.5771
532	4.7354	32.0726	1249.6703	Laminar	1428.7829
533	4.7354	32.0772	1249.4901	Laminar	1428.9890
534	4.7354	32.0819	1249.3098	Laminar	1429.1952
535	4.7354	32.0865	1249.1294	Laminar	1429.4017
536	4.7354	32.0911	1248.9488	Laminar	1429.6084
537	4.7354	32.0958	1248.7681	Laminar	1429.8152
538	4.7354	32.1004	1248.5872	Laminar	1430.0223
539	4.7354	32.1051	1248.4062	Laminar	1430.2297
540	4.7354	32.1097	1248.2251	Laminar	1430.4372

Depth (m)	Annular Velocity(m/s)	τ wall-corrected (Pa)	Reynolds Number	Flow Regime	Frictional Pressure Loss (Pa/m)
541	4.7354	32.1144	1248.0439	Laminar	1430.6449
542	4.7354	32.1191	1247.8625	Laminar	1430.8529
543	4.7354	32.1237	1247.6810	Laminar	1431.0610
544	4.7354	32.1284	1247.4993	Laminar	1431.2694
545	4.7354	32.1331	1247.3176	Laminar	1431.4780
546	4.7354	32.1378	1247.1357	Laminar	1431.6867
547	4.7354	32.1425	1246.9536	Laminar	1431.8957
548	4.7354	32.1472	1246.7715	Laminar	1432.1049
549	4.7354	32.1519	1246.5892	Laminar	1432.3144
550	4.7354	32.1566	1246.4068	Laminar	1432.5240
551	4.7354	32.1613	1246.2242	Laminar	1432.7338
552	4.7354	32.1660	1246.0416	Laminar	1432.9439
553	4.7354	32.1707	1245.8588	Laminar	1433.1541
554	4.7354	32.1755	1245.6758	Laminar	1433.3646
555	4.7354	32.1802	1245.4928	Laminar	1433.5753
556	4.7354	32.1849	1245.3096	Laminar	1433.7861
557	4.7354	32.1897	1245.1263	Laminar	1433.9972
558	4.7354	32.1944	1244.9428	Laminar	1434.2085
559	4.7354	32.1991	1244.7593	Laminar	1434.4200
560	4.7354	32.2039	1244.5756	Laminar	1434.6318
561	4.7354	32.2087	1244.3917	Laminar	1434.8437
562	4.7354	32.2134	1244.2078	Laminar	1435.0558
563	4.7354	32.2182	1244.0237	Laminar	1435.2681
564	4.7354	32.2230	1243.8395	Laminar	1435.4807
565	4.7354	32.2277	1243.6552	Laminar	1435.6934
566	4.7354	32.2325	1243.4707	Laminar	1435.9064
567	4.7354	32.2373	1243.2862	Laminar	1436.1196
568	4.7354	32.2421	1243.1015	Laminar	1436.3329
569	4.7354	32.2469	1242.9167	Laminar	1436.5465
570	4.7354	32.2517	1242.7317	Laminar	1436.7603
571	4.7354	32.2565	1242.5466	Laminar	1436.9743
572	4.7354	32.2613	1242.3615	Laminar	1437.1885
573	4.7354	32.2661	1242.1761	Laminar	1437.4029
574	4.7354	32.2709	1241.9907	Laminar	1437.6175
575	4.7354	32.2757	1241.8052	Laminar	1437.8323
576	4.7354	32.2806	1241.6195	Laminar	1438.0474
577	4.7354	32.2854	1241.4337	Laminar	1438.2626
578	4.7354	32.2902	1241.2477	Laminar	1438.4780
579	4.7354	32.2951	1241.0617	Laminar	1438.6937

Depth (m)	Annular Velocity(m/s)	τ wall-corrected (Pa)	Reynolds Number	Flow Regime	Frictional Pressure Loss (Pa/m)
580	4.7354	32.2999	1240.8755	Laminar	1438.9095
581	4.7354	32.3048	1240.6892	Laminar	1439.1256
582	4.7354	32.3096	1240.5028	Laminar	1439.3418
583	4.7354	32.3145	1240.3163	Laminar	1439.5583
584	4.7354	32.3193	1240.1297	Laminar	1439.7749
585	4.7354	32.3242	1239.9429	Laminar	1439.9918
586	4.7354	32.3291	1239.7560	Laminar	1440.2089
587	4.7354	32.3340	1239.5690	Laminar	1440.4262
588	4.7354	32.3388	1239.3819	Laminar	1440.6436
589	4.7354	32.3437	1239.1946	Laminar	1440.8613
590	4.7354	32.3486	1239.0073	Laminar	1441.0792
591	4.7354	32.3535	1238.8198	Laminar	1441.2973
592	4.7354	32.3584	1238.6322	Laminar	1441.5156
593	4.7354	32.3633	1238.4445	Laminar	1441.7341
594	4.7354	32.3682	1238.2566	Laminar	1441.9528
595	4.7354	32.3731	1238.0687	Laminar	1442.1717
596	4.7354	32.3781	1237.8806	Laminar	1442.3908
597	4.7354	32.3830	1237.6924	Laminar	1442.6101
598	4.7354	32.3879	1237.5041	Laminar	1442.8296
599	4.7354	32.3928	1237.3157	Laminar	1443.0493
600	4.7354	32.3978	1237.1272	Laminar	1443.2692
601	4.7354	32.4027	1236.9385	Laminar	1443.4894
602	4.7354	32.4077	1236.7498	Laminar	1443.7097
603	4.7354	32.4126	1236.5609	Laminar	1443.9302
604	4.7354	32.4176	1236.3719	Laminar	1444.1509
605	4.7354	32.4225	1236.1828	Laminar	1444.3719
606	4.7354	32.4275	1235.9936	Laminar	1444.5930
607	4.7354	32.4325	1235.8042	Laminar	1444.8143
608	4.7354	32.4374	1235.6148	Laminar	1445.0358
609	4.7354	32.4424	1235.4252	Laminar	1445.2576
610	4.7354	32.4474	1235.2355	Laminar	1445.4795
611	4.7354	32.4524	1235.0457	Laminar	1445.7016
612	4.7354	32.4574	1234.8558	Laminar	1445.9240
613	4.7354	32.4624	1234.6658	Laminar	1446.1465
614	4.7354	32.4674	1234.4757	Laminar	1446.3692
615	4.7354	32.4724	1234.2854	Laminar	1446.5922
616	4.7354	32.4774	1234.0951	Laminar	1446.8153
617	4.7354	32.4824	1233.9046	Laminar	1447.0386
618	4.7354	32.4874	1233.7140	Laminar	1447.2621

Depth (m)	Annular Velocity(m/s)	τ wall-corrected (Pa)	Reynolds Number	Flow Regime	Frictional Pressure Loss (Pa/m)
619	4.7354	32.4924	1233.5233	Laminar	1447.4859
620	4.7354	32.4975	1233.3325	Laminar	1447.7098
621	4.7354	32.5025	1233.1416	Laminar	1447.9339
622	4.7354	32.5075	1232.9506	Laminar	1448.1583
623	4.7354	32.5126	1232.7595	Laminar	1448.3828
624	4.7354	32.5176	1232.5682	Laminar	1448.6075
625	4.7354	32.5227	1232.3769	Laminar	1448.8324
626	4.7354	32.5277	1232.1854	Laminar	1449.0576
627	4.7354	32.5328	1231.9938	Laminar	1449.2829
628	4.7354	32.5378	1231.8022	Laminar	1449.5084
629	4.7354	32.5429	1231.6104	Laminar	1449.7341
630	4.7354	32.5480	1231.4185	Laminar	1449.9600
631	4.7354	32.5531	1231.2265	Laminar	1450.1862
632	4.7354	32.5581	1231.0344	Laminar	1450.4125
633	4.7354	32.5632	1230.8421	Laminar	1450.6390
634	4.7354	32.5683	1230.6498	Laminar	1450.8657
635	4.7354	32.5734	1230.4574	Laminar	1451.0926
636	4.7354	32.5785	1230.2648	Laminar	1451.3197
637	4.7354	32.5836	1230.0722	Laminar	1451.5470
638	4.7354	32.5887	1229.8794	Laminar	1451.7745
639	4.7354	32.5938	1229.6866	Laminar	1452.0022
640	4.7354	32.5989	1229.4936	Laminar	1452.2301
641	4.7354	32.6041	1229.3005	Laminar	1452.4582
642	4.7354	32.6092	1229.1073	Laminar	1452.6865
643	4.7354	32.6143	1228.9141	Laminar	1452.9149
644	4.7354	32.6194	1228.7207	Laminar	1453.1436
645	4.7354	32.6246	1228.5272	Laminar	1453.3725
646	4.7354	32.6297	1228.3336	Laminar	1453.6016
647	4.7354	32.6349	1228.1399	Laminar	1453.8308
648	4.7354	32.6400	1227.9461	Laminar	1454.0603
649	4.7354	32.6452	1227.7521	Laminar	1454.2900
650	4.7354	32.6503	1227.5581	Laminar	1454.5198
651	4.7354	32.6555	1227.3640	Laminar	1454.7499
652	4.7354	32.6607	1227.1698	Laminar	1454.9801
653	4.7354	32.6658	1226.9755	Laminar	1455.2105
654	4.7354	32.6710	1226.7810	Laminar	1455.4412
655	4.7354	32.6762	1226.5865	Laminar	1455.6720
656	4.7354	32.6814	1226.3919	Laminar	1455.9030
657	4.7354	32.6866	1226.1971	Laminar	1456.1342

Depth (m)	Annular Velocity(m/s)	τ wall-corrected (Pa)	Reynolds Number	Flow Regime	Frictional Pressure Loss (Pa/m)
658	4.7354	32.6918	1226.0023	Laminar	1456.3657
659	4.7354	32.6970	1225.8073	Laminar	1456.5973
660	4.7354	32.7022	1225.6123	Laminar	1456.8291
661	4.7354	32.7074	1225.4171	Laminar	1457.0611
662	4.7354	32.7126	1225.2219	Laminar	1457.2932
663	4.7354	32.7178	1225.0266	Laminar	1457.5256
664	4.7354	32.7230	1224.8311	Laminar	1457.7582
665	4.7354	32.7283	1224.6356	Laminar	1457.9910
666	4.7354	32.7335	1224.4399	Laminar	1458.2239
667	4.7354	32.7387	1224.2442	Laminar	1458.4571
668	4.7354	32.7440	1224.0483	Laminar	1458.6905
669	4.7354	32.7492	1223.8524	Laminar	1458.9240
670	4.7354	32.7544	1223.6563	Laminar	1459.1577
671	4.7354	32.7597	1223.4602	Laminar	1459.3917
672	4.7354	32.7650	1223.2639	Laminar	1459.6258
673	4.7354	32.7702	1223.0676	Laminar	1459.8601
674	4.7354	32.7755	1222.8712	Laminar	1460.0946
675	4.7354	32.7807	1222.6746	Laminar	1460.3293
676	4.7354	32.7860	1222.4780	Laminar	1460.5642
677	4.7354	32.7913	1222.2812	Laminar	1460.7993
678	4.7354	32.7966	1222.0844	Laminar	1461.0346
679	4.7354	32.8019	1221.8875	Laminar	1461.2701
680	4.7354	32.8071	1221.6905	Laminar	1461.5057
681	4.7354	32.8124	1221.4933	Laminar	1461.7416
682	4.7354	32.8177	1221.2961	Laminar	1461.9776
683	4.7354	32.8230	1221.0988	Laminar	1462.2139
684	4.7354	32.8284	1220.9014	Laminar	1462.4503
685	4.7354	32.8337	1220.7039	Laminar	1462.6869
686	4.7354	32.8390	1220.5063	Laminar	1462.9237
687	4.7354	32.8443	1220.3086	Laminar	1463.1607
688	4.7354	32.8496	1220.1108	Laminar	1463.3979
689	4.7354	32.8550	1219.9129	Laminar	1463.6353
690	4.7354	32.8603	1219.7149	Laminar	1463.8729
691	4.7354	32.8656	1219.5168	Laminar	1464.1107
692	4.7354	32.8710	1219.3187	Laminar	1464.3486
693	4.7354	32.8763	1219.1204	Laminar	1464.5868
694	4.7354	32.8817	1218.9220	Laminar	1464.8251
695	4.7354	32.8870	1218.7236	Laminar	1465.0636
696	4.7354	32.8924	1218.5250	Laminar	1465.3024

Depth (m)	Annular Velocity(m/s)	τ wall-corrected (Pa)	Reynolds Number	Flow Regime	Frictional Pressure Loss (Pa/m)
697	4.7354	32.8977	1218.3264	Laminar	1465.5413
698	4.7354	32.9031	1218.1277	Laminar	1465.7804
699	4.7354	32.9085	1217.9288	Laminar	1466.0197
700	4.7354	32.9139	1217.7299	Laminar	1466.2591
701	4.7354	32.9192	1217.5309	Laminar	1466.4988
702	4.7354	32.9246	1217.3318	Laminar	1466.7387
703	4.7354	32.9300	1217.1326	Laminar	1466.9787
704	4.7354	32.9354	1216.9333	Laminar	1467.2190
705	4.7354	32.9408	1216.7339	Laminar	1467.4594
706	4.7354	32.9462	1216.5345	Laminar	1467.7000
707	4.7354	32.9516	1216.3349	Laminar	1467.9408
708	4.7354	32.9570	1216.1352	Laminar	1468.1818
709	4.7354	32.9624	1215.9355	Laminar	1468.4230
710	4.7354	32.9678	1215.7357	Laminar	1468.6643
711	4.7354	32.9733	1215.5357	Laminar	1468.9059
712	4.7354	32.9787	1215.3357	Laminar	1469.1476
713	4.7354	32.9841	1215.1356	Laminar	1469.3896
714	4.7354	32.9896	1214.9354	Laminar	1469.6317
715	4.7354	32.9950	1214.7351	Laminar	1469.8740
716	4.7354	33.0004	1214.5348	Laminar	1470.1165
717	4.7354	33.0059	1214.3343	Laminar	1470.3592
718	4.7354	33.0113	1214.1337	Laminar	1470.6021
719	4.7354	33.0168	1213.9331	Laminar	1470.8451
720	4.7354	33.0223	1213.7324	Laminar	1471.0884
721	4.7354	33.0277	1213.5316	Laminar	1471.3318
722	4.7354	33.0332	1213.3307	Laminar	1471.5755
723	4.7354	33.0387	1213.1297	Laminar	1471.8193
724	4.7354	33.0441	1212.9286	Laminar	1472.0633
725	4.7354	33.0496	1212.7274	Laminar	1472.3075
726	4.7354	33.0551	1212.5262	Laminar	1472.5518
727	4.7354	33.0606	1212.3248	Laminar	1472.7964
728	4.7354	33.0661	1212.1234	Laminar	1473.0411
729	4.7354	33.0716	1211.9219	Laminar	1473.2861
730	4.7354	33.0771	1211.7203	Laminar	1473.5312
731	4.7354	33.0826	1211.5186	Laminar	1473.7765
732	4.7354	33.0881	1211.3168	Laminar	1474.0220
733	4.7354	33.0936	1211.1149	Laminar	1474.2677
734	4.7354	33.0991	1210.9130	Laminar	1474.5135
735	4.7354	33.1047	1210.7110	Laminar	1474.7596

Depth (m)	Annular Velocity(m/s)	τ wall-corrected (Pa)	Reynolds Number	Flow Regime	Frictional Pressure Loss (Pa/m)
736	4.7354	33.1102	1210.5089	Laminar	1475.0058
737	4.7354	33.1157	1210.3067	Laminar	1475.2522
738	4.7354	33.1213	1210.1044	Laminar	1475.4989
739	4.7354	33.1268	1209.9020	Laminar	1475.7456
740	4.7354	33.1323	1209.6995	Laminar	1475.9926
741	4.7354	33.1379	1209.4970	Laminar	1476.2398
742	4.7354	33.1434	1209.2944	Laminar	1476.4871
743	4.7354	33.1490	1209.0917	Laminar	1476.7347
744	4.7354	33.1546	1208.8889	Laminar	1476.9824
745	4.7354	33.1601	1208.6860	Laminar	1477.2303
746	4.7354	33.1657	1208.4831	Laminar	1477.4784
747	4.7354	33.1713	1208.2800	Laminar	1477.7267
748	4.7354	33.1768	1208.0769	Laminar	1477.9751
749	4.7354	33.1824	1207.8737	Laminar	1478.2238
750	4.7354	33.1880	1207.6704	Laminar	1478.4726
751	4.7354	33.1936	1207.4670	Laminar	1478.7216
752	4.7354	33.1992	1207.2636	Laminar	1478.9708
753	4.7354	33.2048	1207.0601	Laminar	1479.2202
754	4.7354	33.2104	1206.8564	Laminar	1479.4698
755	4.7354	33.2160	1206.6527	Laminar	1479.7195
756	4.7354	33.2216	1206.4490	Laminar	1479.9694
757	4.7354	33.2272	1206.2451	Laminar	1480.2196
758	4.7354	33.2328	1206.0412	Laminar	1480.4699
759	4.7354	33.2385	1205.8372	Laminar	1480.7203
760	4.7354	33.2441	1205.6331	Laminar	1480.9710
761	4.7354	33.2497	1205.4289	Laminar	1481.2219
762	4.7354	33.2554	1205.2246	Laminar	1481.4729
763	4.7354	33.2610	1205.0203	Laminar	1481.7241
764	4.7354	33.2666	1204.8159	Laminar	1481.9755
765	4.7354	33.2723	1204.6114	Laminar	1482.2271
766	4.7354	33.2779	1204.4068	Laminar	1482.4789
767	4.7354	33.2836	1204.2021	Laminar	1482.7308
768	4.7354	33.2893	1203.9974	Laminar	1482.9829
769	4.7354	33.2949	1203.7926	Laminar	1483.2353
770	4.7354	33.3006	1203.5877	Laminar	1483.4878
771	4.7354	33.3063	1203.3827	Laminar	1483.7404
772	4.7354	33.3119	1203.1777	Laminar	1483.9933
773	4.7354	33.3176	1202.9725	Laminar	1484.2463
774	4.7354	33.3233	1202.7673	Laminar	1484.4996

Depth (m)	Annular Velocity(m/s)	τ wall-corrected (Pa)	Reynolds Number	Flow Regime	Frictional Pressure Loss (Pa/m)
775	4.7354	33.3290	1202.5621	Laminar	1484.7530
776	4.7354	33.3347	1202.3567	Laminar	1485.0066
777	4.7354	33.3404	1202.1513	Laminar	1485.2603
778	4.7354	33.3461	1201.9458	Laminar	1485.5143
779	4.7354	33.3518	1201.7402	Laminar	1485.7684
780	4.7354	33.3575	1201.5345	Laminar	1486.0227
781	4.7354	33.3632	1201.3288	Laminar	1486.2772
782	4.7354	33.3689	1201.1229	Laminar	1486.5319
783	4.7354	33.3746	1200.9171	Laminar	1486.7868
784	4.7354	33.3804	1200.7111	Laminar	1487.0418
785	4.7354	33.3861	1200.5050	Laminar	1487.2971
786	4.7354	33.3918	1200.2989	Laminar	1487.5525
787	4.7354	33.3976	1200.0927	Laminar	1487.8080
788	4.7354	33.4033	1199.8865	Laminar	1488.0638
789	4.7354	33.4091	1199.6801	Laminar	1488.3198
790	4.7354	33.4148	1199.4737	Laminar	1488.5759
791	4.7354	33.4206	1199.2672	Laminar	1488.8322
792	4.7354	33.4263	1199.0606	Laminar	1489.0887
793	4.7354	33.4321	1198.8540	Laminar	1489.3454
794	4.7354	33.4378	1198.6473	Laminar	1489.6022
795	4.7354	33.4436	1198.4405	Laminar	1489.8592
796	4.7354	33.4494	1198.2336	Laminar	1490.1164
797	4.7354	33.4552	1198.0267	Laminar	1490.3738
798	4.7354	33.4609	1197.8197	Laminar	1490.6314
799	4.7354	33.4667	1197.6126	Laminar	1490.8892
800	4.7354	33.4725	1197.4054	Laminar	1491.1471
801	4.7354	33.4783	1197.1982	Laminar	1491.4052
802	4.7354	33.4841	1196.9909	Laminar	1491.6635
803	4.7354	33.4899	1196.7835	Laminar	1491.9219
804	4.7354	33.4957	1196.5761	Laminar	1492.1806
805	4.7354	33.5015	1196.3686	Laminar	1492.4394
806	4.7354	33.5073	1196.1610	Laminar	1492.6984
807	4.7354	33.5132	1195.9533	Laminar	1492.9576
808	4.7354	33.5190	1195.7456	Laminar	1493.2170
809	4.7354	33.5248	1195.5378	Laminar	1493.4765
810	4.7354	33.5306	1195.3299	Laminar	1493.7362
811	4.7354	33.5365	1195.1220	Laminar	1493.9961
812	4.7354	33.5423	1194.9140	Laminar	1494.2562
813	4.7354	33.5482	1194.7059	Laminar	1494.5165

Depth (m)	Annular Velocity(m/s)	τ wall-corrected (Pa)	Reynolds Number	Flow Regime	Frictional Pressure Loss (Pa/m)
814	4.7354	33.5540	1194.4977	Laminar	1494.7769
815	4.7354	33.5599	1194.2895	Laminar	1495.0375
816	4.7354	33.5657	1194.0812	Laminar	1495.2983
817	4.7354	33.5716	1193.8728	Laminar	1495.5593
818	4.7354	33.5774	1193.6644	Laminar	1495.8204
819	4.7354	33.5833	1193.4559	Laminar	1496.0818
820	4.7354	33.5892	1193.2473	Laminar	1496.3433
821	4.7354	33.5950	1193.0387	Laminar	1496.6050
822	4.7354	33.6009	1192.8300	Laminar	1496.8668
823	4.7354	33.6068	1192.6212	Laminar	1497.1289
824	4.7354	33.6127	1192.4123	Laminar	1497.3911
825	4.7354	33.6186	1192.2034	Laminar	1497.6535
826	4.7354	33.6245	1191.9944	Laminar	1497.9160
827	4.7354	33.6304	1191.7854	Laminar	1498.1788
828	4.7354	33.6363	1191.5763	Laminar	1498.4417
829	4.7354	33.6422	1191.3671	Laminar	1498.7048
830	4.7354	33.6481	1191.1578	Laminar	1498.9681
831	4.7354	33.6540	1190.9485	Laminar	1499.2316
832	4.7354	33.6599	1190.7391	Laminar	1499.4952
833	4.7354	33.6658	1190.5297	Laminar	1499.7590
834	4.7354	33.6718	1190.3202	Laminar	1500.0230
835	4.7354	33.6777	1190.1106	Laminar	1500.2872
836	4.7354	33.6836	1189.9009	Laminar	1500.5515
837	4.7354	33.6896	1189.6912	Laminar	1500.8160
838	4.7354	33.6955	1189.4814	Laminar	1501.0807
839	4.7354	33.7015	1189.2716	Laminar	1501.3456
840	4.7354	33.7074	1189.0616	Laminar	1501.6106
841	4.7354	33.7134	1188.8517	Laminar	1501.8759
842	4.7354	33.7193	1188.6416	Laminar	1502.1413
843	4.7354	33.7253	1188.4315	Laminar	1502.4068
844	4.7354	33.7312	1188.2213	Laminar	1502.6726
845	4.7354	33.7372	1188.0111	Laminar	1502.9385
846	4.7354	33.7432	1187.8008	Laminar	1503.2046
847	4.7354	33.7492	1187.5904	Laminar	1503.4709
848	4.7354	33.7551	1187.3800	Laminar	1503.7374
849	4.7354	33.7611	1187.1695	Laminar	1504.0040
850	4.7354	33.7671	1186.9589	Laminar	1504.2708
851	4.7354	33.7731	1186.7483	Laminar	1504.5378
852	4.7354	33.7791	1186.5376	Laminar	1504.8049

Depth (m)	Annular Velocity(m/s)	τ wall-corrected (Pa)	Reynolds Number	Flow Regime	Frictional Pressure Loss (Pa/m)
853	4.7354	33.7851	1186.3268	Laminar	1505.0723
854	4.7354	33.7911	1186.1160	Laminar	1505.3398
855	4.7354	33.7971	1185.9051	Laminar	1505.6075
856	4.7354	33.8031	1185.6942	Laminar	1505.8753
857	4.7354	33.8092	1185.4832	Laminar	1506.1433
858	4.7354	33.8152	1185.2721	Laminar	1506.4116
859	4.7354	33.8212	1185.0610	Laminar	1506.6799
860	4.7354	33.8272	1184.8498	Laminar	1506.9485
861	4.7354	33.8333	1184.6385	Laminar	1507.2172
862	4.7354	33.8393	1184.4272	Laminar	1507.4861
863	4.7354	33.8453	1184.2158	Laminar	1507.7552
864	4.7354	33.8514	1184.0044	Laminar	1508.0245
865	4.7354	33.8574	1183.7929	Laminar	1508.2939
866	4.7354	33.8635	1183.5813	Laminar	1508.5635
867	4.7354	33.8695	1183.3697	Laminar	1508.8333
868	4.7354	33.8756	1183.1580	Laminar	1509.1032
869	4.7354	33.8817	1182.9463	Laminar	1509.3733
870	4.7354	33.8877	1182.7345	Laminar	1509.6436
871	4.7354	33.8938	1182.5226	Laminar	1509.9141
872	4.7354	33.8999	1182.3107	Laminar	1510.1848
873	4.7354	33.9060	1182.0987	Laminar	1510.4556
874	4.7354	33.9120	1181.8867	Laminar	1510.7266
875	4.7354	33.9181	1181.6746	Laminar	1510.9977
876	4.7354	33.9242	1181.4624	Laminar	1511.2691
877	4.7354	33.9303	1181.2502	Laminar	1511.5406
878	4.7354	33.9364	1181.0379	Laminar	1511.8123
879	4.7354	33.9425	1180.8256	Laminar	1512.0841
880	4.7354	33.9486	1180.6132	Laminar	1512.3562
881	4.7354	33.9547	1180.4007	Laminar	1512.6284
882	4.7354	33.9608	1180.1882	Laminar	1512.9008
883	4.7354	33.9670	1179.9756	Laminar	1513.1733
884	4.7354	33.9731	1179.7630	Laminar	1513.4460
885	4.7354	33.9792	1179.5503	Laminar	1513.7189
886	4.7354	33.9853	1179.3375	Laminar	1513.9920
887	4.7354	33.9915	1179.1247	Laminar	1514.2652
888	4.7354	33.9976	1178.9119	Laminar	1514.5387
889	4.7354	34.0037	1178.6990	Laminar	1514.8122
890	4.7354	34.0099	1178.4860	Laminar	1515.0860
891	4.7354	34.0160	1178.2729	Laminar	1515.3599

Depth (m)	Annular Velocity(m/s)	τ wall-corrected (Pa)	Reynolds Number	Flow Regime	Frictional Pressure Loss (Pa/m)
892	4.7354	34.0222	1178.0598	Laminar	1515.6340
893	4.7354	34.0284	1177.8467	Laminar	1515.9083
894	4.7354	34.0345	1177.6335	Laminar	1516.1828
895	4.7354	34.0407	1177.4202	Laminar	1516.4574
896	4.7354	34.0468	1177.2069	Laminar	1516.7322
897	4.7354	34.0530	1176.9935	Laminar	1517.0071
898	4.7354	34.0592	1176.7801	Laminar	1517.2823
899	4.7354	34.0654	1176.5666	Laminar	1517.5576
900	4.7354	34.0716	1176.3531	Laminar	1517.8331
901	4.7354	34.0777	1176.1395	Laminar	1518.1087
902	4.7354	34.0839	1175.9258	Laminar	1518.3845
903	4.7354	34.0901	1175.7121	Laminar	1518.6605
904	4.7354	34.0963	1175.4984	Laminar	1518.9367
905	4.7354	34.1025	1175.2845	Laminar	1519.2130
906	4.7354	34.1087	1175.0707	Laminar	1519.4895
907	4.7354	34.1150	1174.8568	Laminar	1519.7662
908	4.7354	34.1212	1174.6428	Laminar	1520.0431
909	4.7354	34.1274	1174.4287	Laminar	1520.3201
910	4.7354	34.1336	1174.2147	Laminar	1520.5973
911	4.7354	34.1398	1174.0005	Laminar	1520.8746
912	4.7354	34.1461	1173.7863	Laminar	1521.1522
913	4.7354	34.1523	1173.5721	Laminar	1521.4299
914	4.7354	34.1585	1173.3578	Laminar	1521.7078
915	4.7354	34.1648	1173.1434	Laminar	1521.9858
916	4.7354	34.1710	1172.9290	Laminar	1522.2640
917	4.7354	34.1773	1172.7145	Laminar	1522.5424
918	4.7354	34.1835	1172.5000	Laminar	1522.8210
919	4.7354	34.1898	1172.2855	Laminar	1523.0997
920	4.7354	34.1960	1172.0708	Laminar	1523.3786
921	4.7354	34.2023	1171.8562	Laminar	1523.6576
922	4.7354	34.2086	1171.6415	Laminar	1523.9369
923	4.7354	34.2148	1171.4267	Laminar	1524.2163
924	4.7354	34.2211	1171.2118	Laminar	1524.4959
925	4.7354	34.2274	1170.9970	Laminar	1524.7756
926	4.7354	34.2337	1170.7820	Laminar	1525.0555
927	4.7354	34.2400	1170.5671	Laminar	1525.3356
928	4.7354	34.2463	1170.3520	Laminar	1525.6159
929	4.7354	34.2526	1170.1369	Laminar	1525.8963
930	4.7354	34.2589	1169.9218	Laminar	1526.1769

Depth (m)	Annular Velocity(m/s)	τ wall-corrected (Pa)	Reynolds Number	Flow Regime	Frictional Pressure Loss (Pa/m)
931	4.7354	34.2652	1169.7066	Laminar	1526.4576
932	4.7354	34.2715	1169.4914	Laminar	1526.7386
933	4.7354	34.2778	1169.2761	Laminar	1527.0197
934	4.7354	34.2841	1169.0608	Laminar	1527.3009
935	4.7354	34.2904	1168.8454	Laminar	1527.5824
936	4.7354	34.2967	1168.6300	Laminar	1527.8640
937	4.7354	34.3031	1168.4145	Laminar	1528.1458
938	4.7354	34.3094	1168.1989	Laminar	1528.4277
939	4.7354	34.3157	1167.9833	Laminar	1528.7098
940	4.7354	34.3221	1167.7677	Laminar	1528.9921
941	4.7354	34.3284	1167.5520	Laminar	1529.2746
942	4.7354	34.3347	1167.3363	Laminar	1529.5572
943	4.7354	34.3411	1167.1205	Laminar	1529.8400
944	4.7354	34.3474	1166.9047	Laminar	1530.1229
945	4.7354	34.3538	1166.6888	Laminar	1530.4060
946	4.7354	34.3601	1166.4729	Laminar	1530.6893
947	4.7354	34.3665	1166.2569	Laminar	1530.9728
948	4.7354	34.3729	1166.0409	Laminar	1531.2564
949	4.7354	34.3792	1165.8248	Laminar	1531.5402
950	4.7354	34.3856	1165.6087	Laminar	1531.8242
951	4.7354	34.3920	1165.3925	Laminar	1532.1083
952	4.7354	34.3984	1165.1763	Laminar	1532.3926
953	4.7354	34.4048	1164.9601	Laminar	1532.6771
954	4.7354	34.4112	1164.7437	Laminar	1532.9617
955	4.7354	34.4176	1164.5274	Laminar	1533.2465
956	4.7354	34.4239	1164.3110	Laminar	1533.5315
957	4.7354	34.4303	1164.0945	Laminar	1533.8167
958	4.7354	34.4368	1163.8780	Laminar	1534.1020
959	4.7354	34.4432	1163.6615	Laminar	1534.3874
960	4.7354	34.4496	1163.4449	Laminar	1534.6731
961	4.7354	34.4560	1163.2283	Laminar	1534.9589
962	4.7354	34.4624	1163.0116	Laminar	1535.2449
963	4.7354	34.4688	1162.7949	Laminar	1535.5310
964	4.7354	34.4753	1162.5781	Laminar	1535.8173
965	4.7354	34.4817	1162.3613	Laminar	1536.1038
966	4.7354	34.4881	1162.1444	Laminar	1536.3905
967	4.7354	34.4946	1161.9275	Laminar	1536.6773
968	4.7354	34.5010	1161.7106	Laminar	1536.9643
969	4.7354	34.5075	1161.4936	Laminar	1537.2514

Depth (m)	Annular Velocity(m/s)	τ wall-corrected (Pa)	Reynolds Number	Flow Regime	Frictional Pressure Loss (Pa/m)
970	4.7354	34.5139	1161.2765	Laminar	1537.5387
971	4.7354	34.5204	1161.0594	Laminar	1537.8262
972	4.7354	34.5268	1160.8423	Laminar	1538.1138
973	4.7354	34.5333	1160.6251	Laminar	1538.4017
974	4.7354	34.5397	1160.4079	Laminar	1538.6896
975	4.7354	34.5462	1160.1906	Laminar	1538.9778
976	4.7354	34.5527	1159.9733	Laminar	1539.2661
977	4.7354	34.5592	1159.7560	Laminar	1539.5546
978	4.7354	34.5656	1159.5386	Laminar	1539.8432
979	4.7354	34.5721	1159.3211	Laminar	1540.1320
980	4.7354	34.5786	1159.1037	Laminar	1540.4210
981	4.7354	34.5851	1158.8861	Laminar	1540.7101
982	4.7354	34.5916	1158.6686	Laminar	1540.9995
983	4.7354	34.5981	1158.4509	Laminar	1541.2889
984	4.7354	34.6046	1158.2333	Laminar	1541.5786
985	4.7354	34.6111	1158.0156	Laminar	1541.8684
986	4.7354	34.6176	1157.7978	Laminar	1542.1583
987	4.7354	34.6241	1157.5801	Laminar	1542.4485
988	4.7354	34.6306	1157.3622	Laminar	1542.7388
989	4.7354	34.6371	1157.1444	Laminar	1543.0293
990	4.7354	34.6437	1156.9265	Laminar	1543.3199
991	4.7354	34.6502	1156.7085	Laminar	1543.6107
992	4.7354	34.6567	1156.4905	Laminar	1543.9017
993	4.7354	34.6633	1156.2725	Laminar	1544.1928
994	4.7354	34.6698	1156.0544	Laminar	1544.4841
995	4.7354	34.6763	1155.8363	Laminar	1544.7755
996	4.7354	34.6829	1155.6181	Laminar	1545.0672
997	4.7354	34.6894	1155.3999	Laminar	1545.3590
998	4.7354	34.6960	1155.1817	Laminar	1545.6509
999	4.7354	34.7026	1154.9634	Laminar	1545.9430
1000	4.7354	34.7091	1154.7451	Laminar	1546.2353
1001	4.7354	34.7157	1154.5267	Laminar	1546.5278
1002	4.7354	34.7223	1154.3083	Laminar	1546.8204
1003	4.7354	34.7288	1154.0899	Laminar	1547.1132
1004	4.7354	34.7354	1153.8714	Laminar	1547.4061
1005	4.7354	34.7420	1153.6529	Laminar	1547.6992
1006	4.7354	34.7486	1153.4343	Laminar	1547.9925
1007	4.7354	34.7551	1153.2157	Laminar	1548.2859
1008	4.7354	34.7617	1152.9970	Laminar	1548.5795

Depth (m)	Annular Velocity(m/s)	τ wall-corrected (Pa)	Reynolds Number	Flow Regime	Frictional Pressure Loss (Pa/m)
1009	4.7354	34.7683	1152.7784	Laminar	1548.8733
1010	4.7354	34.7749	1152.5596	Laminar	1549.1672
1011	4.7354	34.7815	1152.3409	Laminar	1549.4613
1012	4.7354	34.7881	1152.1221	Laminar	1549.7556
1013	4.7354	34.7947	1151.9032	Laminar	1550.0500
1014	4.7354	34.8014	1151.6844	Laminar	1550.3446
1015	4.7354	34.8080	1151.4655	Laminar	1550.6393
1016	4.7354	34.8146	1151.2465	Laminar	1550.9342
1017	4.7354	34.8212	1151.0275	Laminar	1551.2293
1018	4.7354	34.8278	1150.8085	Laminar	1551.5245
1019	4.7354	34.8345	1150.5894	Laminar	1551.8199
1020	4.7354	34.8411	1150.3703	Laminar	1552.1155
1021	4.7354	34.8478	1150.1512	Laminar	1552.4112
1022	4.7354	34.8544	1149.9320	Laminar	1552.7071
1023	4.7354	34.8610	1149.7128	Laminar	1553.0032
1024	4.7354	34.8677	1149.4935	Laminar	1553.2994
1025	4.7354	34.8743	1149.2742	Laminar	1553.5958
1026	4.7354	34.8810	1149.0549	Laminar	1553.8923
1027	4.7354	34.8877	1148.8355	Laminar	1554.1891
1028	4.7354	34.8943	1148.6161	Laminar	1554.4859
1029	4.7354	34.9010	1148.3967	Laminar	1554.7830
1030	4.7354	34.9077	1148.1772	Laminar	1555.0802
1031	4.7354	34.9143	1147.9577	Laminar	1555.3775
1032	4.7354	34.9210	1147.7381	Laminar	1555.6751
1033	4.7354	34.9277	1147.5186	Laminar	1555.9727
1034	4.7354	34.9344	1147.2989	Laminar	1556.2706
1035	4.7354	34.9411	1147.0793	Laminar	1556.5686
1036	4.7354	34.9478	1146.8596	Laminar	1556.8668
1037	4.7354	34.9545	1146.6399	Laminar	1557.1651
1038	4.7354	34.9612	1146.4201	Laminar	1557.4636
1039	4.7354	34.9679	1146.2003	Laminar	1557.7623
1040	4.7354	34.9746	1145.9805	Laminar	1558.0611
1041	4.7354	34.9813	1145.7606	Laminar	1558.3601
1042	4.7354	34.9880	1145.5407	Laminar	1558.6593
1043	4.7354	34.9947	1145.3208	Laminar	1558.9586
1044	4.7354	35.0014	1145.1008	Laminar	1559.2580
1045	4.7354	35.0082	1144.8808	Laminar	1559.5577
1046	4.7354	35.0149	1144.6607	Laminar	1559.8575
1047	4.7354	35.0216	1144.4407	Laminar	1560.1574

Depth (m)	Annular Velocity(m/s)	τ wall-corrected (Pa)	Reynolds Number	Flow Regime	Frictional Pressure Loss (Pa/m)
1048	4.7354	35.0284	1144.2205	Laminar	1560.4576
1049	4.7354	35.0351	1144.0004	Laminar	1560.7578
1050	4.7354	35.0419	1143.7802	Laminar	1561.0583
1051	4.7354	35.0486	1143.5600	Laminar	1561.3589
1052	4.7354	35.0554	1143.3398	Laminar	1561.6597
1053	4.7354	35.0621	1143.1195	Laminar	1561.9606
1054	4.7354	35.0689	1142.8992	Laminar	1562.2617
1055	4.7354	35.0756	1142.6788	Laminar	1562.5629
1056	4.7354	35.0824	1142.4585	Laminar	1562.8644
1057	4.7354	35.0892	1142.2380	Laminar	1563.1659
1058	4.7354	35.0959	1142.0176	Laminar	1563.4677
1059	4.7354	35.1027	1141.7971	Laminar	1563.7696
1060	4.7354	35.1095	1141.5766	Laminar	1564.0716
1061	4.7354	35.1163	1141.3561	Laminar	1564.3739
1062	4.7354	35.1231	1141.1355	Laminar	1564.6762
1063	4.7354	35.1299	1140.9149	Laminar	1564.9788
1064	4.7354	35.1367	1140.6943	Laminar	1565.2815
1065	4.7354	35.1435	1140.4736	Laminar	1565.5844
1066	4.7354	35.1503	1140.2529	Laminar	1565.8874
1067	4.7354	35.1571	1140.0321	Laminar	1566.1906
1068	4.7354	35.1639	1139.8114	Laminar	1566.4939
1069	4.7354	35.1707	1139.5906	Laminar	1566.7974
1070	4.7354	35.1775	1139.3698	Laminar	1567.1011
1071	4.7354	35.1843	1139.1489	Laminar	1567.4049
1072	4.7354	35.1911	1138.9280	Laminar	1567.7089
1073	4.7354	35.1980	1138.7071	Laminar	1568.0131
1074	4.7354	35.2048	1138.4861	Laminar	1568.3174
1075	4.7354	35.2116	1138.2651	Laminar	1568.6219
1076	4.7354	35.2185	1138.0441	Laminar	1568.9265
1077	4.7354	35.2253	1137.8231	Laminar	1569.2313
1078	4.7354	35.2322	1137.6020	Laminar	1569.5363
1079	4.7354	35.2390	1137.3809	Laminar	1569.8414
1080	4.7354	35.2459	1137.1598	Laminar	1570.1466
1081	4.7354	35.2527	1136.9386	Laminar	1570.4521
1082	4.7354	35.2596	1136.7174	Laminar	1570.7577
1083	4.7354	35.2664	1136.4962	Laminar	1571.0634
1084	4.7354	35.2733	1136.2749	Laminar	1571.3693
1085	4.7354	35.2802	1136.0537	Laminar	1571.6754
1086	4.7354	35.2871	1135.8324	Laminar	1571.9816

Depth (m)	Annular Velocity(m/s)	τ wall-corrected (Pa)	Reynolds Number	Flow Regime	Frictional Pressure Loss (Pa/m)
1087	4.7354	35.2939	1135.6110	Laminar	1572.2880
1088	4.7354	35.3008	1135.3896	Laminar	1572.5946
1089	4.7354	35.3077	1135.1682	Laminar	1572.9013
1090	4.7354	35.3146	1134.9468	Laminar	1573.2082
1091	4.7354	35.3215	1134.7254	Laminar	1573.5152
1092	4.7354	35.3284	1134.5039	Laminar	1573.8224
1093	4.7354	35.3353	1134.2824	Laminar	1574.1297
1094	4.7354	35.3422	1134.0608	Laminar	1574.4373
1095	4.7354	35.3491	1133.8393	Laminar	1574.7449
1096	4.7354	35.3560	1133.6177	Laminar	1575.0528
1097	4.7354	35.3629	1133.3960	Laminar	1575.3607
1098	4.7354	35.3698	1133.1744	Laminar	1575.6689
1099	4.7354	35.3767	1132.9527	Laminar	1575.9772
1100	4.7354	35.3837	1132.7310	Laminar	1576.2857
1101	4.7354	35.3906	1132.5092	Laminar	1576.5943
1102	4.7354	35.3975	1132.2875	Laminar	1576.9031
1103	4.7354	35.4045	1132.0657	Laminar	1577.2120
1104	4.7354	35.4114	1131.8439	Laminar	1577.5211
1105	4.7354	35.4183	1131.6220	Laminar	1577.8304
1106	4.7354	35.4253	1131.4002	Laminar	1578.1398
1107	4.7354	35.4322	1131.1783	Laminar	1578.4494
1108	4.7354	35.4392	1130.9563	Laminar	1578.7591
1109	4.7354	35.4462	1130.7344	Laminar	1579.0690
1110	4.7354	35.4531	1130.5124	Laminar	1579.3790
1111	4.7354	35.4601	1130.2904	Laminar	1579.6893
1112	4.7354	35.4670	1130.0684	Laminar	1579.9996
1113	4.7354	35.4740	1129.8463	Laminar	1580.3101
1114	4.7354	35.4810	1129.6242	Laminar	1580.6208
1115	4.7354	35.4880	1129.4021	Laminar	1580.9317
1116	4.7354	35.4949	1129.1800	Laminar	1581.2427
1117	4.7354	35.5019	1128.9578	Laminar	1581.5538
1118	4.7354	35.5089	1128.7357	Laminar	1581.8652
1119	4.7354	35.5159	1128.5134	Laminar	1582.1766
1120	4.7354	35.5229	1128.2912	Laminar	1582.4883
1121	4.7354	35.5299	1128.0690	Laminar	1582.8001
1122	4.7354	35.5369	1127.8467	Laminar	1583.1120
1123	4.7354	35.5439	1127.6244	Laminar	1583.4241
1124	4.7354	35.5509	1127.4020	Laminar	1583.7364
1125	4.7354	35.5579	1127.1797	Laminar	1584.0488

Depth (m)	Annular Velocity(m/s)	τ wall-corrected (Pa)	Reynolds Number	Flow Regime	Frictional Pressure Loss (Pa/m)
1126	4.7354	35.5650	1126.9573	Laminar	1584.3614
1127	4.7354	35.5720	1126.7349	Laminar	1584.6741
1128	4.7354	35.5790	1126.5124	Laminar	1584.9870
1129	4.7354	35.5860	1126.2900	Laminar	1585.3001
1130	4.7354	35.5931	1126.0675	Laminar	1585.6133
1131	4.7354	35.6001	1125.8450	Laminar	1585.9267
1132	4.7354	35.6071	1125.6225	Laminar	1586.2402
1133	4.7354	35.6142	1125.3999	Laminar	1586.5539
1134	4.7354	35.6212	1125.1773	Laminar	1586.8677
1135	4.7354	35.6283	1124.9548	Laminar	1587.1817
1136	4.7354	35.6353	1124.7321	Laminar	1587.4959
1137	4.7354	35.6424	1124.5095	Laminar	1587.8102
1138	4.7354	35.6494	1124.2868	Laminar	1588.1246
1139	4.7354	35.6565	1124.0641	Laminar	1588.4393
1140	4.7354	35.6636	1123.8414	Laminar	1588.7541
1141	4.7354	35.6706	1123.6187	Laminar	1589.0690
1142	4.7354	35.6777	1123.3959	Laminar	1589.3841
1143	4.7354	35.6848	1123.1731	Laminar	1589.6994
1144	4.7354	35.6919	1122.9503	Laminar	1590.0148
1145	4.7354	35.6989	1122.7275	Laminar	1590.3303
1146	4.7354	35.7060	1122.5047	Laminar	1590.6461
1147	4.7354	35.7131	1122.2818	Laminar	1590.9619
1148	4.7354	35.7202	1122.0589	Laminar	1591.2780
1149	4.7354	35.7273	1121.8360	Laminar	1591.5942
1150	4.7354	35.7344	1121.6130	Laminar	1591.9105
1151	4.7354	35.7415	1121.3901	Laminar	1592.2270
1152	4.7354	35.7486	1121.1671	Laminar	1592.5437
1153	4.7354	35.7557	1120.9441	Laminar	1592.8605
1154	4.7354	35.7629	1120.7211	Laminar	1593.1775
1155	4.7354	35.7700	1120.4980	Laminar	1593.4946
1156	4.7354	35.7771	1120.2750	Laminar	1593.8119
1157	4.7354	35.7842	1120.0519	Laminar	1594.1293
1158	4.7354	35.7913	1119.8288	Laminar	1594.4469
1159	4.7354	35.7985	1119.6057	Laminar	1594.7647
1160	4.7354	35.8056	1119.3825	Laminar	1595.0826
1161	4.7354	35.8128	1119.1594	Laminar	1595.4007
1162	4.7354	35.8199	1118.9362	Laminar	1595.7189
1163	4.7354	35.8270	1118.7130	Laminar	1596.0373
1164	4.7354	35.8342	1118.4897	Laminar	1596.3558

Depth (m)	Annular Velocity(m/s)	τ wall-corrected (Pa)	Reynolds Number	Flow Regime	Frictional Pressure Loss (Pa/m)
1165	4.7354	35.8414	1118.2665	Laminar	1596.6745
1166	4.7354	35.8485	1118.0432	Laminar	1596.9934
1167	4.7354	35.8557	1117.8199	Laminar	1597.3124
1168	4.7354	35.8628	1117.5966	Laminar	1597.6315
1169	4.7354	35.8700	1117.3733	Laminar	1597.9508
1170	4.7354	35.8772	1117.1500	Laminar	1598.2703
1171	4.7354	35.8843	1116.9266	Laminar	1598.5899
1172	4.7354	35.8915	1116.7032	Laminar	1598.9097
1173	4.7354	35.8987	1116.4798	Laminar	1599.2297
1174	4.7354	35.9059	1116.2564	Laminar	1599.5497
1175	4.7354	35.9131	1116.0329	Laminar	1599.8700
1176	4.7354	35.9203	1115.8095	Laminar	1600.1904
1177	4.7354	35.9275	1115.5860	Laminar	1600.5110
1178	4.7354	35.9347	1115.3625	Laminar	1600.8317
1179	4.7354	35.9419	1115.1390	Laminar	1601.1525
1180	4.7354	35.9491	1114.9154	Laminar	1601.4736
1181	4.7354	35.9563	1114.6919	Laminar	1601.7947
1182	4.7354	35.9635	1114.4683	Laminar	1602.1161
1183	4.7354	35.9707	1114.2447	Laminar	1602.4376
1184	4.7354	35.9779	1114.0211	Laminar	1602.7592
1185	4.7354	35.9852	1113.7975	Laminar	1603.0810
1186	4.7354	35.9924	1113.5739	Laminar	1603.4029
1187	4.7354	35.9996	1113.3502	Laminar	1603.7250
1188	4.7354	36.0069	1113.1265	Laminar	1604.0473
1189	4.7354	36.0141	1112.9028	Laminar	1604.3697
1190	4.7354	36.0213	1112.6791	Laminar	1604.6923
1191	4.7354	36.0286	1112.4554	Laminar	1605.0150
1192	4.7354	36.0358	1112.2316	Laminar	1605.3379
1193	4.7354	36.0431	1112.0079	Laminar	1605.6609
1194	4.7354	36.0503	1111.7841	Laminar	1605.9841
1195	4.7354	36.0576	1111.5603	Laminar	1606.3075
1196	4.7354	36.0648	1111.3365	Laminar	1606.6310
1197	4.7354	36.0721	1111.1127	Laminar	1606.9546
1198	4.7354	36.0794	1110.8888	Laminar	1607.2784
1199	4.7354	36.0867	1110.6649	Laminar	1607.6024
1200	4.7354	36.0939	1110.4411	Laminar	1607.9265
1201	4.7354	36.1012	1110.2172	Laminar	1608.2508
1202	4.7354	36.1085	1109.9933	Laminar	1608.5752
1203	4.7354	36.1158	1109.7693	Laminar	1608.8998

Depth (m)	Annular Velocity(m/s)	τ wall-corrected (Pa)	Reynolds Number	Flow Regime	Frictional Pressure Loss (Pa/m)
1204	4.7354	36.1231	1109.5454	Laminar	1609.2245
1205	4.7354	36.1304	1109.3214	Laminar	1609.5494
1206	4.7354	36.1377	1109.0975	Laminar	1609.8744
1207	4.7354	36.1450	1108.8735	Laminar	1610.1996
1208	4.7354	36.1523	1108.6495	Laminar	1610.5249
1209	4.7354	36.1596	1108.4254	Laminar	1610.8504
1210	4.7354	36.1669	1108.2014	Laminar	1611.1761
1211	4.7354	36.1742	1107.9774	Laminar	1611.5019
1212	4.7354	36.1815	1107.7533	Laminar	1611.8279
1213	4.7354	36.1888	1107.5292	Laminar	1612.1540
1214	4.7354	36.1962	1107.3051	Laminar	1612.4802
1215	4.7354	36.2035	1107.0810	Laminar	1612.8067
1216	4.7354	36.2108	1106.8569	Laminar	1613.1332
1217	4.7354	36.2181	1106.6327	Laminar	1613.4600
1218	4.7354	36.2255	1106.4086	Laminar	1613.7868
1219	4.7354	36.2328	1106.1844	Laminar	1614.1139
1220	4.7354	36.2402	1105.9602	Laminar	1614.4411
1221	4.7354	36.2475	1105.7360	Laminar	1614.7684
1222	4.7354	36.2549	1105.5118	Laminar	1615.0959
1223	4.7354	36.2622	1105.2876	Laminar	1615.4235
1224	4.7354	36.2696	1105.0634	Laminar	1615.7513
1225	4.7354	36.2769	1104.8391	Laminar	1616.0793
1226	4.7354	36.2843	1104.6149	Laminar	1616.4074
1227	4.7354	36.2917	1104.3906	Laminar	1616.7356
1228	4.7354	36.2990	1104.1663	Laminar	1617.0640
1229	4.7354	36.3064	1103.9420	Laminar	1617.3926
1230	4.7354	36.3138	1103.7177	Laminar	1617.7213
1231	4.7354	36.3212	1103.4933	Laminar	1618.0502
1232	4.7354	36.3286	1103.2690	Laminar	1618.3792
1233	4.7354	36.3360	1103.0446	Laminar	1618.7084
1234	4.7354	36.3433	1102.8203	Laminar	1619.0377
1235	4.7354	36.3507	1102.5959	Laminar	1619.3672
1236	4.7354	36.3581	1102.3715	Laminar	1619.6968
1237	4.7354	36.3655	1102.1471	Laminar	1620.0266
1238	4.7354	36.3730	1101.9227	Laminar	1620.3565
1239	4.7354	36.3804	1101.6982	Laminar	1620.6866
1240	4.7354	36.3878	1101.4738	Laminar	1621.0169
1241	4.7354	36.3952	1101.2493	Laminar	1621.3473
1242	4.7354	36.4026	1101.0249	Laminar	1621.6778

Depth (m)	Annular Velocity(m/s)	τ wall-corrected (Pa)	Reynolds Number	Flow Regime	Frictional Pressure Loss (Pa/m)
1243	4.7354	36.4100	1100.8004	Laminar	1622.0085
1244	4.7354	36.4175	1100.5759	Laminar	1622.3394
1245	4.7354	36.4249	1100.3514	Laminar	1622.6704
1246	4.7354	36.4323	1100.1269	Laminar	1623.0015
1247	4.7354	36.4398	1099.9024	Laminar	1623.3328
1248	4.7354	36.4472	1099.6778	Laminar	1623.6643
1249	4.7354	36.4546	1099.4533	Laminar	1623.9959
1250	4.7354	36.4621	1099.2287	Laminar	1624.3277
1251	4.7354	36.4695	1099.0041	Laminar	1624.6596
1252	4.7354	36.4770	1098.7796	Laminar	1624.9916
1253	4.7354	36.4845	1098.5550	Laminar	1625.3239
1254	4.7354	36.4919	1098.3304	Laminar	1625.6562
1255	4.7354	36.4994	1098.1058	Laminar	1625.9887
1256	4.7354	36.5069	1097.8811	Laminar	1626.3214
1257	4.7354	36.5143	1097.6565	Laminar	1626.6542
1258	4.7354	36.5218	1097.4319	Laminar	1626.9872
1259	4.7354	36.5293	1097.2072	Laminar	1627.3203
1260	4.7354	36.5368	1096.9825	Laminar	1627.6536
1261	4.7354	36.5442	1096.7579	Laminar	1627.9871
1262	4.7354	36.5517	1096.5332	Laminar	1628.3206
1263	4.7354	36.5592	1096.3085	Laminar	1628.6544
1264	4.7354	36.5667	1096.0838	Laminar	1628.9883
1265	4.7354	36.5742	1095.8591	Laminar	1629.3223
1266	4.7354	36.5817	1095.6343	Laminar	1629.6565
1267	4.7354	36.5892	1095.4096	Laminar	1629.9908
1268	4.7354	36.5967	1095.1849	Laminar	1630.3253
1269	4.7354	36.6042	1094.9601	Laminar	1630.6599
1270	4.7354	36.6118	1094.7354	Laminar	1630.9947
1271	4.7354	36.6193	1094.5106	Laminar	1631.3297
1272	4.7354	36.6268	1094.2858	Laminar	1631.6648
1273	4.7354	36.6343	1094.0610	Laminar	1632.0000
1274	4.7354	36.6418	1093.8362	Laminar	1632.3354
1275	4.7354	36.6494	1093.6114	Laminar	1632.6710
1276	4.7354	36.6569	1093.3866	Laminar	1633.0067
1277	4.7354	36.6645	1093.1618	Laminar	1633.3425
1278	4.7354	36.6720	1092.9370	Laminar	1633.6785
1279	4.7354	36.6795	1092.7121	Laminar	1634.0147
1280	4.7354	36.6871	1092.4873	Laminar	1634.3510
1281	4.7354	36.6946	1092.2624	Laminar	1634.6874

Depth (m)	Annular Velocity(m/s)	τ wall-corrected (Pa)	Reynolds Number	Flow Regime	Frictional Pressure Loss (Pa/m)
1282	4.7354	36.7022	1092.0375	Laminar	1635.0240
1283	4.7354	36.7098	1091.8127	Laminar	1635.3608
1284	4.7354	36.7173	1091.5878	Laminar	1635.6977
1285	4.7354	36.7249	1091.3629	Laminar	1636.0347
1286	4.7354	36.7325	1091.1380	Laminar	1636.3719
1287	4.7354	36.7400	1090.9131	Laminar	1636.7093
1288	4.7354	36.7476	1090.6882	Laminar	1637.0468
1289	4.7354	36.7552	1090.4633	Laminar	1637.3844
1290	4.7354	36.7628	1090.2384	Laminar	1637.7222
1291	4.7354	36.7704	1090.0134	Laminar	1638.0602
1292	4.7354	36.7779	1089.7885	Laminar	1638.3983
1293	4.7354	36.7855	1089.5635	Laminar	1638.7365
1294	4.7354	36.7931	1089.3386	Laminar	1639.0750
1295	4.7354	36.8007	1089.1136	Laminar	1639.4135
1296	4.7354	36.8083	1088.8887	Laminar	1639.7522
1297	4.7354	36.8159	1088.6637	Laminar	1640.0911
1298	4.7354	36.8236	1088.4387	Laminar	1640.4301
1299	4.7354	36.8312	1088.2137	Laminar	1640.7692
1300	4.7354	36.8388	1087.9887	Laminar	1641.1085
1301	4.7354	36.8464	1087.7637	Laminar	1641.4480
1302	4.7354	36.8540	1087.5387	Laminar	1641.7876
1303	4.7354	36.8617	1087.3137	Laminar	1642.1273
1304	4.7354	36.8693	1087.0887	Laminar	1642.4673
1305	4.7354	36.8769	1086.8637	Laminar	1642.8073
1306	4.7354	36.8846	1086.6387	Laminar	1643.1475
1307	4.7354	36.8922	1086.4136	Laminar	1643.4879
1308	4.7354	36.8998	1086.1886	Laminar	1643.8284
1309	4.7354	36.9075	1085.9635	Laminar	1644.1690
1310	4.7354	36.9151	1085.7385	Laminar	1644.5098
1311	4.7354	36.9228	1085.5134	Laminar	1644.8508
1312	4.7354	36.9304	1085.2884	Laminar	1645.1919
1313	4.7354	36.9381	1085.0633	Laminar	1645.5331
1314	4.7354	36.9458	1084.8382	Laminar	1645.8745
1315	4.7354	36.9534	1084.6132	Laminar	1646.2161
1316	4.7354	36.9611	1084.3881	Laminar	1646.5578
1317	4.7354	36.9688	1084.1630	Laminar	1646.8996
1318	4.7354	36.9765	1083.9379	Laminar	1647.2416
1319	4.7354	36.9841	1083.7128	Laminar	1647.5838
1320	4.7354	36.9918	1083.4877	Laminar	1647.9260

Depth (m)	Annular Velocity(m/s)	τ wall-corrected (Pa)	Reynolds Number	Flow Regime	Frictional Pressure Loss (Pa/m)
1321	4.7354	36.9995	1083.2626	Laminar	1648.2685
1322	4.7354	37.0072	1083.0375	Laminar	1648.6111
1323	4.7354	37.0149	1082.8124	Laminar	1648.9538
1324	4.7354	37.0226	1082.5873	Laminar	1649.2967
1325	4.7354	37.0303	1082.3621	Laminar	1649.6398
1326	4.7354	37.0380	1082.1370	Laminar	1649.9829
1327	4.7354	37.0457	1081.9119	Laminar	1650.3263
1328	4.7354	37.0534	1081.6867	Laminar	1650.6698
1329	4.7354	37.0611	1081.4616	Laminar	1651.0134
1330	4.7354	37.0688	1081.2365	Laminar	1651.3572
1331	4.7354	37.0766	1081.0113	Laminar	1651.7011
1332	4.7354	37.0843	1080.7862	Laminar	1652.0452
1333	4.7354	37.0920	1080.5610	Laminar	1652.3894
1334	4.7354	37.0997	1080.3359	Laminar	1652.7338
1335	4.7354	37.1075	1080.1107	Laminar	1653.0783
1336	4.7354	37.1152	1079.8856	Laminar	1653.4230
1337	4.7354	37.1230	1079.6604	Laminar	1653.7678
1338	4.7354	37.1307	1079.4352	Laminar	1654.1128
1339	4.7354	37.1384	1079.2101	Laminar	1654.4579
1340	4.7354	37.1462	1078.9849	Laminar	1654.8032
1341	4.7354	37.1539	1078.7597	Laminar	1655.1486
1342	4.7354	37.1617	1078.5345	Laminar	1655.4942
1343	4.7354	37.1695	1078.3093	Laminar	1655.8399
1344	4.7354	37.1772	1078.0842	Laminar	1656.1857
1345	4.7354	37.1850	1077.8590	Laminar	1656.5317
1346	4.7354	37.1928	1077.6338	Laminar	1656.8779
1347	4.7354	37.2005	1077.4086	Laminar	1657.2242
1348	4.7354	37.2083	1077.1834	Laminar	1657.5707
1349	4.7354	37.2161	1076.9582	Laminar	1657.9173
1350	4.7354	37.2239	1076.7330	Laminar	1658.2640
1351	4.7354	37.2317	1076.5078	Laminar	1658.6109
1352	4.7354	37.2395	1076.2826	Laminar	1658.9579
1353	4.7354	37.2473	1076.0574	Laminar	1659.3051
1354	4.7354	37.2550	1075.8322	Laminar	1659.6525
1355	4.7354	37.2628	1075.6070	Laminar	1660.0000
1356	4.7354	37.2707	1075.3818	Laminar	1660.3476
1357	4.7354	37.2785	1075.1566	Laminar	1660.6954
1358	4.7354	37.2863	1074.9314	Laminar	1661.0433
1359	4.7354	37.2941	1074.7062	Laminar	1661.3914

Depth (m)	Annular Velocity(m/s)	τ wall-corrected (Pa)	Reynolds Number	Flow Regime	Frictional Pressure Loss (Pa/m)
1360	4.7354	37.3019	1074.4810	Laminar	1661.7396
1361	4.7354	37.3097	1074.2558	Laminar	1662.0880
1362	4.7354	37.3175	1074.0306	Laminar	1662.4365
1363	4.7354	37.3254	1073.8053	Laminar	1662.7852
1364	4.7354	37.3332	1073.5801	Laminar	1663.1340
1365	4.7354	37.3410	1073.3549	Laminar	1663.4830
1366	4.7354	37.3489	1073.1297	Laminar	1663.8321
1367	4.7354	37.3567	1072.9045	Laminar	1664.1813
1368	4.7354	37.3646	1072.6793	Laminar	1664.5307
1369	4.7354	37.3724	1072.4540	Laminar	1664.8803
1370	4.7354	37.3803	1072.2288	Laminar	1665.2300
1371	4.7354	37.3881	1072.0036	Laminar	1665.5798
1372	4.7354	37.3960	1071.7784	Laminar	1665.9298
1373	4.7354	37.4038	1071.5532	Laminar	1666.2800
1374	4.7354	37.4117	1071.3280	Laminar	1666.6303
1375	4.7354	37.4195	1071.1027	Laminar	1666.9807
1376	4.7354	37.4274	1070.8775	Laminar	1667.3313
1377	4.7354	37.4353	1070.6523	Laminar	1667.6820
1378	4.7354	37.4432	1070.4271	Laminar	1668.0329
1379	4.7354	37.4510	1070.2019	Laminar	1668.3839
1380	4.7354	37.4589	1069.9767	Laminar	1668.7351
1381	4.7354	37.4668	1069.7515	Laminar	1669.0864
1382	4.7354	37.4747	1069.5262	Laminar	1669.4379
1383	4.7354	37.4826	1069.3010	Laminar	1669.7895
1384	4.7354	37.4905	1069.0758	Laminar	1670.1412
1385	4.7354	37.4984	1068.8506	Laminar	1670.4931
1386	4.7354	37.5063	1068.6254	Laminar	1670.8452
1387	4.7354	37.5142	1068.4002	Laminar	1671.1974
1388	4.7354	37.5221	1068.1750	Laminar	1671.5497
1389	4.7354	37.5300	1067.9498	Laminar	1671.9022
1390	4.7354	37.5379	1067.7246	Laminar	1672.2549
1391	4.7354	37.5459	1067.4994	Laminar	1672.6076
1392	4.7354	37.5538	1067.2742	Laminar	1672.9606
1393	4.7354	37.5617	1067.0490	Laminar	1673.3137
1394	4.7354	37.5696	1066.8238	Laminar	1673.6669
1395	4.7354	37.5776	1066.5986	Laminar	1674.0202
1396	4.7354	37.5855	1066.3734	Laminar	1674.3738
1397	4.7354	37.5934	1066.1482	Laminar	1674.7274
1398	4.7354	37.6014	1065.9230	Laminar	1675.0812

Depth (m)	Annular Velocity(m/s)	τ wall-corrected (Pa)	Reynolds Number	Flow Regime	Frictional Pressure Loss (Pa/m)
1399	4.7354	37.6093	1065.6978	Laminar	1675.4352
1400	4.7354	37.6173	1065.4726	Laminar	1675.7893
1401	4.7354	37.6252	1065.2474	Laminar	1676.1435
1402	4.7354	37.6332	1065.0223	Laminar	1676.4979
1403	4.7354	37.6411	1064.7971	Laminar	1676.8525
1404	4.7354	37.6491	1064.5719	Laminar	1677.2072
1405	4.7354	37.6571	1064.3467	Laminar	1677.5620
1406	4.7354	37.6650	1064.1216	Laminar	1677.9170
1407	4.7354	37.6730	1063.8964	Laminar	1678.2721
1408	4.7354	37.6810	1063.6712	Laminar	1678.6274
1409	4.7354	37.6890	1063.4461	Laminar	1678.9828
1410	4.7354	37.6969	1063.2209	Laminar	1679.3383
1411	4.7354	37.7049	1062.9957	Laminar	1679.6940
1412	4.7354	37.7129	1062.7706	Laminar	1680.0499
1413	4.7354	37.7209	1062.5454	Laminar	1680.4059
1414	4.7354	37.7289	1062.3203	Laminar	1680.7620
1415	4.7354	37.7369	1062.0951	Laminar	1681.1183
1416	4.7354	37.7449	1061.8700	Laminar	1681.4747
1417	4.7354	37.7529	1061.6449	Laminar	1681.8313
1418	4.7354	37.7609	1061.4197	Laminar	1682.1881
1419	4.7354	37.7689	1061.1946	Laminar	1682.5449
1420	4.7354	37.7769	1060.9695	Laminar	1682.9019
1421	4.7354	37.7850	1060.7444	Laminar	1683.2591
1422	4.7354	37.7930	1060.5192	Laminar	1683.6164
1423	4.7354	37.8010	1060.2941	Laminar	1683.9739
1424	4.7354	37.8090	1060.0690	Laminar	1684.3315
1425	4.7354	37.8171	1059.8439	Laminar	1684.6892
1426	4.7354	37.8251	1059.6188	Laminar	1685.0471
1427	4.7354	37.8331	1059.3937	Laminar	1685.4051
1428	4.7354	37.8412	1059.1686	Laminar	1685.7633
1429	4.7354	37.8492	1058.9435	Laminar	1686.1216
1430	4.7354	37.8573	1058.7185	Laminar	1686.4801
1431	4.7354	37.8653	1058.4934	Laminar	1686.8387
1432	4.7354	37.8734	1058.2683	Laminar	1687.1975
1433	4.7354	37.8814	1058.0432	Laminar	1687.5564
1434	4.7354	37.8895	1057.8182	Laminar	1687.9154
1435	4.7354	37.8975	1057.5931	Laminar	1688.2746
1436	4.7354	37.9056	1057.3680	Laminar	1688.6340
1437	4.7354	37.9137	1057.1430	Laminar	1688.9935

Depth (m)	Annular Velocity(m/s)	τ wall-corrected (Pa)	Reynolds Number	Flow Regime	Frictional Pressure Loss (Pa/m)
1438	4.7354	37.9218	1056.9180	Laminar	1689.3531
1439	4.7354	37.9298	1056.6929	Laminar	1689.7129
1440	4.7354	37.9379	1056.4679	Laminar	1690.0728
1441	4.7354	37.9460	1056.2428	Laminar	1690.4329
1442	4.7354	37.9541	1056.0178	Laminar	1690.7931
1443	4.7354	37.9622	1055.7928	Laminar	1691.1534
1444	4.7354	37.9703	1055.5678	Laminar	1691.5139
1445	4.7354	37.9784	1055.3428	Laminar	1691.8746
1446	4.7354	37.9865	1055.1178	Laminar	1692.2353
1447	4.7354	37.9946	1054.8928	Laminar	1692.5963
1448	4.7354	38.0027	1054.6678	Laminar	1692.9574
1449	4.7354	38.0108	1054.4428	Laminar	1693.3186
1450	4.7354	38.0189	1054.2178	Laminar	1693.6799
1451	4.7354	38.0270	1053.9929	Laminar	1694.0415
1452	4.7354	38.0351	1053.7679	Laminar	1694.4031
1453	4.7354	38.0432	1053.5429	Laminar	1694.7649
1454	4.7354	38.0514	1053.3180	Laminar	1695.1269
1455	4.7354	38.0595	1053.0930	Laminar	1695.4889
1456	4.7354	38.0676	1052.8681	Laminar	1695.8512
1457	4.7354	38.0758	1052.6432	Laminar	1696.2136
1458	4.7354	38.0839	1052.4182	Laminar	1696.5761
1459	4.7354	38.0920	1052.1933	Laminar	1696.9387
1460	4.7354	38.1002	1051.9684	Laminar	1697.3015
1461	4.7354	38.1083	1051.7435	Laminar	1697.6645
1462	4.7354	38.1165	1051.5186	Laminar	1698.0276
1463	4.7354	38.1246	1051.2937	Laminar	1698.3908
1464	4.7354	38.1328	1051.0688	Laminar	1698.7542
1465	4.7354	38.1409	1050.8439	Laminar	1699.1178
1466	4.7354	38.1491	1050.6191	Laminar	1699.4814
1467	4.7354	38.1573	1050.3942	Laminar	1699.8452
1468	4.7354	38.1654	1050.1694	Laminar	1700.2092
1469	4.7354	38.1736	1049.9445	Laminar	1700.5733
1470	4.7354	38.1818	1049.7197	Laminar	1700.9376
1471	4.7354	38.1900	1049.4948	Laminar	1701.3020
1472	4.7354	38.1982	1049.2700	Laminar	1701.6665
1473	4.7354	38.2063	1049.0452	Laminar	1702.0312
1474	4.7354	38.2145	1048.8204	Laminar	1702.3960
1475	4.7354	38.2227	1048.5956	Laminar	1702.7610
1476	4.7354	38.2309	1048.3708	Laminar	1703.1261

Depth (m)	Annular Velocity(m/s)	τ wall-corrected (Pa)	Reynolds Number	Flow Regime	Frictional Pressure Loss (Pa/m)
1477	4.7354	38.2391	1048.1460	Laminar	1703.4913
1478	4.7354	38.2473	1047.9212	Laminar	1703.8567
1479	4.7354	38.2555	1047.6964	Laminar	1704.2223
1480	4.7354	38.2637	1047.4717	Laminar	1704.5880
1481	4.7354	38.2720	1047.2469	Laminar	1704.9538
1482	4.7354	38.2802	1047.0222	Laminar	1705.3198
1483	4.7354	38.2884	1046.7974	Laminar	1705.6859
1484	4.7354	38.2966	1046.5727	Laminar	1706.0522
1485	4.7354	38.3048	1046.3480	Laminar	1706.4186
1486	4.7354	38.3131	1046.1233	Laminar	1706.7851
1487	4.7354	38.3213	1045.8986	Laminar	1707.1518
1488	4.7354	38.3295	1045.6739	Laminar	1707.5186
1489	4.7354	38.3378	1045.4492	Laminar	1707.8856
1490	4.7354	38.3460	1045.2245	Laminar	1708.2527
1491	4.7354	38.3542	1044.9998	Laminar	1708.6200
1492	4.7354	38.3625	1044.7752	Laminar	1708.9874
1493	4.7354	38.3707	1044.5505	Laminar	1709.3549
1494	4.7354	38.3790	1044.3259	Laminar	1709.7226
1495	4.7354	38.3873	1044.1013	Laminar	1710.0905
1496	4.7354	38.3955	1043.8766	Laminar	1710.4585
1497	4.7354	38.4038	1043.6520	Laminar	1710.8266
1498	4.7354	38.4120	1043.4274	Laminar	1711.1948
1499	4.7354	38.4203	1043.2028	Laminar	1711.5633
1500	4.7354	38.4286	1042.9782	Laminar	1711.9318
1501	4.7354	38.4369	1042.7537	Laminar	1712.3005
1502	4.7354	38.4451	1042.5291	Laminar	1712.6693
1503	4.7354	38.4534	1042.3045	Laminar	1713.0383
1504	4.7354	38.4617	1042.0800	Laminar	1713.4074
1505	4.7354	38.4700	1041.8555	Laminar	1713.7767
1506	4.7354	38.4783	1041.6309	Laminar	1714.1461
1507	4.7354	38.4866	1041.4064	Laminar	1714.5157
1508	4.7354	38.4949	1041.1819	Laminar	1714.8854
1509	4.7354	38.5032	1040.9574	Laminar	1715.2552
1510	4.7354	38.5115	1040.7329	Laminar	1715.6252
1511	4.7354	38.5198	1040.5085	Laminar	1715.9953
1512	4.7354	38.5281	1040.2840	Laminar	1716.3656
1513	4.7354	38.5364	1040.0595	Laminar	1716.7360
1514	4.7354	38.5447	1039.8351	Laminar	1717.1065
1515	4.7354	38.5531	1039.6107	Laminar	1717.4772

Depth (m)	Annular Velocity(m/s)	τ wall-corrected (Pa)	Reynolds Number	Flow Regime	Frictional Pressure Loss (Pa/m)
1516	4.7354	38.5614	1039.3862	Laminar	1717.8480
1517	4.7354	38.5697	1039.1618	Laminar	1718.2190
1518	4.7354	38.5781	1038.9374	Laminar	1718.5901
1519	4.7354	38.5864	1038.7130	Laminar	1718.9614
1520	4.7354	38.5947	1038.4887	Laminar	1719.3328
1521	4.7354	38.6031	1038.2643	Laminar	1719.7044
1522	4.7354	38.6114	1038.0399	Laminar	1720.0760
1523	4.7354	38.6198	1037.8156	Laminar	1720.4479
1524	4.7354	38.6281	1037.5912	Laminar	1720.8198
1525	4.7354	38.6365	1037.3669	Laminar	1721.1920
1526	4.7354	38.6448	1037.1426	Laminar	1721.5642
1527	4.7354	38.6532	1036.9183	Laminar	1721.9366
1528	4.7354	38.6615	1036.6940	Laminar	1722.3092
1529	4.7354	38.6699	1036.4697	Laminar	1722.6818
1530	4.7354	38.6783	1036.2455	Laminar	1723.0547
1531	4.7354	38.6866	1036.0212	Laminar	1723.4276
1532	4.7354	38.6950	1035.7970	Laminar	1723.8007
1533	4.7354	38.7034	1035.5727	Laminar	1724.1740
1534	4.7354	38.7118	1035.3485	Laminar	1724.5474
1535	4.7354	38.7202	1035.1243	Laminar	1724.9209
1536	4.7354	38.7286	1034.9001	Laminar	1725.2946
1537	4.7354	38.7369	1034.6759	Laminar	1725.6684
1538	4.7354	38.7453	1034.4518	Laminar	1726.0424
1539	4.7354	38.7537	1034.2276	Laminar	1726.4165
1540	4.7354	38.7621	1034.0035	Laminar	1726.7907
1541	4.7354	38.7705	1033.7793	Laminar	1727.1651
1542	4.7354	38.7789	1033.5552	Laminar	1727.5397
1543	4.7354	38.7874	1033.3311	Laminar	1727.9143
1544	4.7354	38.7958	1033.1070	Laminar	1728.2891
1545	4.7354	38.8042	1032.8829	Laminar	1728.6641
1546	4.7354	38.8126	1032.6588	Laminar	1729.0392
1547	4.7354	38.8210	1032.4348	Laminar	1729.4144
1548	4.7354	38.8295	1032.2107	Laminar	1729.7898
1549	4.7354	38.8379	1031.9867	Laminar	1730.1653
1550	4.7354	38.8463	1031.7627	Laminar	1730.5410
1551	4.7354	38.8548	1031.5387	Laminar	1730.9168
1552	4.7354	38.8632	1031.3147	Laminar	1731.2927
1553	4.7354	38.8716	1031.0907	Laminar	1731.6688
1554	4.7354	38.8801	1030.8667	Laminar	1732.0450

Depth (m)	Annular Velocity(m/s)	τ wall-corrected (Pa)	Reynolds Number	Flow Regime	Frictional Pressure Loss (Pa/m)
1555	4.7354	38.8885	1030.6428	Laminar	1732.4214
1556	4.7354	38.8970	1030.4188	Laminar	1732.7979
1557	4.7354	38.9054	1030.1949	Laminar	1733.1746
1558	4.7354	38.9139	1029.9710	Laminar	1733.5514
1559	4.7354	38.9224	1029.7471	Laminar	1733.9283
1560	4.7354	38.9308	1029.5232	Laminar	1734.3054
1561	4.7354	38.9393	1029.2993	Laminar	1734.6826
1562	4.7354	38.9478	1029.0755	Laminar	1735.0599
1563	4.7354	38.9562	1028.8516	Laminar	1735.4374
1564	4.7354	38.9647	1028.6278	Laminar	1735.8151
1565	4.7354	38.9732	1028.4040	Laminar	1736.1929
1566	4.7354	38.9817	1028.1802	Laminar	1736.5708
1567	4.7354	38.9902	1027.9564	Laminar	1736.9488
1568	4.7354	38.9986	1027.7326	Laminar	1737.3270
1569	4.7354	39.0071	1027.5088	Laminar	1737.7054
1570	4.7354	39.0156	1027.2851	Laminar	1738.0839
1571	4.7354	39.0241	1027.0613	Laminar	1738.4625
1572	4.7354	39.0326	1026.8376	Laminar	1738.8413
1573	4.7354	39.0411	1026.6139	Laminar	1739.2202
1574	4.7354	39.0497	1026.3902	Laminar	1739.5992
1575	4.7354	39.0582	1026.1665	Laminar	1739.9784
1576	4.7354	39.0667	1025.9429	Laminar	1740.3577
1577	4.7354	39.0752	1025.7192	Laminar	1740.7372
1578	4.7354	39.0837	1025.4956	Laminar	1741.1168
1579	4.7354	39.0922	1025.2720	Laminar	1741.4966
1580	4.7354	39.1008	1025.0484	Laminar	1741.8765
1581	4.7354	39.1093	1024.8248	Laminar	1742.2565
1582	4.7354	39.1178	1024.6012	Laminar	1742.6367
1583	4.7354	39.1264	1024.3776	Laminar	1743.0170
1584	4.7354	39.1349	1024.1541	Laminar	1743.3974
1585	4.7354	39.1435	1023.9306	Laminar	1743.7780
1586	4.7354	39.1520	1023.7070	Laminar	1744.1588
1587	4.7354	39.1606	1023.4835	Laminar	1744.5396
1588	4.7354	39.1691	1023.2601	Laminar	1744.9207
1589	4.7354	39.1777	1023.0366	Laminar	1745.3018
1590	4.7354	39.1862	1022.8131	Laminar	1745.6831
1591	4.7354	39.1948	1022.5897	Laminar	1746.0646
1592	4.7354	39.2033	1022.3663	Laminar	1746.4461
1593	4.7354	39.2119	1022.1429	Laminar	1746.8278

Depth (m)	Annular Velocity(m/s)	τ wall-corrected (Pa)	Reynolds Number	Flow Regime	Frictional Pressure Loss (Pa/m)
1594	4.7354	39.2205	1021.9195	Laminar	1747.2097
1595	4.7354	39.2291	1021.6961	Laminar	1747.5917
1596	4.7354	39.2376	1021.4727	Laminar	1747.9738
1597	4.7354	39.2462	1021.2494	Laminar	1748.3561
1598	4.7354	39.2548	1021.0260	Laminar	1748.7385
1599	4.7354	39.2634	1020.8027	Laminar	1749.1211
1600	4.7354	39.2720	1020.5794	Laminar	1749.5038
1601	4.7354	39.2806	1020.3562	Laminar	1749.8866
1602	4.7354	39.2892	1020.1329	Laminar	1750.2696
1603	4.7354	39.2978	1019.9096	Laminar	1750.6527
1604	4.7354	39.3064	1019.6864	Laminar	1751.0360
1605	4.7354	39.3150	1019.4632	Laminar	1751.4194
1606	4.7354	39.3236	1019.2400	Laminar	1751.8029
1607	4.7354	39.3322	1019.0168	Laminar	1752.1866
1608	4.7354	39.3408	1018.7936	Laminar	1752.5704
1609	4.7354	39.3494	1018.5705	Laminar	1752.9544
1610	4.7354	39.3581	1018.3473	Laminar	1753.3385
1611	4.7354	39.3667	1018.1242	Laminar	1753.7227
1612	4.7354	39.3753	1017.9011	Laminar	1754.1071
1613	4.7354	39.3840	1017.6780	Laminar	1754.4916
1614	4.7354	39.3926	1017.4550	Laminar	1754.8763
1615	4.7354	39.4012	1017.2319	Laminar	1755.2611
1616	4.7354	39.4099	1017.0089	Laminar	1755.6460
1617	4.7354	39.4185	1016.7859	Laminar	1756.0311
1618	4.7354	39.4272	1016.5629	Laminar	1756.4163
1619	4.7354	39.4358	1016.3399	Laminar	1756.8017
1620	4.7354	39.4445	1016.1169	Laminar	1757.1872
1621	4.7354	39.4531	1015.8940	Laminar	1757.5728
1622	4.7354	39.4618	1015.6710	Laminar	1757.9586
1623	4.7354	39.4704	1015.4481	Laminar	1758.3445
1624	4.7354	39.4791	1015.2252	Laminar	1758.7306
1625	4.7354	39.4878	1015.0023	Laminar	1759.1168
1626	4.7354	39.4964	1014.7795	Laminar	1759.5031
1627	4.7354	39.5051	1014.5566	Laminar	1759.8896
1628	4.7354	39.5138	1014.3338	Laminar	1760.2762
1629	4.7354	39.5225	1014.1110	Laminar	1760.6629
1630	4.7354	39.5312	1013.8882	Laminar	1761.0498
1631	4.7354	39.5399	1013.6654	Laminar	1761.4369
1632	4.7354	39.5485	1013.4426	Laminar	1761.8240

Depth (m)	Annular Velocity(m/s)	τ wall-corrected (Pa)	Reynolds Number	Flow Regime	Frictional Pressure Loss (Pa/m)
1633	4.7354	39.5572	1013.2199	Laminar	1762.2113
1634	4.7354	39.5659	1012.9972	Laminar	1762.5988
1635	4.7354	39.5746	1012.7745	Laminar	1762.9864
1636	4.7354	39.5833	1012.5518	Laminar	1763.3741
1637	4.7354	39.5920	1012.3291	Laminar	1763.7620
1638	4.7354	39.6008	1012.1065	Laminar	1764.1500
1639	4.7354	39.6095	1011.8838	Laminar	1764.5381
1640	4.7354	39.6182	1011.6612	Laminar	1764.9264
1641	4.7354	39.6269	1011.4386	Laminar	1765.3148
1642	4.7354	39.6356	1011.2161	Laminar	1765.7034
1643	4.7354	39.6444	1010.9935	Laminar	1766.0921
1644	4.7354	39.6531	1010.7710	Laminar	1766.4809
1645	4.7354	39.6618	1010.5484	Laminar	1766.8699
1646	4.7354	39.6705	1010.3259	Laminar	1767.2590
1647	4.7354	39.6793	1010.1034	Laminar	1767.6483
1648	4.7354	39.6880	1009.8810	Laminar	1768.0377
1649	4.7354	39.6968	1009.6585	Laminar	1768.4272
1650	4.7354	39.7055	1009.4361	Laminar	1768.8169
1651	4.7354	39.7143	1009.2137	Laminar	1769.2067
1652	4.7354	39.7230	1008.9913	Laminar	1769.5966
1653	4.7354	39.7318	1008.7689	Laminar	1769.9867
1654	4.7354	39.7405	1008.5466	Laminar	1770.3770
1655	4.7354	39.7493	1008.3242	Laminar	1770.7673
1656	4.7354	39.7581	1008.1019	Laminar	1771.1578
1657	4.7354	39.7668	1007.8796	Laminar	1771.5485
1658	4.7354	39.7756	1007.6574	Laminar	1771.9392
1659	4.7354	39.7844	1007.4351	Laminar	1772.3302
1660	4.7354	39.7932	1007.2129	Laminar	1772.7212
1661	4.7354	39.8019	1006.9906	Laminar	1773.1124
1662	4.7354	39.8107	1006.7684	Laminar	1773.5038
1663	4.7354	39.8195	1006.5463	Laminar	1773.8952
1664	4.7354	39.8283	1006.3241	Laminar	1774.2869
1665	4.7354	39.8371	1006.1020	Laminar	1774.6786
1666	4.7354	39.8459	1005.8798	Laminar	1775.0705
1667	4.7354	39.8547	1005.6577	Laminar	1775.4625
1668	4.7354	39.8635	1005.4356	Laminar	1775.8547
1669	4.7354	39.8723	1005.2136	Laminar	1776.2470
1670	4.7354	39.8811	1004.9915	Laminar	1776.6394
1671	4.7354	39.8899	1004.7695	Laminar	1777.0320

Depth (m)	Annular Velocity(m/s)	τ wall-corrected (Pa)	Reynolds Number	Flow Regime	Frictional Pressure Loss (Pa/m)
1672	4.7354	39.8987	1004.5475	Laminar	1777.4247
1673	4.7354	39.9076	1004.3255	Laminar	1777.8176
1674	4.7354	39.9164	1004.1036	Laminar	1778.2106
1675	4.7354	39.9252	1003.8816	Laminar	1778.6037
1676	4.7354	39.9340	1003.6597	Laminar	1778.9970
1677	4.7354	39.9429	1003.4378	Laminar	1779.3904
1678	4.7354	39.9517	1003.2159	Laminar	1779.7840
1679	4.7354	39.9605	1002.9941	Laminar	1780.1777
1680	4.7354	39.9694	1002.7722	Laminar	1780.5715
1681	4.7354	39.9782	1002.5504	Laminar	1780.9654
1682	4.7354	39.9871	1002.3286	Laminar	1781.3595
1683	4.7354	39.9959	1002.1068	Laminar	1781.7538
1684	4.7354	40.0048	1001.8851	Laminar	1782.1482
1685	4.7354	40.0136	1001.6633	Laminar	1782.5427
1686	4.7354	40.0225	1001.4416	Laminar	1782.9373
1687	4.7354	40.0313	1001.2199	Laminar	1783.3321
1688	4.7354	40.0402	1000.9982	Laminar	1783.7271
1689	4.7354	40.0491	1000.7766	Laminar	1784.1221
1690	4.7354	40.0580	1000.5549	Laminar	1784.5173
1691	4.7354	40.0668	1000.3333	Laminar	1784.9127
1692	4.7354	40.0757	1000.1117	Laminar	1785.3082
1693	4.7354	40.0846	999.8901	Laminar	1785.7038
1694	4.7354	40.0935	999.6686	Laminar	1786.0995
1695	4.7354	40.1024	999.4471	Laminar	1786.4954
1696	4.7354	40.1112	999.2256	Laminar	1786.8915
1697	4.7354	40.1201	999.0041	Laminar	1787.2876
1698	4.7354	40.1290	998.7826	Laminar	1787.6839
1699	4.7354	40.1379	998.5612	Laminar	1788.0804
1700	4.7354	40.1468	998.3397	Laminar	1788.4770
1701	4.7354	40.1557	998.1183	Laminar	1788.8737
1702	4.7354	40.1647	997.8969	Laminar	1789.2705
1703	4.7354	40.1736	997.6756	Laminar	1789.6675
1704	4.7354	40.1825	997.4542	Laminar	1790.0647
1705	4.7354	40.1914	997.2329	Laminar	1790.4619
1706	4.7354	40.2003	997.0116	Laminar	1790.8593
1707	4.7354	40.2092	996.7904	Laminar	1791.2569
1708	4.7354	40.2182	996.5691	Laminar	1791.6546
1709	4.7354	40.2271	996.3479	Laminar	1792.0524
1710	4.7354	40.2360	996.1267	Laminar	1792.4504

Depth (m)	Annular Velocity(m/s)	τ wall-corrected (Pa)	Reynolds Number	Flow Regime	Frictional Pressure Loss (Pa/m)
1711	4.7354	40.2450	995.9055	Laminar	1792.8485
1712	4.7354	40.2539	995.6843	Laminar	1793.2467
1713	4.7354	40.2628	995.4632	Laminar	1793.6451
1714	4.7354	40.2718	995.2421	Laminar	1794.0436
1715	4.7354	40.2807	995.0210	Laminar	1794.4422
1716	4.7354	40.2897	994.7999	Laminar	1794.8410
1717	4.7354	40.2986	994.5788	Laminar	1795.2399
1718	4.7354	40.3076	994.3578	Laminar	1795.6390
1719	4.7354	40.3166	994.1368	Laminar	1796.0382
1720	4.7354	40.3255	993.9158	Laminar	1796.4375
1721	4.7354	40.3345	993.6948	Laminar	1796.8370
1722	4.7354	40.3435	993.4739	Laminar	1797.2366
1723	4.7354	40.3524	993.2530	Laminar	1797.6363
1724	4.7354	40.3614	993.0321	Laminar	1798.0362
1725	4.7354	40.3704	992.8112	Laminar	1798.4362
1726	4.7354	40.3794	992.5904	Laminar	1798.8363
1727	4.7354	40.3884	992.3695	Laminar	1799.2366
1728	4.7354	40.3974	992.1487	Laminar	1799.6371
1729	4.7354	40.4063	991.9279	Laminar	1800.0376
1730	4.7354	40.4153	991.7072	Laminar	1800.4383
1731	4.7354	40.4243	991.4864	Laminar	1800.8392
1732	4.7354	40.4333	991.2657	Laminar	1801.2401
1733	4.7354	40.4423	991.0450	Laminar	1801.6413
1734	4.7354	40.4513	990.8244	Laminar	1802.0425
1735	4.7354	40.4604	990.6037	Laminar	1802.4439
1736	4.7354	40.4694	990.3831	Laminar	1802.8454
1737	4.7354	40.4784	990.1625	Laminar	1803.2471
1738	4.7354	40.4874	989.9419	Laminar	1803.6489
1739	4.7354	40.4964	989.7214	Laminar	1804.0508
1740	4.7354	40.5055	989.5008	Laminar	1804.4529
1741	4.7354	40.5145	989.2803	Laminar	1804.8551
1742	4.7354	40.5235	989.0598	Laminar	1805.2574
1743	4.7354	40.5326	988.8394	Laminar	1805.6599
1744	4.7354	40.5416	988.6189	Laminar	1806.0625
1745	4.7354	40.5506	988.3985	Laminar	1806.4653
1746	4.7354	40.5597	988.1781	Laminar	1806.8681
1747	4.7354	40.5687	987.9578	Laminar	1807.2712
1748	4.7354	40.5778	987.7374	Laminar	1807.6743
1749	4.7354	40.5868	987.5171	Laminar	1808.0776

Depth (m)	Annular Velocity(m/s)	τ wall-corrected (Pa)	Reynolds Number	Flow Regime	Frictional Pressure Loss (Pa/m)
1750	4.7354	40.5959	987.2968	Laminar	1808.4811
1751	4.7354	40.6049	987.0766	Laminar	1808.8846
1752	4.7354	40.6140	986.8563	Laminar	1809.2883
1753	4.7354	40.6231	986.6361	Laminar	1809.6922
1754	4.7354	40.6321	986.4159	Laminar	1810.0962
1755	4.7354	40.6412	986.1957	Laminar	1810.5003
1756	4.7354	40.6503	985.9756	Laminar	1810.9045
1757	4.7354	40.6594	985.7554	Laminar	1811.3089
1758	4.7354	40.6684	985.5353	Laminar	1811.7134
1759	4.7354	40.6775	985.3152	Laminar	1812.1181
1760	4.7354	40.6866	985.0952	Laminar	1812.5229
1761	4.7354	40.6957	984.8752	Laminar	1812.9278
1762	4.7354	40.7048	984.6552	Laminar	1813.3329
1763	4.7354	40.7139	984.4352	Laminar	1813.7381
1764	4.7354	40.7230	984.2152	Laminar	1814.1435
1765	4.7354	40.7321	983.9953	Laminar	1814.5489
1766	4.7354	40.7412	983.7754	Laminar	1814.9546
1767	4.7354	40.7503	983.5555	Laminar	1815.3603
1768	4.7354	40.7594	983.3356	Laminar	1815.7662
1769	4.7354	40.7685	983.1158	Laminar	1816.1722
1770	4.7354	40.7776	982.8960	Laminar	1816.5784
1771	4.7354	40.7868	982.6762	Laminar	1816.9847
1772	4.7354	40.7959	982.4564	Laminar	1817.3911
1773	4.7354	40.8050	982.2367	Laminar	1817.7977
1774	4.7354	40.8141	982.0170	Laminar	1818.2044
1775	4.7354	40.8233	981.7973	Laminar	1818.6112
1776	4.7354	40.8324	981.5776	Laminar	1819.0182
1777	4.7354	40.8415	981.3580	Laminar	1819.4253
1778	4.7354	40.8507	981.1384	Laminar	1819.8326
1779	4.7354	40.8598	980.9188	Laminar	1820.2399
1780	4.7354	40.8690	980.6993	Laminar	1820.6475
1781	4.7354	40.8781	980.4797	Laminar	1821.0551
1782	4.7354	40.8873	980.2602	Laminar	1821.4629
1783	4.7354	40.8964	980.0407	Laminar	1821.8708
1784	4.7354	40.9056	979.8213	Laminar	1822.2789
1785	4.7354	40.9148	979.6018	Laminar	1822.6871
1786	4.7354	40.9239	979.3824	Laminar	1823.0954
1787	4.7354	40.9331	979.1630	Laminar	1823.5039
1788	4.7354	40.9423	978.9437	Laminar	1823.9125

Depth (m)	Annular Velocity(m/s)	τ wall-corrected (Pa)	Reynolds Number	Flow Regime	Frictional Pressure Loss (Pa/m)
1789	4.7354	40.9515	978.7243	Laminar	1824.3212
1790	4.7354	40.9606	978.5050	Laminar	1824.7301
1791	4.7354	40.9698	978.2858	Laminar	1825.1391
1792	4.7354	40.9790	978.0665	Laminar	1825.5483
1793	4.7354	40.9882	977.8473	Laminar	1825.9576
1794	4.7354	40.9974	977.6281	Laminar	1826.3670
1795	4.7354	41.0066	977.4089	Laminar	1826.7765
1796	4.7354	41.0158	977.1897	Laminar	1827.1862
1797	4.7354	41.0250	976.9706	Laminar	1827.5960
1798	4.7354	41.0342	976.7515	Laminar	1828.0060
1799	4.7354	41.0434	976.5324	Laminar	1828.4161
1800	4.7354	41.0526	976.3134	Laminar	1828.8263
1801	4.7354	41.0618	976.0943	Laminar	1829.2367
1802	4.7354	41.0710	975.8754	Laminar	1829.6472
1803	4.7354	41.0802	975.6564	Laminar	1830.0578
1804	4.7354	41.0894	975.4374	Laminar	1830.4686
1805	4.7354	41.0987	975.2185	Laminar	1830.8795
1806	4.7354	41.1079	974.9996	Laminar	1831.2906
1807	4.7354	41.1171	974.7808	Laminar	1831.7017
1808	4.7354	41.1264	974.5619	Laminar	1832.1131
1809	4.7354	41.1356	974.3431	Laminar	1832.5245
1810	4.7354	41.1448	974.1243	Laminar	1832.9361
1811	4.7354	41.1541	973.9055	Laminar	1833.3478
1812	4.7354	41.1633	973.6868	Laminar	1833.7597
1813	4.7354	41.1726	973.4681	Laminar	1834.1717
1814	4.7354	41.1818	973.2494	Laminar	1834.5838
1815	4.7354	41.1911	973.0308	Laminar	1834.9960
1816	4.7354	41.2003	972.8121	Laminar	1835.4084
1817	4.7354	41.2096	972.5935	Laminar	1835.8210
1818	4.7354	41.2189	972.3750	Laminar	1836.2336
1819	4.7354	41.2281	972.1564	Laminar	1836.6464
1820	4.7354	41.2374	971.9379	Laminar	1837.0594
1821	4.7354	41.2467	971.7194	Laminar	1837.4724
1822	4.7354	41.2559	971.5009	Laminar	1837.8856
1823	4.7354	41.2652	971.2825	Laminar	1838.2990
1824	4.7354	41.2745	971.0641	Laminar	1838.7125
1825	4.7354	41.2838	970.8457	Laminar	1839.1261
1826	4.7354	41.2931	970.6273	Laminar	1839.5398
1827	4.7354	41.3024	970.4090	Laminar	1839.9537

Depth (m)	Annular Velocity(m/s)	τ wall-corrected (Pa)	Reynolds Number	Flow Regime	Frictional Pressure Loss (Pa/m)
1828	4.7354	41.3117	970.1907	Laminar	1840.3677
1829	4.7354	41.3210	969.9724	Laminar	1840.7819
1830	4.7354	41.3303	969.7542	Laminar	1841.1961
1831	4.7354	41.3396	969.5359	Laminar	1841.6106
1832	4.7354	41.3489	969.3177	Laminar	1842.0251
1833	4.7354	41.3582	969.0996	Laminar	1842.4398
1834	4.7354	41.3675	968.8814	Laminar	1842.8546
1835	4.7354	41.3768	968.6633	Laminar	1843.2696
1836	4.7354	41.3861	968.4452	Laminar	1843.6847
1837	4.7354	41.3954	968.2272	Laminar	1844.0999
1838	4.7354	41.4048	968.0091	Laminar	1844.5153
1839	4.7354	41.4141	967.7911	Laminar	1844.9308
1840	4.7354	41.4234	967.5731	Laminar	1845.3464
1841	4.7354	41.4327	967.3552	Laminar	1845.7622
1842	4.7354	41.4421	967.1373	Laminar	1846.1781
1843	4.7354	41.4514	966.9194	Laminar	1846.5941
1844	4.7354	41.4608	966.7015	Laminar	1847.0103
1845	4.7354	41.4701	966.4837	Laminar	1847.4266
1846	4.7354	41.4795	966.2659	Laminar	1847.8430
1847	4.7354	41.4888	966.0481	Laminar	1848.2596
1848	4.7354	41.4982	965.8303	Laminar	1848.6763
1849	4.7354	41.5075	965.6126	Laminar	1849.0931
1850	4.7354	41.5169	965.3949	Laminar	1849.5101
1851	4.7354	41.5262	965.1772	Laminar	1849.9272
1852	4.7354	41.5356	964.9596	Laminar	1850.3445
1853	4.7354	41.5450	964.7420	Laminar	1850.7619
1854	4.7354	41.5543	964.5244	Laminar	1851.1794
1855	4.7354	41.5637	964.3068	Laminar	1851.5970
1856	4.7354	41.5731	964.0893	Laminar	1852.0148
1857	4.7354	41.5825	963.8718	Laminar	1852.4327
1858	4.7354	41.5919	963.6543	Laminar	1852.8508
1859	4.7354	41.6013	963.4369	Laminar	1853.2690
1860	4.7354	41.6106	963.2194	Laminar	1853.6873
1861	4.7354	41.6200	963.0020	Laminar	1854.1057
1862	4.7354	41.6294	962.7847	Laminar	1854.5243
1863	4.7354	41.6388	962.5674	Laminar	1854.9430
1864	4.7354	41.6482	962.3500	Laminar	1855.3619
1865	4.7354	41.6576	962.1328	Laminar	1855.7809
1866	4.7354	41.6670	961.9155	Laminar	1856.2000

Depth (m)	Annular Velocity(m/s)	τ wall-corrected (Pa)	Reynolds Number	Flow Regime	Frictional Pressure Loss (Pa/m)
1867	4.7354	41.6765	961.6983	Laminar	1856.6193
1868	4.7354	41.6859	961.4811	Laminar	1857.0387
1869	4.7354	41.6953	961.2640	Laminar	1857.4582
1870	4.7354	41.7047	961.0468	Laminar	1857.8778
1871	4.7354	41.7141	960.8297	Laminar	1858.2976
1872	4.7354	41.7236	960.6126	Laminar	1858.7176
1873	4.7354	41.7330	960.3956	Laminar	1859.1376
1874	4.7354	41.7424	960.1786	Laminar	1859.5578
1875	4.7354	41.7519	959.9616	Laminar	1859.9782
1876	4.7354	41.7613	959.7446	Laminar	1860.3986
1877	4.7354	41.7707	959.5277	Laminar	1860.8192
1878	4.7354	41.7802	959.3108	Laminar	1861.2400
1879	4.7354	41.7896	959.0939	Laminar	1861.6608
1880	4.7354	41.7991	958.8771	Laminar	1862.0818
1881	4.7354	41.8085	958.6603	Laminar	1862.5030
1882	4.7354	41.8180	958.4435	Laminar	1862.9242
1883	4.7354	41.8275	958.2267	Laminar	1863.3456
1884	4.7354	41.8369	958.0100	Laminar	1863.7672
1885	4.7354	41.8464	957.7933	Laminar	1864.1888
1886	4.7354	41.8558	957.5766	Laminar	1864.6106
1887	4.7354	41.8653	957.3600	Laminar	1865.0326
1888	4.7354	41.8748	957.1434	Laminar	1865.4546
1889	4.7354	41.8843	956.9268	Laminar	1865.8768
1890	4.7354	41.8938	956.7103	Laminar	1866.2992
1891	4.7354	41.9032	956.4938	Laminar	1866.7217
1892	4.7354	41.9127	956.2773	Laminar	1867.1443
1893	4.7354	41.9222	956.0608	Laminar	1867.5670
1894	4.7354	41.9317	955.8444	Laminar	1867.9899
1895	4.7354	41.9412	955.6280	Laminar	1868.4129
1896	4.7354	41.9507	955.4116	Laminar	1868.8360
1897	4.7354	41.9602	955.1953	Laminar	1869.2593
1898	4.7354	41.9697	954.9789	Laminar	1869.6827
1899	4.7354	41.9792	954.7627	Laminar	1870.1062
1900	4.7354	41.9887	954.5464	Laminar	1870.5299
1901	4.7354	41.9982	954.3302	Laminar	1870.9537
1902	4.7354	42.0077	954.1140	Laminar	1871.3777
1903	4.7354	42.0173	953.8978	Laminar	1871.8017
1904	4.7354	42.0268	953.6817	Laminar	1872.2259
1905	4.7354	42.0363	953.4656	Laminar	1872.6503

Depth (m)	Annular Velocity(m/s)	τ wall-corrected (Pa)	Reynolds Number	Flow Regime	Frictional Pressure Loss (Pa/m)
1906	4.7354	42.0458	953.2495	Laminar	1873.0748
1907	4.7354	42.0554	953.0335	Laminar	1873.4994
1908	4.7354	42.0649	952.8175	Laminar	1873.9241
1909	4.7354	42.0744	952.6015	Laminar	1874.3490
1910	4.7354	42.0840	952.3855	Laminar	1874.7740
1911	4.7354	42.0935	952.1696	Laminar	1875.1991
1912	4.7354	42.1031	951.9537	Laminar	1875.6244
1913	4.7354	42.1126	951.7379	Laminar	1876.0498
1914	4.7354	42.1222	951.5220	Laminar	1876.4753
1915	4.7354	42.1317	951.3062	Laminar	1876.9010
1916	4.7354	42.1413	951.0904	Laminar	1877.3268
1917	4.7354	42.1509	950.8747	Laminar	1877.7528
1918	4.7354	42.1604	950.6590	Laminar	1878.1788
1919	4.7354	42.1700	950.4433	Laminar	1878.6050
1920	4.7354	42.1796	950.2277	Laminar	1879.0314
1921	4.7354	42.1891	950.0121	Laminar	1879.4579
1922	4.7354	42.1987	949.7965	Laminar	1879.8845
1923	4.7354	42.2083	949.5809	Laminar	1880.3112
1924	4.7354	42.2179	949.3654	Laminar	1880.7381
1925	4.7354	42.2275	949.1499	Laminar	1881.1651
1926	4.7354	42.2370	948.9344	Laminar	1881.5922
1927	4.7354	42.2466	948.7190	Laminar	1882.0195
1928	4.7354	42.2562	948.5036	Laminar	1882.4469
1929	4.7354	42.2658	948.2882	Laminar	1882.8744
1930	4.7354	42.2754	948.0729	Laminar	1883.3021
1931	4.7354	42.2850	947.8576	Laminar	1883.7299
1932	4.7354	42.2946	947.6423	Laminar	1884.1578
1933	4.7354	42.3042	947.4270	Laminar	1884.5859
1934	4.7354	42.3139	947.2118	Laminar	1885.0141
1935	4.7354	42.3235	946.9966	Laminar	1885.4424
1936	4.7354	42.3331	946.7815	Laminar	1885.8709
1937	4.7354	42.3427	946.5663	Laminar	1886.2995
1938	4.7354	42.3523	946.3512	Laminar	1886.7282
1939	4.7354	42.3620	946.1362	Laminar	1887.1571
1940	4.7354	42.3716	945.9212	Laminar	1887.5861
1941	4.7354	42.3812	945.7062	Laminar	1888.0152
1942	4.7354	42.3909	945.4912	Laminar	1888.4445
1943	4.7354	42.4005	945.2762	Laminar	1888.8739
1944	4.7354	42.4101	945.0613	Laminar	1889.3034

Depth (m)	Annular Velocity(m/s)	τ wall-corrected (Pa)	Reynolds Number	Flow Regime	Frictional Pressure Loss (Pa/m)
1945	4.7354	42.4198	944.8465	Laminar	1889.7331
1946	4.7354	42.4294	944.6316	Laminar	1890.1629
1947	4.7354	42.4391	944.4168	Laminar	1890.5928
1948	4.7354	42.4487	944.2020	Laminar	1891.0228
1949	4.7354	42.4584	943.9873	Laminar	1891.4530
1950	4.7354	42.4681	943.7726	Laminar	1891.8834
1951	4.7354	42.4777	943.5579	Laminar	1892.3138
1952	4.7354	42.4874	943.3432	Laminar	1892.7444
1953	4.7354	42.4970	943.1286	Laminar	1893.1751
1954	4.7354	42.5067	942.9140	Laminar	1893.6060
1955	4.7354	42.5164	942.6994	Laminar	1894.0370
1956	4.7354	42.5261	942.4849	Laminar	1894.4681
1957	4.7354	42.5358	942.2704	Laminar	1894.8993
1958	4.7354	42.5454	942.0560	Laminar	1895.3307
1959	4.7354	42.5551	941.8415	Laminar	1895.7622
1960	4.7354	42.5648	941.6271	Laminar	1896.1939
1961	4.7354	42.5745	941.4128	Laminar	1896.6257
1962	4.7354	42.5842	941.1984	Laminar	1897.0576
1963	4.7354	42.5939	940.9841	Laminar	1897.4896
1964	4.7354	42.6036	940.7698	Laminar	1897.9218
1965	4.7354	42.6133	940.5556	Laminar	1898.3541
1966	4.7354	42.6230	940.3414	Laminar	1898.7866
1967	4.7354	42.6327	940.1272	Laminar	1899.2191
1968	4.7354	42.6424	939.9131	Laminar	1899.6518
1969	4.7354	42.6522	939.6990	Laminar	1900.0847
1970	4.7354	42.6619	939.4849	Laminar	1900.5177
1971	4.7354	42.6716	939.2708	Laminar	1900.9508
1972	4.7354	42.6813	939.0568	Laminar	1901.3840
1973	4.7354	42.6910	938.8428	Laminar	1901.8174
1974	4.7354	42.7008	938.6289	Laminar	1902.2509
1975	4.7354	42.7105	938.4150	Laminar	1902.6845
1976	4.7354	42.7202	938.2011	Laminar	1903.1183
1977	4.7354	42.7300	937.9872	Laminar	1903.5522
1978	4.7354	42.7397	937.7734	Laminar	1903.9862
1979	4.7354	42.7495	937.5596	Laminar	1904.4204
1980	4.7354	42.7592	937.3459	Laminar	1904.8547
1981	4.7354	42.7690	937.1321	Laminar	1905.2891
1982	4.7354	42.7787	936.9184	Laminar	1905.7236
1983	4.7354	42.7885	936.7048	Laminar	1906.1583

Depth (m)	Annular Velocity(m/s)	τ wall-corrected (Pa)	Reynolds Number	Flow Regime	Frictional Pressure Loss (Pa/m)
1984	4.7354	42.7982	936.4911	Laminar	1906.5932
1985	4.7354	42.8080	936.2776	Laminar	1907.0281
1986	4.7354	42.8178	936.0640	Laminar	1907.4632
1987	4.7354	42.8275	935.8505	Laminar	1907.8984
1988	4.7354	42.8373	935.6370	Laminar	1908.3338
1989	4.7354	42.8471	935.4235	Laminar	1908.7692
1990	4.7354	42.8569	935.2101	Laminar	1909.2049
1991	4.7354	42.8667	934.9967	Laminar	1909.6406
1992	4.7354	42.8764	934.7833	Laminar	1910.0765
1993	4.7354	42.8862	934.5700	Laminar	1910.5125
1994	4.7354	42.8960	934.3567	Laminar	1910.9486
1995	4.7354	42.9058	934.1434	Laminar	1911.3849
1996	4.7354	42.9156	933.9302	Laminar	1911.8213
1997	4.7354	42.9254	933.7170	Laminar	1912.2578
1998	4.7354	42.9352	933.5038	Laminar	1912.6945
1999	4.7354	42.9450	933.2907	Laminar	1913.1313
2000	4.7354	42.9548	933.0776	Laminar	1913.5683
2001	4.7354	42.9646	932.8645	Laminar	1914.0053
2002	4.7354	42.9744	932.6515	Laminar	1914.4425
2003	4.7354	42.9843	932.4385	Laminar	1914.8798
2004	4.7354	42.9941	932.2255	Laminar	1915.3173
2005	4.7354	43.0039	932.0126	Laminar	1915.7549
2006	4.7354	43.0137	931.7997	Laminar	1916.1926
2007	4.7354	43.0236	931.5868	Laminar	1916.6305
2008	4.7354	43.0334	931.3739	Laminar	1917.0685
2009	4.7354	43.0432	931.1611	Laminar	1917.5066
2010	4.7354	43.0531	930.9484	Laminar	1917.9448
2011	4.7354	43.0629	930.7356	Laminar	1918.3832
2012	4.7354	43.0728	930.5229	Laminar	1918.8217
2013	4.7354	43.0826	930.3103	Laminar	1919.2604
2014	4.7354	43.0924	930.0976	Laminar	1919.6991
2015	4.7354	43.1023	929.8850	Laminar	1920.1380
2016	4.7354	43.1122	929.6725	Laminar	1920.5771
2017	4.7354	43.1220	929.4599	Laminar	1921.0162
2018	4.7354	43.1319	929.2474	Laminar	1921.4555
2019	4.7354	43.1417	929.0350	Laminar	1921.8950
2020	4.7354	43.1516	928.8225	Laminar	1922.3345
2021	4.7354	43.1615	928.6101	Laminar	1922.7742
2022	4.7354	43.1713	928.3977	Laminar	1923.2141

Depth (m)	Annular Velocity(m/s)	τ wall-corrected (Pa)	Reynolds Number	Flow Regime	Frictional Pressure Loss (Pa/m)
2023	4.7354	43.1812	928.1854	Laminar	1923.6540
2024	4.7354	43.1911	927.9731	Laminar	1924.0941
2025	4.7354	43.2010	927.7608	Laminar	1924.5343
2026	4.7354	43.2109	927.5486	Laminar	1924.9747
2027	4.7354	43.2208	927.3364	Laminar	1925.4152
2028	4.7354	43.2306	927.1243	Laminar	1925.8558
2029	4.7354	43.2405	926.9121	Laminar	1926.2965
2030	4.7354	43.2504	926.7000	Laminar	1926.7374
2031	4.7354	43.2603	926.4880	Laminar	1927.1784
2032	4.7354	43.2702	926.2759	Laminar	1927.6196
2033	4.7354	43.2801	926.0639	Laminar	1928.0608
2034	4.7354	43.2901	925.8520	Laminar	1928.5022
2035	4.7354	43.3000	925.6401	Laminar	1928.9438
2036	4.7354	43.3099	925.4282	Laminar	1929.3854
2037	4.7354	43.3198	925.2163	Laminar	1929.8272
2038	4.7354	43.3297	925.0045	Laminar	1930.2692
2039	4.7354	43.3396	924.7927	Laminar	1930.7112
2040	4.7354	43.3496	924.5809	Laminar	1931.1534
2041	4.7354	43.3595	924.3692	Laminar	1931.5957
2042	4.7354	43.3694	924.1575	Laminar	1932.0382
2043	4.7354	43.3794	923.9459	Laminar	1932.4808
2044	4.7354	43.3893	923.7342	Laminar	1932.9235
2045	4.7354	43.3992	923.5227	Laminar	1933.3663
2046	4.7354	43.4092	923.3111	Laminar	1933.8093
2047	4.7354	43.4191	923.0996	Laminar	1934.2524
2048	4.7354	43.4291	922.8881	Laminar	1934.6956
2049	4.7354	43.4390	922.6767	Laminar	1935.1390
2050	4.7354	43.4490	922.4653	Laminar	1935.5825
2051	4.7354	43.4589	922.2539	Laminar	1936.0261
2052	4.7354	43.4689	922.0425	Laminar	1936.4699
2053	4.7354	43.4789	921.8312	Laminar	1936.9138
2054	4.7354	43.4888	921.6199	Laminar	1937.3578
2055	4.7354	43.4988	921.4087	Laminar	1937.8020
2056	4.7354	43.5088	921.1975	Laminar	1938.2463
2057	4.7354	43.5188	920.9863	Laminar	1938.6907
2058	4.7354	43.5287	920.7752	Laminar	1939.1352
2059	4.7354	43.5387	920.5641	Laminar	1939.5799
2060	4.7354	43.5487	920.3530	Laminar	1940.0247
2061	4.7354	43.5587	920.1420	Laminar	1940.4696

Depth (m)	Annular Velocity(m/s)	τ wall-corrected (Pa)	Reynolds Number	Flow Regime	Frictional Pressure Loss (Pa/m)
2062	4.7354	43.5687	919.9310	Laminar	1940.9147
2063	4.7354	43.5787	919.7200	Laminar	1941.3599
2064	4.7354	43.5887	919.5091	Laminar	1941.8053
2065	4.7354	43.5987	919.2982	Laminar	1942.2507
2066	4.7354	43.6087	919.0874	Laminar	1942.6963
2067	4.7354	43.6187	918.8765	Laminar	1943.1420
2068	4.7354	43.6287	918.6657	Laminar	1943.5879
2069	4.7354	43.6387	918.4550	Laminar	1944.0339
2070	4.7354	43.6487	918.2443	Laminar	1944.4800
2071	4.7354	43.6587	918.0336	Laminar	1944.9262
2072	4.7354	43.6688	917.8229	Laminar	1945.3726
2073	4.7354	43.6788	917.6123	Laminar	1945.8191
2074	4.7354	43.6888	917.4017	Laminar	1946.2658
2075	4.7354	43.6988	917.1912	Laminar	1946.7125
2076	4.7354	43.7089	916.9807	Laminar	1947.1594
2077	4.7354	43.7189	916.7702	Laminar	1947.6065
2078	4.7354	43.7289	916.5598	Laminar	1948.0536
2079	4.7354	43.7390	916.3494	Laminar	1948.5009
2080	4.7354	43.7490	916.1390	Laminar	1948.9483
2081	4.7354	43.7591	915.9287	Laminar	1949.3959
2082	4.7354	43.7691	915.7184	Laminar	1949.8436
2083	4.7354	43.7792	915.5081	Laminar	1950.2914
2084	4.7354	43.7892	915.2979	Laminar	1950.7393
2085	4.7354	43.7993	915.0877	Laminar	1951.1874
2086	4.7354	43.8093	914.8776	Laminar	1951.6356
2087	4.7354	43.8194	914.6674	Laminar	1952.0839
2088	4.7354	43.8295	914.4573	Laminar	1952.5324
2089	4.7354	43.8395	914.2473	Laminar	1952.9810
2090	4.7354	43.8496	914.0373	Laminar	1953.4297
2091	4.7354	43.8597	913.8273	Laminar	1953.8786
2092	4.7354	43.8698	913.6174	Laminar	1954.3276
2093	4.7354	43.8798	913.4075	Laminar	1954.7767
2094	4.7354	43.8899	913.1976	Laminar	1955.2259
2095	4.7354	43.9000	912.9877	Laminar	1955.6753
2096	4.7354	43.9101	912.7779	Laminar	1956.1248
2097	4.7354	43.9202	912.5682	Laminar	1956.5745
2098	4.7354	43.9303	912.3585	Laminar	1957.0242
2099	4.7354	43.9404	912.1488	Laminar	1957.4741
2100	4.7354	43.9505	911.9391	Laminar	1957.9242

Depth (m)	Annular Velocity(m/s)	τ wall-corrected (Pa)	Reynolds Number	Flow Regime	Frictional Pressure Loss (Pa/m)
2101	4.7354	43.9606	911.7295	Laminar	1958.3743
2102	4.7354	43.9707	911.5199	Laminar	1958.8246
2103	4.7354	43.9808	911.3103	Laminar	1959.2750
2104	4.7354	43.9909	911.1008	Laminar	1959.7256
2105	4.7354	44.0011	910.8913	Laminar	1960.1763
2106	4.7354	44.0112	910.6819	Laminar	1960.6271
2107	4.7354	44.0213	910.4725	Laminar	1961.0780
2108	4.7354	44.0314	910.2631	Laminar	1961.5291
2109	4.7354	44.0416	910.0538	Laminar	1961.9803
2110	4.7354	44.0517	909.8445	Laminar	1962.4316
2111	4.7354	44.0618	909.6352	Laminar	1962.8831
2112	4.7354	44.0720	909.4260	Laminar	1963.3347
2113	4.7354	44.0821	909.2168	Laminar	1963.7864
2114	4.7354	44.0922	909.0077	Laminar	1964.2383
2115	4.7354	44.1024	908.7985	Laminar	1964.6902
2116	4.7354	44.1125	908.5894	Laminar	1965.1424
2117	4.7354	44.1227	908.3804	Laminar	1965.5946
2118	4.7354	44.1328	908.1714	Laminar	1966.0470
2119	4.7354	44.1430	907.9624	Laminar	1966.4995
2120	4.7354	44.1532	907.7535	Laminar	1966.9521
2121	4.7354	44.1633	907.5446	Laminar	1967.4049
2122	4.7354	44.1735	907.3357	Laminar	1967.8578
2123	4.7354	44.1837	907.1269	Laminar	1968.3108
2124	4.7354	44.1938	906.9181	Laminar	1968.7639
2125	4.7354	44.2040	906.7093	Laminar	1969.2172
2126	4.7354	44.2142	906.5006	Laminar	1969.6706
2127	4.7354	44.2244	906.2919	Laminar	1970.1242
2128	4.7354	44.2345	906.0833	Laminar	1970.5778
2129	4.7354	44.2447	905.8747	Laminar	1971.0316
2130	4.7354	44.2549	905.6661	Laminar	1971.4856
2131	4.7354	44.2651	905.4575	Laminar	1971.9396
2132	4.7354	44.2753	905.2490	Laminar	1972.3938
2133	4.7354	44.2855	905.0406	Laminar	1972.8481
2134	4.7354	44.2957	904.8321	Laminar	1973.3026
2135	4.7354	44.3059	904.6238	Laminar	1973.7572
2136	4.7354	44.3161	904.4154	Laminar	1974.2119
2137	4.7354	44.3263	904.2071	Laminar	1974.6667
2138	4.7354	44.3365	903.9988	Laminar	1975.1217
2139	4.7354	44.3468	903.7905	Laminar	1975.5768

Depth (m)	Annular Velocity(m/s)	τ wall-corrected (Pa)	Reynolds Number	Flow Regime	Frictional Pressure Loss (Pa/m)
2140	4.7354	44.3570	903.5823	Laminar	1976.0320
2141	4.7354	44.3672	903.3742	Laminar	1976.4874
2142	4.7354	44.3774	903.1660	Laminar	1976.9428
2143	4.7354	44.3877	902.9579	Laminar	1977.3985
2144	4.7354	44.3979	902.7499	Laminar	1977.8542
2145	4.7354	44.4081	902.5418	Laminar	1978.3101
2146	4.7354	44.4184	902.3338	Laminar	1978.7661
2147	4.7354	44.4286	902.1259	Laminar	1979.2222
2148	4.7354	44.4388	901.9180	Laminar	1979.6785
2149	4.7354	44.4491	901.7101	Laminar	1980.1349
2150	4.7354	44.4593	901.5022	Laminar	1980.5914
2151	4.7354	44.4696	901.2944	Laminar	1981.0481
2152	4.7354	44.4798	901.0867	Laminar	1981.5049
2153	4.7354	44.4901	900.8789	Laminar	1981.9618
2154	4.7354	44.5003	900.6712	Laminar	1982.4188
2155	4.7354	44.5106	900.4636	Laminar	1982.8760
2156	4.7354	44.5209	900.2560	Laminar	1983.3333
2157	4.7354	44.5311	900.0484	Laminar	1983.7907
2158	4.7354	44.5414	899.8408	Laminar	1984.2483
2159	4.7354	44.5517	899.6333	Laminar	1984.7060
2160	4.7354	44.5620	899.4258	Laminar	1985.1638
2161	4.7354	44.5722	899.2184	Laminar	1985.6217
2162	4.7354	44.5825	899.0110	Laminar	1986.0798
2163	4.7354	44.5928	898.8036	Laminar	1986.5380
2164	4.7354	44.6031	898.5963	Laminar	1986.9963
2165	4.7354	44.6134	898.3890	Laminar	1987.4548
2166	4.7354	44.6237	898.1818	Laminar	1987.9134
2167	4.7354	44.6340	897.9746	Laminar	1988.3721
2168	4.7354	44.6443	897.7674	Laminar	1988.8310
2169	4.7354	44.6546	897.5603	Laminar	1989.2900
2170	4.7354	44.6649	897.3532	Laminar	1989.7491
2171	4.7354	44.6752	897.1461	Laminar	1990.2083
2172	4.7354	44.6855	896.9391	Laminar	1990.6677
2173	4.7354	44.6958	896.7321	Laminar	1991.1272
2174	4.7354	44.7061	896.5251	Laminar	1991.5868
2175	4.7354	44.7165	896.3182	Laminar	1992.0466
2176	4.7354	44.7268	896.1113	Laminar	1992.5065
2177	4.7354	44.7371	895.9045	Laminar	1992.9665
2178	4.7354	44.7474	895.6977	Laminar	1993.4266

Depth (m)	Annular Velocity(m/s)	τ wall-corrected (Pa)	Reynolds Number	Flow Regime	Frictional Pressure Loss (Pa/m)
2179	4.7354	44.7578	895.4909	Laminar	1993.8869
2180	4.7354	44.7681	895.2842	Laminar	1994.3473
2181	4.7354	44.7784	895.0775	Laminar	1994.8078
2182	4.7354	44.7888	894.8708	Laminar	1995.2685
2183	4.7354	44.7991	894.6642	Laminar	1995.7293
2184	4.7354	44.8095	894.4576	Laminar	1996.1902
2185	4.7354	44.8198	894.2511	Laminar	1996.6513
2186	4.7354	44.8302	894.0446	Laminar	1997.1124
2187	4.7354	44.8405	893.8381	Laminar	1997.5738
2188	4.7354	44.8509	893.6317	Laminar	1998.0352
2189	4.7354	44.8613	893.4253	Laminar	1998.4968
2190	4.7354	44.8716	893.2190	Laminar	1998.9585
2191	4.7354	44.8820	893.0127	Laminar	1999.4203
2192	4.7354	44.8924	892.8064	Laminar	1999.8822
2193	4.7354	44.9027	892.6001	Laminar	2000.3443
2194	4.7354	44.9131	892.3939	Laminar	2000.8065
2195	4.7354	44.9235	892.1878	Laminar	2001.2689
2196	4.7354	44.9339	891.9816	Laminar	2001.7313
2197	4.7354	44.9442	891.7756	Laminar	2002.1939
2198	4.7354	44.9546	891.5695	Laminar	2002.6567
2199	4.7354	44.9650	891.3635	Laminar	2003.1195
2200	4.7354	44.9754	891.1575	Laminar	2003.5825
2201	4.7354	44.9858	890.9516	Laminar	2004.0456
2202	4.7354	44.9962	890.7457	Laminar	2004.5089
2203	4.7354	45.0066	890.5398	Laminar	2004.9722
2204	4.7354	45.0170	890.3340	Laminar	2005.4357
2205	4.7354	45.0274	890.1282	Laminar	2005.8994
2206	4.7354	45.0378	889.9225	Laminar	2006.3631
2207	4.7354	45.0482	889.7168	Laminar	2006.8270
2208	4.7354	45.0587	889.5111	Laminar	2007.2910
2209	4.7354	45.0691	889.3054	Laminar	2007.7552
2210	4.7354	45.0795	889.0999	Laminar	2008.2194
2211	4.7354	45.0899	888.8943	Laminar	2008.6838
2212	4.7354	45.1004	888.6888	Laminar	2009.1484
2213	4.7354	45.1108	888.4833	Laminar	2009.6130
2214	4.7354	45.1212	888.2779	Laminar	2010.0778
2215	4.7354	45.1317	888.0724	Laminar	2010.5427
2216	4.7354	45.1421	887.8671	Laminar	2011.0078
2217	4.7354	45.1525	887.6618	Laminar	2011.4730

Depth (m)	Annular Velocity(m/s)	τ wall-corrected (Pa)	Reynolds Number	Flow Regime	Frictional Pressure Loss (Pa/m)
2218	4.7354	45.1630	887.4565	Laminar	2011.9383
2219	4.7354	45.1734	887.2512	Laminar	2012.4037
2220	4.7354	45.1839	887.0460	Laminar	2012.8693
2221	4.7354	45.1943	886.8408	Laminar	2013.3349
2222	4.7354	45.2048	886.6357	Laminar	2013.8008
2223	4.7354	45.2153	886.4306	Laminar	2014.2667
2224	4.7354	45.2257	886.2255	Laminar	2014.7328
2225	4.7354	45.2362	886.0205	Laminar	2015.1990
2226	4.7354	45.2466	885.8155	Laminar	2015.6653
2227	4.7354	45.2571	885.6106	Laminar	2016.1318
2228	4.7354	45.2676	885.4057	Laminar	2016.5984
2229	4.7354	45.2781	885.2008	Laminar	2017.0651
2230	4.7354	45.2885	884.9960	Laminar	2017.5319
2231	4.7354	45.2990	884.7912	Laminar	2017.9989
2232	4.7354	45.3095	884.5864	Laminar	2018.4660
2233	4.7354	45.3200	884.3817	Laminar	2018.9332
2234	4.7354	45.3305	884.1770	Laminar	2019.4006
2235	4.7354	45.3410	883.9724	Laminar	2019.8681
2236	4.7354	45.3515	883.7678	Laminar	2020.3357
2237	4.7354	45.3620	883.5632	Laminar	2020.8035
2238	4.7354	45.3725	883.3587	Laminar	2021.2713
2239	4.7354	45.3830	883.1542	Laminar	2021.7393
2240	4.7354	45.3935	882.9498	Laminar	2022.2075
2241	4.7354	45.4040	882.7454	Laminar	2022.6757
2242	4.7354	45.4145	882.5410	Laminar	2023.1441
2243	4.7354	45.4250	882.3367	Laminar	2023.6126
2244	4.7354	45.4356	882.1324	Laminar	2024.0813
2245	4.7354	45.4461	881.9281	Laminar	2024.5500
2246	4.7354	45.4566	881.7239	Laminar	2025.0189
2247	4.7354	45.4671	881.5197	Laminar	2025.4880
2248	4.7354	45.4777	881.3156	Laminar	2025.9571
2249	4.7354	45.4882	881.1115	Laminar	2026.4264
2250	4.7354	45.4987	880.9074	Laminar	2026.8958
2251	4.7354	45.5093	880.7034	Laminar	2027.3654
2252	4.7354	45.5198	880.4994	Laminar	2027.8350
2253	4.7354	45.5304	880.2955	Laminar	2028.3048
2254	4.7354	45.5409	880.0916	Laminar	2028.7748
2255	4.7354	45.5515	879.8877	Laminar	2029.2448
2256	4.7354	45.5620	879.6839	Laminar	2029.7150

Depth (m)	Annular Velocity(m/s)	τ wall-corrected (Pa)	Reynolds Number	Flow Regime	Frictional Pressure Loss (Pa/m)
2257	4.7354	45.5726	879.4801	Laminar	2030.1853
2258	4.7354	45.5831	879.2764	Laminar	2030.6558
2259	4.7354	45.5937	879.0727	Laminar	2031.1263
2260	4.7354	45.6043	878.8690	Laminar	2031.5970
2261	4.7354	45.6148	878.6653	Laminar	2032.0678
2262	4.7354	45.6254	878.4618	Laminar	2032.5388
2263	4.7354	45.6360	878.2582	Laminar	2033.0099
2264	4.7354	45.6466	878.0547	Laminar	2033.4811
2265	4.7354	45.6571	877.8512	Laminar	2033.9524
2266	4.7354	45.6677	877.6478	Laminar	2034.4239
2267	4.7354	45.6783	877.4444	Laminar	2034.8955
2268	4.7354	45.6889	877.2410	Laminar	2035.3672
2269	4.7354	45.6995	877.0377	Laminar	2035.8391
2270	4.7354	45.7101	876.8344	Laminar	2036.3110
2271	4.7354	45.7207	876.6312	Laminar	2036.7831
2272	4.7354	45.7313	876.4280	Laminar	2037.2554
2273	4.7354	45.7419	876.2248	Laminar	2037.7277
2274	4.7354	45.7525	876.0217	Laminar	2038.2002
2275	4.7354	45.7631	875.8186	Laminar	2038.6728
2276	4.7354	45.7737	875.6156	Laminar	2039.1456
2277	4.7354	45.7843	875.4126	Laminar	2039.6185
2278	4.7354	45.7950	875.2096	Laminar	2040.0915
2279	4.7354	45.8056	875.0067	Laminar	2040.5646
2280	4.7354	45.8162	874.8038	Laminar	2041.0379
2281	4.7354	45.8268	874.6009	Laminar	2041.5112
2282	4.7354	45.8375	874.3981	Laminar	2041.9848
2283	4.7354	45.8481	874.1953	Laminar	2042.4584
2284	4.7354	45.8587	873.9926	Laminar	2042.9322
2285	4.7354	45.8694	873.7899	Laminar	2043.4061
2286	4.7354	45.8800	873.5873	Laminar	2043.8801
2287	4.7354	45.8906	873.3846	Laminar	2044.3542
2288	4.7354	45.9013	873.1821	Laminar	2044.8285
2289	4.7354	45.9119	872.9795	Laminar	2045.3029
2290	4.7354	45.9226	872.7770	Laminar	2045.7775
2291	4.7354	45.9332	872.5746	Laminar	2046.2521
2292	4.7354	45.9439	872.3722	Laminar	2046.7269
2293	4.7354	45.9546	872.1698	Laminar	2047.2018
2294	4.7354	45.9652	871.9675	Laminar	2047.6769
2295	4.7354	45.9759	871.7652	Laminar	2048.1521

Depth (m)	Annular Velocity(m/s)	τ wall-corrected (Pa)	Reynolds Number	Flow Regime	Frictional Pressure Loss (Pa/m)
2296	4.7354	45.9866	871.5629	Laminar	2048.6274
2297	4.7354	45.9972	871.3607	Laminar	2049.1028
2298	4.7354	46.0079	871.1585	Laminar	2049.5784
2299	4.7354	46.0186	870.9564	Laminar	2050.0541
2300	4.7354	46.0293	870.7543	Laminar	2050.5299
2301	4.7354	46.0400	870.5522	Laminar	2051.0058
2302	4.7354	46.0506	870.3502	Laminar	2051.4819
2303	4.7354	46.0613	870.1482	Laminar	2051.9581
2304	4.7354	46.0720	869.9462	Laminar	2052.4344
2305	4.7354	46.0827	869.7443	Laminar	2052.9109
2306	4.7354	46.0934	869.5425	Laminar	2053.3874
2307	4.7354	46.1041	869.3407	Laminar	2053.8641
2308	4.7354	46.1148	869.1389	Laminar	2054.3410
2309	4.7354	46.1255	868.9371	Laminar	2054.8179
2310	4.7354	46.1362	868.7354	Laminar	2055.2950
2311	4.7354	46.1469	868.5338	Laminar	2055.7723
2312	4.7354	46.1577	868.3321	Laminar	2056.2496
2313	4.7354	46.1684	868.1306	Laminar	2056.7271
2314	4.7354	46.1791	867.9290	Laminar	2057.2047
2315	4.7354	46.1898	867.7275	Laminar	2057.6824
2316	4.7354	46.2006	867.5260	Laminar	2058.1603
2317	4.7354	46.2113	867.3246	Laminar	2058.6382
2318	4.7354	46.2220	867.1232	Laminar	2059.1164
2319	4.7354	46.2327	866.9219	Laminar	2059.5946
2320	4.7354	46.2435	866.7206	Laminar	2060.0730
2321	4.7354	46.2542	866.5193	Laminar	2060.5515
2322	4.7354	46.2650	866.3181	Laminar	2061.0301
2323	4.7354	46.2757	866.1169	Laminar	2061.5088
2324	4.7354	46.2865	865.9157	Laminar	2061.9877
2325	4.7354	46.2972	865.7146	Laminar	2062.4667
2326	4.7354	46.3080	865.5136	Laminar	2062.9458
2327	4.7354	46.3187	865.3125	Laminar	2063.4251
2328	4.7354	46.3295	865.1116	Laminar	2063.9045
2329	4.7354	46.3403	864.9106	Laminar	2064.3840
2330	4.7354	46.3510	864.7097	Laminar	2064.8636
2331	4.7354	46.3618	864.5088	Laminar	2065.3434
2332	4.7354	46.3726	864.3080	Laminar	2065.8233
2333	4.7354	46.3833	864.1072	Laminar	2066.3033
2334	4.7354	46.3941	863.9065	Laminar	2066.7835

Depth (m)	Annular Velocity(m/s)	τ wall-corrected (Pa)	Reynolds Number	Flow Regime	Frictional Pressure Loss (Pa/m)
2335	4.7354	46.4049	863.7058	Laminar	2067.2638
2336	4.7354	46.4157	863.5051	Laminar	2067.7442
2337	4.7354	46.4265	863.3045	Laminar	2068.2247
2338	4.7354	46.4373	863.1039	Laminar	2068.7054
2339	4.7354	46.4481	862.9033	Laminar	2069.1861
2340	4.7354	46.4589	862.7028	Laminar	2069.6671
2341	4.7354	46.4696	862.5024	Laminar	2070.1481
2342	4.7354	46.4805	862.3019	Laminar	2070.6293
2343	4.7354	46.4913	862.1015	Laminar	2071.1106
2344	4.7354	46.5021	861.9012	Laminar	2071.5920
2345	4.7354	46.5129	861.7009	Laminar	2072.0735
2346	4.7354	46.5237	861.5006	Laminar	2072.5552
2347	4.7354	46.5345	861.3004	Laminar	2073.0370
2348	4.7354	46.5453	861.1002	Laminar	2073.5190
2349	4.7354	46.5561	860.9001	Laminar	2074.0010
2350	4.7354	46.5670	860.7000	Laminar	2074.4832
2351	4.7354	46.5778	860.4999	Laminar	2074.9655
2352	4.7354	46.5886	860.2999	Laminar	2075.4480
2353	4.7354	46.5995	860.0999	Laminar	2075.9305
2354	4.7354	46.6103	859.8999	Laminar	2076.4132
2355	4.7354	46.6211	859.7000	Laminar	2076.8960
2356	4.7354	46.6320	859.5002	Laminar	2077.3790
2357	4.7354	46.6428	859.3004	Laminar	2077.8621
2358	4.7354	46.6537	859.1006	Laminar	2078.3453
2359	4.7354	46.6645	858.9008	Laminar	2078.8286
2360	4.7354	46.6754	858.7011	Laminar	2079.3121
2361	4.7354	46.6862	858.5015	Laminar	2079.7956
2362	4.7354	46.6971	858.3018	Laminar	2080.2794
2363	4.7354	46.7079	858.1023	Laminar	2080.7632
2364	4.7354	46.7188	857.9027	Laminar	2081.2472
2365	4.7354	46.7297	857.7032	Laminar	2081.7313
2366	4.7354	46.7405	857.5038	Laminar	2082.2155
2367	4.7354	46.7514	857.3043	Laminar	2082.6998
2368	4.7354	46.7623	857.1050	Laminar	2083.1843
2369	4.7354	46.7732	856.9056	Laminar	2083.6689
2370	4.7354	46.7840	856.7063	Laminar	2084.1536
2371	4.7354	46.7949	856.5071	Laminar	2084.6385
2372	4.7354	46.8058	856.3079	Laminar	2085.1235
2373	4.7354	46.8167	856.1087	Laminar	2085.6086

Depth (m)	Annular Velocity(m/s)	τ wall-corrected (Pa)	Reynolds Number	Flow Regime	Frictional Pressure Loss (Pa/m)
2374	4.7354	46.8276	855.9095	Laminar	2086.0938
2375	4.7354	46.8385	855.7104	Laminar	2086.5792
2376	4.7354	46.8494	855.5114	Laminar	2087.0647
2377	4.7354	46.8603	855.3124	Laminar	2087.5503
2378	4.7354	46.8712	855.1134	Laminar	2088.0360
2379	4.7354	46.8821	854.9145	Laminar	2088.5219
2380	4.7354	46.8930	854.7156	Laminar	2089.0079
2381	4.7354	46.9039	854.5167	Laminar	2089.4940
2382	4.7354	46.9148	854.3179	Laminar	2089.9803
2383	4.7354	46.9258	854.1192	Laminar	2090.4667
2384	4.7354	46.9367	853.9204	Laminar	2090.9532
2385	4.7354	46.9476	853.7217	Laminar	2091.4398
2386	4.7354	46.9585	853.5231	Laminar	2091.9266
2387	4.7354	46.9695	853.3245	Laminar	2092.4134
2388	4.7354	46.9804	853.1259	Laminar	2092.9005
2389	4.7354	46.9913	852.9274	Laminar	2093.3876
2390	4.7354	47.0023	852.7289	Laminar	2093.8749
2391	4.7354	47.0132	852.5305	Laminar	2094.3623
2392	4.7354	47.0241	852.3321	Laminar	2094.8498
2393	4.7354	47.0351	852.1337	Laminar	2095.3374
2394	4.7354	47.0460	851.9354	Laminar	2095.8252
2395	4.7354	47.0570	851.7371	Laminar	2096.3131
2396	4.7354	47.0679	851.5388	Laminar	2096.8011
2397	4.7354	47.0789	851.3406	Laminar	2097.2893
2398	4.7354	47.0899	851.1425	Laminar	2097.7776
2399	4.7354	47.1008	850.9444	Laminar	2098.2660
2400	4.7354	47.1118	850.7463	Laminar	2098.7545
2401	4.7354	47.1228	850.5483	Laminar	2099.2432
2402	4.7354	47.1337	850.3503	Laminar	2099.7319
2403	4.7354	47.1447	850.1523	Laminar	2100.2209
2404	4.7354	47.1557	849.9544	Laminar	2100.7099
2405	4.7354	47.1667	849.7565	Laminar	2101.1991
2406	4.7354	47.1776	849.5587	Laminar	2101.6884
2407	4.7354	47.1886	849.3609	Laminar	2102.1778
2408	4.7354	47.1996	849.1631	Laminar	2102.6673
2409	4.7354	47.2106	848.9654	Laminar	2103.1570
2410	4.7354	47.2216	848.7678	Laminar	2103.6468
2411	4.7354	47.2326	848.5701	Laminar	2104.1367
2412	4.7354	47.2436	848.3726	Laminar	2104.6268

Depth (m)	Annular Velocity(m/s)	τ wall-corrected (Pa)	Reynolds Number	Flow Regime	Frictional Pressure Loss (Pa/m)
2413	4.7354	47.2546	848.1750	Laminar	2105.1170
2414	4.7354	47.2656	847.9775	Laminar	2105.6073
2415	4.7354	47.2766	847.7800	Laminar	2106.0977
2416	4.7354	47.2876	847.5826	Laminar	2106.5883
2417	4.7354	47.2987	847.3852	Laminar	2107.0789
2418	4.7354	47.3097	847.1879	Laminar	2107.5698
2419	4.7354	47.3207	846.9906	Laminar	2108.0607
2420	4.7354	47.3317	846.7933	Laminar	2108.5518
2421	4.7354	47.3427	846.5961	Laminar	2109.0430
2422	4.7354	47.3538	846.3990	Laminar	2109.5343
2423	4.7354	47.3648	846.2018	Laminar	2110.0257
2424	4.7354	47.3758	846.0047	Laminar	2110.5173
2425	4.7354	47.3869	845.8077	Laminar	2111.0090
2426	4.7354	47.3979	845.6107	Laminar	2111.5008
2427	4.7354	47.4090	845.4137	Laminar	2111.9928
2428	4.7354	47.4200	845.2168	Laminar	2112.4848
2429	4.7354	47.4311	845.0199	Laminar	2112.9770
2430	4.7354	47.4421	844.8230	Laminar	2113.4694
2431	4.7354	47.4532	844.6262	Laminar	2113.9618
2432	4.7354	47.4642	844.4295	Laminar	2114.4544
2433	4.7354	47.4753	844.2327	Laminar	2114.9471
2434	4.7354	47.4863	844.0361	Laminar	2115.4400
2435	4.7354	47.4974	843.8394	Laminar	2115.9329
2436	4.7354	47.5085	843.6428	Laminar	2116.4260
2437	4.7354	47.5195	843.4463	Laminar	2116.9192
2438	4.7354	47.5306	843.2497	Laminar	2117.4126
2439	4.7354	47.5417	843.0533	Laminar	2117.9060
2440	4.7354	47.5528	842.8568	Laminar	2118.3996
2441	4.7354	47.5639	842.6604	Laminar	2118.8933
2442	4.7354	47.5749	842.4641	Laminar	2119.3872
2443	4.7354	47.5860	842.2678	Laminar	2119.8812
2444	4.7354	47.5971	842.0715	Laminar	2120.3753
2445	4.7354	47.6082	841.8753	Laminar	2120.8695
2446	4.7354	47.6193	841.6791	Laminar	2121.3638
2447	4.7354	47.6304	841.4830	Laminar	2121.8583
2448	4.7354	47.6415	841.2868	Laminar	2122.3529
2449	4.7354	47.6526	841.0908	Laminar	2122.8477
2450	4.7354	47.6637	840.8948	Laminar	2123.3425
2451	4.7354	47.6748	840.6988	Laminar	2123.8375

Depth (m)	Annular Velocity(m/s)	τ wall-corrected (Pa)	Reynolds Number	Flow Regime	Frictional Pressure Loss (Pa/m)
2452	4.7354	47.6860	840.5028	Laminar	2124.3326
2453	4.7354	47.6971	840.3070	Laminar	2124.8278
2454	4.7354	47.7082	840.1111	Laminar	2125.3232
2455	4.7354	47.7193	839.9153	Laminar	2125.8187
2456	4.7354	47.7304	839.7195	Laminar	2126.3143
2457	4.7354	47.7416	839.5238	Laminar	2126.8100
2458	4.7354	47.7527	839.3281	Laminar	2127.3059
2459	4.7354	47.7638	839.1324	Laminar	2127.8019
2460	4.7354	47.7750	838.9368	Laminar	2128.2980
2461	4.7354	47.7861	838.7413	Laminar	2128.7943
2462	4.7354	47.7973	838.5457	Laminar	2129.2906
2463	4.7354	47.8084	838.3503	Laminar	2129.7871
2464	4.7354	47.8195	838.1548	Laminar	2130.2838
2465	4.7354	47.8307	837.9594	Laminar	2130.7805
2466	4.7354	47.8418	837.7641	Laminar	2131.2774
2467	4.7354	47.8530	837.5688	Laminar	2131.7744
2468	4.7354	47.8642	837.3735	Laminar	2132.2715
2469	4.7354	47.8753	837.1782	Laminar	2132.7688
2470	4.7354	47.8865	836.9831	Laminar	2133.2661
2471	4.7354	47.8977	836.7879	Laminar	2133.7636
2472	4.7354	47.9088	836.5928	Laminar	2134.2613
2473	4.7354	47.9200	836.3977	Laminar	2134.7590
2474	4.7354	47.9312	836.2027	Laminar	2135.2569
2475	4.7354	47.9424	836.0077	Laminar	2135.7549
2476	4.7354	47.9535	835.8128	Laminar	2136.2531
2477	4.7354	47.9647	835.6179	Laminar	2136.7513
2478	4.7354	47.9759	835.4230	Laminar	2137.2497
2479	4.7354	47.9871	835.2282	Laminar	2137.7482
2480	4.7354	47.9983	835.0334	Laminar	2138.2469
2481	4.7354	48.0095	834.8387	Laminar	2138.7456
2482	4.7354	48.0207	834.6440	Laminar	2139.2445
2483	4.7354	48.0319	834.4494	Laminar	2139.7435
2484	4.7354	48.0431	834.2547	Laminar	2140.2427
2485	4.7354	48.0543	834.0602	Laminar	2140.7420
2486	14.2891	221.6033	1646.7940	Laminar	17148.6378
2487	14.2891	221.7026	1646.0564	Laminar	17156.3220
2488	14.2891	221.8019	1645.3190	Laminar	17164.0112
2489	14.2891	221.9014	1644.5818	Laminar	17171.7053
2490	14.2891	222.0009	1643.8448	Laminar	17179.4042

Depth (m)	Annular Velocity(m/s)	τ wall-corrected (Pa)	Reynolds Number	Flow Regime	Frictional Pressure Loss (Pa/m)
2491	14.2891	222.1004	1643.1079	Laminar	17187.1081
2492	14.2891	222.2000	1642.3713	Laminar	17194.8169
2493	14.2891	222.2997	1641.6349	Laminar	17202.5306
2494	14.2891	222.3994	1640.8986	Laminar	17210.2492
2495	14.2891	222.4993	1640.1625	Laminar	17217.9727
2496	14.2891	222.5991	1639.4267	Laminar	17225.7011
2497	14.2891	222.6991	1638.6910	Laminar	17233.4344
2498	14.2891	222.7991	1637.9555	Laminar	17241.1727
2499	14.2891	222.8991	1637.2202	Laminar	17248.9159
2500	14.2891	222.9992	1636.4851	Laminar	17256.6640
2501	14.2891	223.0994	1635.7502	Laminar	17264.4170
2502	14.2891	223.1997	1635.0155	Laminar	17272.1750
2503	14.2891	223.3000	1634.2810	Laminar	17279.9379
2504	14.2891	223.4004	1633.5467	Laminar	17287.7057
2505	14.2891	223.5008	1632.8125	Laminar	17295.4784
2506	14.2891	223.6013	1632.0786	Laminar	17303.2561
2507	14.2891	223.7019	1631.3448	Laminar	17311.0388
2508	14.2891	223.8025	1630.6113	Laminar	17318.8263
2509	14.2891	223.9032	1629.8779	Laminar	17326.6189
2510	14.2891	224.0040	1629.1448	Laminar	17334.4163
2511	14.2891	224.1048	1628.4118	Laminar	17342.2187
2512	14.2891	224.2057	1627.6790	Laminar	17350.0261
2513	14.2891	224.3067	1626.9465	Laminar	17357.8384
2514	14.2891	224.4077	1626.2141	Laminar	17365.6557
2515	14.2891	224.5088	1625.4819	Laminar	17373.4779
2516	14.2891	224.6099	1624.7499	Laminar	17381.3051
2517	14.2891	224.7111	1624.0181	Laminar	17389.1373
2518	14.2891	224.8124	1623.2865	Laminar	17396.9744
2519	14.2891	224.9137	1622.5551	Laminar	17404.8165
2520	14.2891	225.0151	1621.8239	Laminar	17412.6635
2521	14.2891	225.1166	1621.0929	Laminar	17420.5156
2522	14.2891	225.2181	1620.3621	Laminar	17428.3726
2523	14.2891	225.3197	1619.6314	Laminar	17436.2345
2524	14.2891	225.4214	1618.9010	Laminar	17444.1015
2525	14.2891	225.5231	1618.1708	Laminar	17451.9734
2526	14.2891	225.6249	1617.4408	Laminar	17459.8503
2527	14.2891	225.7268	1616.7109	Laminar	17467.7322
2528	14.2891	225.8287	1615.9813	Laminar	17475.6191
2529	14.2891	225.9307	1615.2519	Laminar	17483.5110

Depth (m)	Annular Velocity(m/s)	τ wall-corrected (Pa)	Reynolds Number	Flow Regime	Frictional Pressure Loss (Pa/m)
2530	14.2891	226.0327	1614.5226	Laminar	17491.4079
2531	14.2891	226.1348	1613.7936	Laminar	17499.3097
2532	14.2891	226.2370	1613.0647	Laminar	17507.2166
2533	14.2891	226.3392	1612.3361	Laminar	17515.1285
2534	14.2891	226.4416	1611.6076	Laminar	17523.0453
2535	14.2891	226.5439	1610.8794	Laminar	17530.9672
2536	14.2891	226.6464	1610.1513	Laminar	17538.8941
2537	14.2891	226.7489	1609.4235	Laminar	17546.8260
2538	14.2891	226.8514	1608.6958	Laminar	17554.7628
2539	14.2891	226.9541	1607.9684	Laminar	17562.7048
2540	14.2891	227.0567	1607.2411	Laminar	17570.6517
2541	14.2891	227.1595	1606.5141	Laminar	17578.6036
2542	14.2891	227.2623	1605.7872	Laminar	17586.5606
2543	14.2891	227.3652	1605.0605	Laminar	17594.5226
2544	14.2891	227.4682	1604.3341	Laminar	17602.4896
2545	14.2891	227.5712	1603.6078	Laminar	17610.4616
2546	14.2891	227.6743	1602.8817	Laminar	17618.4387
2547	14.2891	227.7774	1602.1559	Laminar	17626.4208
2548	14.2891	227.8806	1601.4302	Laminar	17634.4079
2549	14.2891	227.9839	1600.7048	Laminar	17642.4001
2550	14.2891	228.0873	1599.9795	Laminar	17650.3973
2551	14.2891	228.1907	1599.2544	Laminar	17658.3995
2552	14.2891	228.2941	1598.5296	Laminar	17666.4068
2553	14.2891	228.3977	1597.8049	Laminar	17674.4192
2554	14.2891	228.5013	1597.0805	Laminar	17682.4365
2555	14.2891	228.6050	1596.3562	Laminar	17690.4590
2556	14.2891	228.7087	1595.6321	Laminar	17698.4865
2557	14.2891	228.8125	1594.9083	Laminar	17706.5190
2558	14.2891	228.9164	1594.1846	Laminar	17714.5566
2559	14.2891	229.0203	1593.4612	Laminar	17722.5993
2560	14.2891	229.1243	1592.7379	Laminar	17730.6470
2561	14.2891	229.2283	1592.0149	Laminar	17738.6998
2562	14.2891	229.3325	1591.2920	Laminar	17746.7577
2563	14.2891	229.4367	1590.5694	Laminar	17754.8206
2564	14.2891	229.5409	1589.8469	Laminar	17762.8886
2565	14.2891	229.6453	1589.1247	Laminar	17770.9617
2566	14.2891	229.7496	1588.4026	Laminar	17779.0399
2567	14.2891	229.8541	1587.6808	Laminar	17787.1231
2568	14.2891	229.9586	1586.9592	Laminar	17795.2115

Depth (m)	Annular Velocity(m/s)	τ wall-corrected (Pa)	Reynolds Number	Flow Regime	Frictional Pressure Loss (Pa/m)
2569	14.2891	230.0632	1586.2377	Laminar	17803.3049
2570	14.2891	230.1679	1585.5165	Laminar	17811.4034
2571	14.2891	230.2726	1584.7955	Laminar	17819.5070
2572	14.2891	230.3774	1584.0746	Laminar	17827.6156
2573	14.2891	230.4822	1583.3540	Laminar	17835.7294
2574	14.2891	230.5871	1582.6336	Laminar	17843.8483
2575	14.2891	230.6921	1581.9134	Laminar	17851.9722
2576	14.2891	230.7972	1581.1934	Laminar	17860.1013
2577	14.2891	230.9023	1580.4736	Laminar	17868.2355
2578	14.2891	231.0075	1579.7540	Laminar	17876.3748
2579	14.2891	231.1127	1579.0346	Laminar	17884.5192
2580	14.2891	231.2180	1578.3154	Laminar	17892.6687
2581	14.2891	231.3234	1577.5964	Laminar	17900.8233
2582	14.2891	231.4288	1576.8776	Laminar	17908.9830
2583	14.2891	231.5343	1576.1590	Laminar	17917.1479
2584	14.2891	231.6399	1575.4406	Laminar	17925.3178
2585	14.2891	231.7456	1574.7224	Laminar	17933.4929
2586	14.2891	231.8513	1574.0045	Laminar	17941.6732
2587	14.2891	231.9570	1573.2867	Laminar	17949.8585
2588	14.2891	232.0629	1572.5691	Laminar	17958.0490
2589	14.2891	232.1688	1571.8518	Laminar	17966.2446
2590	14.2891	232.2748	1571.1346	Laminar	17974.4454
2591	14.2891	232.3808	1570.4177	Laminar	17982.6513
2592	14.2891	232.4869	1569.7010	Laminar	17990.8623
2593	14.2891	232.5931	1568.9844	Laminar	17999.0785
2594	14.2891	232.6993	1568.2681	Laminar	18007.2998
2595	14.2891	232.8056	1567.5520	Laminar	18015.5263
2596	14.2891	232.9120	1566.8361	Laminar	18023.7579
2597	14.2891	233.0185	1566.1203	Laminar	18031.9947
2598	14.2891	233.1250	1565.4048	Laminar	18040.2367
2599	14.2891	233.2315	1564.6895	Laminar	18048.4838
2600	14.2891	233.3382	1563.9744	Laminar	18056.7360
2601	14.2891	233.4449	1563.2596	Laminar	18064.9934
2602	14.2891	233.5517	1562.5449	Laminar	18073.2560
2603	14.2891	233.6585	1561.8304	Laminar	18081.5238
2604	14.2891	233.7654	1561.1161	Laminar	18089.7967
2605	14.2891	233.8724	1560.4021	Laminar	18098.0748
2606	14.2891	233.9794	1559.6882	Laminar	18106.3581
2607	14.2891	234.0865	1558.9746	Laminar	18114.6465

Depth (m)	Annular Velocity(m/s)	τ wall-corrected (Pa)	Reynolds Number	Flow Regime	Frictional Pressure Loss (Pa/m)
2608	14.2891	234.1937	1558.2612	Laminar	18122.9402
2609	14.2891	234.3009	1557.5479	Laminar	18131.2390
2610	14.2891	234.4082	1556.8349	Laminar	18139.5430
2611	14.2891	234.5156	1556.1221	Laminar	18147.8522
2612	14.2891	234.6231	1555.4095	Laminar	18156.1666
2613	14.2891	234.7306	1554.6971	Laminar	18164.4862
2614	14.2891	234.8381	1553.9849	Laminar	18172.8110
2615	14.2891	234.9458	1553.2729	Laminar	18181.1410
2616	14.2891	235.0535	1552.5611	Laminar	18189.4761
2617	14.2891	235.1613	1551.8496	Laminar	18197.8165
2618	14.2891	235.2691	1551.1382	Laminar	18206.1621
2619	14.2891	235.3770	1550.4271	Laminar	18214.5129
2620	14.2891	235.4850	1549.7161	Laminar	18222.8689
2621	14.2891	235.5931	1549.0054	Laminar	18231.2302
2622	14.2891	235.7012	1548.2949	Laminar	18239.5966
2623	14.2891	235.8094	1547.5845	Laminar	18247.9683
2624	14.2891	235.9176	1546.8744	Laminar	18256.3452
2625	14.2891	236.0259	1546.1645	Laminar	18264.7273
2626	14.2891	236.1343	1545.4549	Laminar	18273.1146
2627	14.2891	236.2428	1544.7454	Laminar	18281.5072
2628	14.2891	236.3513	1544.0361	Laminar	18289.9050
2629	14.2891	236.4599	1543.3270	Laminar	18298.3080
2630	14.2891	236.5685	1542.6182	Laminar	18306.7163
2631	14.2891	236.6773	1541.9096	Laminar	18315.1298
2632	14.2891	236.7861	1541.2011	Laminar	18323.5486
2633	14.2891	236.8949	1540.4929	Laminar	18331.9726
2634	14.2891	237.0038	1539.7849	Laminar	18340.4019
2635	14.2891	237.1128	1539.0771	Laminar	18348.8364
2636	14.2891	237.2219	1538.3695	Laminar	18357.2761
2637	14.2891	237.3310	1537.6621	Laminar	18365.7211
2638	14.2891	237.4402	1536.9550	Laminar	18374.1714
2639	14.2891	237.5495	1536.2480	Laminar	18382.6269
2640	14.2891	237.6588	1535.5412	Laminar	18391.0877
2641	14.2891	237.7682	1534.8347	Laminar	18399.5538
2642	14.2891	237.8777	1534.1284	Laminar	18408.0251
2643	14.2891	237.9872	1533.4223	Laminar	18416.5017
2644	14.2891	238.0969	1532.7164	Laminar	18424.9836
2645	14.2891	238.2065	1532.0107	Laminar	18433.4708
2646	14.2891	238.3163	1531.3052	Laminar	18441.9632

Depth (m)	Annular Velocity(m/s)	τ wall-corrected (Pa)	Reynolds Number	Flow Regime	Frictional Pressure Loss (Pa/m)
2647	14.2891	238.4261	1530.5999	Laminar	18450.4609
2648	14.2891	238.5360	1529.8948	Laminar	18458.9639
2649	14.2891	238.6459	1529.1900	Laminar	18467.4722
2650	14.2891	238.7559	1528.4854	Laminar	18475.9858
2651	14.2891	238.8660	1527.7809	Laminar	18484.5047
2652	14.2891	238.9762	1527.0767	Laminar	18493.0288
2653	14.2891	239.0864	1526.3727	Laminar	18501.5583
2654	14.2891	239.1967	1525.6689	Laminar	18510.0931
2655	14.2891	239.3070	1524.9653	Laminar	18518.6331
2656	14.2891	239.4175	1524.2620	Laminar	18527.1785
2657	14.2891	239.5280	1523.5588	Laminar	18535.7292
2658	14.2891	239.6385	1522.8559	Laminar	18544.2852
2659	14.2891	239.7492	1522.1531	Laminar	18552.8465
2660	14.2891	239.8599	1521.4506	Laminar	18561.4131
2661	14.2891	239.9706	1520.7483	Laminar	18569.9851
2662	14.2891	240.0815	1520.0462	Laminar	18578.5624

CURRICULUM VITAE

Surname, Name: Gökdemir, Muzaffer Görkem

EDUCATION

Degree	Institution	Year of Graduation
MS	The University of Tulsa Petroleum Engineering	2010
BS	METU Petroleum and Natural Gas Engineering	2007
High School	Ankara Ataürk Lycee, Ankara	2002

FOREIGN LANGUAGES

Advanced English

PAPERS

1. Gokdemir. M.G., Erkekol S. and Dogan H.A. "Investigation of High Pressure Effect on Drilling Fluid Rheology", OMAE2017-61449, Norway (2017)